ALMA MATER STUDIORUM
UNIVERSITÀ DI BOLOGNA

DOTTORATO DI RICERCA IN

ECONOMICS

Ciclo 37

Settore Concorsuale: 13/A5 - ECONOMETRIA

Settore Scientifico Disciplinare: SECS-P/05 - ECONOMETRIA

ESSAYS ON DYNAMIC FACTOR MODELS AND THEIR APPLICATION IN MACROECONOMETRICS

Presentata da: Claudio Lissona

Coordinatore Dottorato

Matteo Barigozzi

Supervisore

Matteo Barigozzi

Esame finale anno 2026

Essays on Dynamic Factor Models and Their Application in Macroeconometrics

Claudio Lissona
University of Bologna

Abstract

This thesis explores novel applications of large-dimensional dynamic factor models to address key macroeconomic questions in a data-rich environment. Chapter 1 provides a measure of the Euro Area (EA) output gap using a large-dimensional non-stationary dynamic factor model applied to a newly assembled EA dataset. Chapter 2 examines the extent and severity of heterogeneity in downside risks to economic growth across the main EA countries through a factor-augmented quantile regression framework. Chapter 3 quantifies the dynamic effects of common monetary policy across EA countries using a novel large-dimensional dataset for the EA and its ten largest countries. Chapter 4 introduces EA-MD-QD, the large dataset employed throughout the thesis. By leveraging large datasets and modern econometric techniques, the thesis offers a rigorous, data-driven perspective on the macroeconomic stance of the EA and its principal economies.

General Introduction

The growing availability of large time-series datasets, where the cross-sectional dimension is as large as—or even larger than—the temporal one, has enabled researchers to address longstanding questions in macroeconomics within a data-rich environment. To fully exploit this potential, econometric tools capable of handling high-dimensional data are required. Among these, dynamic factor models are particularly well suited for macroeconomic applications, as they accommodate the dense structure of these data.

This thesis investigates three applications of large-dimensional dynamic factor models, drawing on a newly constructed dataset for the Euro Area (EA) and its member countries. Each chapter focuses on a distinct macroeconomic question, with an overarching emphasis on assessing the macroeconomic stance of the EA and its main economies. The results provide new evidence with relevant policy implications, both for the design of EA-wide strategies and for addressing country-specific challenges within the monetary union.

Chapter 1 is based on the paper *Measuring the Euro Area Output Gap*, a joint work with Matteo Barigozzi and Matteo Luciani. The chapter addresses the challenging task of providing reliable estimates of the output gap and potential output—two key quantities for policy analysis at both the Euro Area (EA) and country level. We develop a data-driven approach by combining a large non-stationary dynamic factor model with an unobserved-components trend–cycle decomposition. Our results reveal a marked slowdown in potential output growth following the 2008 recession, which persists to the present and leads to a large, positive output gap in the post-Covid period. Although our estimates are agnostic of any explicit theoretical macroeconomic relationship, they implicitly embed the informational content of standard business cycle models and outperform other statistical alternatives. The findings suggest that the EA's challenges stem from weak potential output rather than cyclical fluctuations. Hence, if the objective is to foster long-run growth, the policy response should focus on structural, supply-side reforms rather than temporary demand-side stimulus.

Chapter 2 is based on the paper *Heterogeneous economic growth vulnerability across Euro Area countries under stressed scenarios*, a joint work with Esther Ruiz. To this end, we estimate country-specific factor-augmented quantile regressions that account for both EA-wide and country-specific macro-financial conditions, captured through factors extracted from a large dataset using a multi-level dynamic factor model. We specifically analyze scenarios where these factors are subject to stress—whether systemic, country-specific, or sectoral.

The results reveal the presence of heterogeneity in exposure to downside risks. For instance, Germany is more sensitive to EA-wide conditions, while Spain is particularly affected by country-specific sectoral dynamics. We further show that financial factors amplify adverse macroeconomic conditions under stress, but even severe sectoral shocks—whether common or country-specific—cannot fully account for the vulnerability observed in stressed environments. These findings highlight the need for policymakers to monitor both local and EA-wide macro-financial conditions in order to design effective measures to mitigate growth vulnerability.

Chapter 3 and 4 are based on the paper *Large datasets for the Euro Area and its member countries and the dynamic effects of the common monetary policy.* Chapter 3 explores the informational content of the EA-MD-QD database, described in Chapter 4, by estimating the potentially heterogeneous dynamic effects of common monetary policy across EA countries. To this end, the analysis employs the novel common-component VAR

(CC-VAR) framework, which allows to exploit the large dimensionality of the data while focusing on multiple target variables of interest at the country level. The results uncover significant asymmetries in the transmission of monetary policy shocks across member states, particularly between core and peripheral countries. These findings underscore the importance of complementing common monetary policy with targeted, country-specific measures, which should be regarded as complementary rather than substitutive tools in achieving effective policy outcomes.

Chapter 4 provides the foundation for the analyses developed throughout the thesis by constructing a comprehensive macroeconomic dataset for the Euro Area (EA) and its ten largest economies. The dataset comprises more than 1,000 series and is continuously updated, offering practitioners a timely and reliable tool for macroeconomic analysis in data-rich environments.

Overal, this thesis contributes to the longstanding literature in macroeconometrics by addressing policy-relevant questions in a data-rich environment through the application of large-dimensional dynamic factor models. Beyond assessing current macroeconomic conditions in the Euro Area and its member countries, it advances the empirical toolkit available to practitioners and policymakers, providing a robust framework to guide policy design and to address future economic challenges.

Contents

Chapter 1

Measuring the Euro Area Output Gap

1.1 Introduction

The decomposition of GDP in potential output—the level of output consistent with current technologies and "normal" use of capital and labor—and the output gap—the percentage deviation of GDP from its potential—is a fundamental task for policymakers. Potential output tells us how fast an economy can grow in the long run; the output gap helps assess the cyclical position of the economy and, thus, potential inflationary pressures (e.g., Jarociński and Lenza, 2018; Bańbura and Bobeica, 2023). Potential output and the output gap are essential for the common Euro Area (EA) monetary policy and the fiscal policy of individual countries—they are among the main pillars of the EA fiscal surveillance framework, ultimately affecting the fiscal capacity of each member country (European Commission, 2018). However, since both quantities are unobserved, policymakers need a model to extract them from the data.

This chapter proposes a new measure of potential output and the output gap for the EA based on a non-stationary dynamic factor model estimated on a large dataset of macroeconomic and financial variables. Compared to the prevailing literature, which focuses on theoretical structural models with few variables of interest, we adopt a distinct approach because we let the data speak by leveraging a large information set conditional on a few key macroeconomic priors—for example, the long-run slowdown in output growth (Cette et al., 2016).

We conduct our analysis on a new large-dimensional dataset comprising 118 EA economic indicators from 2001:Q1 to 2024:Q3. Four main results emerge from our analysis: first, our output gap estimate is in line with those published by the European Commission (EC) and the International Monetary Fund (IMF) until the 2011–2012 Sovereign Debt Recession (henceforth, SDR), after which our output gap measure suggests that the EA economy was tighter than estimated by the EC and the IMF. Moreover, we estimate that potential output growth decelerated after the 2008–2009 Global Financial Crisis (henceforth, GFC), and as of 2024:Q3, potential output growth has yet to return to the pre-GFC pace. In other words, our results suggest that the EA has a potential output issue, not a business cycle issue. Hence, if the goal is to achieve better economic conditions in the EA, European countries should implement structural reforms and promote productivity-enhancing investments that have long-run effects, while policies aiming at stimulating household consumption and residential investments will have only short-term effects at best.

Second, we find that, on average, the Okun's law relationship and the Phillips Curve are satisfied in our model, even though we do not impose either of them; hence, cyclical movements in real activity, unemployment, and inflation are interconnected (see, e.g., Bianchi et al., 2023).

Third, we find that core inflation remained below 2% after the GFC, not because there was slack in the economy, but rather because trend inflation decreased by one percentage point—in line with the idea that inflation expectations de-anchored on the downside after the GFC (Ciccarelli and Osbat, 2017; Corsello et al., 2021). Moreover, we show that the output gap contributed to at least 30% of the post-pandemic increase in core inflation, thus supporting existing literature that suggests demand forces played a substantial role in the rise of post-pandemic inflation (Ascari et al., 2023; Giannone and Primiceri, 2024; Bergholt et al., 2025). Finally, our output gap measure yields better inflation forecasts than those derived from commonly used methods. These results confirm that our data-driven measure is economically meaningful and valuable for policy analysis.

Fourth, we find that growth financed through household debt is not sustainable in the long run, which is why incorporating financial indicators in the dataset, particularly credit indicators, is necessary to pin down the output gap.

To measure potential output and the output gap, we first estimate the non-stationary dynamic factor model by Quasi Maximum Likelihood using the EM algorithm jointly with the Kalman smoother (Doz et al., 2012; Barigozzi and Luciani, 2024). Then, we extract a common trend from the estimated common factors and compute the cyclical component by subtracting the common trend from the common factors. Having estimated the common trend and the common cyclical component, we measure potential output as the part of GDP explained by the common trends and the output gap as the part of GDP explained by the common cyclical component. Our model belongs to the class of unobserved component models, which is among the most indicated ones for extracting the transitory component of GDP (Canova, 2025).

This model is an enhanced version of the model Barigozzi and Luciani (2023) used to measure the US output gap, as it does not require a long sample to identify the trend and deals with the Covid pandemic. Specifically, we use a three-step estimation procedure to account for the latter. First, we estimate the model using only pre-Covid data. Second, we estimate the effects induced by the Covid shock (level-shift and increased volatility). Third, we re-estimate the model on the full dataset after purging the data from Covid-induced dynamics.

Our model is large-dimensional and non-stationary, thus allowing us to capture well-established co-movements in macroeconomic variables while retaining data in levels. It is now widely recognized that cross-sectional aggregation of a large number of series allows to consistently disentangle the co-movements in the data from idiosyncratic dynamics (Stock and Watson, 2016) and that to obtain meaningful estimates of potential output and the output gap a large information set is necessary (Buncic et al., 2023).

Moreover, we go beyond the common practice of pre-transforming data to work with stationary and centered variables. Thus, we can capture features crucial for identifying the common trend, which would be inevitably lost if we were to difference the data to achieve stationarity (Ng, 2018). This is important not only for estimating the output gap but also because accurately accounting for low-frequency movements helps eliminate any potential confounding effect when estimating the relationship between real activity and inflation over the business cycle (Bianchi et al., 2023).

Related literature. How to estimate potential output and the output gap has been a hotly debated topic for several decades (see, e.g., Canova, 2025). The literature has proposed two main approaches: a theoretical approach and a statistical approach.

The theoretical approach uses theoretical models, such as production-function-based models used by the EC (Havik et al., 2014) and the IMF (De Masi, 1997) or New-Keynesian DSGE models (Justiniano et al., 2013; Burlon and D'Imperio, 2020; Furlanetto et al., 2021).

The statistical approach uses (univariate or multivariate) statistical models, sometimes paired with some macroeconomic relationships of interest, e.g., the Phillips Curve. For example, many papers rely on univariate models (e.g., Morley et al., 2003; Kamber et al., 2018; Hamilton, 2018; Phillips and Jin, 2021; Phillips and Shi, 2021; Hartl et al., 2022), while few others employ multivariate non-stationary methods, which are either low-dimensional models (Jarociński and Lenza, 2018; González-Astudillo, 2019; Tóth, 2021; Hasenzagl et al., 2022), or medium-size, but stationary, models (Aastveit and Trovik, 2014; Morley and Wong, 2020; Morley et al., 2023). Most of these works focus on the US, while only a few focus on the EA, the most recent being Morley et al. (2023).

Structure of the chapter. The rest of the chapter is organized as follows. In Section 1.2, we present the data used in our analysis, and in Section 3.2, we present the model and the estimation strategy. Then, in Section 1.4, we present our estimate of potential output and the output gap, and in Section 1.5, we dive deep into the economic content of these estimates, focusing on the Okun's law and the Phillips correlation. Next, we focus on inflation. Section 1.6 interprets inflation dynamics after the GFC through the lens of our model, and Section 1.7 assesses the ability of our output gap estimate to forecast inflation. Finally, Section 1.8 looks into what signals our model takes from financial indicators to estimate the output gap, and Section 2.5 concludes.

A Supplemental Appendix contains additional details on the model, showing various robustness analyses, and reporting additional results. Specifically, Appendix 1.A provides full details on the dataset, while Appendixes 1.B, 1.C, 1.D, and 1.E provide additional details about the model. Next, Appendixes 1.F, 1.G, and 1.H provide robustness analysis. Lastly, Appendix 1.I compares our output gap estimate with that obtained with alternative statistical methodologies, and Appendix 1.J assesses the reliability of our output gap estimate.

1.2 A large Euro Area dataset

We construct a large macroeconomic dataset of $n = 118$ EA series, observed from 2001:Q1 to 2024:Q3 ($T = 95$). The dataset contains a wide range of macroeconomic indicators, including national account statistics, industrial production and turnover indicators, labor market and compensation indicators, price indexes, oil prices, natural gas prices, house prices, exchange rates, interest rates, a stock market index, monetary aggregates, non-financial assets and liabilities, and confidence indexes.

In terms of broad categories of data, we include in the dataset the usual suspects normally considered for high-dimensional macroeconomic analysis (see, for example, McCracken and Ng, 2016, 2020).

In terms of which and how many series to include for each category, we use a mix of economic and statistical reasoning. On the one hand, to identify the common factors driving the co-movement in the data, it is crucial to pool information from many indicators; hence, a larger information set should be preferred. On the other hand, a key assumption of the model is the presence of mild cross-sectional correlation among the idiosyncratic components: violating this assumption leads to a deterioration of the model's performance (Boivin and Ng, 2006; Luciani, 2014). Thus, when building a dataset for factor analysis, we face a trade-off between the need for a larger information set and the risk of introducing too much idiosyncratic correlation. For this reason, we selected the variables to include in the dataset to maximize economic signal while limiting the noise, with exceptions motivated by economic reasoning. For instance, we include GDP and its components since their informational content justifies a relatively high level of idiosyncratic correlations. Similarly, consumption and employment are decomposed according to durability and sectoral composition, respectively, while assets and liabilities are decomposed by ownership. In contrast, we keep the consumer price index for energy while dropping the producer price index for energy, as they carry the same signal (their correlation is greater than 0.95). Likewise, we drop the consumer price index for industrial goods because it has a correlation greater than 0.95 with the goods consumer price index.

As for the treatment of the series, we take logarithms for all variables except for confidence indicators and those already expressed in percentage points. We keep all variables in levels except for price indicators, for which we take first differences; i.e., we work with inflation rates. This is a common approach used in the literature to avoid spurious dynamics resulting from the potential $I(2)$ behavior in price indexes (Stock and Watson, 2016; McCracken and Ng, 2016, 2020). Appendix 1.A provides the complete list of variables included in the dataset, along with their sources and treatment.

1.3 Methodology

In Section 1.3.1, we outline the model and its main features—we discuss all the details, formal assumptions, and further comments in Appendix 1.B. In Section 1.3.2, we sketch how we estimate the model while referring the reader to Appendix 1.C for a step-by-step guide on how estimation is carried out in practice and Appendix 1.D for the bootstrap procedure used to measure uncertainty around our estimates.

1.3.1 The model

We denote the observed i-th time series at a given quarter t as y_{it}, with $1 \leq i \leq 118$ and 2001:Q1 $\leq t \leq$ 2024:Q3. In our non-stationary dynamic factor model, each variable is the sum of (i) a secular component D_{it}, which is treated either as deterministic or stochastic, (ii) q common factors $\mathbf{f}_t = (f_{1t} \cdots f_{qt})'$, which capture the macroeconomic long- and short-run co-movements and have a dynamics governed by a VAR, and (iii) an idiosyncratic component ξ_{it}, which captures local dynamics or measurement errors and is possibly correlated across i and t.

We partition the n series according to two features. First, according to the nature of the secular component, that is, whether D_{it} is a stochastic or a deterministic process. Second, according to the nature of the idiosyncratic component, that is, whether ξ_{it} has a stochastic trend or it is stationary.

In particular, we model D_{it} as a local linear trend for GDP to account for the well-documented slowdown in productivity (Cette et al., 2016) and for households' financial liabilities (HHLB) and households' long-term loans (HHLB.LLN), which make up more than 80% of total household's liabilities, whose average growth rate has slowed down consistently since the GFC. For these variables, we say that $i \in \mathcal{L}_1$. Moreover, we model D_{it} as a local level model for the unemployment rate (UNETOT) to account for relevant labor market features (Cette et al., 2016)—this includes the reallocation of employees across sectors, which contributed to the slowdown in the EA productivity growth—and for all consumer price inflation indexes (HICPOV, HICPNEF, HICPG, HICPSV, HICPNG, HICPFD) as well as oil and natural gas prices (POIL, PNGAS) to account for the slowdown in inflation occurred after the GFC—accounting for low-frequency dynamics in inflation is crucial to avoid potential confounding effects which may alter the relation between inflation and real activity over the business cycle (Bianchi et al., 2023). For these variables, we say that $i \in \mathcal{L}_0$.[1] For all other series, D_{it} is either a linear trend with a constant slope, in which case we say that $i \in \mathcal{I}_b$, or D_{it} is just a constant equal to D_{i0}. To determine $\mathcal{I}_b$, we test the significance of the sample mean of Δy_{it} (see Appendix 1.A).

As for the idiosyncratic components, if $\xi_{it} \sim I(1)$, then we say that $i \in \mathcal{I}_1$ and we model ξ_{it} as a random walk, while if $\xi_{it} \sim I(0)$, we say that $i \notin \mathcal{I}_1$ and we leave its dynamics unspecified to avoid over-parametrization of the model. To determine $\mathcal{I}_1$, we employ the test proposed by Bai and Ng (2004) for the null hypothesis of an idiosyncratic unit root (see Appendix 1.A).

Furthermore, we capture the effect of the Covid shock, which generated a large shift both in the levels (Ng, 2021; Stock and Watson, 2025), and in the volatility (Lenza and Primiceri, 2022; Carriero et al., 2024) of most macroeconomic EA series, through an additional common factor g_t (Stock and Watson, 2025), and a scalar s_t scaling the conditional volatility of the latent factors (Lenza and Primiceri, 2022). While we model the former to have an impact on all series only in 2020 and 2021, we allow the latter to have an effect that persists even after the recovery from the pandemic. These choices reflect the fact that mobility restrictions and lockdowns in the EA have been on and off until early 2022, while in the US, they were enforced only at the beginning of the pandemic.

Formally, the model reads as follows:

$$
\begin{aligned}
y_{it} &= \mathrm{D}_{it} + \boldsymbol{\lambda}_i'\mathbf{f}_t + \gamma_i g_t \mathbb{I}_{2020:\mathrm{Q}1 \le t \le 2021:\mathrm{Q}4} + \xi_{it}, && 1 \le i \le 1; 2001{:}\mathrm{Q}1 \le t \le 2024{:}\mathrm{Q}3, && (1.1)\\
\mathrm{D}_{it} &= \mathrm{D}_{it-1} + b_{i,t-1}\mathbb{I}_{i\in\mathcal{I}_b} + \epsilon_{it}, && \epsilon_{it} \sim (0, \sigma^2_{\epsilon_i}\mathbb{I}_{i\in\mathcal{L}_0}), && (1.2)\\
b_{it} &= b_{it-1} + \eta_{it}, && \eta_{it} \sim (0, \sigma^2_{\eta_i}\mathbb{I}_{i\in\mathcal{L}_1}), && (1.3)\\
\mathbf{f}_t &= \sum_{j=1}^{p} \mathbf{A}_j \mathbf{f}_{t-j} + \{s_t \mathbb{I}_{t \ge 2020:\mathrm{Q}1} + \mathbb{I}_{t < 2020:\mathrm{Q}1})\}\mathbf{u}_t, && \mathbf{u}_t \overset{i.i.d.}{\sim} (\mathbf{0}, \boldsymbol{\Sigma}_u), && (1.4)\\
\xi_{it} &= \xi_{it-1}\mathbb{I}_{i\in\mathcal{I}_1} + e_{it}, && e_{it} \sim (0, \sigma^2_{e_i}), && (1.5)
\end{aligned}
$$

where $\mathbb{I}_A = 1$, if A is true, and $\mathbb{I}_A = 0$, otherwise. We set $p = 2$ based on the BIC criterion for a VAR on the estimated factors, and $q = 4$ based on standard information criteria (Bai and Ng, 2002; Hallin and Liška, 2007). Details are in Appendix 1.E.

Furthermore, we assume that one common trend, τ_t, which we model as a random walk, drives the non-stationarity in the factors $\mathbf{f}_t$, an assumption in line with many theoretical models assuming a common trend as the sole driver of long-run dynamics (e.g.,

[1] Appendix 1.H shows robustness results for the estimate of the output gap when removing the time variation in the secular trends.

Del Negro et al., 2007). In contrast, we remain agnostic on the law of motion of the residual, i.e., the stationary cyclical component, which we denote as $\boldsymbol{\omega}_t$. Specifically, we consider the decomposition:

$$\mathbf{f}_t = \boldsymbol{\psi}\tau_t + \boldsymbol{\omega}_t, \qquad \boldsymbol{\omega}_t \sim (\mathbf{0}, \boldsymbol{\Sigma}_\omega), \tag{1.6}$$

$$\tau_t = \tau_{t-1} + \nu_t, \qquad \nu_t \sim (0, \sigma_\nu^2). \tag{1.7}$$

We can then identify the common trend τ_t by properly initializing the variance σ_ν^2, which is analogous to controlling the signal-to-noise ratio. Details are in the next section. This identification strategy for the common trend is consistent with the results of Kim and Kim (2022), who show that extracting a common trend modeled with an unconstrained random walk component overfits GDP, thus producing a potential output that fluctuates too much and generating the so-called "pile-up" problem.

It is important to stress that we do not impose any parametric model for the dynamic evolution of either ν_t or $\boldsymbol{\omega}_t$. Regarding ν_t, we notice that if we modeled it as an ARMA process, our approach would be equivalent to Morley et al. (2024) approach, who achieve identification by rescaling the estimated parameters of an estimated ARMA for $\Delta\tau_t$ (see Appendix 1.F for a comparison between the two approaches). Regarding $\boldsymbol{\omega}_t$ we notice that the common practice of modeling it as an AR(2) poses identification problems since the same state-space representation can also be obtained with an ARMA(2,1) specification (Kim and Kim, 2022).

The model we just described is a modified version of the model Barigozzi and Luciani (2023) (BL) used to estimate the output gap in the US. We modified BL's model to overcome two important limitations. First, their model relies on estimating cointegrating relationships to identify the common trends, thus requiring long time series to get a reliable estimate. As such, BL's model can be estimated only on US macroeconomic data for which more than 50 years of quarterly data are available. Second, BL estimate their model on pre-Covid data; thus, to incorporate more recent observations, some modification is needed to handle the different co-movements brought about by the Covid pandemic. In this chapter, we solve both limitations by introducing (1.6)-(1.7), which we can estimate even on short samples, and by incorporating recently proposed methods to handle the Covid period in the estimation strategy.

Combining Equations (1.1) and (1.6), we obtain the decomposition of each observed variable:

$$y_{it} = \mathrm{D}_{it} + \boldsymbol{\lambda}_i'\boldsymbol{\psi}\tau_t + \boldsymbol{\lambda}_i'\boldsymbol{\omega}_t + \gamma_i g_t \mathbb{I}_{2020:\mathrm{Q1} \leq t \leq 2021:\mathrm{Q4}} + \xi_{it}. \tag{1.8}$$

Focusing on GDP, we define potential output, PO_t, and the output gap, OG_t, as:

$$\mathrm{PO}_t = \mathrm{D}_{\mathrm{GDP},t} + \boldsymbol{\lambda}_{\mathrm{GDP}}'\boldsymbol{\psi}\tau_t, \tag{1.9}$$

$$\mathrm{OG}_t = \boldsymbol{\lambda}_{\mathrm{GDP}}'\boldsymbol{\omega}_t. \tag{1.10}$$

Hence, in our framework, potential output is the sum of the time-varying secular trend of GDP ($\mathrm{D}_{\mathrm{GDP},t}$), which captures the long-run decline in EA output growth, and the part of GDP driven by the common trend component (τ_t); the output gap is the part of GDP driven by the stationary cyclical component ($\boldsymbol{\omega}_t$).

From the definition of potential output (1.9) and output gap (1.10), we left out the idiosyncratic component, $\xi_{\mathrm{GDP},t}$, and the Covid component, $\gamma_{\mathrm{GDP}} g_t$. While the idiosyncratic component is likely to be just a measurement error (Aruoba et al., 2016), hence, it is clear why we are leaving it out; the exclusion of the Covid shock deserves an explanation.

The Covid component represents the co-movements from 2020:Q1 to 2021:Q4 that neither potential output nor the output gap captures. In principle, this component could be allocated to the output gap, which would be equivalent to assuming that the productive capacity of the EA "froze" due to the lockdowns. While this view is commonly accepted by European institutions (Thum-Thysen et al., 2022), it is still unclear whether, and by what amount, the EA productive capacity has been affected by the Covid shock. Thus, we remain agnostic on the allocation of the Covid component between potential output and the output gap, and we will present it as a standalone component.

1.3.2 Estimating the model

To estimate potential output and the output gap, we first estimate the DFM (1.1)-(1.5) using a three-step estimation procedure, and then we estimate the model for the common trend (1.6)-(1.7) on the estimated factors.

Estimating the dynamic factor model. To estimate the model in (1.1)-(1.5), we need to extract the latent states $\mathbf{f}_t$, g_t, $\mathrm{D}_{\mathrm{i},t}$ (if $i \in \mathcal{L}_1$ or $i \in \mathcal{L}_0$), and ξ_{it} (if $i \in \mathcal{I}_1$), and estimate the parameters $\boldsymbol{\lambda}_i$, γ_i, $\mathbf{A}_j$, s_t, $\boldsymbol{\Sigma}_u$, $\sigma^2_{e_i}$, a_i, and b_i (if $i \in \mathcal{I}_b$), while we calibrate $\sigma^2_{\epsilon_i}$ (if $i \in \mathcal{L}_0$) and $\sigma^2_{\eta_i}$ (if $i \in \mathcal{L}_1$) following Del Negro et al. (2017).[2] To do so, we use a three-step estimation procedure that we summarize below.

STEP 1: ESTIMATE THE MODEL UP TO 2019:Q4 (PRE-COVID STEP). We obtain a preliminary estimate of the parameters using non-stationary PCA (Bai and Ng, 2004; Barigozzi et al., 2021; Onatski and Wang, 2021). Then, we run the EM algorithm, jointly with the Kalman smoother, as described in Barigozzi and Luciani (2024) in the high-dimensional case.

STEP 2: ESTIMATE THE COVID FACTOR AND VOLATILITY (COVID STEP). Using the parameter estimated over the pre-Covid period, we apply the Kalman filter and smoother to extract the latent states using data up to the end of the sample. To address the influence of the Covid outliers on the estimates, we truncate the Kalman smoother at 2020:Q1, and then we continue the backward iterations by re-initializing the Kalman smoother using the Kalman filter estimate for 2019:Q4. This truncation avoids any backward spurious effect from the Covid period to the pre-Covid estimates but creates a structural break in the estimated secular components in 2020:Q1. For this reason, we adjust the level of the smoothed secular components by judgmentally allocating the break in 2020:Q1 to the idiosyncratic component, as suggested by Ahn and Luciani (2024).[3]

[2] We calibrate the variances of the stochastic secular components so that when $i \in \mathcal{L}_1$, the standard deviation of the secular trend is approximately 1% over 100 years, while when $i \in \mathcal{L}_0$, the standard deviation of the secular trend is approximately 1% over 50 years.

[3] An alternative approach we could have taken consists of adjusting for outliers on a series-by-series basis. However, we did not pursue this option because much of the additional volatility during the Covid shock is "economic" volatility induced by the pandemic, not measurement error (Ng, 2021). A univariate outlier adjustment method cannot distinguish between the two, so it likely removes economically relevant information. Indeed, if we do univariate outlier adjustment, we get that the Covid factor is essentially zero, and the output gap is flat as if nothing happened.

At this point, we have an estimate of the states over the entire sample given the information set prior to the Covid shock. This implies that the co-movements in the Covid period are left unaccounted for and are captured by the idiosyncratic component ξ_{it}. Thus, since Covid was a common shock affecting most of (if not all) the series in the dataset, we estimate the Covid factor $\widehat{g}_t$ and its loadings $\widehat{\gamma}_i$ by PCA on the variance-covariance matrix of the idiosyncratic component for the period 2020:Q1-2021:Q4, following Stock and Watson (2025).

Lastly, we estimate the Covid volatilities $\widehat{s}_t$ for the period 2020:Q1-2024:Q3 by maximum likelihood and by using the factors extracted using pre-Covid parameters. We find that $\widehat{s}_t$ jumps from 1 to about 3.5 at the onset of the Covid pandemic, and then remain larger than 2 until the end of 2022, thus justifying our choice of imposing a time-varying volatility until the end of the sample. In Appendix 1.G, we show how our measures would change if we do not explicitly model the effect of Covid, or if we use the exponential decay parametrization proposed by Lenza and Primiceri (2022).

Step 3: Full sample estimation. We estimate all the parameters and latent states up to the end of the sample, by using data net of the Covid component, i.e., with $y_{it} - \widehat{\gamma}_i\widehat{g}_t$. Specifically, by using the factors estimated over the whole sample in Step 2 rescaled by $\widehat{s}_t$ in the last part of the sample, we estimate the parameters, $\widehat{\boldsymbol{\lambda}}_i$, $\widehat{\mathbf{A}}_j$, $\widehat{\boldsymbol{\Sigma}}_u$, $\widehat{\sigma}^2_{e_i}$, $\widehat{a}_i$, and $\widehat{b}_i$, by maximizing the expected likelihood. Finally, with the estimated parameters in hand, we obtain a final estimate of the states, $\widehat{\mathbf{f}}_t$, $\widehat{\mathrm{D}}_{i,t}$, and $\widehat{\xi}_{it}$, through the Kalman smoother again truncated in 2020:Q1 and reinitialized before iterating backward, as explained in Step 2.

Estimating the common trend. Having estimated the model parameters and unobserved states, we can now estimate the common trend. To this end, we estimate the state-space model in (1.6)-(1.7) using the EM algorithm by replacing the true factors with the estimated factors. In particular, we initialize σ^2_ν in such a way that the standard deviation of the trend is approximately 1% over 100 years (Del Negro et al., 2017).

At convergence of the EM algorithm, we obtain a final estimate of the parameters, $\widehat{\boldsymbol{\psi}}$, $\widehat{\boldsymbol{\Sigma}}_\omega$, and $\widehat{\sigma}^2_\nu$, and using these estimates, we have a final estimate of the trend $\widehat{\tau}_t$ and of the cyclical component $\widehat{\boldsymbol{\omega}}_t = \widehat{\mathbf{f}}_t - \widehat{\boldsymbol{\psi}}\widehat{\tau}_t$, obtained through the Kalman smoother. Given the estimates of the common trend and the cyclical common component, we compute our final estimates of potential output and the output gap according to (1.9) and (1.10), respectively.

As shown in Barigozzi and Luciani (2024), the estimation procedure we just outlined delivers consistent estimators of all parameters and of the factors, provided that n and T grow to infinity and the EM algorithm is initialized with the estimator of the loadings and factors introduced by Barigozzi et al. (2021). Furthermore, to prove this result, we neither have to impose the Gaussianity assumption nor have to require uncorrelatedness of the idiosyncratic components (ξ_{it} if $i \notin \mathcal{I}_1$ or e_{it} if $i \in \mathcal{I}_1$) across i or t. Rather, we just have to impose standard moment conditions, such as existence and summability of 4th-order cumulants.

1.4 Potential output and output gap of the Euro Area

Figure 1.1 presents our potential output estimate (black line), both in 100 × log levels (left plot) and in year-on-year (YoY) growth rates (right plot). The right plot also includes potential output growth estimates from the EC (red line) and IMF (blue line).

Three main results emerge from Figure 1.1. First, potential output growth decelerated after the GFC, and the SDR further compounded this deceleration—average potential output growth was 2.1% in 2008, and the subsequent peak was 1.6% right before the Covid pandemic. This result is consistent with the results of Elfsbacka Schmöller and Spitzer (2021), who show that the decline in total factor productivity that occurred during the two recessions induced hysteresis effects on the level of GDP. Second, while the EC and IMF also estimate a slowdown in potential growth after the GFC, they do not estimate any effects of the SDR on potential growth. Third, it is still too soon to determine whether the Covid recession had a long-term effect on potential output growth—the prevailing institutional perspective is that it did not (Thum-Thysen et al., 2022)—because while potential growth rebounded fast after the Covid shock, reaching a peak in 2022:Q4 at 2%, it then slowly declined to 0.95% in 2024:Q3, below the pre-Covid pace.

Figure 1.1: *Potential output*

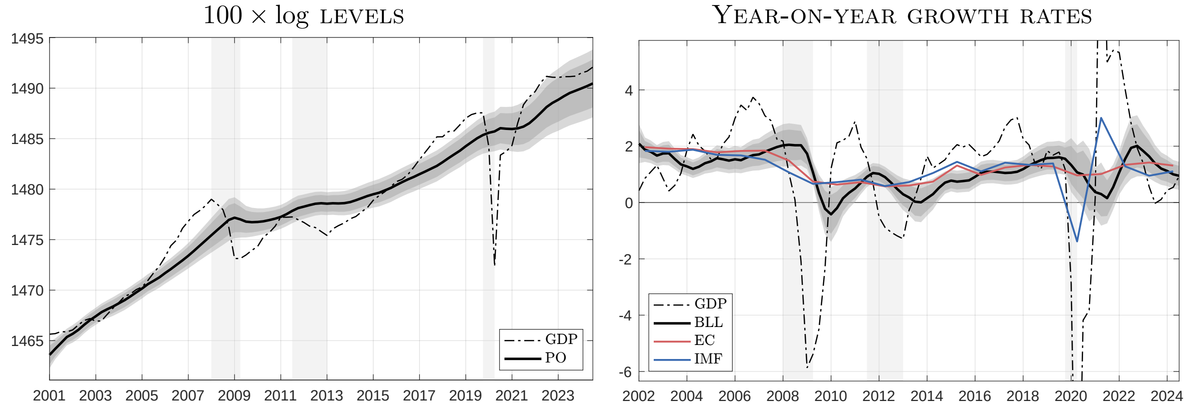

NOTES: In all charts, the black solid line is our estimate of potential output, the grey shaded areas are the 68% and 84% confidence bands, and the dashed black line is GDP—we truncated the y-axis in the right chart for readability. In the right chart, the blue and red lines are the potential output estimates published by the European Commission and the IMF, respectively. The IMF estimate of YoY potential output growth reported in the right chart is the result of our own calculation. Indeed, the IMF publishes only an estimate of the output gap from which we backed out potential output. Thus, the blue line in the right chart does not account for any adjustment for Covid that the IMF might have done.

Figure 1.2 presents the estimated output gap, together with the estimates from the EC and the IMF. Our output gap estimate looks similar to those of the EC and IMF in that the dating of the turning points perfectly coincides. Moreover, the three estimates closely align until the SDR, as they all suggest a substantial overheating of the economy in the pre-GFC period, followed by a persistently negative output gap during the two recessions. However, our measure increased after the SDR, hovering at about 2% from 2017 to the Covid pandemic, thus signaling a much tighter economy than the EC or the IMF. Likewise, our measure indicates a much tighter economy after the Covid shock than the EC and the IMF.

To conclude, Figure 1.3 decomposes GDP growth into the contribution of potential output, the output gap, the Covid factor, and the idiosyncratic component. During the

FIGURE 1.2: *Output gap*

LEVELS | YEAR-ON-YEAR GROWTH RATES

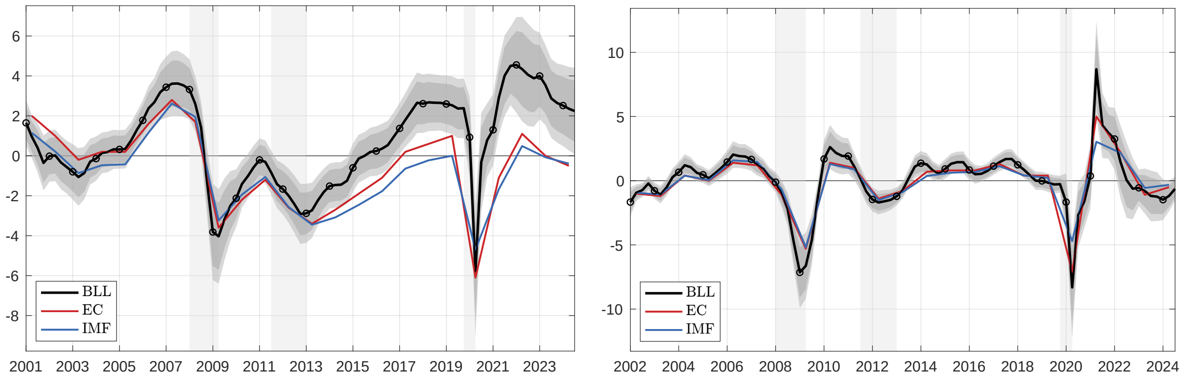

NOTES: The black line is our estimate of the output gap (OG) in levels (left plot) and YoY growth rates (right plot)—the level of the output gap is the percentage deviation from potential, the YoY growth rates is $\mathrm{OG}_t - \mathrm{OG}_{t-4}$. Each black marker denotes one year (four quarters), starting from 2001:Q1. The grey shaded areas are the 68% and 84% confidence bands. The red and blue lines are the output gap estimates published by the European Commission and the IMF, respectively.

Covid pandemic, the output gap subtracted 27.2 percentage points (p.p.) from quarter-on-quarter (QoQ) annualized GDP growth in 2020:Q2 (inset box, right chart). With QoQ annualized GDP growth rate declining at a -47%, a 27.2 p.p. contribution from the output gap seems dubious. However, as explained in Section 1.3.2, our output gap estimate captures only business-as-usual co-movements, while the Covid factor captures the additional co-movements induced by the Covid shock. As shown by the inset box in the right plot in Figure 1.3, the Covid factor accounts for an additional -15 p.p. of the QoQ GDP growth rate plunge in 2020:Q2. Since then, the Covid factor added around 23 p.p. in 2020:Q3, and its contribution declined in the following six quarters, alternating between negative contribution when mobility restrictions were in place and positive contribution during the reopening.

FIGURE 1.3: *Decomposition of GDP growth*

YEAR-ON-YEAR GROWTH RATE | QUARTER-ON-QUARTER ANNUALIZED GROWTH RATES

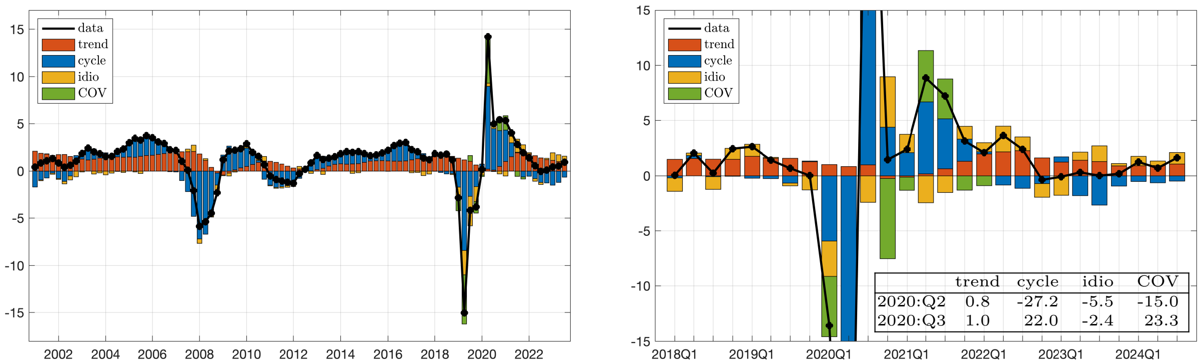

Notes: The black line with dot markers is GDP growth. The bars represent the contribution of each component to GDP growth. The left plot shows YoY growth rates, while the right plot shows QoQ growth at an annual rate. Growth rates are computed using the log approximation.

In summary, Figures 1.1–1.3 show that the EA has a potential output issue, not a business cycle issue. Since the seminal work of Blanchard and Quah (1989), it is common to assume that supply shocks have permanent effects, while demand shocks have only transitory effects. Empirical studies support this assumption. Specifically, Forni et al. (2025) show that the impulse response functions to a supply (demand) shock are almost identical to those of a permanent (transitory shock). Additionally, Benati and

Lubik (2021) find that it is essentially impossible to detect aggregate demand shocks that permanently affect GDP.

Based on this evidence, we assume that the common trend τ_t—hence, potential output—is mainly driven by supply forces, while the cyclical common component $\boldsymbol{\omega}_t$—hence, the output gap—is mainly driven by demand forces. Consequently, to achieve better economic conditions in the EA, European countries should implement structural reforms and promote productivity-enhancing investments that have long-run effects. In contrast, policies aiming at stimulating household consumption and residential investments will have only short-term effects at best because, as we will show in Section 1.8, growth financed through household debt is not sustainable in the long run.

1.5 What about the Okun's law and the Phillips curve?

Our estimate of the output gap has a different meaning than that of the EC and IMF, which derive the output gap and potential output according to the so-called "production function approach" (Kiley, 2013). In production-function-based models, the output and unemployment gaps are related through the Okun's law, and the output gap is related to inflation through the Phillips curve. Thus, in these models, the unemployment gap decreases whenever the output gap increases, and vice-versa, and low inflation suggests a negative output gap, while high inflation indicates a positive gap.

In our model (like any statistical model), we do not impose any Okun's law or Phillips curve. Thus, we must be careful when we compare our estimate with that of the EC or the IMF because their output gap measures are designed to indicate potential inflation pressure, whereas ours is not. Nonetheless, in Sections 1.5.1 and 1.5.2, we show that, on average, our model satisfies the Okun's law relationship and exhibits Phillips correlation.

1.5.1 The Okun's law

The left plot in Figure 1.4 shows that in our model, the unemployment rate gap and the output gap are negatively correlated; that is, our model captures the Okun's law relationship in the data. Over the whole sample, on average, for every percentage point increase in the output gap, the unemployment gap decreases 0.6 p.p. (grey dotted line). Moreover, this correlation has decreased after Covid from -0.56 (blue dash-dotted line) to -0.23 (red solid line), suggesting a (temporary) disconnect between the labor and goods and services market post-Covid in the EA as also noted by Berson et al. (2024). The right plot in Figure 1.4 shows the expanding window estimate of the Okun's law coefficient β in the regression $(\mathrm{UR}_t - D_{\mathrm{UR},t}) = \alpha + \beta \mathrm{OG}_t + \varepsilon_{\mathrm{UR},t}$, where $D_{\mathrm{UR},t}$ is the time-varying mean of the unemployment rate defined in (1.2). On average, the Okun's law coefficient varies between -0.55 to -0.60.[4]

To further corroborate the intuition that there is a tight relationship between our output gap estimate and labor market indicators, Figure 1.5 shows the Generalized Impulse Response Functions (GIRFs) of the common component of the unemployment rate, GDP, potential output, and the output gap to a 1 p.p. shock to the common component of the unemployment rate.[5] Results confirm that our model, on average, associates an

[4]We also estimated the relationship between the output gap and hours worked gap and find a positive correlation in line with the results of Morley et al. (2023).

[5]The lag-h GIRF of all variables is obtained by computing the differences between the h-step ahead

Figure 1.4: *Okun's Law*

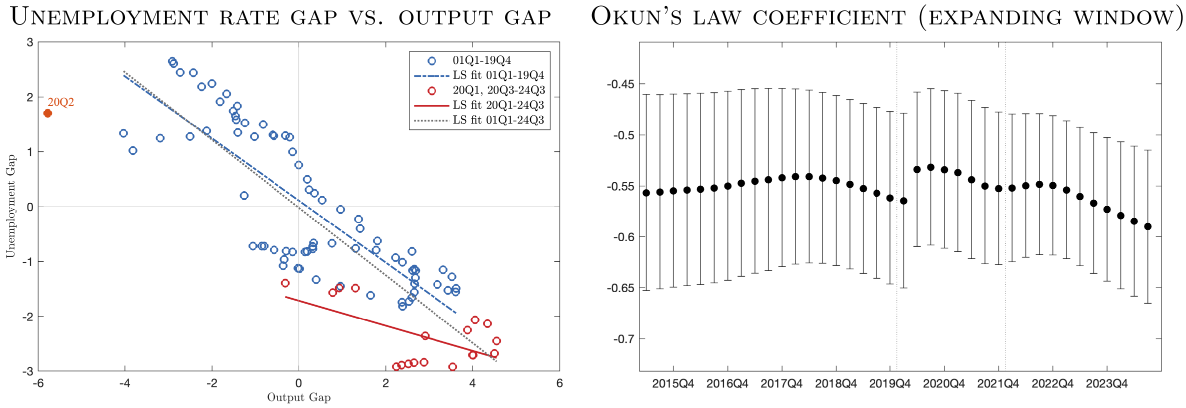

Notes: The left chart shows the Okun's law relationship with the output gap on the horizontal axis and the unemployment rate gap on the vertical axis. Each circle corresponds to an output gap - unemployment gap pair at a given time t. The grey dotted, blue dashed-dotted, and red solid lines are the least squares fit lines for the full, pre-Covid, and post-Covid samples, respectively, obtained by omitting the observation for 2020:Q2 (orange dot).

The right chart shows the least squares estimate, based on an expanding window starting from 2015:Q1, of the Okun's law slope β given by the regression $(\text{UR}_t - D_{\text{UR},t}) = \alpha + \beta \text{OG}_t + \varepsilon_{\text{UR},t}$, where $D_{\text{UR},t}$ is the time-varying mean of the unemployment rate defined in (1.2). Each dot is an estimate of β while the whiskers are $\pm$ one HAC standard errors.

unemployment rate increase with an output gap decrease. After the shock, the common component of the unemployment rate remains 1 p.p. (or more) above the baseline for about a year and a half before decreasing and slowly returning to zero. In response, GDP decreases and keeps decreasing, reaching a through a year after the shock; then, it slowly returns to baseline. The model attributes most of the GDP response to movements in the output gap, while potential output slightly decreases only after a few quarters. The shock is fully absorbed in about 4 years.

Figure 1.5: *Generalized Impulse Response Functions to a shock to the unemployment rate*

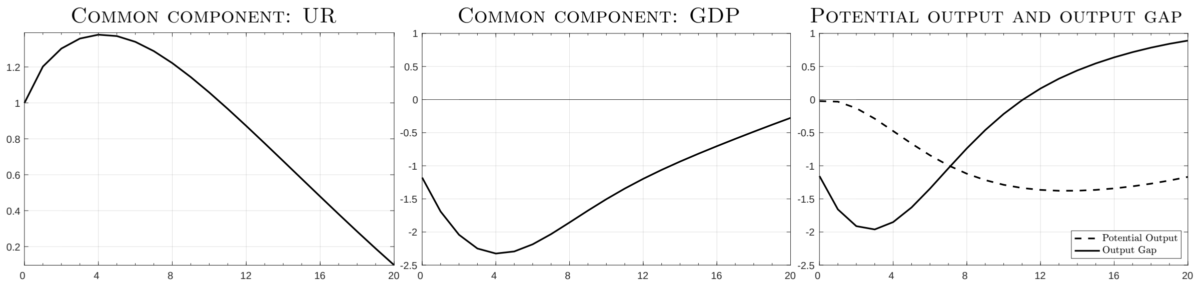

Notes: The black solid/dashed lines are the GIRFs to a 1 p.p. shock to the common component of the unemployment rate. The major ticks in the x-axis represent quarters after the shock.

1.5.2 The Phillips curve

The left plot in Figure 1.6 shows that in our model, the core inflation rate gap (i.e., the cyclical common component of core inflation) and the output gap are positively correlated; that is, there is Phillips correlation in the data, and our model captures it. Over the whole sample, on average, for every percentage point increase in the output

forecast of their common component conditional on a shock to a given variable at time $T+1$ minus the h-step ahead unconditional forecast of the common component, i.e., when no shock is imposed. Both forecasts are computed conditional on all information available at time T (the last observation in our sample) by means of the Kalman filter (Bańbura et al., 2015; Crump et al., 2021).

gap, the core inflation gap increases 4 basis points (dotted grey line). Moreover, this correlation has increased significantly after Covid from 0.022 (dashed-dotted blue line) to 0.079 (solid red line). The right plot in Figure 1.6 shows the expanding window estimate of the slope of the Phillips curve α in the following expectation-augmented specification (e.g., Conti, 2021): $\pi_t = c + \alpha \mathrm{OG}_t + \beta\pi_{t-1} + \gamma\pi_t^e + \varepsilon_{\pi,t}$, where π_t is core inflation and π_t^e are the long-run (5-year ahead) inflation expectations in the Survey of Professional Forecasters. The results suggest that the relationship between inflation and the output gap has strengthened after Covid, a point also made by Lane (2024).

FIGURE 1.6: *Phillips Curve*

CORE INFLATION GAP VS OUTPUT GAP — PHILLIPS CURVE SLOPE (EXPANDING WINDOW)

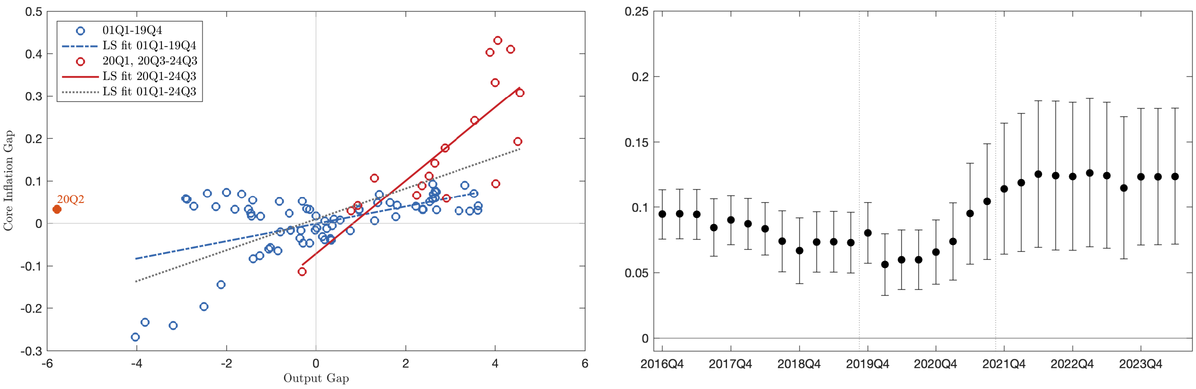

NOTES: The left chart shows the Phillips curve relationship with the output gap on the horizontal axis and the core inflation gap on the vertical axis. Each circle corresponds to an output gap - core inflation gap pair at time t. The grey dotted, blue dashed-dotted, and red solid lines are the least squares fit lines for the full, pre-Covid, and post-Covid samples, respectively, obtained by omitting the observation for 2020:Q2 (orange dot).

The right chart shows the least squares estimate, based on an expanding window starting from 2015:Q1, of the slope of the Phillips curve given by the following expectation-augmented specification: $\pi_t = c + \alpha \mathrm{OG}_t + \beta\pi_{t-1} + \gamma\pi_t^e + \varepsilon_{\pi,t}$, where π_t is core inflation and π_t^e are the long-run (5-year ahead) inflation expectations in the Survey of Professional Forecasters. Each dot is an estimate of α while the whiskers are $\pm$ one HAC standard errors.

To further corroborate the intuition that there is a relationship between our output gap estimate and inflation indicators, Figure 1.7 shows the GIRFs of the common component of core inflation, GDP, potential output, and the output gap to a 0.5 p.p. shock to the common component of core inflation. Results confirm that our model, on average, associates an increase in inflation with an output gap increase. The GIRF of the common component of core inflation peaks one quarter after the shocks before decreasing and slowly returning to zero. In response, GDP initially increases, but after about a year, it starts decreasing, reaching a trough about 2 years after the shock—the shock is fully absorbed in 5 years. The response of potential output is negative and persistent. The output gap initially increases, then decreases, and increases again before returning to zero.

1.6 Inflation dynamics through the lens of our model

In Section 1.5.2, we show that, although we did not create it specifically to signal inflationary pressures, our output gap measure does provide insights related to inflation dynamics. In light of these results, further inspection of Figure 1.2 raises two important questions: How can we reconcile an output gap of 2% between 2017 and 2019 when inflation was just 1%, well below the 2% ECB target? How does our model interpret post-pandemic inflation dynamics?

Figure 1.7: *Generalized Impulse Response Functions to a shock to core inflation*

Common component: core HICP — Common component: GDP — Potential output and output gap

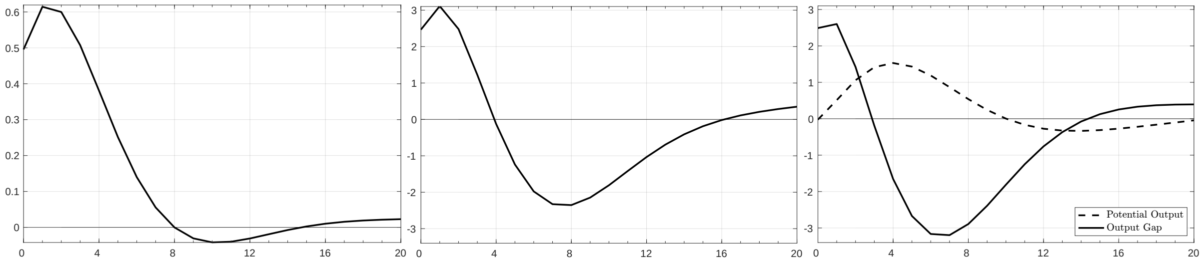

Notes: The black solid/dashed lines are the GIRF to a 0.5 p.p. shock to the common component of core inflation. The major ticks in the x-axis represent quarters after the shock.

To answer these questions, in Figure 1.8, we plot the decomposition of core inflation (HICPNEF) implied by our model:

$$y_{\text{HICPNEF},t} = \bar{\pi}_t^c + \tilde{\pi}_t^c + \gamma_{\text{HICPNEF}} g_t \mathbb{I}_{2020:\text{Q}1 \le t \le 2021:\text{Q}4} + \xi_{\text{HICPNEF},t}, \tag{1.11}$$

$$\bar{\pi}_t^c = \text{D}_{\text{HICPNEF},t} + \boldsymbol{\lambda}'_{\text{HICPNEF}} \psi \tau_t, \tag{1.12}$$

$$\tilde{\pi}_t^c = \boldsymbol{\lambda}'_{\text{HICPNEF}} \boldsymbol{\omega}_t, \tag{1.13}$$

where $\bar{\pi}_t^c$ is trend inflation, and $\tilde{\pi}_t^c$ is the inflation gap. Similar to Hasenzagl et al. (2019), we estimate that after the GFC, trend inflation decreased from 2% to about 1% in 2016, a level at which it stabilized until the Covid pandemic. This result aligns with the findings of Ciccarelli and Osbat (2017) and Corsello et al. (2021), who show that inflation expectations de-anchored on the downside after the SDR. Thus, we conclude that after the GFC, core inflation remained below 2% primarily because trend inflation decreased, not because there was slack in the economy, which explains why we estimate an output gap above 2% when core inflation was 1%.

Figure 1.8: *Decomposition of core inflation*

Year-on-year inflation — Quarter-on-quarter annualized inflation

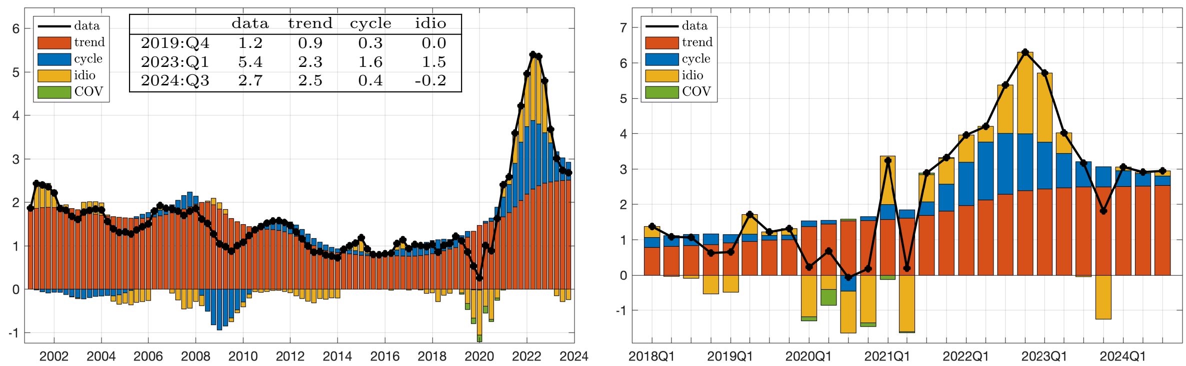

Notes: The black line with dot markers is core inflation. The bars represent the contribution of each component to core inflation. The left plot shows YoY inflation, while the right plot shows QoQ inflation at an annual rate.

Next, we turn our attention to post-pandemic inflation dynamics. As shown in the inset box of the left chart in Figure 1.8, YoY core inflation increased about 4.2 p.p. between 2019:Q4 and 2023:Q1. Trend inflation and the core inflation gap jointly account for about 65% of this 4.2 p.p. increase, while idiosyncratic factors drive the remaining portion. Since its 5.4% peak in 2023:Q1, YoY core inflation decreased to 2.7% in 2024:Q3. The core inflation gap accounts 40 basis points of this decline, and the idiosyncratic components for 250 basis points, while trend inflation increased 20 basis points.

As we explained at the end of Section 1.4, the cyclical common component—therefore, the core inflation gap—primarily reflects demand forces. Under this assumption, the results of the decomposition in Figure 1.8 show that demand forces accounted for at least 30% of the post-pandemic increase in core inflation, thus supporting existing literature that indicates that demand dynamics played a significant role in the inflation surge following the pandemic (Ascari et al., 2023; Giannone and Primiceri, 2024; Bergholt et al., 2025).

Figure 1.8 clearly shows that other significant factors shaping post-pandemic inflation dynamics are idiosyncratic. For example, lingering Covid-specific effects (e.g., supply chain bottlenecks) that are not captured by the Covid factor. Another possibility is that the concurrent sharp rise in oil and natural gas prices following the onset of the Russia-Ukraine war induced second-round effects beyond those experienced in the pre-Covid sample. Finally, labor market tightness might have induced a non-linear response of prices that our linear model fails to capture. These factors might have a more or less persistent effect. Thus, our estimate of the role of demand forces should be considered a lower bound.

1.7 Has our output gap measure predictive power for inflation?

Any output gap measure *must* be good at predicting inflation to be considered a credible indicator of current/future inflationary pressure. Thus, to assess the forecasting properties of our output gap estimate, we replicate the analysis conducted in Bańbura and Bobeica (2023), and we employ the following model:

$$\pi_{t+4} = \alpha\pi_t + \beta OG_t + v_{t+4}, \tag{1.14}$$

where $\pi_t = 100\log(P_t/P_{t-1})$ is the quarter-on-quarter inflation rate in quarter t, P_t is the harmonized consumer price index (either headline or core), $\pi_{t+4} = \sum_{i=1}^{4}\pi_{t+i}$ is year-on-year inflation in quarter $t+4$, and OG_t is the output gap. Bańbura and Bobeica (2023) labeled model (1.14) the "benchmark model," and they show that, despite being very simple, it delivers decent forecasts compared to more complex alternative models.

Our exercise compares the inflation forecast obtained using the benchmark model (1.14) with a forecast obtained by replacing our estimate of the output gap with different univariate and multivariate statistical models: the HP filter, the filter by Hamilton (2018), the boosted HP filter by Phillips and Shi (2021), the Butterworth filter as recommended by Canova (2025), and the large Bayesian VAR approach by Morley et al. (2023)—Appendix 1.I describes these alternative models. We carry out the forecasting exercise on expanding windows, where the first window is a 60-quarter window. We look at the forecasting performance of the different output gap measures over two distinct samples: a pre-Covid sample, 2015:Q4–2019:Q4, and a post-Covid sample, 2022:Q1–2024:Q3.

Table 1.1 compares the forecasting performance of the different output gap measures in terms of relative Root Mean Squared Error (RMSE)—numbers lower than one indicate a better forecasting performance when using our output gap estimate. As shown in rows (1)-(8), in the pre-Covid period, when inflation was low and stable, our output gap measure performed better than all the other alternatives in forecasting headline inflation and better than most alternatives when forecasting core inflation. However, in the post-Covid period, when inflation surged and then declined, our model outperformed all the other measures, sometimes substantially.

In conclusion, the results in this section prove that our output gap measure is not only a measure of the cyclical position of the economy but also a reliable inflation gauge.

1.8 The role of credit indicators

Borio et al. (2017) argue that financial indicators are crucial to meaningfully assess the business

TABLE 1.1: *4-quarter ahead year-on-year inflation forecasting*
Relative Root Mean Squared Errors

		2015:Q4-2019:Q4		2022:Q1-2024:Q3	
	Output Gap Measure	Headline	Core	Headline	Core
(1)	HP Filter ($\lambda = 1600$)	0.91	1.00	0.97	0.89
(2)	HP Filter ($\lambda = 51200$)	0.92	1.01	0.94	0.89
(3)	Hamilton Filter	0.99	0.97	0.97	0.90
(4)	Boosted HP Filter ($\lambda = 1600$)	0.90	0.95	0.89	0.87
(5)	Boosted HP Filter ($\lambda = 51200$)	0.90	0.99	0.91	0.88
(6)	Christiano-Fitzgerald Filter	0.90	0.82	0.98	0.88
(7)	Butterworth Filter	0.95	0.95	0.96	0.88
(8)	Multivariate Beveridge-Nelson	0.91	0.97	-	-

NOTES: The table shows the relative RMSE of forecasting year-on-year inflation using (1.14), where OG_t is either our output gap estimate, or an alternative output gap estimate. Our benchmark output gap estimate is always the numerator of the RMSE, thus numbers lower than 1 indicate a better forecasting performance when using our benchmark output gap estimate. Rows (1)–(8) compare our benchmark estimate with alternative models. In row (8) forecasts are obtained with the output gap measure by Morley et al. (2023) which is available only until 2021:Q3. Therefore, we only present results for the pre-Covid forecasting exercise.

cycle, as credit expansions often lead to economic overheating, especially from the late 1990s onward. In support of this result, Berger et al. (2022) find that a large share of the US economy overheating in the build-up of the financial crisis was due to financial imbalances in the credit and housing market. Moreover, Claessens et al. (2012), Rünstler and Vlekke (2018), and Winter et al. (2022) find that the business and financial cycles are correlated and co-move in the medium run.

To understand what signals our model takes from financial indicators to estimate the output gap, we focus on household liabilities because they have become an important driver of the business cycle in many advanced economies since the early 2000s (Mian et al., 2017). Indeed, while in the 1990s, non-financial corporations were the main driver of the financial cycle, households were behind both the pre-GFC excess leverage, which boosted household demand, and the subsequent deleveraging, which curtailed household's demand (Mian and Sufi, 2018; Plagborg-Møller et al., 2020; Reichlin et al., 2020). In terms of the EA area, Gambetti and Musso (2017) find that loan supply shocks significantly affect the EA business cycle.

Figure 1.9 shows the impact of a scenario in which household liabilities increase faster than projected in the baseline for about 3½ years. In this scenario, household liabilities reach a level about 6¼ p.p. higher than in the baseline before returning to baseline after about 8 years.[6]

The lower charts in Figure 1.9 show the dynamic effects of this scenario on the log level of GDP and on the output gap and potential output.[7] Specifically, GDP increases for a little over three years, reaching a peak at 3 p.p. above the baseline. Then, it declines and, after six years, turns negative. The response of the output gap mimics that of GDP, but it is a little faster. Potential output slowly increases for the first five years and then returns to the baseline. These results show that growth financed through household debt is not sustainable in the long run.

To conclude, we repeat the inflation forecasting exercise in Table 1.1 using the output gap estimated when omitting all credit indicators. We find that, in this case, the predictive

[6] To calibrate this scenario, we computed the difference between the actual times series of household liabilities between 2003:Q1 and 2011:Q4 and a counterfactual scenario in which household liabilities would have grown linearly during this period (the red line in the upper-left chart of Figure 1.9). Then, we smoothed this difference with a 5-th order degree polynomial and added it to the unconditional forecast of household liabilities (the red line in the upper-right chart in Figure 1.9), which gives us a path for household liabilities (blue line) conditional on which we can obtain forecasts for all the variables in the model.

[7] This is equivalent to computing the effect of a sequence of shocks. Hence, it is estimated the same way we estimated the GIRFs in Section 1.5.

Figure 1.9: *Scenario analysis*

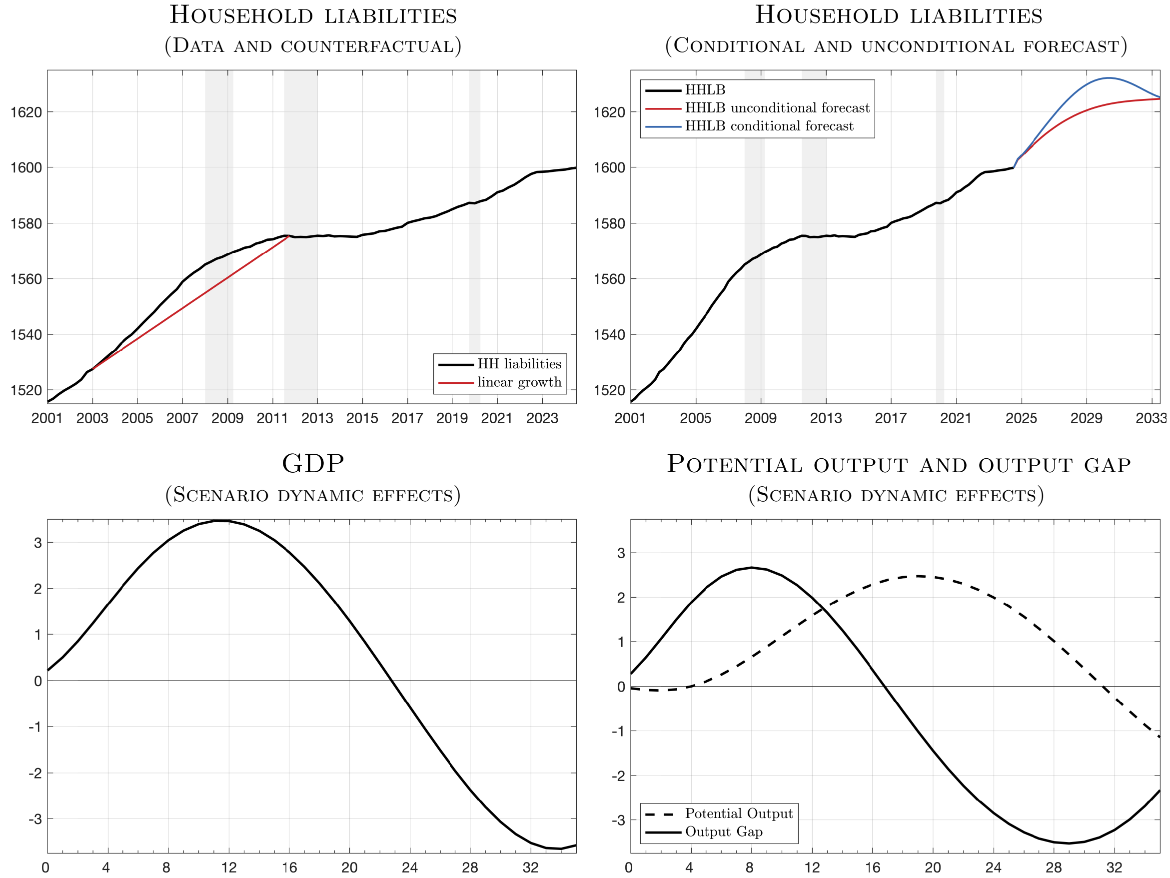

Notes: In the upper-left chart, the black line is the data (in 100×log-levels), and the red line is a linear path starting from the value of household liabilities in 2003:Q1 and ending in 2011:Q4. In the upper-right chart, the black line are the data,the blue line is the scenario we simulate, and the red line is the forecast of household liabilities when no alternative scenario is imposed. In the lower charts, the black solid/dashed lines are the dynamic effects of the simulated scenario.

performance of the output gap is about 5% worse than our benchmark measure. This result supports our claim that including credit variables in the dataset when estimating the output gap is crucial, as the model including credit indicators outperforms the model excluding credit indicators.

1.9 Conclusions

This chapter proposes a new measure of potential output and the output gap for the EA based on letting a large number of macroeconomic and financial indicators speak. To do so, we estimate a large-dimensional non-stationary dynamic factor model, which allows us to capture co-movements across series while incorporating relevant macroeconomic priors, such as the long-run decline in output growth.

Our output gap estimate is in line with those published by the EC and the IMF in most of the sample. However, our estimate diverges significantly after the SDR when our output gap measure suggests that the EA economy was tighter than estimated by the EC and the IMF. This result suggests that the EA has a potential output issue, not a business cycle issue. Hence, if the goal is to achieve better economic conditions in the EA, European countries should implement structural reforms and promote productivity-enhancing investments that have long-run effects. In contrast, policies aiming at stimulating household consumption and residential investments will have only short-term effects at best, as our findings indicate that growth financed through household debt is not sustainable in the long run.

Moreover, although we did not create our output gap measure specifically to signal inflationary pressures, it does provide insights related to inflation dynamics because, on average, the Phillips Curve is satisfied. In particular, we find that core inflation remained below 2% after the GFC, not because there was slack in the economy, but rather because trend inflation decreased by one percentage point—in line with the idea that inflation expectations de-anchored on the downside after the GFC (Ciccarelli and Osbat, 2017; Corsello et al., 2021). Finally, we show that the output gap contributed to at least 30% of the post-pandemic increase in core inflation, thus supporting existing literature that suggests demand forces played a substantial role in the rise of post-pandemic inflation (Ascari et al., 2023; Giannone and Primiceri, 2024; Bergholt et al., 2025).

Chapter 2

Heterogeneous economic growth vulnerability across Euro Area countries under stressed scenarios

2.1 Introduction

Understanding the risks of severe economic downturns–referred to as downside risks to economic growth or growth vulnerability–has become a central concern for policymakers and market participants (see, e.g., Kilian and Manganelli, 2008; Alessi et al., 2014). The potential for sudden, large and unexpected contractions in economic activity poses significant challenges for macro-financial stability. As a consequence of the influential work of Adrian, Boyarchenko, and Giannone (2019), it is popular to quantify downside risks to economic growth with Growth-at-Risk (GaR), which nowadays is part of the toolbox of academics and policy makers (Prasad et al., 2019; Suarez, 2022; Furno and Giannone, 2024).

While a substantial body of research on growth vulnerability focuses on the US, there is growing interest in examining such risks within the Euro Area (EA). Accurately assessing and anticipating growth vulnerability is critical for the timely implementation of both EA-wide and country-specific policies aimed at mitigating the impact of adverse shocks. Given the interconnectedness of EA economies together with the diverse structural conditions across member countries, it is essential to develop models that can capture both global (EA-wide) and country-specific factors influencing growth vulnerability within EA countries.

In this chapter, we analyse economic growth vulnerability across the four largest EA economies–Germany (DE), France (FR), Italy (IT), and Spain (ES).[1] For each country, we model the distribution of GDP growth conditional on both global EA and country-specific macro and financial conditions and compute the corresponding GaRs. By doing so, we are able to evaluate the heterogeneous effects of global and country-specific macro and financial conditions on vulnerable growth across the largest economies in the EA. We then generate scenarios for growth vulnerability when these conditions are under stress to understand how downside risks to GDP growth differ from those observed during "normal" times.

Our methodology relies on three main steps. First, for each country, we compute the GaR following Adrian, Boyarchenko, and Giannone (2019), estimating the growth density after fitting factor-augmented quantile regressions (FA-QRs) separately for each country. The factors used in the FA-QRs, which quantify EA-wide and country-specific macroeconomic and financial

[1]As of 2023, Germany, Spain, France, and Italy account for approximately two-third of overall GDP of the EA and are frequently used as representative countries for economic analysis; see, for example, Angelini et al. (2019).

conditions, are extracted using a multilevel dynamic factor model (ML-DFM) estimated via the EM algorithm (Delle Chiaie et al., 2022; Barigozzi and Luciani, 2024). Specifically, we extract pervasive EA-wide global factors and semi-pervasive country-specific factors from a large dataset of macroeconomic and financial indicators, as provided by Barigozzi, Lissona, and Tonni (2024). This approach allows us to disentangle common dynamics, shared across EA economies, from country-specific macro-financial conditions. We document the presence of macroeconomic and financial factors, which capture comovements across EA countries, serving as proxies for aggregate macro-financial conditions in the EA. Additionally, the inclusion of country-specific factors provides a detailed view of local sectoral dynamics, allowing for a comprehensive analysis of how EA-wide and local macro-financial conditions jointly shape economic growth vulnerability in each country.

Second, González-Rivera, Rodríguez-Caballero, and Ruiz (2024) show that, under stressed conditions, which are critical for policymakers, standard growth vulnerability measures like GaR tend to underestimate downside risks to growth. In the context of Principal Components (PC) factor extraction, they introduce Growth-in-Stress (GiS) as a complementary measure that assesses vulnerability when the underlying factors are jointly stressed using their probability countours. In this chapter, we extend the methodology proposed by González-Rivera et al. (2024) to factors extracted from ML-DFMs using the EM algorithm instead of PC. For each of the four EA economies considered, we construct scenarios to evaluate growth vulnerability under economic stress, generating scenarios for extreme deviations in macroeconomic and financial conditions, both within and across countries and obtain the GiS under these scenarios. Our findings reveal significant heterogeneity across countries, with those more exposed to EA-wide conditions, such as Germany, and those driven by strong country-specific dynamics, such as Spain, exhibiting higher levels of growth vulnerability. This underscores the importance of considering both common and local dynamics in evaluating risks to domestic economic growth.

Moreover, we make a further step to disentangle the drivers of growth vulnerability within each country by exploring alternative stress-testing scenarios. We move beyond joint stress scenarios by separately stressing alternative factors. First, we consider a scenario where only macroeconomic factors are stressed, while financial factors remain at their average levels. This exercise reveals that vulnerability is systematically underestimated when financial conditions are not included in the stress test, highlighting the crucial amplifying role that financial stress plays in driving adverse economic outcomes. Second, we examine the impact of large sectoral shocks, both common and country-specific, to determine whether extreme shocks to individual sector can replicate the large vulnerabilities observed when the economy is jointly stressed. This analysis provides novel evidence on the amplifying role of financial variables in adverse economic conditions and underscores the risks to growth posed by economy-wide stress compared to local, yet very large, sector-specific shocks. Our findings show that large sectoral shocks fail to produce the same levels of vulnerability as those observed under joint stress, reinforcing the idea that growth vulnerability across EA countries is largely shaped by the interaction between both EA-wide and country-specific macroeconomic, and financial conditions.

This chapter is related with previous work on the quantification of growth vulnerability across different dimensions. One of the earliest attempts to measure EA growth vulnerability is Proietti et al. (2017), who construct a monthly density indicator for GDP. Later, Figueres and Jarociński (2020) and Ferrara et al. (2022) employed the GaR framework to model tail risk in the EA, documenting the importance of financial indicators to model downturn risk for GDP growth.[2] Similarly, Szendrei and Varga (2023) employ a frequentist Adaptive LASSO approach to identify key variables driving different parts of the EA growth distribution, emphasizing the significance of financial, particularly bank-related, variables. Conversely, Lhuissier (2022) proposes a regime-switching skew-normal model for the EA growth distribution. Unlike other

[2]Specifically, they consider the Composite Indicator of Systemic Stress (CISS), obtained by non-linear aggregation of individual financial indicators; see Hollo et al. (2012) for a description of CISS.

studies, his findings indicate a limited contribution of financial variables, when included in time-varying probabilities used to anticipate shifts in growth skewness. Overall, a broad literature underscores the joint role of macroeconomic and financial conditions in shaping macroeconomic tail risks, extending beyond economic growth alone. For instance, Botelho et al. (2024) examine tail risk in the EA (and US) labour market, modelling it as a function of both real and financial indicators and emphasizing the role of non-linearities in the transmission of shocks to unemployment. Additionally, Morana (2024) propose constructing composite indicators for the EA that integrate macroeconomic and financial drivers, capturing both short- and long-term fluctuations in these variables.

While substantial research has focused on modelling growth vulnerability for the EA as a whole, EA countries exhibit significant heterogeneity in labour markets, financial structures, and fiscal positions (Gilchrist and Mojon, 2018; Hoffmann et al., 2020). Within EA members states, economic vulnerabilities may differ substantially due to various factors, which may reflect either EA-wide or country-specific macro-financial conditions, leading to heterogeneous effects on downside growth risks across countries; see, for example, Eickmeier (2009). The COVID-19 shock, for instance, despite being a common shock, had asymmetric effects on EA countries in both timing and magnitude—an aspect that would be averaged out when focusing solely on aggregate EA growth. Yet, the analysis of growth vulnerability at the individual country level remains limited.

Our work contributes to this literature along different dimensions. First, we move beyond a standard aggregate approach by modelling economic growth vulnerability within each of the main EA economies as a function of both common and country-specific economic conditions. By doing so, we are able to account for potential cross-country spillovers, as well as local dynamics which would be otherwise neglected in an EA-wide analysis. Second, we explicitly model economic growth vulnerability as a function of macroeconomic and financial conditions, which allows us to assess the relative contribution of each sector to growth risks. We achieve this by leveraging multiple economic sources within our ML-DFM, effectively incorporating all relevant information across sectors and countries. Finally, our stressed scenarios provide valuable insights that extend beyond standard measures of downside GDP risk. Specifically, they highlight the role of financial variables in amplifying economic downturns and the significance of local dynamics in shaping the exposure of each country to macro-financial risks. To the best of our knowledge, we are the first to model downside risks to GDP at the individual EA country level while simultaneously accounting for both EA-wide and country-specific conditions. As far as we are aware, only Busetti et al. (2021) explicitly model the growth distribution for Italy, using expectile regressions based on both domestic and international real and financial indicators. Furthermore, in contrast to the existing literature, we do so by utilizing a novel high-dimensional dataset.

In light of the literature, the framework adopted in this chapter offers a comprehensive approach to understanding growth risks across EA countries, highlighting the need to monitor both EA-wide and local macro-financial conditions. Our results emphasize the systemic nature of growth risks, providing evidence on the pivotal role that the interplay between macroeconomic and financial conditions plays in shaping vulnerabilities across economies. We offer valuable insights for policymakers, emphasizing the importance of coordinated macro-prudential policies, alongside monetary and fiscal tools, tailored to address both common and country-specific vulnerabilities. Such measures are essential to mitigate growth risks effectively and ensure economic stability within the EA.

The rest of the chapter is structured as follows. In Section 3.2 we describe the methodology and estimation strategy. Section 2.3 describes the data used in the analysis. The main results of the chapter appear in Section 2.4, which deals with the empirical estimation of growth vulnerability in each of the four largest EA economies and presents different stressed scenarios. Section 2.5 concludes.

2.2 Methodology

In this section, we describe the methodology used to estimate the conditional distribution of GDP growth in each country, and the corresponding GaR and GiS measures of vulnerability. On top of describing the FA-QR model, we also describe the ML-DFM used to extract the latent factors driving macroeconomic and financial conditions.

2.2.1 The conditional distribution of GDP growth: GaR and GiS

We characterize the distribution of GDP growth conditional on underlying macroeconomic and financial factors under two distinct scenarios: (i) during "normal" times, with the latent factors held at their average levels, and (ii) under stress, when the economic conditions represented by the factors are subject to significant macroeconomic and/or financial pressures.

Conditional distribution in normal times: growth at risk (GaR)

To analyse the relationship between GDP growth and past macroeconomic and financial conditions, we fit a FA-QR model for each country, with the quantiles modelled as functions of a few latent macro/financial factors capturing both EA-wide comovements across countries, as well as domestic dynamics within each country. The four EA countries–Germany (DE), Spain (ES), France (FR), and Italy (IT)–are indexed by $c \in \mathcal{C} := \{\text{DE,ES,FR,IT}\}$. Let $y_t^{(c)}$ denote the quarterly GDP growth rate in period t for country $c \in \mathcal{C}$, and let $\mathbf{F}_t^{(c)} = (\mathbf{f}_t^{(\text{F})\prime}, \mathbf{f}_t^{(\text{M})\prime}, \mathbf{f}_t^{(c,\text{F})\prime}, \mathbf{f}_t^{(c,\text{M})\prime})'$ denote the vector of factors assumed to characterize its distribution. The $r^{(\text{F})}$ factors in $\mathbf{f}_t^{(\text{F})}$ are financial factors common to all four countries, while the $r^{(c,\text{F})}$ factors in $\mathbf{f}_t^{(c,\text{F})}$ are financial factors specific to country c. Similarly, $\mathbf{f}_t^{(\text{M})}$ and $\mathbf{f}_t^{(c,\text{M})}$, with dimensions $r^{(\text{M})}$ and $r^{(c,\text{M})}$, respectively, are common and country-specific macroeconomic factors, respectively. The total number of factors is $r = r^{(\text{F})} + \sum_{c\in\mathcal{C}} r^{(c,\text{F})} + r^{(\text{M})} + \sum_{c\in\mathcal{C}} r^{(c,\text{M})}$. Let the two economic sectors–macroeconomic (M) and financial (F)–be indexed by $s \in \mathcal{S} := \{\text{F, M}\}$. For each country within $\mathcal{C}$, and quantile $\tau = 0.05, 0.10, \ldots, 0.95$, we fit the following FA-QR model:[3]

$$q_\tau(y_{t+1}^{(c)}, |y_t^{(c)}, \mathbf{F}_t^{(c)}) \;=\; \mu^{(c,\tau)} + \phi^{(c,\tau)} y_t^{(c)} + \sum_{s\in\mathcal{S}} \boldsymbol{\beta}^{(c,s,\tau)\prime}\mathbf{f}_t^{(s)} + \sum_{s\in\mathcal{S}} \boldsymbol{\gamma}^{(c,s,\tau)\prime}\mathbf{f}_t^{(c,s)} \tag{2.1}$$

where $q_\tau(y_{t+1}^{(c)}, |y_t^{(c)}, \mathbf{F}_t^{(c)})$ is the one-step-ahead forecast of the $\tau-$quantile of the conditional distribution of GDP growth for country c, while $\mu^{(c,\tau)}$, $\phi^{(c,\tau)}$, $\boldsymbol{\beta}^{(c,s,\tau)} = \left(\beta_1^{(c,s,\tau)}, \ldots, \beta_{r(s)}^{(c,s,\tau)}\right)$ and $\boldsymbol{\gamma}^{(c,s,\tau)} = \left(\gamma_1^{(c,s,\tau)}, \ldots, \gamma_{r(c,s)}^{(c,s,\tau)}\right)$ are parameters to be estimated. Since the factors are unobserved, they are replaced in practice by their estimated counterparts. The model employed to extract the factors and their estimation are treated in detail in Section 2.2.2.

The FA-QR model in (2.1) is a flexible yet parsimonious tool that effectively captures potential non-linear and asymmetric relationships between economic growth and the underlying macroeconomic and financial conditions, with EA-wide economic conditions represented by the common factors and country-specific dynamics captured by the country-level factors. This dual perspective is crucial for evaluating the presence, if any, of heterogeneous responses to common (EA-wide) shocks and their interactions with local macroeconomic and financial conditions.

The parameters of model (2.1) are estimated following the methodology introduced in Koenker and Bassett (1978), using the algorithm of Koenker and d'Orey (1987), with the

[3]Although the analysis in this chapter focus on one-step-ahead growth, it can be easily extended to other multi-period forecast horizons.

corresponding standard errors computed as described in Koenker (2005) assuming i.i.d. errors; see Bai and Ng (2008) for the consistency of the estimated parameters, and Ando and Tsay (2011), and Giglio et al. (2016) for the consistency of the forecasts of the quantiles when the factors are extracted using PC. The goodness of fit of the model is assessed using the R^1 measure described in Koenker and Machado (1999). Specifically, let $\hat{v}_{t+1}^{(c,\tau)} = y_{t+1}^{(c)} - \widehat{\mu}^{(c,\tau)} - \widehat{\phi}^{(c,\tau)} y_t^{(c)} - \sum_{s\in\mathcal{S}} \widehat{\boldsymbol{\beta}}^{(c,s,\tau)} \mathbf{f}_t^{(s)} - \sum_{s\in\mathcal{S}} \widehat{\boldsymbol{\gamma}}^{(c,s,\tau)} \mathbf{f}_t^{(c,s)}$ denote the residuals from model (1) fitted to the τ-quantile of growth in country c. For each quantile and country, we compute $R^1(c,\tau) = 1 - \frac{\sum_{t=2}^{T-h} \hat{v}_t^{(c,\tau)}[\tau\mathbb{I}(\hat{v}_t^{(c,\tau)}\geq 0)+(\tau-1)\mathbb{I}(\hat{v}_t^{(c,\tau)}<0)]}{\sum_{t=2}^{T-h}(y_t^{(c)}-\bar{y}^{(c)})[\tau(\mathbb{I}(y_t^{(c)}\geq\bar{y}^{(c)})+(\tau-1)\mathbb{I}(y_t^{(c)}<\bar{y}^{(c)})]}$, where $\bar{y}^{(c)}$ is the sample mean of y_t for country c and $\mathbb{I}(\cdot)$ is the indicator function, which takes a value of 1 if its argument is true, and 0 otherwise.

After estimating model (1), we follow Adrian et al. (2019) and obtain a smooth estimate of the conditional distribution of growth for each country and period t by fitting the Skewed-t distribution introduced by Azzalini (1985) to the estimated $\tau = 0.25, 0.5, 0.75, 0.95$ quantiles[4]. The estimated conditional distribution of GDP growth for each country is denoted as $\widehat{f}_0(y_{t+1}^{(c)}|, y_t^{(c)}, \mathbf{F}_t^{(c)})$. Finally, we compute the one-step-ahead GaR_t as the 5% quantile of this distribution.

Conditional distribution under stress: growth in stress (GiS)

In contrast to GaR, which assesses growth vulnerability under "normal" conditions–i.e. when the factors are fixed at their average values–GiS evaluates growth vulnerability under stressed conditions by considering factors that deviate significantly from their average value; see González-Rivera et al. (2019) and González-Rivera et al. (2024). Indeed, extreme structural economic conditions tend to exacerbate growth vulnerability, a phenomenon that is likely underestimated by GaR.

In order to estimate the density of growth under stressed factors, we focus on the 5% quantile and find the value of the factors, when constrained at their α-probability contour, that minimize $q_{0.05}(y_{t+1}^{(c)}|y_t^{(c)}, \mathbf{F}_t^{(c)})$ as follows:

$$\min_{\mathbf{F}_t^{(c)}} \quad q_{0.05}(y_{t+1}^{(c)}|y_t^{(c)}, \mathbf{F}_t^{(c)}) \qquad \text{s.t.} \quad g(\mathbf{F}_t^{(c)}, \alpha) = 0 \tag{2.2}$$

where $g(\mathbf{F}_t^{(c)}, \alpha)$ represents the α-contour of the factors for each country, with α being a predetermined probability level that defines the severity of the underlying economic stress. Higher values of α correspond to more extreme underlying stress levels for the macroeconomic and financial conditions represented by factors. Here, we consider $\alpha = 0.95$. Furthermore, note that the joint probability contours $g(\cdot)$ for each country are shaped by both EA-wide and country-specific factors. Therefore, for the same level of underlying stress, the composition of underlying economic factors can be different for each country. These differences depend on the transmission of common shocks to individual countries and the significance of local macro-financial conditions within each economy.

In practice, when the number of factors is larger than 2, as in our case, the minimization problem in (2.2) is solved using the binary mesh algorithm proposed by Flood and Korenko (2015).[5] Finally, the factors that solve the minimization problem in (2.2) are substituted into

[4]The results are nearly identical to those obtained by using additional quantiles as, for example, $\tau = 0.05, 0.10, 0.90$.

[5]This algorithm is widely employed in stress-testing exercises by financial institutions in order to leverage the dependence structure among the underlying factors to create plausible and severe scenarios with minimal parametrization; see on Basel Committee on Banking Supervision (2009). The binary mesh algorithm requires selecting a tuning parameter δ that determines the granularity of the mesh. Higher values of δ increase the number of scenarios considered, at the cost of a greater computational burden.

the estimated FA-QRs for $\tau = 0.25$,0.50,0.75 and 0,95 to obtain the corresponding quantiles to which we fit the Skew-t distribution. This approach yields a conditional density of GDP growth under stressed conditions. For a given probability level α and each country c, we denote this estimated density as $\widehat{f}_\alpha(y_{t+h}^{(c)}|y_t^{(c)}, \mathbf{F}_t^{(c)})$. The one-step-ahead GiS_t is defined as the 5% quantile of this density. The GiS provides a measure of the vulnerability of economic growth to adverse structural economic conditions under different scenarios, serving as a valuable tool for policymakers.

2.2.2 Factor extraction: Multilevel DFM

We fit two separate ML-DFMs to the sets of macroeconomic (M) and financial (F) variables to extract the corresponding latent factors. Within each ML-DFM, we assume that the block structure of the data is known, with the factors being either common to all countries or specific of each country. We test for the presence of common factors overlapping both sets of variables by implementing the bootstrap tests proposed by Gonçalves et al. (2025), who after estimating factors separately in each set of variables, test whether the factors in different sets are correlated. Denote as $\mathbf{x}_t^{(s)} = (\mathbf{x}_t^{(\text{DE},s)\prime}, \mathbf{x}_t^{(\text{ES},s)\prime}, \mathbf{x}_t^{(\text{FR},i)\prime}, \mathbf{x}_t^{(\text{IT},i)\prime})'$ the N_s-dimensional vector of variables for sector $s \in \mathcal{S}$ at time t, such that, for country $c \in \mathcal{C}$, $\mathbf{x}_t^{(c,s)} = (x_{1,t}^{(c,s)}, \dots, x_{n_{c,s},t}^{(c,s)})'$ represents the $N_{c,s}-$dimensional vector of country-sector specific variables. The model for each sector s can be expressed as follows:

$$\mathbf{x}_t^{(s)} = \left[\begin{array}{c|cccc} \mathbf{\Lambda}^{(\text{DE},s)} & \mathbf{\Psi}^{(\text{DE},s)} & \mathbf{0} & \mathbf{0} & \mathbf{0} \\ \mathbf{\Lambda}^{(\text{ES},s)} & \mathbf{0} & \mathbf{\Psi}^{(\text{ES},s)} & \mathbf{0} & \mathbf{0} \\ \mathbf{\Lambda}^{(\text{FR},s)} & \mathbf{0} & \mathbf{0} & \mathbf{\Psi}^{(\text{FR},s)} & \mathbf{0} \\ \mathbf{\Lambda}^{(\text{IT},s)} & \mathbf{0} & \mathbf{0} & \mathbf{0} & \mathbf{\Psi}^{(\text{IT},s)} \end{array}\right] \left[\begin{array}{c} \mathbf{f}_t^{(s)} \\ \hline \mathbf{f}_t^{(\text{DE},s)} \\ \mathbf{f}_t^{(\text{ES},s)} \\ \mathbf{f}_t^{(\text{FR},s)} \\ \mathbf{f}_t^{(\text{IT},s)} \end{array}\right] + \boldsymbol{\xi}_t^{(s)} \tag{2.3}$$

$$\begin{aligned} \mathbf{f}_t^{(s)} &= \mathbf{A}^{(s)}(L)\mathbf{f}_{t-1}^{(s)} + \mathbf{u}_t^{(s)} \\ \mathbf{f}_t^{(c,s)} &= \mathbf{B}^{(c,s)}(L)\mathbf{f}_{t-1}^{(c,s)} + \mathbf{v}_t^{(c,s)} \end{aligned}$$

where the factors are defined as in model (2.1) and $\mathbf{\Lambda}^{(s)} = (\mathbf{\Lambda}^{(\text{DE},s)}, \mathbf{\Lambda}^{(\text{ES},s)}, \mathbf{\Lambda}^{(\text{FR},s)}, \mathbf{\Lambda}^{(\text{IT},s)})$ is the $N^{(s)} \times r^{(s)}$ matrix of loadings for sector s common to all countries, with $\mathbf{\Lambda}^{(c,s)} = (\boldsymbol{\lambda}_1^{(c,s)\prime}, \dots, \boldsymbol{\lambda}_{n_c}^{(c,s)\prime})'$ being the $N^{(c,s)} \times r^{(c,s)}$ matrix of loadings for country c. Similarly, $\mathbf{f}_t^{(c,s)}$ is the $r^{(c,s)}-$dimensional vector of loadings corresponding to the country-specific factors. Finally, $\boldsymbol{\xi}_t^{(s)} = (\boldsymbol{\xi}_t^{(\text{DE},s)\prime}, \boldsymbol{\xi}_t^{(\text{ES},s)\prime}, \boldsymbol{\xi}_t^{(\text{FR},s)\prime}, \boldsymbol{\xi}_t^{(\text{IT},s)\prime})'$, is the $N^{(s)}$-dimensional vector of white noise idiosyncratic components, with $\boldsymbol{\xi}_t^{(c,s)} = (\xi_{1,t}^{(c,s)}, \dots, \xi_{n_{c,s},t}^{(c,s)})'$; see, among others, Breitung and Eickmeier (2016), Choi et al. (2018), Andreou et al. (2019), Freyaldenhoven (2022) and Gonçalves et al. (2025) for the characterization of the ML-DFM. The identification of factor and loadings requires that, within each block of variables, the factors should be orthonormal with the corresponding loadings being orthogonal; see Breitung and Eickmeier (2016).[6] Furthermore, we assume that the dynamic dependence of the factors is described by a VAR(1) model with $\mathbf{A}^{(s)}$ and $\mathbf{B}^{(c,s)}$ being $r^{(s)} \times r^{(s)}$ and $r^{(c,s)} \times r^{(c,s)}$, respectively. The $r^{(s)}$- and $r^{(c,s)}$-dimensional vectors $\mathbf{u}_t^{(s)}$ and $\mathbf{v}_t^{(c,s)}$ are white noise residuals; see Appendix 2.A for the complete state-space representation of the ML-DFM in (2.3).

Consistent with González-Rivera et al. (2024), we set $\delta = 8$, corresponding to $\approx$3000 scenarios. Results are unchanged with higher mesh levels (e.g. $\delta = 10$, with ≈ 5500 scenarios).

[6] Note that Freyaldenhoven (2022) also requires orthogonality between blocks.

The number of factors within each sector and country is determined by examining the corresponding scree plots, as well as the covariance matrix of estimated idiosyncratic components, to ensure that no relevant comovements are left unexplained by the model.[7]

The ML-DFM in (2.3) is finally estimated using the Expectation-Maximization (EM) algorithm, as outlined by Delle Chiaie et al. (2022).[8] The EM algorithm consists of two iterative steps that are repeated until convergence. First, in the Expectation step (E-step), the latent factors are estimated using the Kalman Smoother, based on an initial set of consistent parameter estimates. These estimated factors are then used in the Maximization step (M-step), where the model parameters are updated via linear projections, accounting for the uncertainty in the factor estimation (Doz et al., 2012). Convergence is assessed based on the likelihood derived from the Kalman filter in the E-step. Upon convergence, the algorithm provides quasi-maximum likelihood estimates for all model parameters. A final application of the Kalman Smoother yields consistent estimates of the latent factors; see Barigozzi and Luciani (2024) for a detailed discussion on the EM algorithm and its asymptotic properties.

Initial estimates of all the parameters in the ML-DFM are obtained after estimating the loadings of all factors (pervasive and country-specific) via a top-down principal component (PC) procedure, which also provides initial estimates of the factors; see Aastveit et al. (2016). Subsequently, these estimated factors are used to obtain initial estimates of the autoregressive parameters through separate least squares regressions for each factor; see Appendix 2.A for a comprehensive explanation of the algorithm, its initialization, and comparisons with alternative estimation methods.

Finally, the Kalman Smoother also generates estimates of the Mean Squared Errors (MSEs) associated with the estimated factors. The MSEs of the factors delibered by the Kalman Smoother are obtained by assuming that the model specification is correct and that the estimated parameters coincide with the true model parameters. In order to incorporate parameter uncertainty into the MSE of the factors, we extend the subsampling procedure proposed by Maldonado and Ruiz (2021) in the context of PC factor extraction, to the ML-DFM estimated using the EM algorithm; see Appendix 2.A. We obtain the confidence regions for factors (and loadings) as proposed by Barigozzi and Luciani (2022) under the assumption of cross-sectionally uncorrelated idiosyncratic components; see Appendix 2.A for a complete description of the procedure. Using these MSEs and assuming further normality, one can obtain the probabilistic contours of the factors needed to stress them. Note that the factors that enter into the FA-QR are both macroeconomic and financial factors. Even though these factors are extracted separately, they should be stressed based on their joint distribution. Consequently, when finding the joint contours of the factors, we assume that macroeconomic and financial factors are mutually independent; recall that their independence can be tested using the bootstrap procedure proposed by Gonçalves et al. (2025).

2.3 Data

For each country, quarter-on-quarter GDP growth rates are observed quarterly from 2000Q2 to 2024Q3. The factors used to explain the one-step-ahead quantiles of the distribution of growth are extracted from the macroeconomic and financial variables contained in the EA-MD-

[7]Several procedures to determine the number of factors in ML-DFMs have been proposed in the literature; see, for example, Freyaldenhoven (2022) and Choi et al. (2023).

[8]Alternative estimation strategies include, among others, sequential least squares (Rodríguez-Caballero and Caporin, 2019) and sequential principal component approaches (Wang, 2010); see Breitung and Eickmeier (2016) for a review of alternative estimation strategies.

QD database, as described by Barigozzi et al. (2024).[9] Missing values due to ragged edges at the beginning/end of the sample are imputed using the EM algorithm procedure outlined by McCracken and Ng (2020). All variables are transformed so to achieve stationarity. In order to net out extreme observations, particularly due to the COVID-19 pandemic, outliers, which are defined as observations that deviate from the sample median by more than ten interquartile ranges, are replaced with a local median, computed using the nearest neighbourhood of 10 observations; see McCracken and Ng (2016, 2020). A complete description of the variables in the data base together with their corresponding transformations is reported in Appendix 4.A. All series are finally demeaned and standardized. For each country, the macroeconomic and financial series used to extract the factors, alongside GDP growth, are plotted in Figure 2.1.

We estimate the unconditional distribution of GDP growth for each country by fitting a quantile regression with just a constant term, for $\tau = 0.25, 0.50, 0.75$ and 0.95. Then, the estimated quantiles are used to fit the Skew-t distribution as described in Section 3.2. Figure 2.2, which plots the estimated unconditional density for each country, shows that the four countries considered differ not only in terms of their means, but also across the entire GDP growth distribution. We can observe that, although the average growth is larger in Spain, it also has the most skewed distribution to the left. The average growths are similar in Germany and France. Furthermore, both have approximately symmetric unconditional distributions. Finally, the average growth in Italy is smaller with an approximately symmetric distribution. The unconditional densities in all countries but France seem to have heavy tails; see also Table 2.1 that reports the parameters characterizing the estimated unconditional Skewed-t distributions. Specifically, Germany and Italy exhibit minimal skewness, as indicated by the parameter λ, with Italy showing the lowest mean GDP growth among the countries analysed. Despite this, both countries display the largest concentration of values in the tails, with their Skew-t distributions characterized by $\nu = 2$ degrees of freedom. In contrast, a different pattern emerges for France and Spain, particularly for the latter, which shows a notable degree of left skewness. Both countries also exhibit the highest average GDP growth, with France displaying the largest value of ν, which suggests a relatively lower frequency of observations in the tails. Therefore, we align with the vast literature supporting the presence of heterogeneity between EA countries across different dimensions; see, for example, Barigozzi et al. (2014), Gilchrist and Mojon (2018), Hoffmann et al. (2020), and Azqueta-Gavaldón et al. (2023).

TABLE 2.1: *Unconditional Distribution of GDP growth: Estimated parameters of Skewed-t densities.*

Country	μ	σ^2	λ	ν
DE	0.32	0.50	0.02	2
ES	1.05	0.63	-1.88	3
FR	0.51	0.39	-0.55	4
IT	0.14	0.43	-0.01	2

The table reports, for each country, the four parameters characterizing the Skew-t distributions: location (μ), scale (σ^2), skewness (λ) and shape (ν).

2.4 Estimating growth vulnerability in EA countries

In this section, after extracting the factors from the ML-DFM, we fit FA-QRs to estimate the quantiles of economic growth in each country. Finally, different scenarios of the corresponding

[9]Series are observed at the monthly level and aggregated at the quarterly level by simple quarterly averages.

Figure 2.1: *Quarterly GDP growth, and macroeconomic and financial series.*

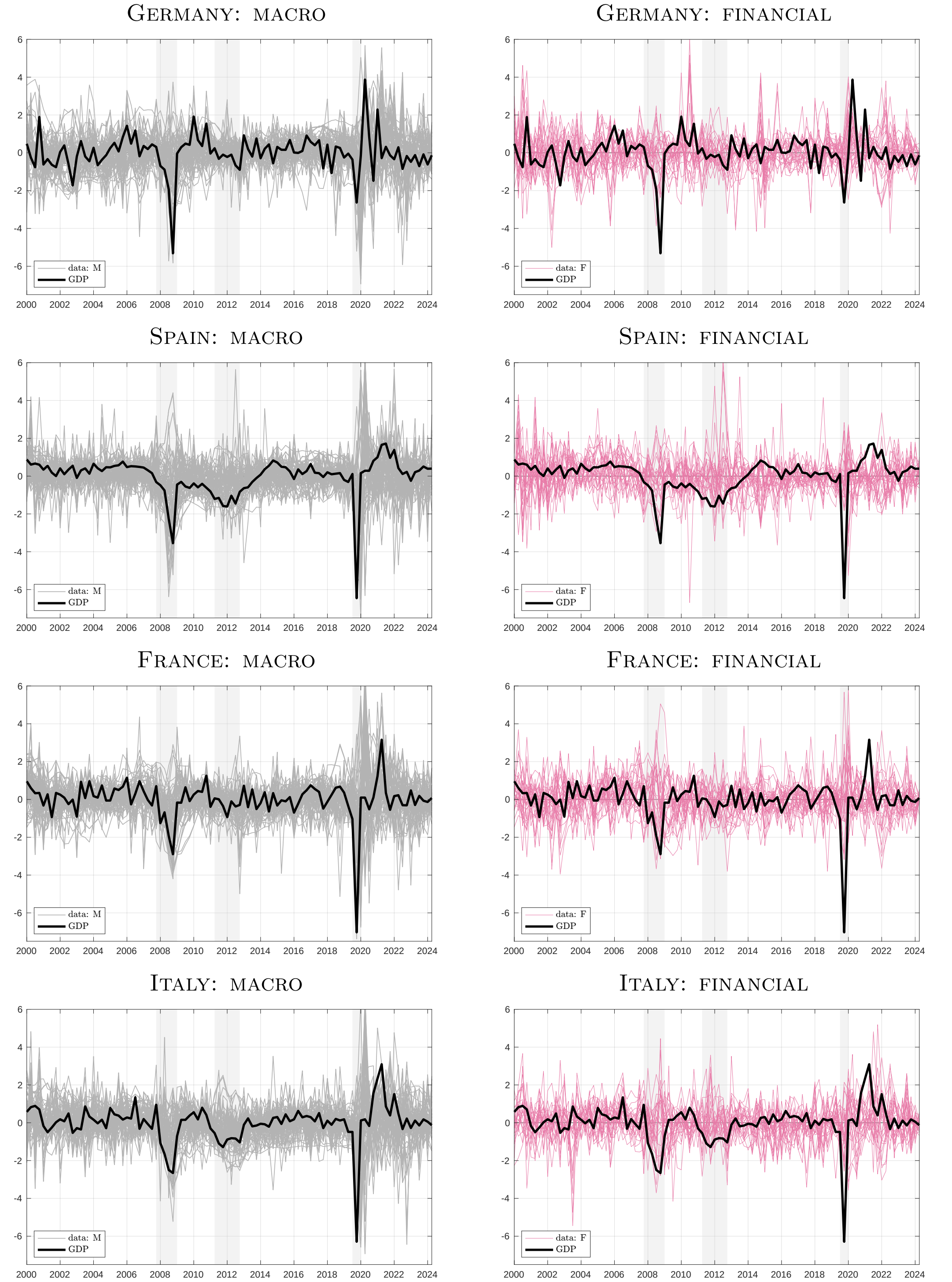

For each country, the figure plots GDP growth (black bold line) and macroeconomic (left panels) and financial (right panels) series observed quarterly from 2000Q2 to 2024Q3. Data are demeaned, standardized and cleaned for outliers, which explains the small drops in GDP growth during the Covid period.

conditional densities are obtained after stressing the factors.

Figure 2.2: *Unconditional distribution of GDP growth in each country.*

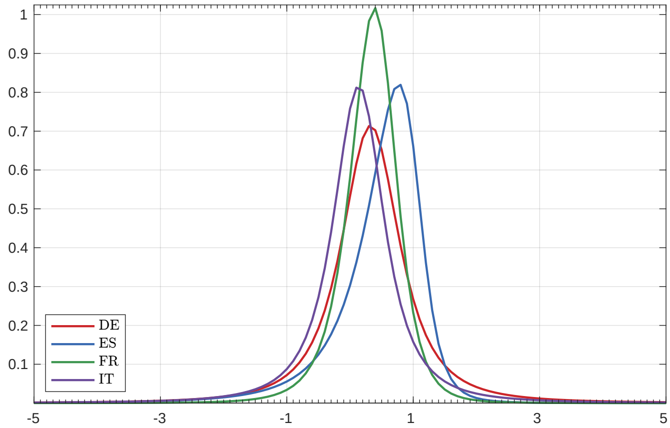

2.4.1 Extracting underlying factors

The ML-DFM in (2.3) is fitted separately to the macroeconomic and financial sets of variables to extract EA-wide and country-specific macroeconomic and financial factors, respectively. This modelling choice is backed by the bootstrap test of Gonçalves et al. (2025), which indicates the absence of a common factor across the two datasets.[10] After a preliminary analysis of the scree plots and the properties of the covariance matrices of the idiosyncratic noises, we determine for each data set one global factor ($r^{(\mathrm{F})} = r^{(\mathrm{M})} = 1$). The number of country-specific macroeconomic factors is two per country($r^{(c,\mathrm{M})} = 2\ \forall c \in \mathcal{C}$), while the number of country-specific financial factors is one per country ($r^{(c,\mathrm{F})} = 1\ \forall c \in \mathcal{C}$). Consequently, the total number of factors is $r = 14$ with 9 macroeconomic factors and 5 financial factors; see Appendix 2.A for a complete discussion of the model specification.

The factors are extracted using the EM algorithm as outlined in Section 2.2.2. Figure 2.3 plots the estimated global and country-specific macroeconomic and financial factors together with their corresponding 75% and 90% confidence bounds obtained from the Kalman Smoother. The first two panels plot the global factors, which are crucial for understanding the interdependence among countries. We can observe that the global macroeconomic factor evolves smoothly with big impacts of the global financial crisis and the COVID-19 pandemic, while the dynamic evolution of the global financial factor is more erratic. The remaining panels plot the country-specific macroeconomic and financial factors. These factors allow for the assessment of the relative position of each country in comparison to the aggregate EA-wide stance. The first country-specific macroeconomic factor is rather strong and shows the different patterns of the global crisis in each country. The second macroeconomic factor is rather erratic in Germany and Italy, while it jumps during the global financial crisis and the COVID19 pandemic in France and Spain. The magnitude of these factors is comparable to that of the global macroeconomic factor. It is remarkable the large uncertainty associated to the second macroeconomic factor, related to prices, in France and Spain. Finally, the local financial factors, which are comparable in magnitude to the global financial factor, are also rather erratic without showing any remarkable pattern.

The loadings corresponding to the estimated factors are plotted in Figure 2.4. Consider first the results corresponding to the loadings of the macroeconomic factors. Note that the global factors loads on all variables across all countries but the variables corresponding to Confidence Indexes (C), some labour variables (Real Labour Productivity, Wages and Salaries, and Employer's Social Contribution, denote these variables as L_1), and all price variables (P). Remarkably, the first country specific macroeconomic factor loads in the variables in C and L_1. Furthermore, the second country-specific factor loads in all P variables. Therefore, while

[10]We run the test with $B = 10000$ bootstrap replications, with a resulting p-value of 2×10^{-4}.

FIGURE 2.3: *Global and country-specific factors.*

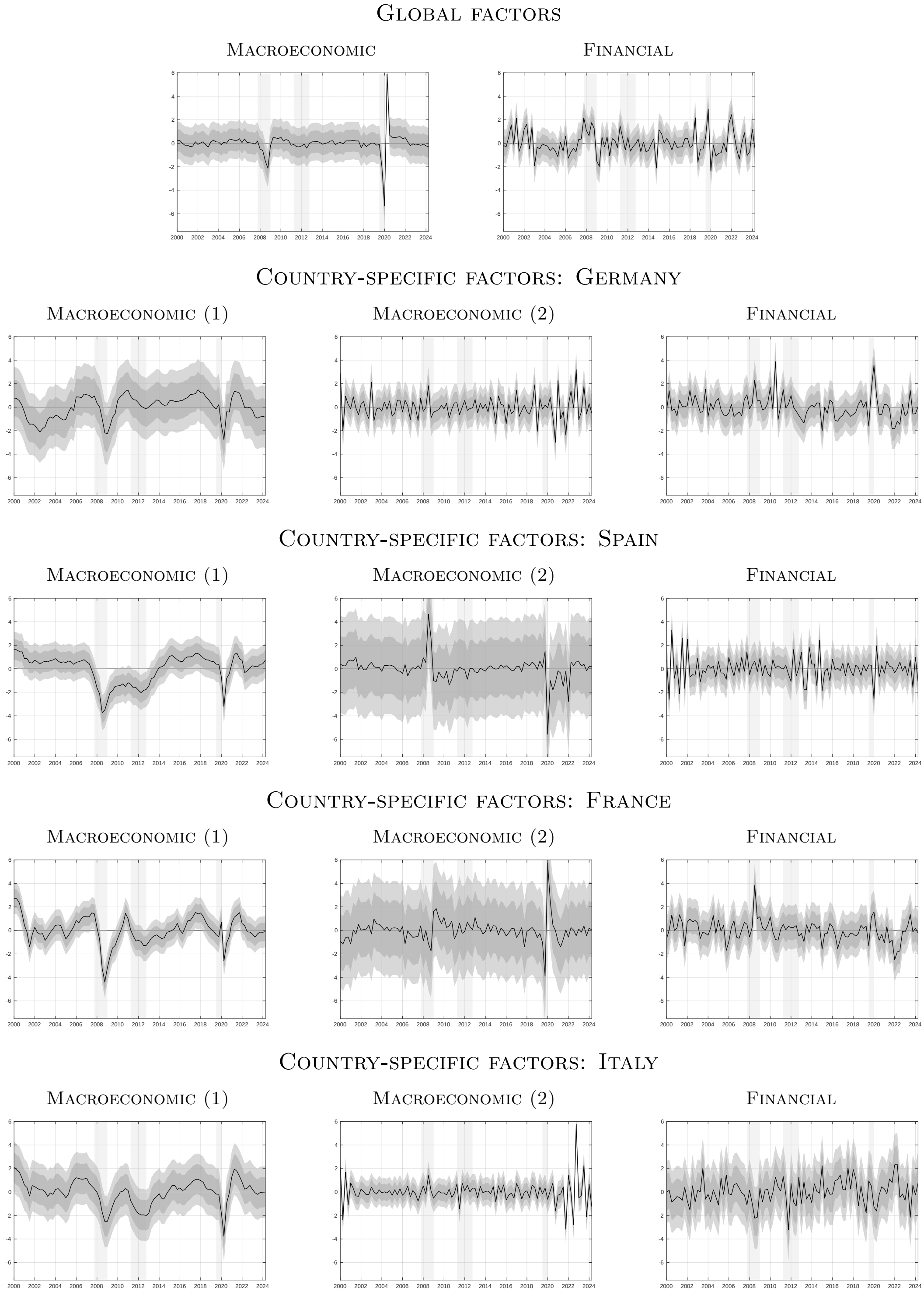

The figure plots the global and country-specific factors for each country (black solid lines), along with their 75% and 95% confidence bands (gray shaded areas).

the factor underlying Industrial Production (IP), National Accounts (NA), Others (O) and the labour variables that are not in L_1 (denote these variables as L_2) is truly common across countries, the two factors underlying prices and confidence indexes, respectively, are country-specific. Furthermore, we can observe that the loadings of the global factor are positive for all countries and variables in IP, NA, O, and L_2 variables but for some IP variables. This last group of IP variables have negative weights in all countries but in Germany, in which they have zero weights. These results reinforce the presence of strong comovements across countries within the macroeconomic sector, aligning with the literature, which highlights the existence of international business cycles (Kose et al., 2003; Rünstler and Vlekke, 2018; Oman, 2019). Looking at the loadings of the first country-specific macroeconomic factor, linked to confidence indexes and productivity, we can observe that they are positive for the first group of variables while they are negative for the second. This second factor highlights the heterogeneity among countries linked to confidence and productivity, highlighting the impact of country-specific economic conditions (Rünstler and Vlekke, 2018; Barigozzi et al., 2024). Finally, the second country-specific macroeconomic factor loads negatively in prices in Germany and Italy. However, the loadings of the price factor are close to zero in France and very mild in Spain. Once more, we observe an strong heterogeneity between countries with respect to the price factor.

FIGURE 2.4: *Global and country-specific loadings.*

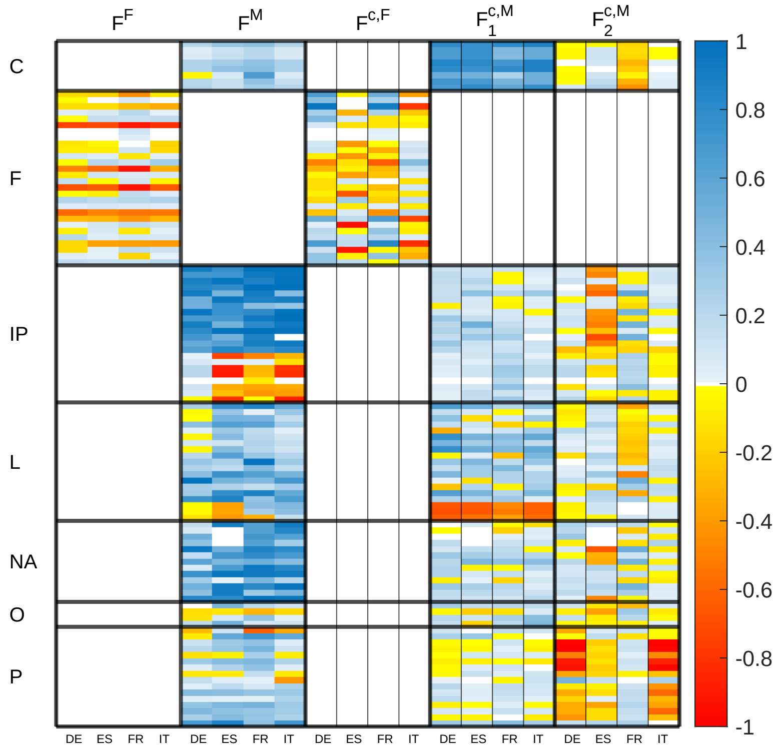

The heatmap shows the magnitude of the estimated loadings of the global and country-specific factors for each country for financial (F) and macroeconomic variables, the latter grouped as: Confidence indices (C), Industrial Production (IP), Labour Market (L), National Accounts (NA), Others (O) and Prices (P). Bold vertical lines divide factors while thin lines divide countries within country-specific factors. By construction, the global financial and macroeconomic factors load on the sectoral variables across all countries, hence the absence of thin vertical separators.

Moving to the loadings of the financial factors, we can observe that the global factor loads uniformly in all countries with negative weights which are stronger on the stock market, while positive ones being mostly concentrated on long-term interest rates and exchange rates. However, the country-specific financial factors load on different variables in different countries.

Together, the common and country-specific factors offer a parsimonious yet comprehensive representation of the underlying macroeconomic and financial conditions in each country.

2.4.2 GiS and GaR across Euro Area countries

In this section, we assess the power of global EA-wide and country-specific factors to predict the quantiles of economic growth in each country, and, consequently, its economic vulnerability. We also investigate whether their impact varies across EA countries, and estimate growth vulnerability not only in "normal" times but also when the factors are representative of a "stressed" economy.

Heterogeneity of the conditional growth distribution in each economy can arise either from the different impact of global EA-wide shocks affecting all countries or from the impact of country-specific macroeconomic and financial factors, which account for differences in sectoral behaviour across countries. The interplay between global and country-specific factors ultimately determines their overall impact on the distribution of economic growth and, consequently, on its vulnerability, measured by a extreme left quantile of this distribution.

FIGURE 2.5: *Estimated parameters of factor-augmented quantile regressions.*

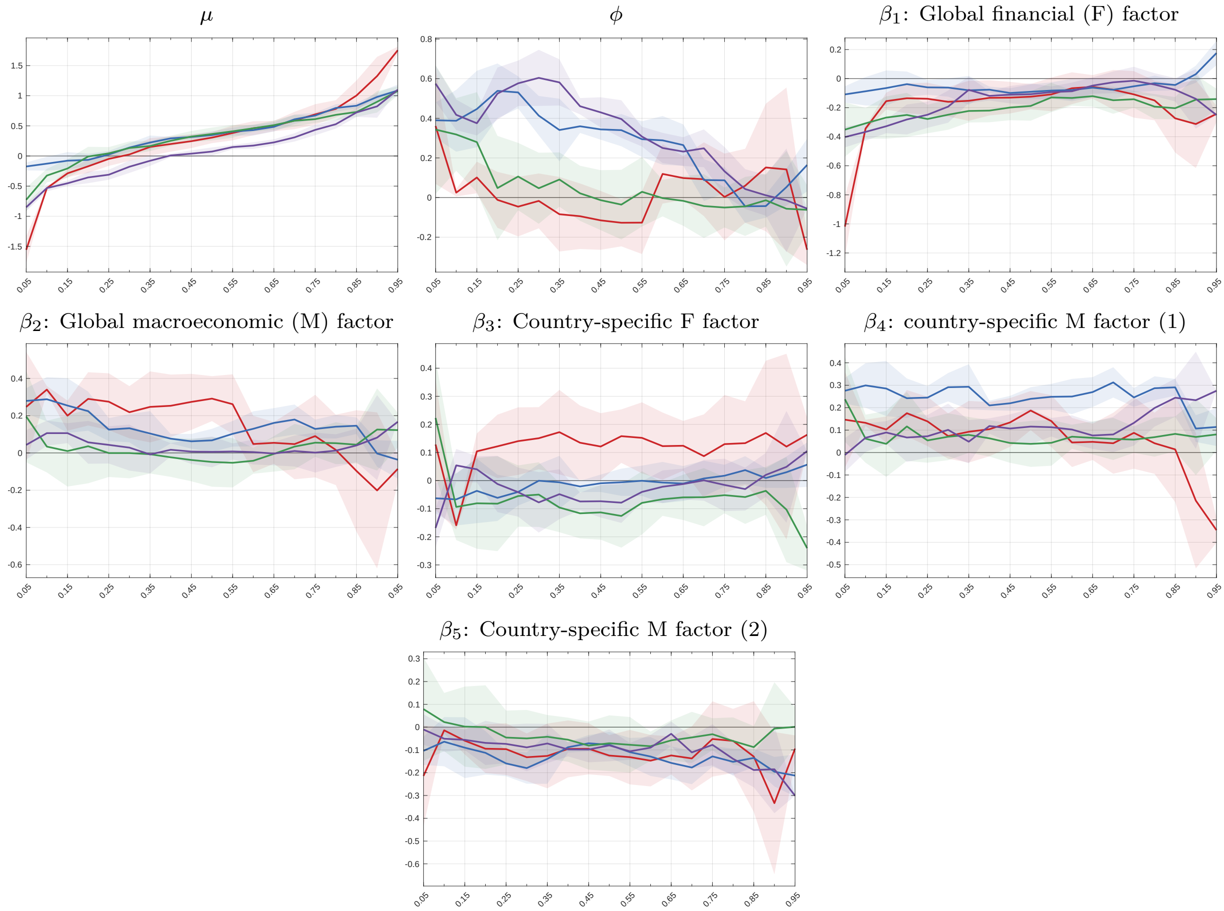

The figure plots the estimated coefficients of the FA-QRs at each quantile τ, from $\tau = 0.05$ to $\tau = 0.95$, with steps of 0.05, for each country: Germany (red solid lines), France (green solid lines), Spain (blue solid lines) and Italy (purple solid lines). Shades areas represent 95% confidence bounds with the same colours for each country.

For each country, Figure 2.5 plots the estimated parameters of the FA-QR models in (2.1) together with their 95% confidence bounds as a function of the quantile of growth for $\tau = 0.05$ to 0.95 with steps of 0.05. The first conclusion from Figure 2.5 is that, regardless of the particular country considered, the estimated factors play a significant role in shaping the distribution of GDP growth. This effect is stronger in the tails, particularly at the left tail. Second, it is remarkable the large and evident heterogeneity of conditional growth in the four economies analysed. Look first at the constant of the FA-QRs, μ. They are all similar at the median, but for Italy, which has a clearly smaller parameter μ. It is also remarkable that μ is clearly larger for Germany when looking at the right quantiles of the distribution of growth, implying a larger growth in expansions than that observed in any other economy. Also, there is a large heterogeneity in the level of growth in the left 0.05 quantile. The heterogeneity between the growth distribution in the four economies considered is even larger when looking at the dependence of this distribution with respect to past growth, measured by the parameter ϕ.

This parameter is hardly significant for the two largest economies, Germany and France, in which we only observe certain significant dependence of the extreme left quantiles. However, the conditional distribution of growth in Italy and Spain is clearly positively influenced by past growth, with this dependence decreasing as the quantile increases. For these two latter economies, past growth is more relevant in recessions than in expansions.

Finally, even more interesting is the heterogeneity observed in the dependence of growth with respect to the underlying macroeconomic and financial factors. Regardless of the economy, the global financial factor, $f_t^{(F)}$, is significant and negative. However, its influence is very strong in Germany and weak in Spain. The effect of the global macroeconomic factor is smaller in Italy and France and stronger in Germany. With respect to the country-specific factors, which represent different underlying mechanisms across countries, we can observe a very strong first macroeconomic factor, linked to confidence, in Spain while the country-specific financial factor is strong in France.

To have a closer look at the impact of the factors on growth, Table 2.2 reports the estimated parameters of the FA-QRs for some selected quantiles, in particular, the 5%, 50% and 95% quantiles in each country, together with the corresponding p-values and R^1 coefficients. Given that one of the main interests of estimating the conditional density of growth is measuring vulnerability, we focus on the results for the 5% quantile. The financial factors are not relevant in Spain, with the country-specific factor not being even significant to explain the 5% quantile of growth. However, the macroeconomic factors are very relevant in Spain; see that the R^1 coefficient is 0.40. However, in Germany France and Italy, the global macroeconomic factor is not significant while the global financial factor is very strong. These findings align with the literature, which highlights the interplay between local macro-financial conditions and EA-wide factors in shaping heterogeneous responses across countries; see Cavallo and Ribba (2015) and Rathke et al. (2022).

TABLE 2.2: *Estimated parameters of factor-augmented quantile regressions.*

	Germany			Spain			France			Italy		
Coefficients	$\tau = .05$	$\tau = .50$	$\tau = .95$	$\tau = .05$	$\tau = .50$	$\tau = .95$	$\tau = .05$	$\tau = .50$	$\tau = .95$	$\tau = .05$	$\tau = .50$	$\tau = .95$
μ	-1.55	0.30	1.76	-0.17	0.35	1.09	-0.72	0.37	1.08	-0.85	0.07	1.10
	(0.00)	(0.00)	(0.00)	(0.00)	(0.00)	(0.00)	(0.00)	(0.00)	(0.00)	(0.00)	(0.00)	(0.00)
ϕ	0.36	-0.12	-0.26	0.39	0.34	0.16	0.34	-0.04	0.06	0.58	0.40	-0.06
	(0.01)	(0.03)	(0.04)	(0.00)	(0.00)	(0.01)	(0.01)	(0.44)	(0.35)	(0.00)	(0.00)	(0.26)
$\beta^{(F)}$	-1.01	-0.13	-0.24	-0.11	-0.10	0.18	-0.35	-0.19	-0.14	-0.40	-0.11	-0.25
	(0.00)	(0.01)	(0.02)	(0.01)	(0.02)	(0.00)	(0.00)	(0.00)	(0.01)	(0.00)	(0.01)	(0.00)
$\beta^{(M)}$	0.25	0.31	-0.09	0.28	0.07	-0.04	0.20	-0.05	0.12	0.04	0.06	0.17
	(0.09)	(0.00)	(0.22)	(0.00)	(0.38)	(0.11)	(0.10)	(0.24)	(0.08)	(0.26)	(0.42)	(0.01)
$\beta^{(F,c)}$	0.13	0.15	0.16	-0.06	-0.01	0.06	0.22	-0.13	-0.24	-0.17	-0.08	0.11
	(0.27)	(0.03)	(0.09)	(0.07)	(0.00)	(0.10)	(0.04)	(0.01)	(0.00)	(0.01)	(0.05)	(0.02)
$\beta_1^{(M,c)}$	0.15	0.21	-0.35	0.28	0.24	0.11	0.24	0.04	0.08	-0.01	0.12	0.28
	(0.11)	(0.00)	(0.00)	(0.00)	(0.00)	(0.00)	(0.01)	(0.27)	(0.00)	(0.40)	(0.01)	(0.07)
$\beta_2^{(M,c)}$	-0.21	-0.13	-0.10	-0.10	-0.07	-0.21	0.08	-0.07	-0.01	-0.01	-0.08	-0.30
	(0.03)	(0.01)	(0.20)	(0.02)	(0.00)	(0.00)	(0.26)	(0.11)	(0.41)	(0.45)	(0.03)	(0.00)
R^1	0.20	0.06	0.28	0.40	0.35	0.22	0.24	0.08	0.17	0.29	0.14	0.22

The table reports the estimated parameters from the quantile regression together with their p-values in parenthesis, for the quantiles $\tau = .05$ and $\tau = .95$, along with the median ($\tau = .50$), for each country. For each quantile, the table also reports the R^1 of the regression.

All in all, the estimated parameters reported in Table 2.2 show that the role of the common and country-specific macroeconomic and financial factors is rather different in the four largest economies of the EA considered. Overall, the global financial factor plays a pivotal role for all countries, while the global macroeconomic factors seems to be less relevant in light of the inclusion of local macroeconomic conditions. At the country-level, on the contrary, local macroeconomic conditions are important for all countries, while country-specific financial conditions prove to be less relevant.

Based on the estimated parameters of the FA-QR models reported in Table 2.2, we estimate the conditional growth density in each country under two different scenarios. The densities are first estimated as in Adrian et al. (2019), when the factors are fixed at their conditional mean, i.e. under the "business as usual" scenario. Alternatively, the conditional growth densities are obtained as in González-Rivera et al. (2024), when the factors are stressed at their 95th percentile level to minimize the 5% quantile of growth. Figure 2.6 plots the conditional densities estimated under normal conditions (blue areas) and under stress (red areas). First, comparing the conditional densities obtained under the "business as usual" scenario with the unconditional densities plotted in Figure 2.2, we can observe that, regardless of the particular country considered, the underlying factors explain movements not only of the mean and variance of the growth distribution but also its asymmetries, which are stronger in periods of economic crisis. Second, compared to normal times, the stressed densities exhibit two key characteristics: (i) they peak at lower levels of GDP growth and (ii) they show an increased skewness toward the right tail of the distribution. This pattern is consistent across all countries, although it appears to be more pronounced in Germany and Spain, particularly during periods of economic crisis, such as the Great Recession and the Covid-19 pandemic. It is also remarkable that, while the effect of stressing the underlying economic factors on the growth densities of France, Italy and Germany is rather marginal, the stressed growth densities corresponding to Spain are strongly different from those obtained under the "business as usual" scenario, showing the larger vulnerability of the Spanish economy.

FIGURE 2.6: *Smoothed skew-t densities.*

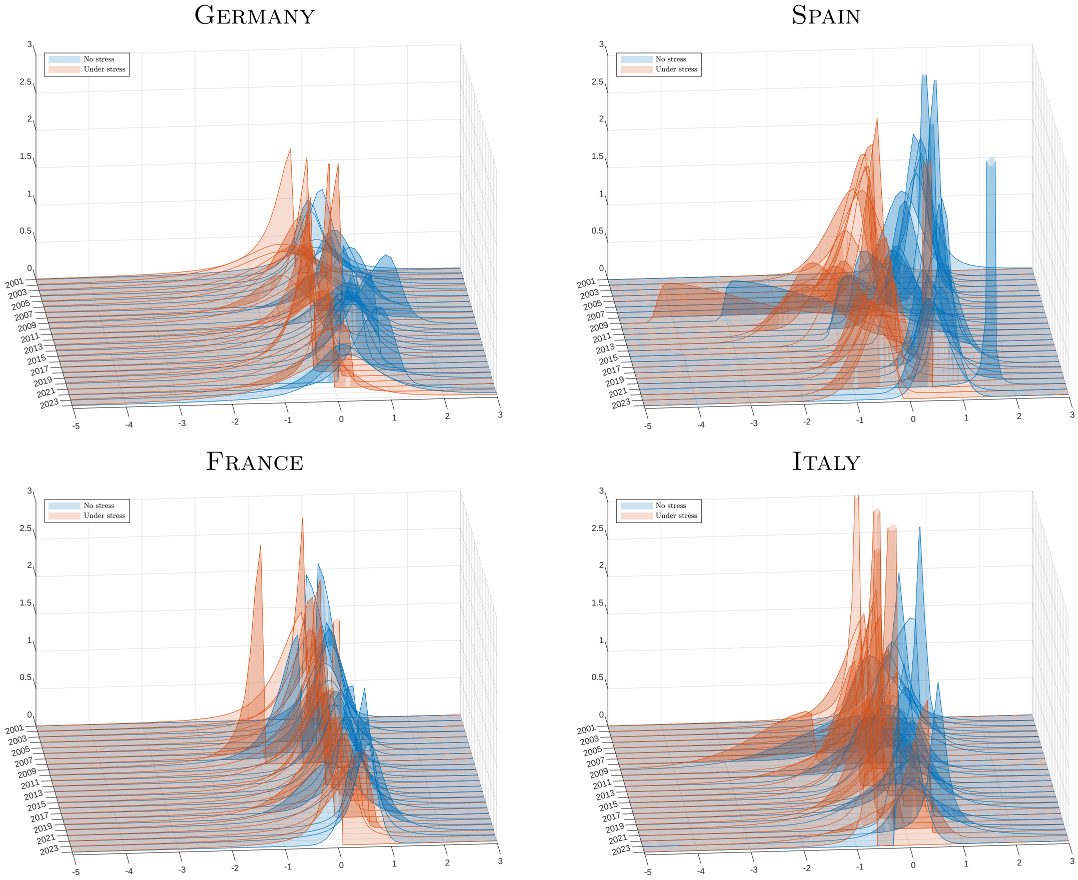

The figure plots, for each country, the smoothed Skew-t conditional densities, both without stress, i.e. when factors are fixed at their conditional mean (blue areas) and under stress, i.e. when the factors are jointly stressed at their 95% level (red areas). Each area correspond to one time period (bottom-left axis), covering the last quarter of each year, starting from 2001Q1.

Finally, we analyse the impact of the factors on both the GaR and the GiS of each country, defined as the 5th percentile of the corresponding GDP growth distribution obtanied under "business-as-usual" and stressed scenarios and computed as described in Section 2.4.2. Figure 2.7 plots the (observed) GDP growth in each country, along with the corresponding GaR and GiS. Across all countries, stressed macroeconomic and financial conditions–both at the EA-wide and local levels–result in significantly higher growth vulnerability compared to the GaR measure. Specifically, under stressed conditions, the 5th percentile of GDP growth is, on average, between ≈3 percentage points lower for Germany and 1.1 percentage points lower for Italy, relative to the corresponding percentile under the "business-as-usual" scenario.

FIGURE 2.7: *Estimated GaR and GiS*

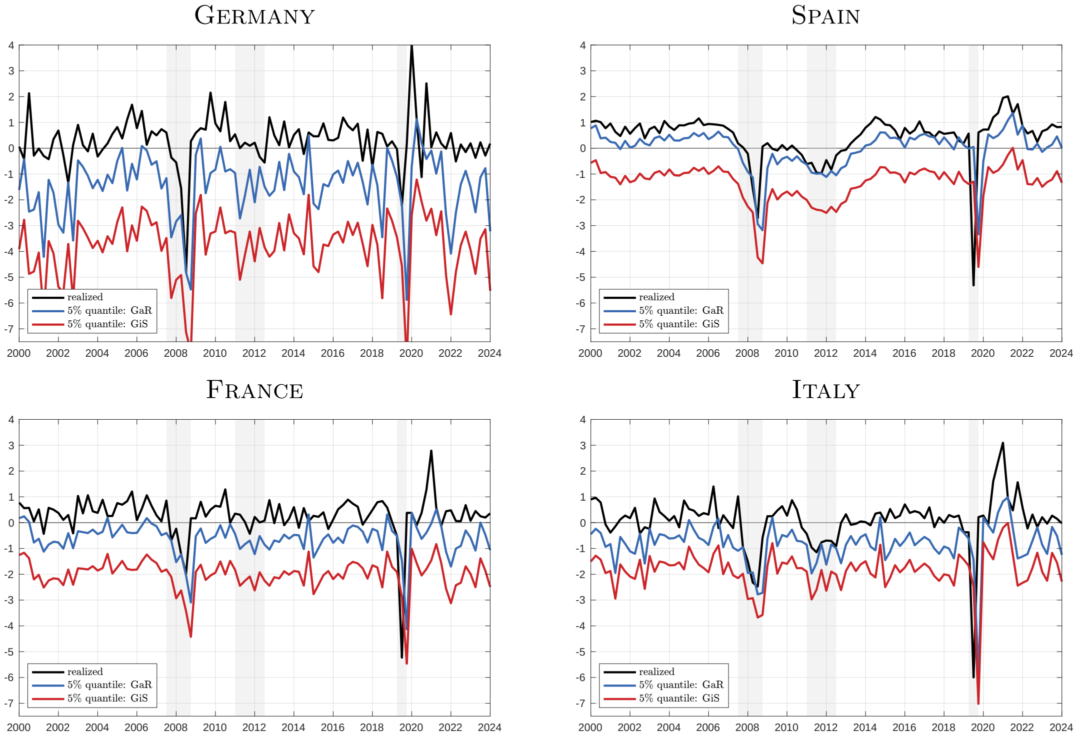

The figure plots observed GDP growth (black solid line), together with the estimated 5% GaR (red solid line) and the 5% GiS (blue solid line) when the underlying factors are jointly stressed at their 95% probability level.

The findings highlight the significance of macroeconomic and financial conditions, both at the EA-wide and country-specific levels, in shaping the distribution of GDP growth, particularly at the tails.[11] Moreover, the effects of common and country-specific economic conditions differ markedly across countries. For instance, some countries, such as Spain, are heavily influenced by local conditions, while others, particularly Italy, are predominantly impacted by EA-wide factors. These findings align with the literature, which highlights the interplay between local macro-financial conditions and EA-wide factors in shaping heterogeneous responses across countries; see Cavallo and Ribba (2015) and Rathke et al. (2022).

Note that, despite the compelling evidence of cross-country heterogeneity in the impact of underlying economic factors on the distribution of growth, we are left with the question on the nature of the underlying sources of this heterogeneity. It is unclear how "stressed" economic conditions differ across countries and whether their effects can be driven by a small subset of factors being under stress, or whether stressing all factors is essential to the results observed thus far. Answering this important question will be the objective of the next subsection.

[11] While in this chapter we focus on vulnerable growth, the results from Table 2.2 suggest that similar patterns emerge during periods of economic prosperity, when GDP growth is at the upper 95th percentile.

2.4.3 The role of macroeconomic and financial conditions in the Euro Area

In this subsection, we delve deeper into the nature of the shocks underlying the distribution of economic growth by exploring two key questions. First, we investigate whether stressed financial conditions, in addition to macroeconomic ones, are relevant for explaining economic growth vulnerability. Second, we examine whether the composition of the shocks driving the factors under stress has a significant impact.

First, to assess the role of financial shocks in the stressed growth distributions obtained above, we fix global and country-specific financial factors at their conditional mean and construct stressed scenarios for global and country-specific macroeconomic factors by stressing them at their 95% probability level.[12] We incorporate financial information into the model while isolating the effect of macroeconomic shocks. Table 2.3 reports the average through time of the absolute deviations of factors stressed at their 95% level when minimizing the 5% quantile of growth, with respect to their average in the "business-as-usual" scenario.[13] The first column of Table 2.3 reports these deviations when all factors are jointly stressed while the second column reports the deviations when only the macroeconomic factors are stressed. The corresponding GiS are plotted in Figure 2.8. Once more, we can conclude that financial factors do not contribute much to stressing the distribution of growth in Spain. Figure 2.8 shows that the GiS obtained when all factors are stressed and when only macroeconomic factors are stressed are nearly the same. Furthermore, the magnitude of the shocks to the macroeconomic factors is also very similar in both situations. However, in Germany, the shocks to the macroeconomic factors has to much larger when the financial factors are kept at their "business-as-usual" levels and, still the GiS is much smaller in absolute value in this last case. A similar situation can be observed in France and Italy with macroeconomic factors having much larger shocks and still the GiS being smaller in absoulte value when only the macroeconomic sector is under stress. This indicates that a higher degree of stress is necessary when focusing on a single sector alone. Stressing macroeconomic conditions alone, while leaving financial conditions unchanged, fails to produce the substantial levels of growth vulnerability observed under simultaneous stress of all factors. The case of Italy is remarkable with the 5% quantile of growth obtained when only macroeconomic factors are stressed being not different from the 5% quantile estimated in the "business-as-usual" scenario. This highlights the critical role of financial factors in amplifying adverse outcomes. Furthermore, the magnitude of this effect varies across countries, revealing different levels of exposure to financial conditions, both EA-wide and local. For instance, Germany and Spain appear more reliant on macroeconomic dynamics, whereas France and Italy–particularly the former–are significantly influenced by financial conditions. In these countries, neglecting financial shocks leads to a marked underestimation of downside risk to GDP, highlighting the importance of accounting for financial stress when assessing growth vulnerability.

Second, we also assess the role of the composition of shocks driving the stressed factors by allowing for univariate shocks in the factors. We do so by considering the 95% quantile of the corresponding marginal distributions of the common and country-specific factors; see Table 2.3 for the average magnitude of these univariate shocks. Through this exercise, we aim to determine whether the observed low economic growth under stressed conditions results

[12] It is important to note that this exercise is feasible as we are extracting factors separately from the set of financial and macroeconomic variables.

[13] Since factors are identified only up to a sign, the sign of the factors alone is uninformative without a proper identification scheme, which allows for meaningful interpretation. Given that factors influence GDP growth quantiles through the quantile regression in (2.1), the sign of the coefficients already indicates the role of each factor in shaping the conditional distribution of economic growth within each country.

Table 2.3: *Deviations of stressed factors from average values under alternative scenarios*

Country		**Factors**	Joint Stress		Univariate Stress				
			Fin & Macro	Only Macro	Common Fin	Common Macro	Local Fin	Local Macro 1	Local Macro 2
Country	DE	f^{F}	1.36	0	2.48	0	0	0	0
		f^{M}	1.41	1.03	0	2.57	0	0	0
		$f^{(DE,\mathrm{F})}$	0.59	0	0	0	2.70	0	0
		$f_1^{(DE,\mathrm{M})}$	2.58	2.87	0	0	0	4.77	0
		$f_2^{(DE,\mathrm{M})}$	0.83	1.36	0	0	0	0	2.77
	ES	f^{F}	0.54	0	2.48	0	0	0	0
		f^{M}	1.44	1.03	0	2.57	0	0	0
		$f^{(ES,\mathrm{F})}$	0.20	0	0	0	2.81	0	0
		$f_1^{(ES,\mathrm{M})}$	1.68	1.36	0	0	0	2.32	0
		$f_2^{(ES,\mathrm{M})}$	3.82	4.25	0	0	0	0	6.79
	FR	f^{F}	1.30	0	2.48	0	0	0	0
		f^{M}	0.92	1.13	0	2.57	0	0	0
		$f^{(FR,\mathrm{F})}$	1.89	0	0	0	3.61	0	0
		$f_1^{(FR,\mathrm{M})}$	1.05	1.31	0	0	0	1.23	0
		$f_2^{(FR,\mathrm{M})}$	3.60	4.64	0	0	0	0	4.46
	IT	f^{F}	1.42	0	2.48	0	0		0
		f^{M}	1.47	2.02	0	2.57	0	0	0
		$f^{(IT,\mathrm{F})}$	2.45	0	0	0	4.26	0	0
		$f_1^{(IT,\mathrm{M})}$	0.29	1.10	0	0	0	3.87	0
		$f_2^{(IT,\mathrm{M})}$	0.14	0.14	0	0	0	0	2.03

For each country, the table reports the average absolute deviation of the factors stressed at their 95% level when minimizing the 5% quantile of growth, with respect to their mean at the "business-as-usual" scenario. We consider two different scenarios: (i) all factors are under stress (first column); and (ii) only macroeconomic factors are stressed (second column). Univariate shocks to each factor obtained as the 95% quantile of their corresponding marginal distributions are reported in the second panel of the table.

from the joint depression of underlying macroeconomic and financial conditions, or whether very large shocks to individual sectors–either at the EA-wide level or at the country level–can explain the observed levels of vulnerability. Observe that the univariate shocks reported in Table 2.3 are much larger than those observed in their respective sectors when all factors are jointly stressed. Figure 2.9 plots the estimated 5% quantiles of growth when the factors are stressed one-by-one, together with the benchmark GiS, obtained when all factors are jointly stressed. We can observe that the high levels of economic growth vulnerability observed in Section 2.4.2 result from the overall economy–both in each economy and in the EA as a whole–being under pressure. Large idiosyncratic shocks to individual sectors, whether EA-wide or country-specific, are insufficient to fully account for the observed levels of economic growth vulnerability. An interesting exception is observed in the case of Italy, where large financial shocks, either global or specific, lead to a level of growth under stress comparable to that in the joint stress scenario. However, note that the implied financial shock is approximately 13 times larger than that observed when the economy is under general stress. This result could be explained by the high levels of debt observed in Italy, which make its financial conditions particularly sensitive to the EA-wide financial stance (see, e.g., Busetti et al., 2021). Furthermore, the effect of individual shocks–both common and country-specific–display significant heterogeneity across countries, reflecting the different impact of the macroeconomic and financial conditions on local markets.

This analysis yields two important insights. First, financial conditions under stress play a critical role in explaining GDP growth at its tails in all economies but Spain. Neglecting financial shocks leads to an underestimation of economic growth vulnerability, particularly during periods

FIGURE 2.8: *GiS under different stress scenarios.*

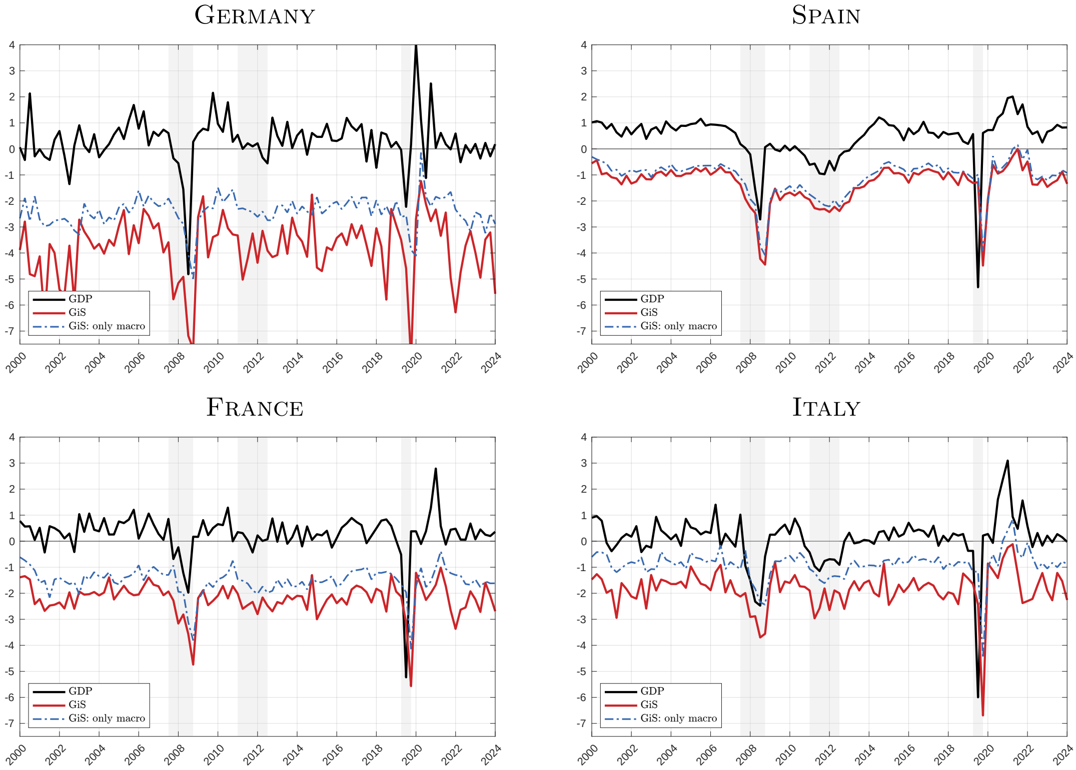

For each country, the figure plots observed GDP growth (black solid line), the estimated GiS when all factors are jointly stressed (red solid line) and when only macroeconomic factors are stressed (blue dashed line).

of stress when underlying economic conditions are strained.

Second, it is essential to account for both EA-wide and country-specific economic conditions as key drivers of the distribution of economic growth in each country. Large shocks to either of these factors have a sizeable impact on economic growth vulnerability although, alone, they are not able to fully explain the large negative values observed when the entire underlying economy is under stress. This distinction has important policy implications. Common shocks across EA countries often require coordinated responses, with macroprudential policies playing a key role in safeguarding financial stability and mitigating systemic risks. These policies can complement monetary policy actions, particularly in addressing vulnerabilities stemming from cross-border spillovers and shared financial exposures (Bussière et al., 2021). Conversely, country-specific shocks are best managed through targeted macroprudential measures tailored to local conditions, among others (Claessens, 2015). However, the interplay between these shocks–both across sectors and countries–can amplify systemic risks, underscoring the importance of an integrated policy approach. Coordinated macroprudential interventions, alongside monetary and fiscal tools, are essential to stabilize GDP growth and reduce the likelihood of severe negative economic outcomes when both EA-wide and country-specific conditions are under stress (Borio, 2014; Cecchetti, 2016).

2.5 Conclusions

We study the heterogeneous dynamics of economic growth vulnerability across the four largest Euro Area economies under stressed macroeconomic and financial conditions. Using a multilevel dynamic factor model, we extract the pervasive EA-wide macroeconomic and financial factors and semi-pervasive country-specific factors driving the distribution of GDP growth. This approach allows us to isolate the contributions of both EA-wide global and local country-specific

Figure 2.9: *Alternative stress scenarios: univariate sectoral shocks*

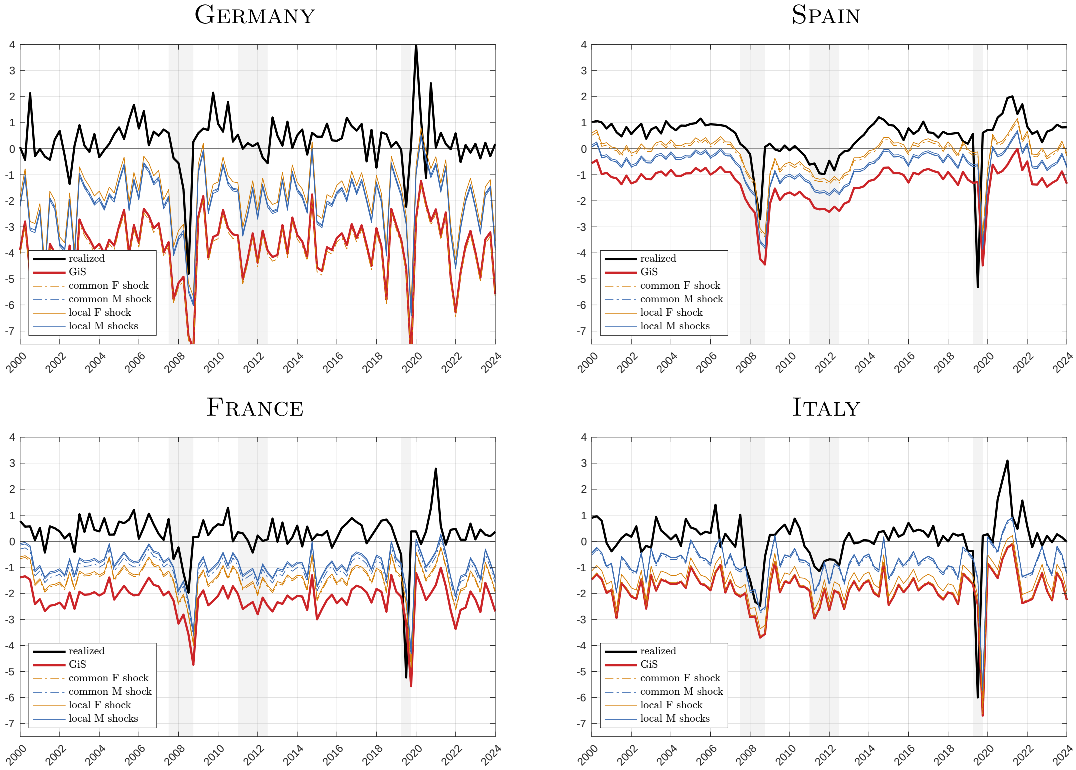

For each country, the figure plots observed GDP growth (black solid line), the estimated GiS when all factors are stressed (red solid line) and the GiS obtained in different scenarios; i) Only the global macroeconomic factor is stressed (dahsed blue line); ii) Only the global financial factor is stressed (dahsed orange line); iii) Only the country-specific macroeconomic factors are stressed (solid blue line); and iv) Only the country-specific financial factor is stressed (solid orange line).

macro-financial conditions, to understand their impact on growth vulnerabilities across countries. By focusing on the lower quantiles of the conditional distribution of GDP growth, we quantify vulnerability in scenarios where economic conditions deviate significantly from those observed during normal times, i.e. when the underlying factors are set at their average values.

The methodology adopted in this study offers a robust framework for analyzing growth vulnerabilities under stress. Factor-augmented quantile regression is a flexible yet parsimonious tool for capturing non-linear and asymmetric relationships between growth and economic conditions. This is complemented by the smooth estimation of conditional distributions using Skew-t densities to provide a detailed representation of downside risks to GDP growth. Finally, the integration of these elements with factor-based stress testing allows us to simulate adverse scenarios and assess growth vulnerability under systemic economic stress.

Our findings reveal distinct patterns of economic growth vulnerability, shaped by differences in exposure to EA-wide conditions and the strength of local dynamics. Specifically, countries heavily influenced by EA-wide conditions, such as Germany, and those driven by dominant country-specific dynamics, like Spain, display larger levels of growth vulnerability. The results of the construction of scenarios under stressed conditions reveal that, when only macroeconomic factors are stressed, while financial factors remain at their average levels, growth vulnerability is consistently smaller, underscoring the critical role of financial conditions in amplifying adverse economic outcomes. Furthermore, large sectoral shocks, whether global or country-specific, fail to fully explain the vulnerability observed under systemic stress, highlighting the interconnected and systemic nature of growth vulnerability across EA countries.

These results carry significant implications for policymaking. The evident heterogeneity in growth vulnerability underscores the necessity for a coordinated policy framework that integrates EA-wide macroprudential interventions with tailored country-specific measures. The interplay between common and local shocks emphasizes the importance of leveraging macro-prudential tools alongside monetary and fiscal policies to address systemic risks and mitigate growth vulnerabilities effectively.

Chapter 3

Assessing the dynamic effects of the common monetary policy in the Euro Area using large data

3.1 Introduction

Understanding how monetary policy affects economic activity across countries within a monetary union is a long-standing challenge in macroeconomics. While a common policy framework is intended to ensure coherence and stability, differences in national economic structures, financial systems, and labor markets can generate heterogeneous responses to a single monetary policy shock. Such asymmetries complicate the design and calibration of euro area (EA) policy and remain a central issue in debates about economic convergence and resilience.

In this paper, we study the heterogeneous transmission of monetary policy shocks across EA member countries. We use a newly assembled large-scale dataset, EA-MD-QD, which covers macroeconomic and financial variables for the euro area and its ten largest economies from 2000 to 2025. The availability of country-level data enables policymakers to account for cross-country heterogeneity, which may ultimately influence both the effectiveness and the transmission of the common monetary policy. In this context, understanding whether, and to what extent, heterogeneous dynamics arise across countries is essential for designing and implementing more effective EA-level policies.

To this end, we fit to the data the recently developed Common Component Vector Auto Regression (CC-VAR) model by Forni et al. (2025), which relies on the assumption of an underlying factor structure in the data. In a first step, standard Principal Component Analysis (PCA) is employed to extract the common factors and compute the common components of all variables. In a second step, a VAR model is estimated on some selected common components of interest along with other observables. The share of variance explained by the common factors provides a preliminary assessment of the degree of comovement among EA countries across different economic dimensions. We find non-negligible differences in the degree of comovement across countries, mainly concentrated in unemployment and interest rates, whereas industrial production, stock indices, and prices display a higher degree of homogeneity.

Then, to assess the extent to which this heterogeneity translates into different responses to a structural monetary policy shock, we identify an EA-wide common monetary policy shock using the Instrumental Variables (IV) approach proposed by Stock and Watson (2012) and Mertens and Ravn (2013), in combination with the High-Frequency Identification (HFI) strategy of Gertler and Karadi (2015). We test several instruments from the pool provided by Altavilla et al. (2019) and select the one associated with the highest first-stage F-statistic. Results at the EA level are consistent with stardard ecomic theory, with industrial production, prices, stock market index declining while interest rates and unemployment rise following a contractionary monetary policy shock. The magnitude of these responses aligns with other results in the literature on EA outcomes (Jarociński and Karadi, 2020).

Given these results, we assess and quantify the heterogeneous dynamics across countries by computing, for each variable of interest, the difference between the national IRFs and the corresponding EA-level IRF. The magnitude and statistical significance of these differences provide a measure of the degree of asymmetry in the transmission of monetary policy shocks across countries.

Overall, our results point to the presence of moderate yet non-negligible heterogeneity across EA countries. This heterogeneity is most pronounced in price and interest rate dynamics and, to a lesser extent, in production and labor market responses. At the country level, the clearest patterns emerge for Germany and Greece: Germany tends to move closely in line with the EA aggregate, whereas Greece displays more pronounced deviations.

Finally, to explore potential drivers of the observed heterogeneity, we follow Corsetti et al. (2022) and conduct an empirical exercise computing the correlations between the peak country-level IRFs and selected country characteristics related to labor markets, households, firms, and the economic structure of each country. Although no structural claim can be made from this exercise, our results suggest that monetary policy transmission is either dampened or amplified by several economic channels, including homeownership rates and savings dynamics, among others.

Over the years, a large body of literature has studied the effects of common monetary policy in the euro area (EA) (Jarociński and Karadi, 2020; Andrade and Ferroni, 2021, among others). In this chapter, we take a step further by analysing potential asymmetries in the transmission mechanism across EA member countries. Our findings extend previous studies investigating cross-country heterogeneity in the transmission of EA monetary policy shocks (Barigozzi et al., 2014; Georgiadis, 2015; Corsetti et al., 2022; Mandler et al., 2022). Specifically, we employ a novel large-dimensional dataset, more recent data vintages, and a novel econometric framework to formally assess the presence, and statistical significance, of cross-country differences in the transmission of monetary policy shocks. Despite differences in sample coverage, our results broadly align with those of Barigozzi et al. (2014), who document similar cross-country patterns in prices and unemployment rates, partly driven by a core–periphery dynamic within the EA. Although the magnitude of responses varies across countries, our results show that prices decline in all EA economies following a contractionary monetary policy shock, consistent with standard economic theory. This contrasts with Corsetti et al. (2022), who report price increases for several countries in response to monetary tightening. Nevertheless, despite this difference in sign, the relative cross-country patterns we identify are broadly consistent with their findings. Conversely, Mandler et al. (2022) obtain an inverted cross-country ranking in price responses compared with our results. Along similar lines, Burriel and Galesi (2018) study the presence of cross-country heterogeneity in responses to unconventional monetary policy shocks.

The chapter is organized as follows. Section 3.2 outlines the econometric framework employed for the monetary policy application. Section 3.3 reports the main findings on the degree of comovement across countries and the dynamic responses of the EA and its member countries to a common monetary policy shock, as well as the analysis of cross-country heterogeneity and its potential drivers. Section 3.4 concludes. The Supplementary Appendix provides a detailed list of all data sources, additional empirical results, and robustness checks.

3.2 Methodology

In this section, we exploit the EA-MD-QD database introduced in Chapter 4 to study the transmission of EA monetary policy across countries, with the goal of highlighting the advantages the database offers for structural macroeconomic analysis. It is well established that, within a monetary union, the effects of a common monetary policy shock may differ across regions (Barigozzi et al., 2014; Corsetti et al., 2022). By exploiting the country-level information in the data, we can assess both the presence and the magnitude of such asymmetries.

3.2.1 Factor extraction

As a first step, we exploit the high dimensionality of our dataset to test for and extract common factors from a monthly panel of EA- and country-specific series. Specifically, we construct a panel $\mathbf{x} = x_{it}, i = 1, \ldots, N; t = 1, \ldots, T$ consisting of 47 EA-wide monthly variables and 200 national series, for a total of $N = 247$.[1]

All variables used to extract the factors are differenced once, except for interest rates and confidence indicators, which are kept in levels. These transformations are consistent with the literature on identifying monetary policy shocks in high-dimensional settings (see, e.g., Corsetti et al., 2022). Results based on an alternative set of transformations, where all variables are differenced according to standard stationarity tests, are reported in Appendix 3.D, while results keeping all rates in levels (including the unemployment rate) are reported in Appendix 3.E.

The panel is balanced and covers the period 2002:M1–2023:M10, corresponding to $T = 263$ monthly observations. We begin the analysis in 2002:M1, following the literature on the identification of EA monetary policy shocks via instrumental variables (IV) (Altavilla et al., 2019; Andrade and Ferroni, 2021), since liquidity in the OIS market was limited before then, hindering identification. The sample ends in 2023:M10, which is the latest date for which monetary policy surprises from Altavilla et al. (2019)—used to identify the shocks—are currently available.

We assume that the $N-$dimensional vector of observed data at time t, $\mathbf{x}_t$, follows a factor model:

$$\mathbf{x}_t \;=\; \boldsymbol{\mu} + \boldsymbol{\Lambda}\mathbf{f}_t + \boldsymbol{\xi}_t \;=\; \boldsymbol{\chi}_t + \boldsymbol{\xi}_t \qquad t = 1, \ldots, T, \tag{3.1}$$

where $\boldsymbol{\Lambda}$ is the $N \times r$ vector of loadings associated to the r-dimensional vector of zero-mean static factors $\mathbf{f}_t$, $\boldsymbol{\xi}_t$ is a $N \times 1$ vector of zero-mean idiosyncratic components, and $\boldsymbol{\mu}$ is a $N \times 1$ vector of constants, such that $\mathbb{E}[\mathbf{x}_t] = \boldsymbol{\mu}$.

Both the factors and the idiosyncratic components are allowed to be serially correlated. Moreover, when N is large is reasonable to allow the idiosyncratic components to be also (weakly) cross-sectionally correlated, and, in this case, we say that $\mathbf{x}_t$ follows an approximate factor structure. We refer to Bai (2003) for the formal assumptions.

The loadings and the factors in (3.1) are not identified, since the factor model can equivalently be expressed with $\boldsymbol{\Lambda}\mathbf{H}$ as the loadings matrix and $\mathbf{H}^{-1}\mathbf{f}_t$ as the factors vector, for some invertible $r \times r$ matrix $\mathbf{H}$. To identify the factors additional assumptions would be needed (Bai and Ng, 2013), but since in this chapter our interest is only in estimating the common component $\boldsymbol{\chi}_t = \boldsymbol{\mu} + \boldsymbol{\Lambda}\mathbf{f}_t$, we do not explore this path further. Indeed, $\boldsymbol{\chi}_t$ is always identified once we determine the number of factors r, so that we can disentangle it from the idiosyncratic component.

Under an approximate factor structure, the number of factors r is identified provided that $N \to \infty$ (Bai and Ng, 2002), a condition necessary also for consistently estimating the common component (Stock and Watson, 2002a; Bai, 2003). This in practice shows the necessity of working with a high-dimensional panel in order to consistently disentangle the common components capturing all main comovements from the idiosyncratic ones.

[1]We append the following national variables to the EA dataset: industrial production indexes (IPMN, IPCAG, IPCOG, IPDCOG, IPNDCOG, IPING, IPNRQ), Harmonized Indexes of Consumer Prices (HICPOV, HICPNEF, HICPG, HICPIN, HICPSV, HICPNG), Producer Price Indexes (PPICAG, PPICOG, PPINDCOG, PPIDCOG, PPIING, PPINRG), long-term interest rate (LTIRT), stock price index (SHIX), and unemployment rate (UNETOT).

We determine the number of common factors employing different methods. Namely, we apply the log-information criterion (IC2) of Bai and Ng (2002), implemented also when tuning the penalty as suggested by Alessi et al. (2010), as well as the eigenvalue-ratio criterion by Ahn and Horenstein (2013) and the test by Onatski (2010). Given the results in Table 3.1 we set $r = 6$ for both datasets.[2] Then, following the suggestion by Forni et al. (2025), we estimate the model for different values of r within a neighborhood of $r = 6$ and, starting from the lower bound, we progressively increase r until the IRFs stabilize (see Section 3.2.2 below). This approach leads us to select $r = 6$.

TABLE 3.1: *Estimated number of factors*

Method	Factors
Bai and Ng (2002)	8
Onatski (2010)	2
Ahn and Horenstein (2013)	2
Alessi et al. (2010)	6

Estimation is performed using the classical PCA approach. Here we follow the approach by Stock and Watson (2002a) and we estimate the loadings, denoted as $\widehat{\mathbf{\Lambda}}$, as $\sqrt{N}$ times the r normalized eigenvectors corresponding to the r-largest eigenvalues of the sample covariance matrix of the standardized data $\mathbf{x}_t$, i.e., of $T^{-1}\sum_{t=1}^{T}\widehat{\mathbf{\Omega}}^{-1/2}(\mathbf{x}_t - \widehat{\boldsymbol{\mu}})(\mathbf{x}_t - \widehat{\boldsymbol{\mu}})'\widehat{\mathbf{\Omega}}^{-1/2}$, where $\widehat{\boldsymbol{\mu}}$ and $\widehat{\mathbf{\Omega}}$ are, respectively, the N dimensional vector of sample means and a diagonal $N \times N$ matrix with entries the N sample variances of each element of $\mathbf{x}_t$. Then, the factors, $\widehat{\mathbf{f}}_t$, are obtained by projecting the estimated loadings onto the data, i.e., $\widehat{\mathbf{f}}_t = (\widehat{\mathbf{\Lambda}}'\widehat{\mathbf{\Lambda}})^{-1}\widehat{\mathbf{\Lambda}}'\widehat{\mathbf{\Omega}}^{-1/2}(\mathbf{x}_t - \widehat{\boldsymbol{\mu}}) = N^{-1}\widehat{\mathbf{\Lambda}}'\widehat{\mathbf{\Omega}}^{-1/2}(\mathbf{x}_t - \widehat{\boldsymbol{\mu}})$ (due normalization of the eigenvectors). The estimated common components are then de-standardized and de-centered by multiplying them by the standard deviation of the original series and adding the corresponding mean. The resulting common component N-dimensional vector is denoted as $\widehat{\boldsymbol{\chi}}_t = \widehat{\boldsymbol{\mu}} + \widehat{\mathbf{\Omega}}^{1/2}\widehat{\mathbf{\Lambda}}\widehat{\mathbf{f}}_t$. From the results in Stock and Watson (2002a) it immediately follows that $\widehat{\boldsymbol{\chi}}_t$ is a consistent estimator of $\boldsymbol{\chi}_t$, as $N, T \to \infty$.

For a given variable, the share of total variance explained by the common component offers a straightforward measure of cross-country comovement. Specifically, for a given country and variable, a high proportion of variance explained by the common component indicates that the variable is primarily driven by EA-wide common factors rather than by country-specific idiosyncratic dynamics. Confidence intervals for the explained variance are obtained using the bootstrap procedure of Barigozzi et al. (2018). Specifically, for each factor $l \in 1, \dots, r$, and each bootstrap repetition $b = 1, \dots, B$, we generate a $T-$dimensional bootstrap sample $\widehat{\mathbf{f}}_l^{(b)}$ via a block bootstrap algorithm. The common components are then reconstructed as $\widehat{\boldsymbol{\chi}}_t^{(b)} = \widehat{\boldsymbol{\mu}} + \widehat{\mathbf{\Omega}}^{1/2}\widehat{\mathbf{\Lambda}}\widehat{\mathbf{f}}_t^{(b)}$. The bootstrap sample of the idiosyncratic components, denoted by the $N \times T$ matrix $\widehat{\boldsymbol{\xi}}^{(b)}$, is obtained by jointly resampling the estimated idiosyncratic components $\widehat{\boldsymbol{\xi}}$ across variables, thereby preserving potential cross-sectional dependence. In contrast, the factors are resampled independently, given their orthogonality by construction. The bootstrap data are then constructed as $\widehat{\mathbf{x}}^{(b)} = \widehat{\boldsymbol{\chi}}^{(b)} + \widehat{\boldsymbol{\xi}}^{(b)}$. For each bootstrap iteration, the share of variance explained by the common component for variable i is computed as $\text{var}(\widehat{\boldsymbol{\chi}}_i^{(b)})/\text{var}(\widehat{\mathbf{x}}_i^{(b)})$. This procedure is repeated for $B = 1000$ iterations.

[2]For small samples as the quarterly data the methods by Onatski (2010) and Ahn and Horenstein (2013) are known to be often too parsimonious

3.2.2 Estimation via Common Component-VAR

For estimation, we adopt the CC-VAR approach of Forni et al. (2025), constructing an $n \times 1$ vector $\mathbf{Y}_t$ of endogenous variables with $n \ll N$. This vector contains the estimated common component of selected variables from $\mathbf{x}_t$, $\widehat{\boldsymbol{\chi}}_t$, along with additional observables of interest, if any. Following Forni et al. (2025), and denoting by n^* the number of elements from $\widehat{\boldsymbol{\chi}}_t$ included in $\mathbf{Y}_t$, we impose $n^* = r$, where r is the number of common factors. This restriction is sufficient to guarantee the fundamentalness of the recovered structural shocks (Alessi et al., 2011).

Indeed, as long as $n^* = r$ in the CC-SVAR, the space of shocks spanning all N common components $\widehat{\boldsymbol{\chi}}_t$ is identified, since these are linear combinations of the underlying r common factors. This, in turn, allows us to rotate the common components included in $\mathbf{Y}_t$ to recover the IRFs for all N variables used in the factor extraction. Unlike in a standard VAR or FAVAR, modifying the set of endogenous variables included in $\mathbf{Y}_t$ has no effect on the estimated IRFs. This property is particularly valuable in our setting, where we aim to analyze the response of a large set of national variables to a well-identified monetary policy shock within a single model, thereby ensuring the internal consistency of the estimates. For a detailed comparison with alternative models, see Appendix 3.C.

Specifically, we fit the following reduced-form VAR:

$$\mathbf{Y}_t = \mathbf{C} + \sum_{i=1}^{p} \mathbf{B}_i \mathbf{Y}_{t-i} + \sigma_t \mathbf{u}_t, \quad t = 1, \dots, T, \tag{3.2}$$

where $\mathbf{C}$ is a $n \times 1$ vector of reduced-form constants, $\mathbf{B}_i$, $i = 1, \dots p$, are $n \times n$ matrices of reduced-form coefficients and $\mathbf{u_t}$ is the $n \times 1$ zero-mean vector of reduced-form errors, with zero mean and covariance matrix $\boldsymbol{\Sigma}$.

The scaling factor σ_t is included to address the significant fluctuations observed during the Covid period by adjusting the model residual volatility, as suggested by Lenza and Primiceri (2022). In particular, σ_t, takes a value of 1 for all periods preceding the Covid onset period, while from 2020:M3 until the end of the sample, at T = 2023:M10, σ_t is estimated in each period by maximum likelihood.[3]

Estimation of the VAR in (3.2) gives the estimated coefficients $\widehat{\mathbf{B}}_i$ and by VAR inversion we obtain the estimated reduced form IRFs.[4] Consistency, as $N, T \to \infty$, of these estimated IRFs can be directly proved by combining consistency of the estimated common components with the results in Forni et al. (2009), which are similar to the results for PCA based Factor augmented VARs obtained by Bai and Ng (2006).

Table 3.2 reports the elements of the vector $\mathbf{Y}_t$ used in our analysis. Our specification includes, as an observable, the policy rate—specifically, the 2-year interest rate in the EA, denoted R_t. In addition, we incorporate the common component for key EA variables: industrial production growth in manufacturing (IPMN), HICP inflation, long-term interest rates (LTIRT), stock price growth (SHIX), and the monthly change in the unemployment rate (UR). Finally, we include the common component of a single national variable of interest, for which we aim to study the IRF. For each national variable, we re-estimate the model while keeping the same set of EA common components and the policy rate, sequentially rotating across the common components of all national variables of interest, each included as the last component in $\mathbf{Y}_t$. This procedure ensures that the requirement $n^* = r$ is always satisfied, so that the estimated IRFs derive from a unique model, regardless of which national component is included last. Consequently, the estimated IRFs for both EA and national variables are invariant to the choice of the last common component in $\mathbf{Y}_t$.[5]

[3] Our approach differs slightly from the approach of Lenza and Primiceri (2022) as their approach is

Table 3.2: *Components of $\mathbf{Y}_t$ in the CC-VAR*

notation	ID	name
R_t	-	EA 2 Years Interest Rate
$\widehat{\chi}_t^{\text{IP EA}}$	IPMN	EA Industrial Production (common component)
$\widehat{\chi}_t^{\text{HICP EA}}$	HICPOV	EA HICP overall (common component)
$\widehat{\chi}_t^{\text{R long EA}}$	LTIRT	EA Long Term Interest Rate (common component)
$\widehat{\chi}_t^{\text{SHIX EA}}$	SHIX	EA Share Prices (common component)
$\widehat{\chi}_t^{\text{UR EA}}$	UNETOT	EA Unemployment Rate (common component)
$\widehat{\chi}_t^{\text{nat.}}$	-	National variable (common component)

Structural Identification

The structural counterpart of (3.2) is:

$$\mathbf{A}_0\mathbf{Y}_t = \mathbf{C}^* + \sum_{i=1}^{p}\mathbf{A}_i\mathbf{Y}_{t-i} + \sigma_t\boldsymbol{\varepsilon}_t, \quad t = 1, \ldots, T, \tag{3.3}$$

where the reduced-form errors $\mathbf{u}_t$ are related to the structural errors $\boldsymbol{\varepsilon}_t$ through the following relationship:

$$\mathbf{u}_t = \mathbf{A}_0^{-1}\boldsymbol{\varepsilon}_t, \quad t = 1, \ldots, T. \tag{3.4}$$

Hereafter, let $\mathbf{S} \equiv \mathbf{A}_0^{-1}$ for simplicity of notation.

As is well known in the VAR literature, the matrix $\mathbf{S}$ is unobserved and we need an identification strategy to estimate it and give an economic interpretation to the elements of $\boldsymbol{\varepsilon}_t$. For our application, focused on the monetary policy shock only, it is sufficient to identify the associated elements in the column of the matrix $\mathbf{S}$. We denote such column as $\mathbf{s}$ and the corresponding monetary policy shock as ε_t^p, while all other structural shocks are collected into the vector $\boldsymbol{\varepsilon}_t^q$. The entry of $\mathbf{s}$ corresponding to ε_t^p, which is the contemporaneous impact of the monetary policy shock on the interest rate, is denoted as s^p, while all other entries are collected into the vector $\mathbf{s}^q$. Once the EA wide monetary policy shock is identified the corresponding IRFs are then computed from the, truncated, VMA(∞) representation of the estimated structural VAR defined in (3.3).

To identify $\mathbf{s}$ and ε_t^p, we employ the high-frequency Proxy-SVAR method from Gertler and Karadi (2015).[6] This approach requires jointly specifying two types of variables: a policy indicator, denoted as R_t, and a monetary policy instrument, denoted as Z_t. The policy indicator is a variable capturing the central bank's monetary policy stance and, in our case, this is the interest rate R_t, which is included in $\mathbf{Y}_t$ and thus enters directly into the CC-VAR model. Our selection of policy indicator R_t candidates includes EA interest rates across different maturities. In particular, for the 1-, 2-, and 3-year rates, we employed data from the Eurostat database. Our choice for the pool of instrument candidates Z_t is drawn from the work of Altavilla et al. (2019)[7].

based on US data. Nevertheless, the variations introduced do not significantly affect our results.

[4]Throughout, we choose $p = 8$ lags in the VAR

[5]Adjusting the IRFs for Covid introduces slight deviations from this invariance due to changes in the volatility parameter σ_t, leading to unwanted dispersion in the EA IRFs. To address this, we first estimate σ_t for each specification differing only in the last variable. We then take the median of the estimated σ_t vectors across specifications to obtain an average volatility, which is subsequently used to compute the national IRFs as described.

[6]In the Supplementary Appendix 3.F we also exploit an alternative identification strategy based on sign restrictions

[7]To convert high-frequency data into monthly frequency, daily observations are cumulated over the last 30 days of each month and then averaged, following Gertler and Karadi (2015). This procedure substantially mitigates the temporal aggregation bias (Kilian, 2024).

The monetary policy instrument is a variable Z_t satisfying two characteristics. First, it must be correlated with the monetary policy shock:

$$\mathrm{E}[Z_t \varepsilon_t^p] > 0. \tag{3.5}$$

Second, it must be exogenous to all other shocks, collected in the vector $\boldsymbol{\varepsilon}_t^q$, i.e.,

$$\mathrm{E}[Z_t \boldsymbol{\varepsilon}_t^q] = \mathbf{0}. \tag{3.6}$$

After choosing R_t and Z_t, estimating the reduced-form VAR described in (3.2), and obtaining the vector of estimated reduced-form residuals $\widehat{\mathbf{u}}_t$, we identify $\mathbf{s}$ using a two-step procedure. First, we project the residual of the policy indicator R_t, which we denote as $\widehat{u}_t^p$, on the instrument Z_t. That is, we estimate the linear regression:

$$\widehat{u}_t^p = \alpha + \beta Z_t + \zeta_t, \quad t = 1, \dots, T. \tag{3.7}$$

Then, letting $\widehat{\alpha}$ and $\widehat{\beta}$ be the OLS estimates of α and β and letting $\widehat{\widehat{u}}_t^p = \widehat{\alpha} + \widehat{\beta} Z_t$, we estimate the linear regression,

$$\widehat{\mathbf{u}}_t^q = \boldsymbol{\gamma}\, \widehat{\widehat{u}}_t^p + \boldsymbol{\delta}_t, \quad t = 1, \dots, T, \tag{3.8}$$

where $\widehat{\mathbf{u}}_t^q$ are all other the reduced-form residuals. The OLS estimate of $\boldsymbol{\gamma}$, denoted as $\widehat{\boldsymbol{\gamma}}$, is then an estimate of $\mathbf{s}^q/s^p$. This identifies $\mathbf{s}$ up to a scaling factor. To fully identify $\mathbf{s}$, we normalize the impact of the monetary policy shock on the interest rate to one, i.e. we set $s^p = 1$, so that $\widehat{\boldsymbol{\gamma}} = \widehat{\mathbf{s}}^q$. This results into an identified monetary policy shock which increases at impact the interest rate of one percentage point.

As in Gertler and Karadi (2015), we test different combinations of instrument-policy indicators, selecting the pair that exhibits the highest F-statistic related to Equation 3.7. The F-statistic is used to test the null hypothesis of instrument irrelevance (low F-statistic) against the alternative hypothesis of instrument relevance (high F-statistic), with a threshold of 10 commonly used to distinguish between strong and weak instruments (Stock et al., 2002). Based on this test we choose R_t as the EA 2-years interest rate, while for Z_t we choose the 1-year EONIA swap giving a standard F-statistic equal to 14.5 and a robust F-statistic, computed following Olea and Pflueger (2013), equal to 10.5.[8]

The EONIA swap price is measured immediately before and after both the ECB's press statement and press conference. The policy surprise measure is derived by summing these two price differences. The rationale is that, preceding the ECB policy announcements, the swap price incorporates market expectations regarding the future path of EONIA. Therefore, any adjustment in the price immediately after the policy announcements is interpreted as a recalibration of market expectations in response to an unforeseen monetary policy surprise. This satisfies the correlation requirement in (3.5). Regarding the exogeneity condition in (3.6), we assume that no other significant macroeconomic shock occurs in the time span between the press statement and the press conference. Additionally, we distinguish conventional monetary policy shocks from information shocks (Jarociński and Karadi, 2020; Andrade and Ferroni, 2021) by retaining only those high-frequency observations for the EONIA swap price that are associated with a simultaneous movement of opposite sign in the swap price on the Euro Stoxx 50 index. To quantify uncertainty around the estimated IRFs, we employ a standard Wild boostrap (Gonçalves and Kilian, 2004) with $B = 1000$ bootstrap repetitions, also accounting for the well-known bias due to the estimation of the VAR in finite samples (Kilian, 1998).

[8]We obtained similar results using other instrument-policy variable combinations. Specifically, we also tested the 1-year swap together with the 1-year interest rate (F-stat 12.8), the 1-year swap together with the 3-year interest rate (F-stat 10.7) and the 2-year swap together with the 2-year interest rate (F-stat 11.1). All these specifications yielded similar results.

3.2.3 Assessing cross-country heterogeneity

Examining the estimated country-specific IRFs, obtained as described in Section 3.2.2, provides initial insights into the presence of heterogeneous responses of EA countries to the common monetary policy shock. To move beyond this descriptive assessment, we next quantify the magnitude of these differences and, most importantly, evaluate their statistical significance. Specifically, we quantify heterogeneity across EA countries by computing, for each variable of interest, the difference between the national IRFs and the corresponding EA IRF. We leverage the properties of the CC-VAR to facilitate this comparison. As described in Section 3.2.2, we sequentially re-estimate the CC-VAR, including the common component of each national variable of interest while retaining all other EA-wide common components in the specification. Thus, at each iteration $k = 1, \ldots, 49$, we can directly compare the IRF of the common component for a given national variable with its EA counterpart. This is straightforward in our setting because, as long as $n^* = r$, changing which common components are included in the VAR does not affect the IRFs. For each iteration, the space of shocks driving these components is fully represented, ensuring comparability across iterations.

This procedure allows for a direct comparison across individual countries. Specifically, at each horizon $h = 0, \ldots, H$, a positive (negative) value indicates that the national response lies above (below) the corresponding EA response. Importantly, this relative positioning does not necessarily imply a stronger or weaker response in absolute terms, as it depends on the sign and magnitude of both IRFs. For instance, a positive difference may arise either when both IRFs are positive and the national response is larger, or when both are negative and the national response is smaller. By repeating this procedure for each bootstrap repetition $b = 1, \ldots, B$ (with $B = 1000$), we can also quantify the uncertainty around these point estimates.

3.3 The dynamic effects of the EA monetary policy

3.3.1 Comovements across EA countries

To provide an intuition of the explanatory power of the common factors, Table 3.3 reports the share of variance explained by the common component for selected key variables. This analysis offers a preliminary assessment of the degree of synchronization across EA countries. Indeed, if country dynamics were perfectly aligned, we would expect relatively similar levels of comovement across countries for each variable.

The results reveal a non-negligible level of heterogeneity both across countries and relative to the EA. Comovement across variables is relatively high at the EA level, reflecting the influence of both EA-wide and country-specific information. At the country level, however, some heterogeneity emerges across indicators. For industrial production, the countries that deviate from the high commonality observed for the EA are Belgium, Greece, the Netherlands, and, to a lesser extent, Portugal. In general, larger industrial economies are more closely aligned with the EA, whereas smaller economies exhibit a higher degree of idiosyncratic variation in production. In contrast, prices display a relatively more homogeneous pattern across countries. Nevertheless, the average share of variance explained for consumer prices is considerably lower than for industrial production, as prices have been shown to comove less than real variables in standard large macroeconomic datasets (Lissona and Ruiz, 2025). The degree of commonality for interest rates exhibits a clear core–periphery pattern: central European countries display a high level of commonality, whereas interest rate dynamics in southern countries appear more driven by country-specific factors. However, even within this group, the extent of idiosyncrasy

Table 3.3: *Share of Explained Variance by the common factors*

Country	Indutrial Production (IPMN)	Prices (HICPOV)	Interest Rate (LTIRT)	Stock Index (SHIX)	Unemployment Rate (UNETOT)
EA	0.88	0.82	0.93	0.90	0.64
	(0.81-0.92)	(0.73-0.86)	(0.86-1.00)	(0.86-0.94)	(0.56-0.69)
AT	0.63	0.68	0.93	0.78	0.10
	(0.50-0.70)	(0.58-0.74)	(0.86-0.99)	(0.73-0.83)	(0.08-0.12)
BE	0.18	0.50	0.94	0.81	0.11
	(0.12-0.24)	(0.40-0.57)	(0.89-0.99)	(0.76-0.86)	(0.09-0.13)
DE	0.72	0.58	0.91	0.81	0.14
	(0.59-0.78)	(0.48-0.64)	(0.82-0.98)	(0.76-0.86)	(0.11-0.17)
EL	0.15	0.42	0.13	0.61	0.12
	(0.10-0.18)	(0.34-0.48)	(0.10-0.15)	(0.55-0.66)	(0.10-0.14)
ES	0.81	0.64	0.79	0.77	0.55
	(0.70-0.87)	(0.55-0.70)	(0.66-0.94)	(0.72-0.82)	(0.46-0.62)
FR	0.86	0.65	0.94	0.88	0.17
	(0.76-0.91)	(0.54-0.71)	(0.88-0.98)	(0.83-0.92)	(0.14-0.20)
IE	-	0.57	0.65	0.71	0.29
	(—)	(0.46-0.64)	(0.52-0.80)	(0.65-0.77)	(0.23-0.33)
IT	0.77	0.52	0.81	0.85	0.41
	(0.64-0.83)	(0.42-0.58)	(0.70-0.95)	(0.81-0.89)	(0.32-0.47)
NL	0.29	0.37	0.92	0.83	0.27
	(0.20-0.35)	(0.29-0.43)	(0.84-0.98)	(0.77-0.87)	(0.22-0.30)
PT	0.52	0.47	0.41	0.67	0.32
	(0.37-0.61)	(0.38-0.53)	(0.31-0.51)	(0.61-0.72)	(0.26-0.35)

Notes: Each entry in the table corresponds to the share of variability within each variable (in the columns) for each country (in the rows) explained by the common component, $\chi_{i,t}$. Numbers in parentheses indicate the lower and upper bounds of the 68% confidence interval, computed using the bootstrap procedure described in Section 3.2.1.

varies considerably: Italy and Spain comove more strongly with other countries, while Greece is almost entirely idiosyncratic. Stock market indices show a relatively high and homogeneous degree of commonality across countries, with the partial exception of Greece and Portugal.

The variable exhibiting the highest degree of heterogeneity is the unemployment rate. Here, many central countries display a low level of synchronization with EA dynamics, in contrast to some peripheral countries such as Italy and Spain. Nevertheless, no clear core–periphery pattern emerges for unemployment.

Overall, these results provide preliminary insights into the degree of heterogeneity across variables and EA countries. While no structural claims can be made at this stage, they motivate a deeper analysis to determine whether this heterogeneity persists conditional on a monetary policy shock. In Section 3.3.4, we further explore the relationship between the asymmetric response to a monetary policy shock and the degree of commonality in the corresponding variable. A more rigorous analysis of comovements across EA variables would require explicitly accounting for lag and lead relationships both across variables and countries, as in D'Agostino et al. (2016) and Cascaldi-Garcia et al. (2024). However, given the large dimensionality of our data–both within and across countries–such an approach is beyond the scope of this chapter.

3.3.2 EA IRFs

Figure 3.1 presents the estimated IRFs of the Euro Area variables included in the CC-SVAR in (3.2) in response to a 100 basis-point (bps) shock to the 2-year interest rate, along with their one-standard-deviation confidence intervals.

A contractionary monetary policy shock leads to an increase in both short-term and long-term interest rates, with the latter rising to roughly half the magnitude of the former at impact. This pattern is expected, as monetary policy shocks typically have a stronger effect on shorter maturities than on the upper end of the yield curve (Altavilla et al., 2019). As anticipated, industrial production, prices, and stock prices in the EA decline. In contrast, the unemployment rate rises with a lag of a few months, although the response is not statistically significant. After rescaling the interest rate increase to 100 basis points, the magnitudes of the responses in the HICP and stock price indices is comparable to those reported by Jarociński and Karadi (2020),

Figure 3.1: *Euro Area impulse responses*

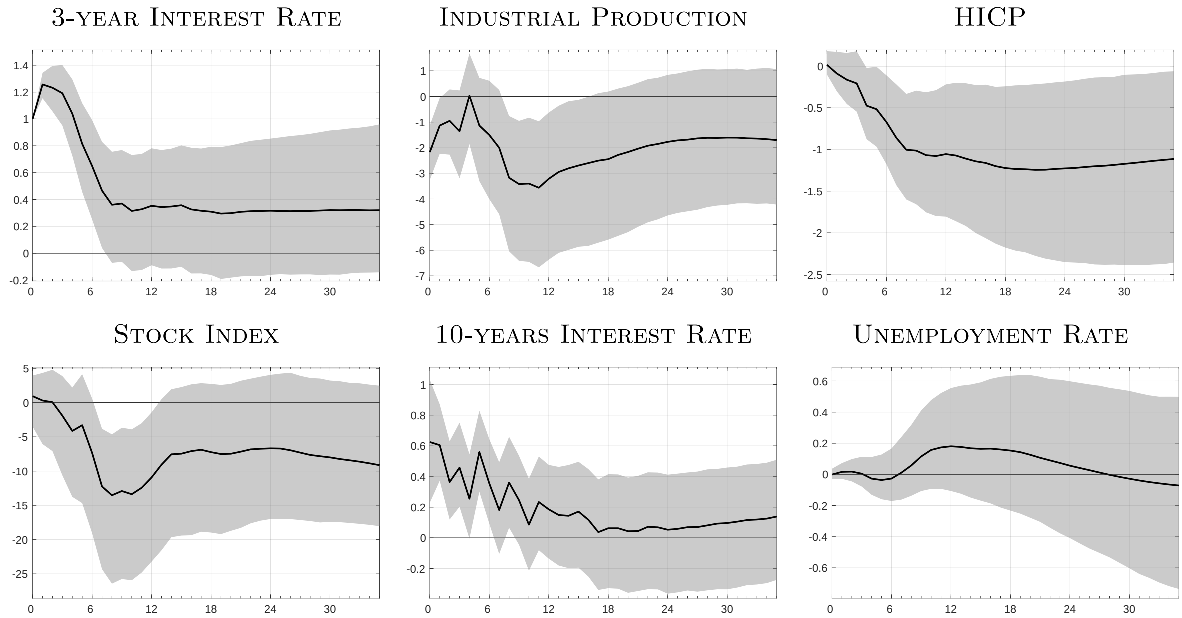

Notes: Each sub-figure plots the impulse response of one EA variable to a 100bps contractionary monetary policy shock. The black solid line is the point estimate in our baseline setting, while the gray shaded area is the corresponding 68% confidence interval.

but contrasts with Corsetti et al. (2022), who document a muted reaction of the HICP. This difference likely reflects our explicit control for so-called *information shocks* when constructing the instruments, consistent with the findings of Andrade and Ferroni (2021) and Jarociński and Karadi (2020). The response of the unemployment rate is similar in magnitude to that reported by Corsetti et al. (2022), although it remains statistically insignificant.

Overall, our results are quantitatively in line with other findings in the literature. Specifically, once having properly re-scaled the monetary policy shock, we find our estimates for the Euro Area to be close to those obtained by Jarociński and Karadi (2020), reinforcing the robustness of our methodology.

To assess the robustness of our results, Appendix 3.F repeats the exercise using an alternative identification strategy based on sign restrictions. The direction and shape of the IRFs remain largely unchanged, and their magnitudes are similar to those observed in the main specification.

3.3.3 Heterogeneous country responses

Turning to individual countries, Figure 3.2 presents the IRFs for the corresponding national variables. At each horizon $h = 1, \ldots, 36$, responses that are significant at the one-standard-deviation confidence level are shown with solid lines, while non-significant responses are depicted with dotted lines. Individual responses with their confidence intervals can be found in Appendix 3.A.

Figure 3.2: *Country-level impulse responses*

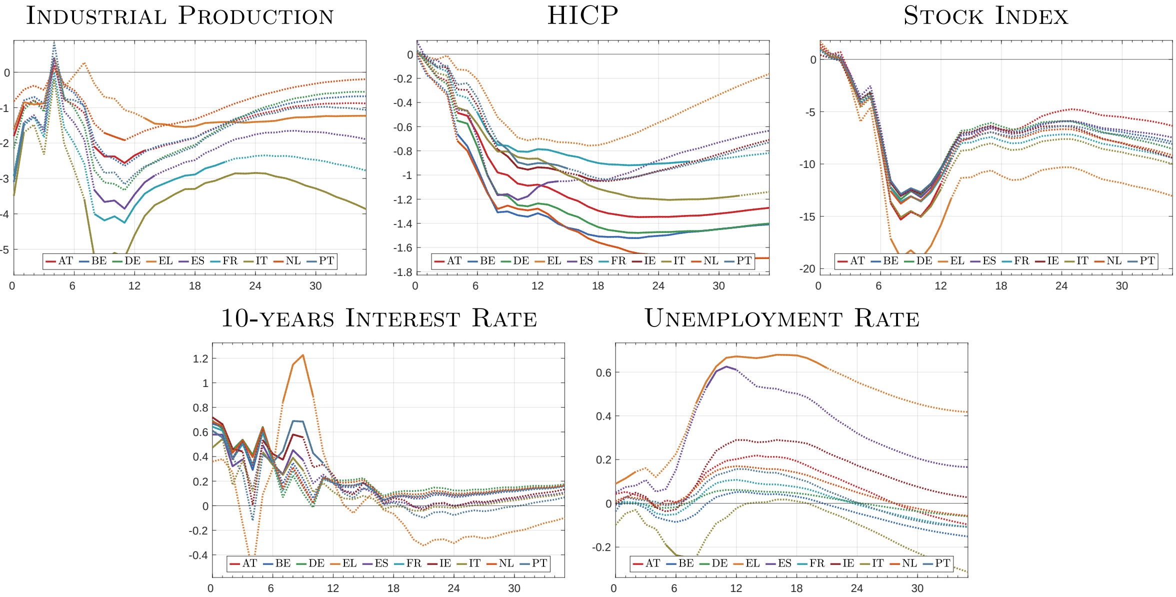

Notes: Each sub-figure plots the impulse responses, for all countries, of one variable to a 100bps contractionary monetary policy shock. Within each sub-figure, at each horizon $h = 0, \ldots, 36$ the country-level impulse responses are denoted with a solid line if the IRF is statistically significant at the 68% level at that horizon, and with a dotted line otherwise.

As with the aggregate, the direction of the impulse responses for each country is consistent with standard economic theory. Moreover, the IRFs exhibit broadly similar dynamics across countries, with the main differences appearing in the magnitude of the response. For industrial production, the peak decline in the impulse responses ranges from approximately 6% for Italy to around 2% for Greece, which stands out both in terms of magnitude and the shape of its response relative to other countries. These results highlight how the largest manufacturing economies in the EA are more strongly affected by the adverse effects of a contractionary shock. Price responses are particularly homogeneous across countries, with a slightly more muted reaction in Greece. The maximum difference between the impulse responses is approximately 1.5 percentage points, indicating only minor misalignments across countries.

Similar patterns are observed for stock prices, although Greece exhibits a particularly strong response to the contractionary shock, with stock prices declining by roughly 20%.

On the interest rate side, Greece again stands out with an exceptionally strong response, peaking at around 120 bps. More generally, interest rates increase more in other peripheral countries (i.e., Portugal, Ireland, Italy, and Spain) compared to core countries.

This core–periphery distinction is less clear for unemployment. While Greece and Spain experience notably higher unemployment responses, Italy shows a counterintuitive, though mostly non-significant, effect. Overall, most unemployment responses are borderline significant at best.

These results suggest only moderate heterogeneity across countries, which is mostly concentrated in a few selected cases. However, this analysis alone does not allow us to fully assess this claim, as these observed differences may be entirely obscured by estimation uncertainty.

To determine the presence of heterogeneous dynamics across countries, we compute, for each variable, the difference between a country's response and the corresponding EA aggregate response, as described in detail in Section 3.2.3. Figure 3.3 presents these differences along with one-standard-deviation confidence intervals.

For industrial production, France and Italy stand out from the other countries, as they are the only ones exhibiting a stronger downward response relative to the EA aggregate. This pattern differs for Germany, which, despite being one of the main manufacturing economies in the EA like Italy and France, shows no substantial deviation from the EA aggregate response. All other countries display weaker responses compared with the EA, particularly core economies such as Austria, Belgium, and the Netherlands. In contrast, for prices, some differences emerge between core and peripheral countries. Core countries are either closely aligned with the EA aggregate (e.g., Austria) or exhibit a stronger response (e.g., Germany), whereas peripheral countries generally show a more muted reaction, with the exception of Spain, where the difference is not statistically significant. This pattern seems to suggests that the transmission of monetary policy to prices differs between core and peripheral countries (Barigozzi et al., 2014). Stock prices present a relatively homogeneous picture, with only Germany, Italy, and Greece showing statistically significant deviations from the EA aggregate. However, the magnitude of these differences varies markedly: Germany and Italy deviate by at most approximately 2%, whereas Greece exhibits a substantially stronger response, with a difference exceeding 5% compared to the EA counterpart. An interesting pattern emerges for interest rates. First, for nearly all countries, the peak differences relative to the EA occur between 6 and 8 months, coinciding with the horizon at which most responses are statistically significant. Second, there is a hint of a core–periphery pattern: responses in peripheral countries tend to lie above the EA aggregate at medium horizons, whereas those of core countries peak below the EA at the same horizons. Notably, the magnitude of the response for Greece is particularly strong. On the labor market side, the most pronounced differences are observed for Greece and Spain, whose responses exceed the EA aggregate, and for Italy and France, whose responses are comparatively lower. These pattern is coherent with the one observed by (Barigozzi et al., 2014), despite the sample differences. These results are coherent with those obtained using quarterly data and sign restrictions, as well as those obtained with alternative sets of transformations

Overall, our results indicate the presence of moderate, yet non-negligible, heterogeneity across EA countries. This heterogeneity is most pronounced in price and interest rate dynamics, and, to a lesser extent, in production and labor market responses. At the country level, the clearest patterns emerge for Germany and Greece: Germany is generally more aligned with the EA aggregate, whereas Greece exhibits pronounced deviations.

These results do not signal major concerns for the conduct and transmission of monetary policy in the Euro Area. However, they highlight the importance of closely monitoring within-country dynamics to further smooth policy transmission and mitigate adverse effects on domestic production, labor market outcomes, and—most importantly—financing costs, particularly in light of the recent post-Covid surge in public spending.

FIGURE 3.3: *Difference between EA and country-level IRFs*

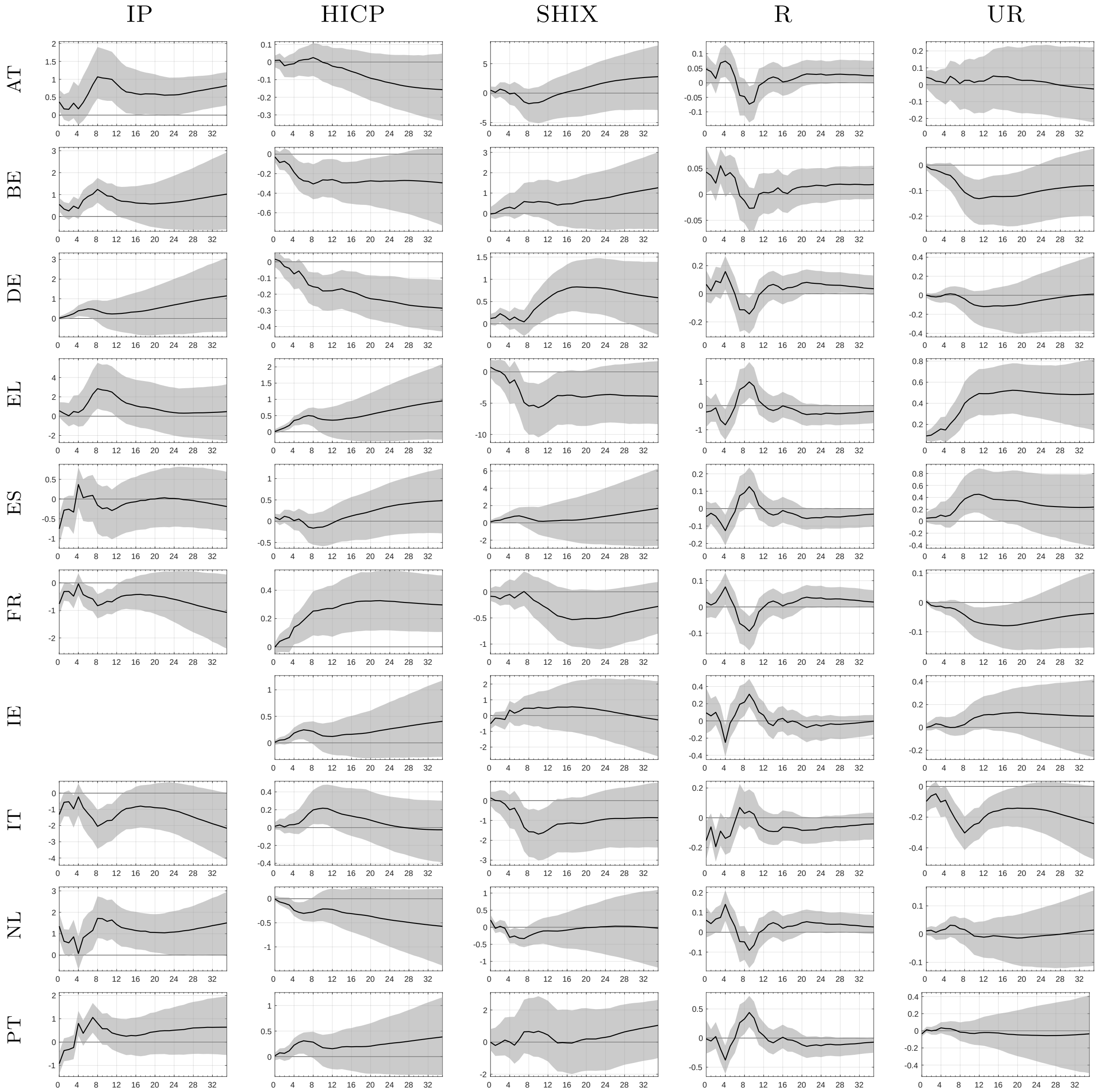

NOTES: Each sub-figure plots the difference between the country-level IRF and the corresponding EA counterpart for one variable and one country. Each column of the graph represents a variable, while each row represents a country. The black solid line is the point estimate in our baseline setting, while the gray shaded area is the corresponding 68% confidence interval. The scale in the vertical axis differs across variables and countries.

3.3.4 Cross-country characteristics and heterogeneous IRF dynamics

To investigate cross-country differences in responses to monetary policy shocks, we follow the methodology outlined in Corsetti et al. (2022). For each country, we compile data on selected institutional characteristics, including–but not limited to–labor market features, the financial conditions of firms and households, wage and price dynamics, and other country-specific factors. Whenever possible, these variables are averaged over the sample period; otherwise, we use data up to the most recent available period. We then compute the correlation between each explanatory variable and the peak response of the country-specific IRFs. Variables for this exercise are chosen following Corsetti et al. (2022), with additional indicators included where relevant according to the existing literature. The results of this analysis are reported in Table 3.4.

Table 3.4: *Cross-country characteristics and IRFs dynamics: correlation analysis*

ID	Variable	IP	HICP	R	SHIX	UR
1	Employment Protection	-0.03	-0.20	-0.03	-0.10	-0.32
		(0.38)	(0.35)	(0.35)	(0.35)	(0.34)
2	Wage Adj. Frequency: more than once a year	0.28	-0.28	0.31	0.33	-0.46
		(0.43)	(0.39)	(0.39)	(0.39)	(0.36)
3	Wage Adj. Frequency: once a year	0.55	-0.08	0.32	-0.06	0.35
		(0.37)	(0.41)	(0.39)	(0.41)	(0.38)
4	Wage Adj. Frequency: less than once a year	-0.61	0.01	-0.54	-0.35	-0.46
		(0.35)	(0.41)	(0.34)	(0.38)	(0.36)
5	Price Flexibility	0.17	-0.39	-0.21	0.65	-0.02
		(0.44)	(0.41)	(0.44)	(0.34)	(0.45)
6	NFC Leverage	0.22	-0.38	-0.33	0.62*	-0.21
		(0.37)	(0.33)	(0.33)	(0.28)	(0.35)
7	Homeownership	-0.06	0.37	0.14	-0.07	0.44
		(0.38)	(0.33)	(0.35)	(0.35)	(0.32)
8	Homeownership with mortgage	0.35	-0.66**	-0.33	0.60*	-0.26
		(0.35)	(0.27)	(0.33)	(0.28)	(0.34)
9	Homeownership without mortgage	-0.33	0.76**	0.35	-0.54	0.47
		(0.36)	(0.23)	(0.33)	(0.30)	(0.31)
10	Fixed-Rate Mortgages	-0.07	-0.59*	-0.34	0.37	-0.63*
		(0.38)	(0.28)	(0.33)	(0.33)	(0.28)
11	Loan to Value	-0.17	-0.27	-0.37	0.61*	-0.20
		(0.40)	(0.36)	(0.35)	(0.30)	(0.37)
12	Share of HtM	0.33	0.41	0.39	0.06	0.38
		(0.36)	(0.32)	(0.33)	(0.35)	(0.33)
13	Share of WHtM	0.26	0.53	0.50	-0.10	0.53
		(0.37)	(0.30)	(0.31)	(0.35)	(0.30)
14	Saving Rate	-0.08	-0.78***	-0.65**	0.63*	-0.44
		(0.38)	(0.22)	(0.27)	(0.28)	(0.32)
15	Explained Variance	-0.82***	0.12	-0.78***	0.47	0.25
		(0.22)	(0.35)	(0.22)	(0.31)	(0.34)

Notes: Each entry of the table corresponds to the correlation between each indicator (in the row) and the peak of the impulse response for a specific variable (in the columns). Standard errors in parentheses, asterisks denote statistical significance at 99% (***), 95% (**), and 90% (*). The first row reports the Employment Protection Index (OECD). Rows 2–4 show the frequency of wage adjustments by firms (Branten et al., 2018), while row 1 reports the frequency with which firms adjust output prices (Gautier et al., 2024). Row 6 shows the leverage of non-financial corporations relative to GDP (Eurostat). Row 7 reports the homeownership rate as a share of the population (Eurostat). Rows 8 and 9 indicate, respectively, the shares of residential properties with and without an outstanding mortgage (Eurostat). Row 10 reports the share of fixed-rate mortgages (De Stefani and Mano, 2025). Row 11 shows the average household loan-to-value ratio from the Eurosystem Household Finance and Consumption Survey (HFCS). Rows 12 and 13 display, respectively, the shares of "wealthy hand-to-mouth" and "poor hand-to-mouth" households, constructed as in Slacalek et al. (2020) based on HFCS data. Row 14 reports the household saving rate as a percentage of GDP (OECD). Finally, row 15 corresponds to the share of variance explained by the common factors for each variable in the columns, as reported in Table 3.3.

We begin by examining labor market indicators, including wage flexibility and job security. For wages, we consider three levels of wage adjustment frequency: more than once a year, once a year, and less than once a year. We find no statistically significant relationship between downward wage rigidity and heterogeneous responses across countries. Nevertheless, the signs of the correlations suggest that higher wage rigidity is associated with a stronger response in real activity and a more muted response in prices, consistent with a flatter aggregate demand curve (Christiano et al., 2005). Results for the employment protection index are weaker: as expected, higher employment protection corresponds to a smaller increase in unemployment, but its effect on other variables is relatively muted. Turning to firm characteristics, lower price stickiness is associated with a stronger transmission of monetary policy to prices, along with a more muted response in real activity (see, e.g. Alvarez et al., 2016). Regarding the financial structure of firms, the results suggest that a higher leverage ratio of non-financial corporations relative to GDP is linked to a weaker response in real activity and stock prices, but a stronger response in prices. Similar findings are reported by Dedola and Lippi (2005), as higher leverage proxies for borrowing capacity and, consequently, firm performance. For households, we focus on their housing situation and consumption behavior. Our results indicate that homeownership per se provides little information on cross-country heterogeneity. In contrast, the method of financing housing appears more relevant. Countries with a higher share of homeowners with a mortgage experience a stronger impact on prices (and a weaker impact on stock prices), whereas the opposite holds for homeowners without a mortgage. This finding is consistent with recent literature, which, building on rational inattention models, shows that households with mortgages are more attentive to central bank communication and interest rate decisions, thereby enhancing monetary policy transmission (Ahn et al., 2024). We do not find any meaningful relationship between the type of mortgages (i.e., fixed versus floating) and country-specific responses. However, in countries where households have higher loan-to-value ratios on their mortgages, the impact on stock prices is smaller, further reinforcing the mechanism described in Dedola and Lippi (2005). Unlike Corsetti et al. (2022), we do not find any statistically significant results related to households' consumption habits. However, the direction of our findings is consistent with theirs. Specifically, hand-to-mouth households tend to dampen the transmission of monetary policy to prices, production, and the labor market, while increasing its impact on interest rates and having no effect on stock prices. Similar patterns are observed for wealthy hand-to-mouth consumers. From a broader perspective, higher saving rates are associated with a stronger impact on prices. In contrast, long-term interest rates exhibit a less pronounced increase, while the negative effects on stock prices are mitigated. Finally, we examine how the degree of cross-sectional comovement for each variable, as quantified in Section 3.3.1, influences dynamic responses across countries. We find that countries whose industrial production is more closely aligned with the rest of the panel are notably more affected by the contractionary shock. This finding is consistent with Table 3.3, which shows the largest comovements in industrial production among the main manufacturing countries in the EA. In contrast, the impact on long-term interest rates is smaller for countries that are more aligned with the panel. This reflects the fact that countries with more idiosyncratic dynamics experience the strongest transmission of monetary policy to sovereign yield movements.

Overall, the results highlight several interesting channels through which a common monetary policy is transmitted across countries. However, these findings should be interpreted with caution, as they are based on variability across a relatively small cross-section of countries and should be regarded primarily as descriptive.

3.4 Conclusions

Using the newly developed EA-MD-QD dataset, this chapter examines the transmission of a common monetary policy shock across euro area (EA) countries through a Common Component Structural VAR framework. Our results reveal moderate but meaningful heterogeneity in the propagation of monetary policy. Differences are most evident in price and interest rate dynamics, while responses in output and labor market variables are comparatively more homogeneous. Among individual countries, Germany's reactions closely track the EA aggregate, whereas Greece exhibits stronger deviations.

By correlating peak impulse responses with country-specific characteristics, we provide suggestive evidence that structural factors–such as homeownership and saving behavior—help explain cross-country differences in transmission strength. These findings underscore that, even under a common monetary policy, national economic structures and institutions play a key role in shaping adjustment dynamics.

Overall, the analysis highlights that achieving policy effectiveness and convergence within the EA requires continued attention to structural asymmetries across member states. Future research could extend this framework to assess how these heterogeneities evolve over time, particularly in response to changing financial conditions and unconventional monetary policies.

Chapter 4

Large datasets for the Euro Area and its member countries

4.1 Introduction

The recent and ongoing "data revolution" has enabled researchers to collect and process large amounts of information, thereby broadening the scope of macroeconomic research. The availability of high-dimensional datasets—where the number of series, N, can be comparable to or even exceed the time dimension, T—allows researchers to exploit the rich information contained in large sets of macroeconomic and financial indicators. This, in turn, facilitates addressing relevant policy questions using econometric methods specifically designed to handle, and in some cases benefit from, such large datasets.

In this chapter, we present and document a new large-scale dataset for macroeconomic analysis, denoted as EA-MD-QD. The dataset comprises time series for both the euro area (EA) as a whole and its ten largest member countries, providing an accessible and comprehensive resource for policy analysis of EA-wide outcomes. It also enables comparisons across data vintages and empirical studies. Overall, EA-MD-QD includes 1136 time series, spanning the period 2000–2025 (with continuous updates), at either monthly or quarterly frequency depending on data availability. The countries covered are Austria, Belgium, France, Germany, Greece, Ireland, Italy, the Netherlands, Portugal, and Spain. All the series are retrieved from institutional sources, namely Eurostat, ECB, OECD and FRED.

Although the cost of data collection has substantially decreased in recent years, several sunk costs still hinder data availability and, consequently, the reproducibility of economic research. First, the manual updating of time series becomes increasingly burdensome as the dimensionality of the dataset grows, highlighting the need for systematic procedures to facilitate data acquisition. Second, once collected, data are often not immediately suitable for analysis due to issues such as seasonality, non-stationarity, and missing values, which require additional preprocessing. In this work, we aim to reduce—if not entirely eliminate—these costs by providing a dataset that is periodically updated and accompanied by codes enabling users to generate, within seconds, a research-ready dataset. The complete datasets, together with the codes for data transformation, missing-value imputation, and the treatment of outliers and the COVID period, are publicly available online.[1]

As data are updated on a monthly basis, the dataset includes real-time monthly vintages that are made available to users. Specifically, updates occur at the end of each calendar month, either on the last working day or on the day when all updates scheduled for that month by the data providers have been released. Making vintages publicly available serves two main purposes.

[1] https://zenodo.org/doi/10.5281/zenodo.10514667

First, it enables users to account for the effects of data revisions across different periods, which have been shown to matter in many macroeconomic applications (see, e.g., Orphanides and van Norden, 2002). Second, it fosters the reproducibility of research findings, as users can identify and retrieve the exact data vintage employed in a given analysis.

Building on the seminal contribution of Stock and Watson (1996), several large-scale datasets have been developed to foster macroeconomic research. Among the most prominent examples are FRED-MD and FRED-QD (McCracken and Ng, 2016, 2020), two publicly available collections of monthly and quarterly macroeconomic and financial time series for the United States. Similarly, Fortin-Gagnon et al. (2022) constructed a large dataset for Canada for macroeconomic analysis.

To the best of our knowledge, this is the first attempt to provide a comprehensive dataset for macroeconomic research that encompasses both the euro area (EA) as a whole and its largest member countries. The closest reference to our work using EA data is the real-time database developed by Giannone et al. (2012), which relies on the information contained in the ECB's Monthly Bulletins, i.e. the rawest information set available to policymakers on the data of the ECB governing council. Our dataset differs from theirs along several dimensions. First, the shorter amount of vintages of our data prevents a fully real-time analysis of the type conducted by Giannone et al. (2012). Second, both the timing of data collection and the information content of our dataset do not correspond to any specific policy meeting or information set available to policymakers. Instead, we provide a snapshot of macroeconomic conditions in the EA and its largest member countries at a given point in time. Hence, the purpose and scope of the two datasets is different. Finally, unlike Giannone et al. (2012), our dataset also covers the largest EA countries, with the aim of offering comparable information at both the national and EA aggregate levels. In doing so, we provide practitioners with all the tools needed to make the dataset readily usable for empirical macroeconomic research.

By reducing the sunk costs of data collection, harmonization, and maintenance, EA-MD-QD aims to serve as a public good for the macroeconomic research community. It can be used for a wide range of applications—from forecasting and structural analysis to studying business-cycle synchronization or monetary transmission.

The chapter is organized as follows. Section 4.1.1 presents the series included in the dataset. Section 4.2 defines the pre-treatment applied to each series. Section 4.3 describes all data transformations, while Section 4.4 defines the treatment of outliers. Section 4.5 concluded. The Supplementary Appendix provides a detailed list of all data sources, and describes the transformations applied in Chapter 3.

4.1.1 Data Description

The dataset is constructed according to three guiding principles: (i) *accessibility*: all series are sourced from public, institutional databases; (ii) *timeliness*: the dataset is fully web-scraped, enabling monthly updates of all series in the panel according to their respective release calendars; and (iii) *coverage*: it includes variables representing the most relevant sources for modern macro-financial analysis. Importantly, the monthly update provides practitioners with a new vintage of the dataset each month, incorporating all data releases and revisions to previously published series, if any. All monthly vintages are available from the initial release of EA-MD-QD in January 2024.

Euro Area. The EA dataset comprises $N = 118$ series, of which $N_Q = 71$ are quarterly and $N_M = 47$ are monthly. All series span from 2000:Q1 (2000:M1) to the most recent available observation. The selection of variables follows established datasets for the US (McCracken and Ng, 2016, 2020) and covers: (1) National Accounts, (2) Labor Market Indicators, (3) Credit Aggregates, (4) Labor Costs, (5) Exchange Rates, (6) Financial Markets, (7) Industrial Production and Turnover, (8) Prices, (9) Confidence Indicators and (10) Monetary Aggregates.

Among the 118 series, 104 are sourced from Eurostat, 10 from the ECB Data Warehouse, 3 from the OECD Statistical Database, and 1 from the FRED portal.

Countries. In addition to the EA dataset, we provide datasets for the ten largest EA countries: Austria, Belgium, France, Germany, Greece, Ireland, Italy, the Netherlands, Portugal, and Spain. Each country-specific dataset is constructed according to the same principles used for the EA data, with a few exceptions. For instance, variables related to Monetary Aggregates are not included at the country level, as they cannot be straightforwardly attributed to individual countries. Other groups of variables (e.g., Credit Aggregates or Industrial Production and Turnover) are smaller for some countries, such as Ireland, due solely to data availability.

Table 4.1 provides a summary of the series included in the dataset, along with a brief description, the measurement unit, seasonal adjustment, frequency and provider. For each series, the last columns of Table 4.1 indicate the countries for which the series is available. A checkmark denotes availability, while a dash indicates that the series is not available for that country.

Finally, Table 4.2 provides a more detailed breakdown of the series by country, organized according to the ten macro-categories included in the dataset. Broadly, each category is similarly represented across countries, with two notable exceptions: indicators of industrial production and turnover are unavailable for Ireland, and producer prices are missing for both Ireland and Portugal. Consequently, the frequency of individual series is generally uniform across countries. Specifically, for both the EA and each individual country, approximately 60% of the series are quarterly, while the remaining 40% (20% for Ireland) are monthly. For a detailed description of all series, see Table M2 in Supplementary Appendix 4.A.

4.2 Pre-treatment of the series

Due to their mixed-frequency nature, the datasets are inherently unbalanced, with quarterly series recorded in the first month of each corresponding quarter and missing values in the remaining months.[2] The datasets are accompanied by codes that allow users to handle this unbalanced structure. Practitioners can choose to: (i) retain the mixed-frequency format; (ii) subset the datasets to include only monthly or only quarterly variables; or (iii) aggregate all data to the quarterly frequency, thus obtaining a balanced dataset for each country. In the latter case, monthly series are aggregated to the quarterly level by summing the values of monthly *flow* variables and taking the mean of monthly *stock* variables.[3]

After the aggregation procedure, the datasets remain unbalanced due to both data availability and ragged edges arising from the asynchronous release of different series. Regarding data availability, while most series begin at or before 2000:Q1 (2000:M1), some start later.[4] As for release timing, the series are updated at different intervals across categories: some variables (e.g., National Accounts) are published roughly one to two months after the end of the reference quarter, while others (e.g., Credit Aggregates) may be released up to four months later. The companion codes provided with the dataset allow practitioners to impute these missing values. A formal discussion of the imputation procedure is presented in Section 4.4.

[2]For example, GDP for 2023:Q1 is recorded in January 2023, while the values for February and March are left as missing.

[3]Alternatively, one could take the value from the last month of the reference quarter as the quarterly observation. However, this approach would overlook intra-quarter dynamics that may be informative. For instance, if 2020:Q2 were represented solely by June 2020 data, much of the COVID-19 shock observed in April 2020 would be disregarded.

[4]For instance, Unit Labor Costs for the Euro Area are available only from 2001:Q1, resulting in four missing observations for the period 2000:Q1–2000:Q4.

Table 4.1: *Data Description by country*

Identifiers								Countries										
N	**ID**	**Series**	**Unit**	**SA**	**F**	**P**	**C**	**EA**	**AT**	**BE**	**DE**	**EL**	**ES**	**FR**	**IE**	**IT**	**NL**	**PT**
(1) **National Accounts**																		
1	GDP	Real Gross Domestic Product	CLV15	SCA	Q	EUR	R	✓	✓	✓	✓	✓	✓	✓	✓	✓	✓	✓
2	EXPGS	Real Export Goods and services	CLV15	SCA	Q	EUR	R	✓	✓	✓	✓	✓	✓	✓	✓	✓	✓	✓
3	IMPGS	Real Import Goods and services	CLV15	SCA	Q	EUR	R	✓	✓	✓	✓	✓	✓	✓	✓	✓	✓	✓
4	GFCE	Real Government Final consumption expenditure	CLV15	SCA	Q	EUR	R	✓	✓	✓	✓	✓	✓	✓	✓	✓	✓	✓
5	HFCE	Real Households consumption expenditure	CLV15	SCA	Q	EUR	R	✓	✓	✓	✓	✓	✓	✓	✓	✓	✓	✓
6	CONSD	Real Households consumption expenditure: Durable Goods	CLV15	SCA	Q	EUR	R	✓	✓	✓	✓	✓	✓	✓	✓	✓	✓	✓
7	CONSSD	Real Households consumption expenditure: Semi-Durable Goods	CLV15	SCA	Q	EUR	R	-	✓	-	✓	-	-	✓	✓	✓	✓	-
8	CONSSV	Real Households consumption expenditure: Services	CLV15	SCA	Q	EUR	R	-	✓	-	✓	-	-	✓	✓	✓	✓	-
9	CONSND	Real Households consumption expenditure: Non-Durable Goods	CLV15	SCA	Q	EUR	R	✓	✓	-	✓	-	-	✓	✓	✓	✓	-
10	GCF	Real Gross capital formation	CLV15	SCA	Q	EUR	R	✓	✓	✓	✓	✓	✓	✓	✓	✓	✓	✓
11	GCFC	Real Gross fixed capital formation	CLV15	SCA	Q	EUR	R	✓	✓	✓	✓	✓	✓	✓	✓	✓	✓	✓
12	GFACON	Real Gross Fixed Capital Formation: Construction	CLV15	SCA	Q	EUR	R	✓	✓	-	✓	✓	✓	✓	✓	✓	✓	✓
13	GFAMG	Real Gross Fixed Capital Formation: Machinery and Equipment	CLV15	SCA	Q	EUR	R	✓	✓	-	✓	✓	✓	✓	✓	✓	✓	✓
14	AHRDI	Adjusted Households Real Disposable Income	%chg	SCA	Q	EUR	R	✓	-	-	-	-	-	-	-	-	-	-
15	AHFCE	Actual Final Consumption Expenditure of Households	%chg	SCA	Q	EUR	R	✓	-	-	-	-	-	-	-	-	-	-
16	GNFCPS	Gross Profit Share of Non-Financial Corporations	%	SCA	Q	EUR	R	✓	✓	✓	✓	✓	✓	✓	✓	✓	✓	✓
17	GNFCIR	Gross Investment Share of Non-Financial Corporations	%	SCA	Q	EUR	R	✓	✓	✓	✓	✓	✓	✓	✓	✓	✓	✓
18	GHIR	Gross Investment Rate of Households	%	SCA	Q	EUR	R	✓	✓	-	✓	-	✓	✓	✓	✓	✓	✓
19	GHSR	Gross Households Savings Rate	%	SCA	Q	EUR	R	✓	✓	✓	✓	-	✓	✓	✓	✓	✓	✓
(2) **Labor Market Indicators**																		
20	TEMP	Total Employment (domestic concept)	1000p	SCA	Q	EUR	R	✓	✓	✓	✓	✓	✓	✓	✓	✓	✓	✓
21	EMP	Employees (domestic concept)	1000p	SCA	Q	EUR	R	✓	✓	✓	✓	✓	✓	✓	✓	✓	✓	✓
22	SEMP	Self Employment (domestic concept)	1000p	SCA	Q	EUR	R	✓	✓	✓	✓	✓	✓	✓	✓	✓	✓	✓
23	THOURS	Hours Worked: Total	I15	SCA	Q	EUR	R	✓	✓	-	✓	✓	✓	✓	✓	✓	✓	✓
24	EMPAG	Quarterly Employment: Agriculture, Forestry, Fishing	1000p	SCA	Q	EUR	R	✓	✓	✓	✓	✓	✓	✓	✓	✓	✓	✓
25	EMPIN	Quarterly Employment: Industry	1000p	SCA	Q	EUR	R	✓	✓	✓	✓	✓	✓	✓	✓	✓	✓	✓
26	EMPMN	Quarterly Employment: Manufacturing	1000p	SCA	Q	EUR	R	✓	✓	✓	✓	✓	✓	✓	✓	✓	✓	✓
27	EMPCON	Quarterly Employment: Construction	1000p	SCA	Q	EUR	R	✓	✓	✓	✓	✓	✓	✓	✓	✓	✓	✓
28	EMPRT	Quarterly Employment: Wholesale/Retail trade, transport, food	1000p	SCA	Q	EUR	R	✓	✓	✓	✓	✓	✓	✓	✓	✓	✓	✓
29	EMPIT	Quarterly Employment: Information and Communication	1000p	SCA	Q	EUR	R	✓	✓	✓	✓	✓	✓	✓	✓	✓	✓	✓
30	EMPFC	Quarterly Employment: Financial and Insurance activities	1000p	SCA	Q	EUR	R	✓	✓	✓	✓	✓	✓	✓	✓	✓	✓	✓
31	EMPRE	Quarterly Employment: Real Estate	1000p	SCA	Q	EUR	R	✓	✓	✓	✓	✓	✓	✓	✓	✓	✓	✓
32	EMPPR	Quarterly Employment: Professional, Scientific, Technical activities	1000p	SCA	Q	EUR	R	✓	✓	✓	✓	✓	✓	✓	✓	✓	✓	✓
33	EMPPA	Quarterly Employment: PA, education, health ad social services	1000p	SCA	Q	EUR	R	✓	✓	✓	✓	✓	✓	✓	✓	✓	✓	✓
34	EMPENT	Quarterly Employment: Arts and recreational activities	1000p	SCA	Q	EUR	R	✓	✓	✓	✓	✓	✓	✓	✓	✓	✓	✓
35	UNETOT	Unemployment: Total (% active population)	%	SA	M	EUR	R	✓	✓	✓	✓	✓	✓	✓	✓	✓	✓	✓
36	UNEO25	Unemployment: Over 25 years (% active population)	%	SA	M	EUR	R	✓	✓	✓	✓	✓	✓	✓	✓	✓	✓	✓
37	UNEU25	Unemployment: Under 25 years (% active population)	%	SA	M	EUR	R	✓	✓	✓	✓	✓	✓	✓	✓	✓	✓	✓
38	RPRP	Real Labour Productivity (person)	I15	SCA	Q	EUR	R	✓	✓	✓	✓	✓	✓	✓	✓	✓	✓	✓
39	WS	Wages and salaries	CP	SCA	Q	EUR	N	✓	✓	✓	✓	✓	✓	✓	✓	✓	✓	✓
40	ESC	Employers' Social Contributions	CP	SCA	Q	EUR	N	✓	✓	✓	✓	✓	✓	✓	✓	✓	✓	✓
(3) **Credit Aggregates**																		
41	TASS.SDB	Total Economy - Assets: Short-Term Debt Securities	MLN€	MSA	Q	EUR	F	✓	✓	✓	✓	✓	✓	✓	✓	✓	✓	✓
42	TASS.LDB	Total Economy - Assets: Long-Term Debt Securities	MLN€	MSA	Q	EUR	F	✓	✓	✓	✓	✓	✓	✓	✓	✓	✓	✓
43	TASS.SLN	Total Economy - Assets: Short-Term Loans	MLN€	MSA	Q	EUR	F	✓	✓	✓	✓	✓	✓	✓	✓	✓	✓	✓
44	TASS.LLN	Total Economy - Assets: Long-Term Loans	MLN€	MSA	Q	EUR	F	✓	✓	✓	✓	✓	✓	✓	✓	✓	✓	✓
45	TLB.SDB	Total Economy - Liabilities: Short-Term Debt Securities	MLN€	MSA	Q	EUR	F	✓	✓	✓	✓	-	✓	✓	✓	✓	✓	✓
46	TLB.LDB	Total Economy - Liabilities: Long-Term Debt Securities	MLN€	MSA	Q	EUR	F	✓	✓	✓	✓	✓	✓	✓	✓	✓	✓	✓
47	TLB.SLN	Total Economy - Liabilities: Short-Term Loans	MLN€	MSA	Q	EUR	F	✓	✓	✓	✓	✓	✓	✓	✓	✓	✓	✓
48	TLB.LLN	Total Economy - Liabilities: Long-Term Loans	MLN€	MSA	Q	EUR	F	✓	✓	✓	✓	✓	✓	✓	✓	✓	✓	✓
49	NFCASS	Non-Financial Corporations: Total Financial Assets	MLN€	MSA	Q	EUR	F	✓	✓	✓	✓	✓	✓	✓	✓	✓	✓	✓
50	NFCASS.SLN	Non-Financial Corporations - Assets: Short-Term Loans	MLN€	MSA	Q	EUR	F	✓	✓	✓	✓	-	✓	✓	✓	✓	✓	✓
51	NFCASS.LLN	Non-Financial Corporations - Assets: Long-Term Loans	MLN€	MSA	Q	EUR	F	✓	✓	✓	✓	-	✓	✓	✓	✓	✓	✓
52	NFCLB	Non-Financial Corporations: Total Financial Liabilities	MLN€	MSA	Q	EUR	F	✓	✓	✓	✓	✓	✓	✓	✓	✓	✓	✓
53	NFCLB.SLN	Non-Financial Corporations - Liabilities - Short-Term Loans	MLN€	MSA	Q	EUR	F	✓	✓	✓	✓	✓	✓	✓	-	✓	✓	✓
54	NFCLB.LLN	Non-Financial Corporations - Liabilities - Long-Term Loans	MLN€	MSA	Q	EUR	F	✓	✓	✓	✓	✓	✓	✓	-	✓	✓	✓
55	GGASS	General Government: Total Financial Assets	MLN€	MSA	Q	EUR	F	✓	✓	✓	✓	✓	✓	✓	✓	✓	✓	✓
56	GGASS.SLN	General Government - Assets: Short-Term Loans	MLN€	MSA	Q	EUR	F	✓	✓	-	-	-	-	-	-	-	✓	-
57	GGASS.LLN	General Government - Assets: Short-Term Loans	MLN€	MSA	Q	EUR	F	✓	✓	-	✓	-	-	✓	-	-	✓	✓
58	GGLB	General Government: Total Financial Liabilities	MLN€	MSA	Q	EUR	F	✓	✓	✓	✓	✓	✓	✓	✓	✓	✓	✓
59	GGLB.SLN	General Government - Liabilities: Short-Term Loans	MLN€	MSA	Q	EUR	F	✓	✓	✓	✓	-	✓	✓	✓	✓	✓	✓
60	GGLB.LLN	General Government - Liabilities: Long-Term Loans	MLN€	MSA	Q	EUR	F	✓	✓	✓	✓	-	✓	✓	✓	✓	✓	✓
61	HHASS	Households: Total Financial Assets	MLN€	MSA	Q	EUR	F	✓	✓	✓	✓	✓	✓	✓	✓	✓	✓	✓
62	HHASS.SLN	Households - Assets: Short-Term Loans	MLN€	MSA	Q	EUR	F	✓	-	-	-	-	-	✓	-	-	-	-
63	HHASS.LLN	Households - Assets: Long-Term Loans	MLN€	MSA	Q	EUR	F	✓	-	-	-	-	-	✓	-	-	✓	✓
64	HHLB	Households: Total Financial Liabilities	MLN€	MSA	Q	EUR	F	✓	✓	✓	✓	✓	✓	✓	✓	✓	✓	✓
65	HHLB.SLN	Households - Liabilities: Short-Term Loans	MLN€	MSA	Q	EUR	F	✓	✓	✓	✓	✓	✓	✓	-	✓	✓	✓
66	HHLB.LLN	Households - Liabilities: Long-Term Loans	MLN€	MSA	Q	EUR	F	✓	✓	✓	✓	✓	✓	✓	-	✓	✓	✓
(4) **Labor Costs**																		
67	ULCIN	Nominal Unit Labor Costs: Industry	I16	SCA	Q	EUR	N	✓	✓	✓	✓	✓	✓	✓	✓	✓	✓	✓
68	ULCMQ	Nominal Unit Labor Costs: Mining and Quarrying	I16	SCA	Q	EUR	N	✓	✓	✓	-	✓	-	✓	✓	-	✓	✓
69	ULCMN	Nominal Unit Labor Costs: Manufacturing	I16	SCA	Q	EUR	N	✓	✓	✓	✓	✓	✓	✓	✓	✓	✓	✓
70	ULCCON	Nominal Unit Labor Costs: Construction	I16	SCA	Q	EUR	N	✓	✓	✓	✓	✓	✓	✓	-	✓	✓	✓
71	ULCRT	Nominal Unit Labor Costs: Wholesale/Retail Trade, Transport, Food, IT	I16	SCA	Q	EUR	N	✓	✓	✓	✓	✓	✓	✓	✓	✓	✓	✓
72	ULCFC	Nominal Unit Labor Costs: Financial Activities	I16	SCA	Q	EUR	N	✓	✓	✓	✓	✓	✓	✓	✓	✓	✓	✓
73	ULCRE	Nominal Unit Labor Costs: Real Estate	I16	SCA	Q	EUR	N	✓	✓	✓	✓	✓	✓	✓	-	✓	✓	✓
74	ULCPR	Nominal Unit Labor Costs: Professional, Scientific, Technical activities	I16	SCA	Q	EUR	N	✓	✓	✓	✓	✓	✓	✓	✓	✓	✓	✓
(5) **Financial Markets**																		
75	REER42	Real Exchange Rate (42 main industrial countries)	I10	NSA	M	EUR	F	✓	✓	✓	✓	✓	✓	✓	✓	✓	✓	✓
76	ERUS	Exchange Rate (US dollar)	I10	NSA	M	EUR	F	✓	-	-	-	-	-	-	-	-	-	-
77	SHIX	Share Prices	I10	SA	M	OECD	F	✓	✓	✓	✓	✓	✓	✓	✓	✓	✓	✓
(6) **Interest Rates**																		
79	IRT3M	3-Months Interest Rates	%	NSA	M	EUR	F	✓	-	-	-	-	-	-	-	-	-	-
79	IRT6M	6-Months Interest Rates	%	NSA	M	EUR	F	✓	-	-	-	-	-	-	-	-	-	-
80	LTIRT	Long-Term Interest Rates (EMU Criterion)	%	NSA	M	EUR	F	✓	✓	✓	✓	✓	✓	✓	✓	✓	✓	✓

Table 4.1: *Data Description by country*

Identifiers								Countries										
N	**ID**	**Series**	**Unit**	**SA**	**F**	**P**	**C**	**EA**	**AT**	**BE**	**DE**	**EL**	**ES**	**FR**	**IE**	**IT**	**NL**	**PT**
(7) **Industrial Production and Turnover**																		
81	IPMN	Industrial Production Index: Manufacturing	I21	SCA	M	EUR	R	✓	✓	✓	✓	✓	✓	✓	-	✓	✓	✓
82	IPCAG	Industrial Production Index: Capital Goods	I21	SCA	M	EUR	R	✓	✓	✓	✓	✓	✓	✓	-	✓	✓	✓
83	IPCOG	Industrial Production Index: Consumer Goods	I21	SCA	M	EUR	R	✓	✓	✓	✓	✓	✓	✓	-	✓	-	-
84	IPDCOG	Industrial Production Index: Durable Consumer Goods	I21	SCA	M	EUR	R	✓	✓	✓	✓	✓	✓	✓	-	✓	✓	✓
85	IPNDCOG	Industrial Production Index: Non Durable Consumer Goods	I21	SCA	M	EUR	R	✓	✓	✓	✓	✓	✓	✓	-	✓	✓	✓
86	IPING	Industrial Production Index: Intermediate Goods	I21	SCA	M	EUR	R	✓	✓	✓	✓	✓	✓	✓	-	✓	✓	✓
87	IPNRG	Industrial Production Index: Energy	I21	SCA	M	EUR	R	✓	✓	✓	✓	✓	✓	✓	-	✓	✓	✓
88	TRNMN	Turnover Index: Manufacturing	I21	SCA	M	EUR	R	✓	✓	✓	✓	✓	✓	✓	-	-	✓	✓
89	TRNCAG	Turnover Index: Capital Goods	I21	SCA	M	EUR	R	✓	✓	✓	✓	✓	✓	✓	-	✓	✓	✓
90	TRNCOG	Turnover Index: Consumer Goods	I15	SCA	M	EUR	R	✓	✓	✓	✓	✓	✓	✓	-	✓	✓	✓
91	TRNDCOG	Turnover Index: Durable Consumer Goods	I21	SCA	M	EUR	R	✓	✓	✓	✓	✓	✓	✓	-	✓	✓	✓
92	TRNNDCOG	Turnover Index: Non Durable Consumer Goods	I21	SCA	M	EUR	R	✓	✓	✓	✓	✓	✓	✓	-	✓	✓	✓
93	TRNING	Turnover Index: Intermediate Goods	I21	SCA	M	EUR	R	✓	✓	✓	✓	✓	✓	✓	-	✓	✓	✓
94	TRNNRG	Turnover Index: Energy	I21	SCA	M	EUR	R	✓	✓	✓	✓	✓	✓	✓	-	✓	-	✓
95	CAREG	Passenger's Cars Registrations	1000U	SCA	M	ECB	R	✓	-	-	-	-	-	-	-	-	-	-
(8) **Prices**																		
96	PPICAG	Producer Price Index: Capital Goods	I21	MSA	M	EUR	N	✓	✓	✓	✓	✓	✓	✓	-	✓	✓	-
97	PPICOG	Producer Price Index: Consumer Goods	I21	MSA	M	EUR	N	✓	✓	✓	✓	✓	✓	✓	-	✓	✓	-
98	PPIDCOG	Producer Price Index: Durable Consumer Goods	I21	MSA	M	EUR	N	✓	✓	✓	✓	✓	✓	✓	-	✓	✓	-
99	PPINDCOG	Producer Price Index: Non Durable Consumer Goods	I21	MSA	M	EUR	N	✓	✓	✓	✓	✓	✓	✓	-	✓	✓	-
100	PPIING	Producer Price Index: Intermediate Goods	I21	MSA	M	EUR	N	✓	✓	✓	✓	✓	✓	✓	-	✓	✓	-
101	PPINRG	Producer Price Index: Energy	I21	MSA	M	EUR	N	✓	✓	✓	✓	✓	✓	✓	-	✓	✓	-
102	HICPOV	Harmonized Index of Consumer Prices: Overall Index	I10	SCA	M	ECB	N	✓	✓	✓	✓	✓	✓	✓	✓	✓	✓	✓
103	HICPNEF	Harmonized Index of Consumer Prices: All Items, no Energy&Food	I10	SCA	M	ECB	N	✓	✓	✓	✓	✓	✓	✓	✓	✓	✓	✓
104	HICPG	Harmonized Index of Consumer Prices: Goods	I10	SCA	M	ECB	N	✓	✓	✓	✓	✓	✓	✓	✓	✓	✓	✓
105	HICPIN	Harmonized Index of Consumer Prices: Industrial Goods	I10	SCA	M	ECB	N	✓	✓	✓	✓	✓	✓	✓	✓	✓	✓	✓
106	HICPSV	Harmonized Index of Consumer Prices: Services	I10	SCA	M	ECB	N	✓	✓	✓	✓	✓	✓	✓	✓	✓	✓	✓
107	HICPNG	Harmonized Index of Consumer Prices: Energy	I10	MSA	M	EUR	N	✓	✓	✓	✓	✓	✓	✓	✓	✓	✓	✓
108	DFGDP	Real Gross Domestic Product Deflator	I15	SCA	Q	EUR	N	✓	✓	✓	✓	✓	✓	✓	✓	✓	✓	✓
109	HPRC	Residential Property Prices (BIS)	MLN€	SCA	Q	FRED	N	✓	✓	✓	✓	-	✓	✓	✓	✓	✓	-
(9) **Confidence Indicators**																		
110	ICONFIX	Industrial Confidence Indicator	Index	SA	M	EUR	C	✓	✓	✓	✓	✓	✓	✓	✓	✓	✓	✓
111	CCONFIX	Consumer Confidence Index	Index	SA	M	EUR	C	✓	✓	✓	✓	✓	✓	✓	✓	✓	✓	✓
112	ESENTIX	Economic Sentiment Indicator	Index	SA	M	EUR	C	✓	✓	✓	✓	✓	✓	✓	✓	✓	✓	✓
113	KCONFIX	Construction Sentiment Indicator	Index	SA	M	EUR	C	✓	✓	✓	✓	✓	✓	✓	✓	✓	✓	✓
114	RTCONFIX	Retail Confidence Indicator	Index	SA	M	EUR	C	✓	✓	✓	✓	✓	✓	✓	✓	✓	✓	✓
115	SCONFIX	Services Confidence Indicator	Index	SA	M	EUR	C	✓	✓	✓	✓	✓	✓	✓	✓	✓	✓	✓
116	BCI	Business Confidence Index	2010=100	SA	M	OECD	C	✓	✓	✓	✓	✓	✓	✓	✓	✓	✓	✓
117	CCI	Consumer Confidence Index	2010=100	SA	M	OECD	C	✓	✓	✓	✓	✓	✓	✓	✓	✓	✓	✓
(10) **Monetary Aggregates**																		
118	CURR	Money Stock: Currency	MLN€	SCA	M	ECB	F	✓	-	-	-	-	-	-	-	-	-	-
119	M1	Money Stock: M1	MLN€	SCA	M	ECB	F	✓	-	-	-	-	-	-	-	-	-	-
120	M2	Money Stock: M2	MLN€	SCA	M	ECB	F	✓	-	-	-	-	-	-	-	-	-	-

Table 4.2: *Number of series: EA and individual countries*

	EA	**AT**	**BE**	**DE**	**EL**	**ES**	**FR**	**IE**	**IT**	**NL**	**PT**	**TOTAL**
(1) National Accounts	17	17	11	17	12	14	17	17	17	17	14	161
(2) Labor Market Indicators	21	21	20	21	21	21	21	21	21	21	21	229
(3) Credit Aggregates	26	24	22	23	17	22	25	18	22	25	24	248
(4) Labor Costs	8	8	8	7	8	7	8	6	7	8	8	85
(5) Financial Markets	3	2	2	2	2	2	2	2	2	2	2	23
(6) Interest Rates	3	1	1	1	1	1	1	1	1	1	1	12
(7) Production and Turnover	14	14	14	14	14	14	14	0	13	12	13	136
(8) Prices	14	14	14	14	13	14	14	8	14	14	7	140
(9) Confidence Indicators	8	8	8	8	8	8	8	8	8	8	8	88
(10) Monetary Aggregates	3	0	0	0	0	0	0	0	0	0	0	3
(1)-(10) TOTAL	118	109	100	107	96	103	110	81	105	108	99	1136

While most series in the datasets are already seasonally adjusted at the source, some are only available in raw form. For these, we retrieve the unadjusted series and apply seasonal adjustment *ex post*. In particular, we employ standard seasonal filtering methods (Findley et al., 1998) for monthly variables, while quarterly variables are adjusted using a simple dummy-variable approach.[5] Across the EA and country-level datasets, only *Credit Aggregates* and *Producer Prices* are not seasonally adjusted at the source, accounting on average for about 30% of the total series in each dataset. Starting from the October 2025 release, we also provide users with raw data, where these series remain unadjusted, allowing researchers to apply their own seasonal adjustment procedures if desired.

[5] It is well known that filtering techniques can suffer from end-of-sample issues, requiring many observations to obtain reliable estimates of the trend component. Given the limited time span at the quarterly frequency, end-of-period estimates for seasonally adjusted quarterly variables obtained with these filters are therefore unreliable.

4.3 Transformations to stationarity

Being composed of variables that capture a wide range of economic and financial aggregates, the datasets include both stationary and non-stationary series. Although recent advances in econometric methods allow for the presence of non-stationarity in large-dimensional settings (Barigozzi et al., 2021), many empirical applications still require stationary data. For this reason, together with the raw data, we provide users with benchmark transformation codes designed to achieve stationarity.

The proposed set of transformations aims to remove any $I(1)$ or $I(2)$ dynamics from the level of the series, allowing for multiple differencing where necessary. To identify whether a series exhibits $I(1)$ or $I(2)$ behavior, we apply the non-parametric test of Phillips and Perron (1988) to both the levels and first differences of each variable. In some instances, we override the test results to ensure a degree of homogeneity within groups of related series.[6] Overall, both across variable categories and countries, only a small number of series exhibit $I(2)$ dynamics. Most of these belong to the group of Credit Aggregates, distributed relatively evenly across countries, with a few notable exceptions related to Unit Labor Costs and Labor Market Indicators. Conversely, the majority of the series in the panel are $I(1)$ and thus require differencing to achieve stationarity. A smaller subset of variables is instead $I(0)$, primarily concentrated among confidence indicators and, for some countries, national accounts variables.

The transformations are applied uniformly across countries, with only minor deviations reflecting country-specific idiosyncrasies that generate dynamics differing from those of the corresponding EA series. A complete list of all series, their respective transformations, and a cross-country comparison is provided in Table 4.A2 in the Supplementary Appendix 4.A.

4.4 Treatment of missing values and outliers

As discussed in Section 4.2, regardless of the dataset frequency, missing values remain due to ragged edges arising from data availability and the asynchronous timing of data releases. Moreover, the transformations applied to the series, as described in Section 4.3, introduce additional missing values because of observation losses (e.g., when taking first differences). While the untreated data are always provided, the companion codes to the dataset allow practitioners to choose among different strategies for handling missing values.

Specifically, outliers can be imputed using the Expectation–Maximization (EM) algorithm proposed by Stock and Watson (2002b) and also employed by McCracken and Ng (2016). This represents the most straightforward approach commonly used in the literature for imputing both outliers and missing values, though not necessarily the most sophisticated. Alternative procedures have been proposed, among which the algorithm by Bańbura and Modugno (2014) is particularly suitable when the data exhibit a factor structure with autocorrelated factors. In our context, however, the number of missing values to be imputed is limited (both with and without outlier adjustment), so the two imputation methods deliver virtually identical results, leaving the main findings unaffected.[7]

Furthermore, the dataset may contain outliers and we follow McCracken and Ng (2020) for their definition and treatment. Namely, an observation is considered an outlier if it deviates from the sample median by more than ten interquartile ranges and it is imputed by means of the EM algorithm, exploiting the information contained in the other series in the panel. This applies to all sample except the Covid period.

[6] For example, if only a subset of price series displays $I(1)$ dynamics, we treat all price variables as $I(1)$ to maintain consistency across the group.

[7] The companion codes provided allow users to select the imputation algorithm for missing values, enabling them to choose the approach that best suits their needs.

Unlike "standard" outliers, the COVID shock is pervasive, affecting most series in the panel–particularly those representing the real economy–with substantial heterogeneity even within these series. Moreover, it is unclear how much of the COVID shock should be attributed to economic versus exogenous forces (Ng, 2021). In light of these considerations, treating the COVID period as composed of sporadic outliers would result in the loss of potentially important economic information relevant for understanding the current economic stance.

4.5 Conclusions

This chapter introduces EA-MD-QD, a new high-dimensional dataset covering both the euro area (EA) and its ten largest member countries. The dataset provides a unified, continuously updated, and fully documented resource for macroeconomic research. By combining national and aggregate data from institutional sources and making both the data and accompanying codes publicly available, EA-MD-QD reduces the sunk costs of data collection, transformation, and maintenance that often hinder reproducibility in empirical economics.

The dataset is designed to serve a broad range of research and policy applications, from forecasting and nowcasting to structural and cross-country analyses. Its monthly vintages make it particularly suited for studies of real-time data revisions and the evolution of economic assessments over time. By offering harmonized, research-ready data across multiple countries, EA-MD-QD contributes to improving the transparency and comparability of macroeconomic analysis in the euro area.

Appendix to Chapter 1

1.A Data Description

Table 4.A2 provides a brief description for each of the 118 series in our dataset. Moreover, for each variable, Table 4.A2 indicates the source, the unit of measure, the seasonal adjustment treatment, the transformation (if any), model for the deterministic component for the idiosyncratic component. Table 1.A1 presents a glossary to proper understand the data description presented in Table 4.A2.

All the series were retrieved in February 2025, with the sample starting in January 2000 and ending in October 2024, the last observation available for all the series. After dropping missing values and transforming the variables, the actual starting point for the analysis is 2001:Q1. Monthly series, which constitute around one-third of the dataset, are aggregated at the quarterly level by simple averages; hence, the sample used for the analysis is 2001:Q1-2024:Q3 ($T = 95$).

Most of the series in the dataset are available already seasonally adjusted from the source, while others, e.g., financial variables and producer price indexes, are only available not seasonality adjusted. In these cases, we deseasonalize the series using a simple dummy variable approach.

TABLE 1.A1: *Glossary*

Source	**Unit**
EUR = Eurostat	CLV= Chain-linked volumes
OECD = Organization for Economic Co-operation and Development	1000-ppl= Thousands of persons
ECB = European Central Bank	1000-U = Thousands of Units
FRED = Federal Reserve Economic Data	CP = Current Prices

SA	**F**	**Trans**	**Trend**	**Idio**
NSA = No Seasonal Adjustment	Q = Quarterly	0 = No Transformation	0 = No Trend	0 = I(0)
SA = Seasonal Adjustment	M = Monthly	1 = First Differences	1 = Deterministic Trend	1 = I(1)
SCA = Seasonal and Calendar Adjustment		2 = Log-Transformations	2 = Time-Varying Trend	
MSA = Manual adjustment		3 = First-Differences in Logs	3 = Time-varying Mean	

TABLE 1.A2: *Data description: Euro Area*

ID	Ticker	Series	Unit	SA	F	Source	Trans	Trend	Idio
		(1) **National Accounts**							
1	GDP	Real Gross Domestic Product	CLV(2015)	SCA	Q	EUR	2	2	0
2	EXPGS	Real Export Goods and services	CLV(2015)	SCA	Q	EUR	2	1	0
3	IMPGS	Real Import Goods and services	CLV(2015)	SCA	Q	EUR	2	1	0
4	GFCE	Real Government Final consumption expenditure	CLV(2015)	SCA	Q	EUR	2	1	0
5	HFCE	Real Households consumption expenditure	CLV(2015)	SCA	Q	EUR	2	1	1
6	CONSD	Real Households consumption expenditure: Durable Goods	CLV(2015)	SCA	Q	EUR	2	1	1
7	CONSND	Real Households consumption expenditure: Non-Durable Goods and Services	CLV(2015)	SCA	Q	EUR	2	1	1
8	GCF	Real Gross capital formation	CLV(2015)	SCA	Q	EUR	2	0	0
9	GCFC	Real Gross fixed capital formation	CLV(2015)	SCA	Q	EUR	2	0	1
10	GFACON	Real Gross Fixed Capital Formation: Construction	CLV(2015)	SCA	Q	EUR	2	0	1
11	GFAMG	Real Gross Fixed Capital Formation: Machinery and Equipment	CLV(2015)	SCA	Q	EUR	2	0	1
12	AHRDI	Adjusted Households Real Disposable Income	%change	SCA	Q	EUR	0	0	0
13	AHFCE	Actual Final Consumption Expenditure of Households	%change	SCA	Q	EUR	0	0	0
14	GNFCPS	Gross Profit Share of Non-Financial Corporations	Percent	SCA	Q	EUR	0	0	0
15	GNFCIR	Gross Investment Share of Non-Financial Corporations	Percent	SCA	Q	EUR	0	0	0
16	GHIR	Gross Investment Rate of Households	Percent	SCA	Q	EUR	0	1	0
17	GHSR	Gross Households Savings Rate	Percent	SCA	Q	EUR	0	0	0
		(2) **Labor Market Indicators**							
18	TEMP	Total Employment (domestic concept)	1000-ppl	SCA	Q	EUR	2	1	1
19	EMP	Employees (domestic concept)	1000-ppl	SCA	Q	EUR	2	1	1
20	SEMP	Self Employment (domestic concept)	1000-ppl	SCA	Q	EUR	2	0	1
21	THOURS	Hours Worked: Total	2015=100	SCA	Q	EUR	2	0	1
22	EMPAG	Quarterly Employment: Agriculture, Forestry, Fishing	1000-ppl	SCA	Q	EUR	2	1	0
23	EMPIN	Quarterly Employment: Industry	1000-ppl	SCA	Q	EUR	2	0	0
24	EMPMN	Quarterly Employment: Manufacturing	1000-ppl	SCA	Q	EUR	2	0	0
25	EMPCON	Quarterly Employment: Construction	1000-ppl	SCA	Q	EUR	2	0	1
26	EMPRT	Quarterly Employment: Wholesale/Retail trade, transport, food	1000-ppl	SCA	Q	EUR	2	1	1
27	EMPIT	Quarterly Employment: Information and Communication	1000-ppl	SCA	Q	EUR	2	1	1
28	EMPFC	Quarterly Employment: Financial and Insurance activities	1000-ppl	SCA	Q	EUR	2	0	1
29	EMPRE	Quarterly Employment: Real Estate	1000-ppl	SCA	Q	EUR	2	0	0
30	EMPPR	Quarterly Employment: Professional, Scientific, Technical activities	1000-ppl	SCA	Q	EUR	2	1	1
31	EMPPA	Quarterly Employment: PA, education, health ad social services	1000-ppl	SCA	Q	EUR	2	1	1
32	EMPENT	Quarterly Employment: Arts and recreational activities	1000-ppl	SCA	Q	EUR	2	1	0
33	UNETOT	Unemployment: Total	%active	SA	M	EUR	0	3	0
34	UNEO25	Unemployment: Over 25 years	%active	SA	M	EUR	0	1	0
35	UNEU25	Unemployment: Under 25 years	%active	SA	M	EUR	0	1	0
36	RPRP	Real Labour Productivity (person)	2015=100	SCA	Q	EUR	2	1	1
37	WS	Wages and salaries	CP	SCA	Q	EUR	2	1	0
38	ESC	Employers' Social Contributions	CP	SCA	Q	EUR	2	1	0
		(3) **Credit Aggregates**							
39	TAS.SDB	Total Economy - Assets: Short-Term Debt Securities	MLN€	MSA	Q	EUR	2	0	1
40	TAS.LDB	Total Economy - Assets: Long-Term Debt Securities	MLN€	MSA	Q	EUR	2	1	0
41	TAS.SLN	Total Economy - Assets: Short-Term Loans	MLN€	MSA	Q	EUR	2	1	0
42	TAS.LLN	Total Economy - Assets: Long-Term Loans	MLN€	MSA	Q	EUR	2	1	1
43	TLB.SDB	Total Economy - Liabilities: Short-Term Debt Securities	MLN€	MSA	Q	EUR	2	0	1
44	TLB.LDB	Total Economy - Liabilities: Long-Term Debt Securities	MLN€	MSA	Q	EUR	2	1	1
45	TLB.SLN	Total Economy - Liabilities: Short-Term Loans	MLN€	MSA	Q	EUR	2	1	1
46	TLB.LLN	Total Economy - Liabilities: Long-Term Loans	MLN€	MSA	Q	EUR	2	1	1
47	NFCAS	Non-Financial Corporations: Total Financial Assets	MLN€	MSA	Q	EUR	2	1	0
48	NFCAS.SLN	Non-Financial Corporations - Assets: Short-Term Loans	MLN€	MSA	Q	EUR	2	1	0
49	NFCAS.LLN	Non-Financial Corporations - Assets: Long-Term Loans	MLN€	MSA	Q	EUR	2	1	0
50	NFCLB	Non-Financial Corporations: Total Financial Liabilities	MLN€	MSA	Q	EUR	2	1	0
51	NFCLB.SLN	Non-Financial Corporations - Liabilities - Short-Term Loans	MLN€	MSA	Q	EUR	2	1	1
52	NFCLB.LLN	Non-Financial Corporations - Liabilities - Long-Term Loans	MLN€	MSA	Q	EUR	2	1	1
53	GGAS	General Government: Total Financial Assets	MLN€	MSA	Q	EUR	2	1	0
54	GGAS.SLN	General Government - Assets: Short-Term Loans	MLN€	MSA	Q	EUR	2	1	0
55	GGAS.LLN	General Government - Assets: Short-Term Loans	MLN€	MSA	Q	EUR	2	0	1
56	GGLB	General Government: Total Financial Liabilities	MLN€	MSA	Q	EUR	2	1	1
57	GGLB.SLN	General Government - Liabilities: Short-Term Loans	MLN€	MSA	Q	EUR	2	1	0
58	GGLB.LLN	General Government - Liabilities: Long-Term Loans	MLN€	MSA	Q	EUR	2	0	1
59	HHAS	Households: Total Financial Assets	MLN€	MSA	Q	EUR	2	1	1
60	HHAS.SLN	Households - Assets: Short-Term Loans	MLN€	MSA	Q	EUR	2	1	0
61	HHAS.LLN	Households - Assets: Long-Term Loans	MLN€	MSA	Q	EUR	2	1	0
62	HHLB	Households: Total Financial Liabilities	MLN€	MSA	Q	EUR	2	2	0
63	HHLB.SLN	Households - Liabilities: Short-Term Loans	MLN€	MSA	Q	EUR	2	0	0
64	HHLB.LLN	Households - Liabilities: Long-Term Loans	MLN€	MSA	Q	EUR	2	2	0

TABLE 1.A2: *Data description: Euro Area*

ID	Ticker	Series	Unit	SA	F	Source	Trans	Trend	Idio
		(4) **Labor Costs**							
65	ULCIN	Nominal Unit Labor Costs: Industry	2016=100	SCA	Q	EUR	2	1	0
66	ULCMQ	Nominal Unit Labor Costs: Mining and Quarrying	2016=100	SCA	Q	EUR	2	1	0
67	ULCMN	Nominal Unit Labor Costs: Manufacturing	2016=100	SCA	Q	EUR	2	1	0
68	ULCCON	Nominal Unit Labor Costs: Construction	2016=100	SCA	Q	EUR	2	1	0
69	ULCRT	Nominal Unit Labor Costs: Wholesale/Retail Trade, Transport, Food, IT	2016=100	SCA	Q	EUR	2	1	0
70	ULCFC	Nominal Unit Labor Costs: Financial Activities	2016=100	SCA	Q	EUR	2	1	0
71	ULCRE	Nominal Unit Labor Costs: Real Estate	2016=100	SCA	Q	EUR	2	1	0
72	ULCPR	Nominal Unit Labor Costs: Professional, Scientific, Technical activities	2016=100	SCA	Q	EUR	2	1	0
		(5) **Exchange Rates**							
73	REER42	Real Exchange Rate (42 main industrial countries)	2010=100	NSA	M	EUR	2	0	0
74	ERUS	Exchange Rate (US dollar)	2010=100	NSA	M	EUR	2	0	0
		(6) **Interest Rates**							
75	IRT3M	3-Months Interest Rates	Percent	NSA	M	EUR	0	0	1
76	IRT6M	6-Months Interest Rates	Percent	NSA	M	EUR	0	0	1
77	LTIRT	Long-Term Interest Rates (EMU Criterion)	Percent	NSA	M	EUR	0	0	1
		(7) **Industrial Production and Turnover**							
78	IPMN	Industrial Production Index: Manufacturing	2021=100	SCA	M	EUR	2	0	1
79	IPCAG	Industrial Production Index: Capital Goods	2021=100	SCA	M	EUR	2	0	1
80	IPCOG	Industrial Production Index: Consumer Goods	2021=100	SCA	M	EUR	2	1	0
81	IPDCOG	Industrial Production Index: Durable Consumer Goods	2021=100	SCA	M	EUR	2	1	0
82	IPNDCOG	Industrial Production Index: Non Durable Consumer Goods	2021=100	SCA	M	EUR	2	1	0
83	IPING	Industrial Production Index: Intermediate Goods	2021=100	SCA	M	EUR	2	0	1
84	IPNRG	Industrial Production Index: Energy	2021=100	SCA	M	EUR	2	1	0
85	TRNMN	Turnover Index: Manufacturing	2021=100	SCA	M	EUR	2	1	1
86	TRNCAG	Turnover Index: Capital Goods	2021=100	SCA	M	EUR	2	1	1
87	TRNDCOG	Turnover Index: Durable Consumer Goods	2021=100	SCA	M	EUR	2	0	0
88	TRNNDCOG	Turnover Index: Non Durable Consumer Goods	2021=100	SCA	M	EUR	2	1	0
89	TRNING	Turnover Index: Intermediate Goods	2021=100	SCA	M	EUR	2	0	0
90	TRNNRG	Turnover Index: Energy	2021=100	SCA	M	EUR	2	0	0
		(8) **Prices**							
91	PPICAG	Producer Price Index: Capital Goods	2021=100	MSA	M	EUR	3	0	0
92	PPIDCOG	Producer Price Index: Durable Consumer Goods	2021=100	MSA	M	EUR	3	0	0
93	PPINDCOG	Producer Price Index: Non Durable Consumer Goods	2021=100	MSA	M	EUR	3	0	0
94	PPIING	Producer Price Index: Intermediate Goods	2021=100	MSA	M	EUR	3	0	0
95	PPIFD	Producer Price Index: Food	2021=100	MSA	M	EUR	3	0	1
96	HICPOV	Harmonized Index of Consumer Prices: Overall Index	2010=100	SCA	M	ECB	3	0	1
97	HICPNEF	Harmonized Index of Consumer Prices: All Items: no Energy & Food	2010=100	SCA	M	ECB	3	3	0
98	HICPG	Harmonized Index of Consumer Prices: Goods	2010=100	SCA	M	ECB	3	3	0
99	HICPSV	Harmonized Index of Consumer Prices: Services	2010=100	SCA	M	ECB	3	3	0
100	HICPNG	Harmonized Index of Consumer Prices: Energy	2010=100	MSA	M	EUR	3	3	0
101	HICPFD	Harmonized Index of Consumer Prices: Food	2010=100	MSA	M	EUR	3	3	0
102	DFGDP	Real Gross Domestic Product Deflator	2015=100	SCA	Q	EUR	3	0	0
103	HPRC	Residential Property Prices (BIS)	MLN€	SCA	Q	FRED	3	0	0
104	POIL	Crude Oil Prices: Brent - Europe	€/barrel	MSA	Q	FRED	3	3	0
105	PNGAS	Global price of Natural gas, EU	€/MMbtu	MSA	Q	FRED	3	3	0
		(9) **Confidence Indicators**							
106	ICONFIX	Industrial Confidence Indicator	Index	SA	M	EUR	0	0	1
107	CCONFIX	Consumer Confidence Indicator	Index	SA	M	EUR	0	0	0
108	ESENTIX	Economic Sentiment Indicator	Index	SA	M	EUR	0	0	1
109	KCONFIX	Construction Confidence Indicator	Index	SA	M	EUR	0	0	1
110	RTCONFIX	Retail Confidence Indicator	Index	SA	M	EUR	0	0	0
111	SCONFIX	Services Confidence Indicator	Index	SA	M	EUR	0	1	1
112	BCI	Cyclically-Adjusted Business Confidence Index	2010=100	SA	M	OECD	0	0	1
113	CCI	Cyclically-Adjusted Consumer Confidence Index	2010=100	SA	M	OECD	0	0	0
		(10) **Monetary Aggregates**							
114	CURR	Money Stock: Currency	MLN€	SCA	M	ECB	2	1	1
115	M1	Money Stock: M1	MLN€	SCA	M	ECB	2	1	1
116	M2	Money Stock: M2	MLN€	SCA	M	ECB	2	1	1
		(11) **Others**							
117	SHIX	Share Prices	2010=100	SA	M	OECD	2	0	1
118	CAREG	Passenger's Cars Registrations	1000-U	SCA	M	ECB	2	0	1

1.B Assumptions

In this section, we state all the formal assumptions underlying the model outlined in Section 1.3.1, and we provide both econometric and economic justifications for these assumptions. Throughout the text, we let t_{19Q4}, t_{20Q1} and t_{21Q4} denote 2019:Q4, 2020:Q1 and 2021:Q4, respectively.

Identifying assumptions for the space spanned by the factors.

(1) The number of factors q is such that $q < n$ and is independent of n.

(2) The q-dimensional vector $\mathbf{f}_t$ is such that $\mathbb{E}[\Delta\mathbf{f}_t] = \mathbf{0}$ and $\mathbb{E}[\Delta\mathbf{f}_t\Delta\mathbf{f}_t'] = \mathbf{I}$.

(3) The $n \times q$ matrix $\boldsymbol{\Lambda} = (\boldsymbol{\lambda}_1 \cdots \boldsymbol{\lambda}_n)'$, with $\boldsymbol{\lambda}_i = (\lambda_{i1} \cdots \lambda_{iq})'$, $1 \leq i \leq n$, is such that $\lim_{n\to\infty} n^{-1}\boldsymbol{\Lambda}'\boldsymbol{\Lambda} = \mathbf{H}$ positive definite.

(4) The scalar g_t is such that $\mathbb{E}[\Delta g_t] = 0$ and $\mathbb{E}[(\Delta g_t)^2] = 1$.

(5) The n-dimensional vector $\boldsymbol{\gamma} = (\gamma_1 \cdots \gamma_n)'$, is such that $\lim_{n\to\infty} n^{-1}\boldsymbol{\gamma}'\boldsymbol{\gamma} > 0$.

(6) The q-dimensional vector $\mathbf{u}_t$ is such that $\mathbb{E}[\mathbf{u}_t] = \mathbf{0}$, $\mathbb{E}[\mathbf{u}_t\mathbf{u}_t'] = \boldsymbol{\Sigma}_u$ is positive definite, and $\mathbb{E}[\mathbf{u}_t\mathbf{u}_{t-k}'] = \mathbf{0}$ for $k \neq 0$. Moreover, s_t is deterministic with $s_t > 0$.

(7) The idiosyncratic innovations e_{it}, $1 \leq i \leq n$, are such that $\mathbb{E}[e_{it}] = 0$, $\mathbb{E}[e_{it}^2] = \sigma_{e_i}^2 > 0$ for all t. Moreover, there exist finite constants $M_{ij} > 0$ independent of t and $0 < \rho < 1$ independent of t, i, and j such that $|\mathbb{E}[e_{it}e_{j,t-k}]| \leq M_{ij}\rho^{|k|}$ for all $k \in \mathbb{Z}$, with $\sum_{i=1,i\neq j}^n M_{ij} \leq M$ and $\sum_{j=1,j\neq i}^n M_{ij} \leq M$ for some finite constant $M > 0$ independent of i, j, and n.

(8) $\mathbb{E}[e_{it}\mathbf{u}_s] = \mathbf{0}$, for all i, t, s.

Assumptions (1)-(3) require the q factors $\mathbf{f}_t$ to be pervasive so that they have a non-negligible effect on the variables of interest (Bai and Ng, 2004; Barigozzi et al., 2021). Following Stock and Watson (2025), these assumptions are extended in parts (4) and (5) to the Covid factor, g_t, where pervasiveness stems from the common nature of the Covid shock affecting most of the series included in the dataset. Including both 2020 and 2021 in the Covid period is consistent with the evolution of the pandemic in Europe.

Assumption (6) assumes white noise innovations whose volatility changes over time after the Covid shock—time-varying volatility is not a prominent feature in the pre-2020 sample (Jarociński and Lenza, 2018). Accounting for the change in volatility due to Covid has proven to be fundamental both for estimation and forecasting, and here we adopt an approach similar to Lenza and Primiceri (2022) by introducing a scaling term s_t modeled independently for each period starting from 2020:Q1. Lenza and Primiceri (2022) analyze monthly US data and impose an exponential decay for s_t starting in June 2020. In contrast, we estimate one parameter for each period starting in 2020:Q1 because many series exhibit large variation even after the first half of 2020, which is not surprising given that (i) mobility restriction measures in the EA were much more restrictive than in the US, lasted for longer, and were also implemented in 2021, and (2) the Russia-Ukraine war had a much larger impact on Europe by pushing natural gas prices (and gasoline prices to a lesser extent) to the roof, and in creating a lot of macro-financial uncertainty. Moreover, as Morley et al. (2023) pointed out, quarterly data do not allow for a sharp identification of the decay parameter.

Assumption (7) allows the idiosyncratic innovations to be mildly cross-sectionally correlated and serially correlated with summable autocovariances, thus compatible with stationary ARMA dynamics (Bai and Ng, 2004; Barigozzi et al., 2021). Last, Assumption (8) requires the idiosyncratic and factor innovations to be uncorrelated at all leads and lags, a requirement consistent with the idea of global macroeconomic shocks being unrelated to local dynamics.

Assumptions on the dynamic specifications on the non-stationary idiosyncratic components and the secular components.

(9) Let $\mathcal{I}_1$ be the set of indexes such that $\xi_{it} \sim I(1)$ if $i \in \mathcal{I}_1$, then $n_I = \#\{i : i \in \mathcal{I}_1\}$ is such that $0 < n_I < n$.

(10) Let $\mathcal{I}_b$ be the set of indexes such that $b_{it} \neq 0$ if $i \in \mathcal{I}_b$, then $n_B = \#\{i : \ i \in \mathcal{I}_b\}$ is such that $0 < n_B < n$. Moreover, $\mathrm{D}_{i0} = a_i \neq 0$, for all i.

(11) Let $\widehat{\sigma}^2_{\Delta y_i}$ and $\widehat{\sigma}^2_{y_i}$ be the sample variances of Δy_{it} and y_{it} respectively, computed for $1 \leq t \leq t_{\text{19Q4}}$ and $t_{\text{21Q4}} + 1 \leq t \leq T$.

   (a) Let $\mathcal{L}_1 := \{\text{GDP, HHLB, HHLB.LLN}\}$ be the set of indexes such that for $i \in \mathcal{L}_1$ we have $\sigma^2_{\eta_i} \neq 0$, then $\mathbb{E}[\eta_{it}] = 0$ and we set $\sigma^2_{\eta_i} = (1600\widehat{\sigma}^2_{\Delta y_i})^{-1}$.

   (b) Let $\mathcal{L}_0 := \{\text{UNETOT, HICPOV, HICPNEF, HICPG, HICPSV, HICPFD, POIL, PNGAS}\}$ be the set of indexes such that for $i \in \mathcal{L}_0$ we have $\sigma^2_{\epsilon_i} \neq 0$, then $\mathbb{E}[\epsilon_{it}] = 0$ and we set $\sigma^2_{\epsilon_i} = (800\widehat{\sigma}^2_{y_i})^{-1}$.

Assumption (9) allows the idiosyncratic component to be $I(1)$ for some, but not all, of the series. This assumption is crucial when estimating the model on a large dataset. Imposing the assumption of all idiosyncratic components being $I(0)$ would be overly restrictive, as it implies cointegration for any q-dimensional vector of series (Barigozzi et al., 2021). While cointegration may hold for certain series, it is highly unlikely to hold for many others. To accommodate potential cointegration, we allow only a limited number n_I of variables to possess a non-stationary idiosyncratic component. Our dataset, where only $n_I = 57$ out of $n = 118$ series exhibit a non-stationary idiosyncratic component, supports this assumption.

Assumption (10) allows for a non-stationary secular component for some, but not all, of the variables in the dataset. This modeling choice is coherent with the properties of a standard macroeconomic dataset. Specifically, variables related to the real sector of the economy, such as consumption or investments, commonly display a distinct (upward) trend. Conversely, this may not hold for other variables, such as inflation rates or interest rates, for example. This intuition finds support in the empirical data, where only $n_B = 58$ out of $n = 118$ series exhibit a linear trend.

Assumptions (10) and (11a) imply that GDP, households' financial liabilities and long-term loans, have a secular component given by the local linear trend model

$$\mathrm{D}_{it} = a_i + b_{it}t, \qquad b_{it} = b_{i,t-1} + \eta_{it}, \qquad i \in \mathcal{L}_1, \tag{1.B1}$$

where $a_i = \mathrm{D}_{i0}$.

We introduce a local-linear trend for GDP to capture the gradual drift in the secular decline in long-run output growth documented both for the US and the EA (Cette et al., 2016; Antolin-Diaz et al., 2017; Gordon, 2018). The literature has identified several factors contributing to this slowdown, with particular emphasis on declining productivity growth. This decline has been more pronounced in the EA due to heterogeneity between core and peripheral countries, as peripheral countries are experiencing a larger misallocation of economic resources (Cette et al., 2016). Therefore, it is crucial to accurately account for these features to assess GDP's long-run dynamics. This assessment is essential for estimating potential output, as it avoids spuriously inflating the output gap with unexplained predictable variation (Ng, 2018).

We introduce a local-linear trend for household financial liabilities and long-term loans, which constitute about 85% of total household liabilities, to capture the slowdown in their average growth rates that occurred since the GFC.

Assumptions (10) and Assumption (11b) implies that the unemployment rate, all consumer price inflation indexes, oil and natural gas prices have a secular component given by the local level model

$$\mathrm{D}_{it} = a_{it}, \qquad a_{it} = a_{i,t-1} + \epsilon_{it}, \qquad i \in \mathcal{L}_0, \tag{1.B2}$$

This specification captures relevant labor and demographic factors that may affect the unemployment rate secular trend, such as, for example, the aging of the population and the misallocation of resources in the labor market due to "soft budget constraints" or stringent labor market policies can lead to a mismatch between employers' needs and the skill-set of the unemployed (Cette et al., 2016). Similarly, this specification also allows us to account for the slowdown in inflation occurred after the GFC.

All the other variables in the dataset have either a deterministic linear trend or a constant mean, i.e, $\mathrm{D}_{it} = a_i + b_i t$ if $i \in \mathcal{I}_b$, or $\mathrm{D}_{it} = a_i$ otherwise. Although it is technically possible to model a time-varying component for all the variables in the dataset, such an approach would introduce complexities in the estimation framework, with the number of latent states increasing linearly with the number of series.

In Assumption (11) we fix the variances of the stochastic secular components following Del Negro et al. (2017) in order to effectively capture the gradual and persistent nature of the secular trends. This specification implies that when $i \in \mathcal{L}_1$, the standard deviation of the secular trend is approximately 1% over 100 years, while when $i \in \mathcal{L}_0$, the standard deviation of the secular trend is approximately 1% over 50 years. This choice consistent with the notion of a slow-moving secular component.

Assumptions on the dynamics of the factors, trend, and cycles.

(12) The polynomial $\det(\mathbf{I} - \sum_{j=1}^{p} \mathbf{A}_j z^j) = 0$ has 1 root in $z = 1$ and the remaining $q-1$ roots in $|z| > 1$.

(13) The q-dimensional vector $\boldsymbol{\psi}$ is such that $\boldsymbol{\beta}'\boldsymbol{\psi} = \mathbf{0}$, where $\boldsymbol{\beta}$ is the $q \times (q-1)$ matrix having as columns the cointegrating vectors of $\mathbf{f}_t$, i.e., such that $\boldsymbol{\beta}'\mathbf{f}_t$ is weakly stationary.

(14) The q-dimensional vector $\boldsymbol{\omega}_t$ is weakly stationary and such that $\mathbb{E}[\boldsymbol{\omega}_t] = \mathbf{0}$ and $\mathbb{E}[\boldsymbol{\omega}_t\boldsymbol{\omega}_t'] = \boldsymbol{\Sigma}_\omega$ is positive definite.

(15) The scalar ν_t is such that $\mathbb{E}[\nu_t] = 0$ and $\mathbb{E}[\nu_t^2] = \sigma_\nu^2 > 0$.

(16) $\mathbb{E}[\nu_t \boldsymbol{\omega}_t] = \mathbf{0}$ for all t.

Assumption (12) imposes that 1 common trend drives the non-stationarity in the common factors, hence, that the factors are cointegrated with $q-1$ cointegrating relations—our data provide strong support for the presence of just one common trend. This is a standard assumption in the literature, which often assumes that common productivity trend is the sole driver of long-run economic growth (see, e.g., Del Negro et al., 2007).

Assumptions (13) and (14) imply that $\boldsymbol{\omega}_t$, defined in (1.6), belongs to the cointegration space of the common factors. This view is consistent with theoretical models assuming that the output gap represents deviations from long-run equilibria determined by a common productivity trend (Del Negro et al., 2007).

Assumption (15) assumes that ν_t is a stochastic process—hence τ_t is a common stochastic trend—but it does not constraint ν_t to be a white noise—hence τ_t to be a random walk. Indeed, our estimates suggest that ν_t is autocorrelated, in line with the theoretical arguments by Lippi and Reichlin (1994).

Finally, Assumption (16) implies contemporaneous orthogonality between potential output and the output gap, which is also assumed in the non-parametric approaches used by Barigozzi and Luciani (2023).

Then, the extended state-space form of the model is given by:

$$y_{it} = \mathrm{D}_{it} + \boldsymbol{\lambda}_i' \mathbf{f}_t + \gamma_i g_t \mathbb{I}_{t_{20Q1} \le t \le t_{21Q4}} + \zeta_{it} + z_{it}, \qquad 1 \le i \le n, \ 1 \le t \le T, \tag{1.B3a}$$

$$\mathbf{f}_t = \sum_{j=1}^{p} \mathbf{A}_j \mathbf{f}_{t-j} + \{s_t \mathbb{I}_{t \ge t_{20Q1}} + (1 - \mathbb{I}_{t \ge t_{20Q1}})\} \mathbf{u}_t, \qquad \mathbf{u}_t \overset{i.i.d.}{\sim} (\mathbf{0}, \boldsymbol{\Sigma}_u), \tag{1.B3b}$$

$$\mathrm{D}_{it} = \begin{cases} a_i + b_i t & \text{if } i \in \mathcal{I}_b, \\ \mathrm{D}_{it-1} + b_{it-1}, \ b_{it} = b_{it-1} + \eta_{it} & \text{if } i \in \mathcal{L}_1, \quad \eta_{it} \sim (0, \sigma^2_{\eta_i}), \\ \mathrm{D}_{it-1} + \epsilon_{i,t} & \text{if } i \in \mathcal{L}_0, \quad \epsilon_{it} \sim (0, \sigma^2_{\epsilon_i}), \\ a_i & \text{otherwise,} \end{cases} \tag{1.B3c}$$

$$\zeta_{it} = \begin{cases} \xi_{it}, \ \xi_{it} = \xi_{i,t-1} + e_{it} & \text{if } i \in \mathcal{I}_1, \quad e_{it} \sim (0, \sigma^2_{e_i}), \\ 0 & \text{if } i \notin \mathcal{I}_1, \end{cases} \tag{1.B3d}$$

$$z_{it} = \begin{cases} z^*_{it} & \text{if } i \in \mathcal{I}_1, \quad z^*_{it} \overset{i.i.d.}{\sim} (0, R_i), \\ e_{it} & \text{if } i \notin \mathcal{I}_1, \quad e_{it} \sim (0, R_i), \end{cases} \tag{1.B3e}$$

$$R_i = \begin{cases} \sigma^2_z & \text{if } i \in \mathcal{I}_1, \\ \sigma^2_{e_i} & \text{if } i \notin \mathcal{I}_1. \end{cases} \tag{1.B3f}$$

As defined in Assumption (9), $\mathcal{I}_1$ denotes the set of series with an $I(1)$ idiosyncratic component. As defined in Assumption (10), $\mathcal{I}_b$ denotes the set of series with a deterministic linear trend. Finally, as defined in Assumption (11), $\mathcal{L}_1$ denotes the set of series with a time-varying trend modeled as a local-linear trend, while $\mathcal{L}_0$ denotes the set of series with a time-varying mean modeled as a random walk.

1.C Estimation in detail

In this section, we provide details on the estimation procedure described in Section 1.3.2.

Estimating the dynamic factor model

Initialization

In order to apply the Kalman filter and smoother, we need initial estimates of all the quantities described in Equations (1.B3a)-(1.B3f), with the exception of $\sigma^2_{\eta_i}$, $\sigma^2_{\epsilon_i}$, both set as in Assumption 11, and σ^2_z set to 10^{-2}, as suggested by Opschoor and van Dijk (2023) who show that smaller values might be detrimental for the performance of the algorithm.

We denote with the superscript "19" all quantities computed with data up to 2019. Let

$\breve{y}_{it}^{19} = (y_t^{19} - \breve{a}_i^{(0),19} - \breve{b}_i^{(0),19} \cdot t)/\widehat{\sigma}^2_{\Delta y_i^{19}}$, where $\widehat{\sigma}^2_{\Delta y_i^{19}}$ is the sample variance of Δy_{it}^{19}, and $\breve{a}_i^{(0),19}$ and $\breve{b}_i^{(0),19}$ are estimated by regressing y_{it}^{19} on a constant and a time trend, whenever $i \in \mathcal{I}_b$ or $i \in \mathcal{L}_1$. If $i \in \mathcal{I}_a$ or $i \in \mathcal{L}_0$ we let $\breve{y}_{it} = y_{it}^{19} - \breve{a}_i^{(0),19}$, where $\breve{a}_i^{(0),19}$ is the sample average of y_{it}. The standardized slopes are denoted as $\widehat{b}_i^{(0),19} = \breve{b}_i^{(0),19}/\widehat{\sigma}^2_{\Delta y_i^{19}}$. We initialize the loadings using the estimator of Barigozzi et al. (2021): the $n \times q$ matrix of estimated loadings $\widehat{\boldsymbol{\Lambda}}^{(0),19} = (\widehat{\boldsymbol{\lambda}}_1^{(0),19}, \ldots, \widehat{\boldsymbol{\lambda}}_q^{(0),19})'$ is obtained by principal components on the standardized first differences of the data, i.e. $(\Delta y_{it}^{19} - \overline{\Delta y_i^{19}})/\widehat{\sigma}^2_{\Delta y_i^{19}}$, where $\overline{\Delta y_i^{19}}$ is the sample mean of Δy_{it}^{19}. Given the loadings, we also obtain a first estimate of the q common factors, $\widehat{\mathbf{f}}_t^{(0),19} = n^{-1}\widehat{\boldsymbol{\Lambda}}^{(0),19\prime}\breve{\mathbf{y}}_t^{19}$ and of the idiosyncratic components, $\widehat{\xi}_{it}^{(0),19} = \breve{y}_{it}^{19} - \widehat{\boldsymbol{\lambda}}_i^{(0),19\prime}\widehat{\mathbf{f}}_t^{(0),19}$. Furthermore, we obtain $\widehat{\mathbf{A}}_j^{(0),19}$, $j = 1, \ldots, p$, by fitting a VAR(p) on $\widehat{\mathbf{f}}_t^{(0),19}$. Given the residuals $\widehat{\mathbf{u}}_t^{(0),19} = \widehat{\mathbf{f}}_t^{(0),19} - \widehat{\mathbf{A}}^{(0),19}\widehat{\mathbf{f}}_{t-1}^{(0),19}$, where $\widehat{\mathbf{A}}^{(0),19}$ is the companion form representation of the autoregressive matrices $\widehat{\mathbf{A}}_1^{(0),19}, \ldots, \widehat{\mathbf{A}}_p^{(0),19}$, an estimate of the latent covariance is given by $\widehat{\boldsymbol{\Sigma}}_u^{(0),19} = \widehat{\mathrm{Cov}}(\widehat{\mathbf{u}}_t^{(0),19})$, where $\widehat{\mathrm{Cov}}$ is the sample covariance matrix. Finally, when $i \notin \mathcal{I}_1$ we set $\widehat{R}_i^{(0),19} = (\widehat{\sigma}_{e_i}^{(0),19})^2 = \widehat{\mathrm{Var}}(\widehat{\xi}_{it}^{(0),19})$, where $\widehat{\mathrm{Var}}$ is the sample variance. And when $i \in \mathcal{I}_1$ we set $(\widehat{\sigma}_{e_i}^{(0),19})^2 = \widehat{\mathrm{Var}}(\Delta\widehat{\xi}_{it}^{(0),19})$.

TABLE 1.C1: *Initialization of states for the Kalman filter*

$\mathbf{f}_{0\|0}^{19} = \widehat{\mathbf{f}}_0^{(0),19}$	
$\mathrm{vec}\left(\mathbf{P}_{0\|0}^{19}\right) = \left(\mathbf{I}_{pq^2} - \widehat{\mathbf{A}}^{(0),19} \otimes \widehat{\mathbf{A}}^{(0),19}\right)^{-1} \mathrm{vec}\left(\widehat{\boldsymbol{\Sigma}}_u^{(0),19}\right)$	
$\mathrm{D}_{i,0\|0}^{19} = \widehat{b}_i^{(0),19}$	if $i \in \{\mathcal{I}_b, \mathcal{L}_1\}$
$\mathrm{D}_{i,0\|0}^{19} = 0$	if $i \in \mathcal{L}_0$
$\mathrm{D}_{i,0\|0}^{19} = 0$	if $i \notin \{\mathcal{I}_b, \mathcal{L}_0, \mathcal{L}_1\}$
$b_{i,0\|0}^{19} = \widehat{b}_i^{(0),19}$	if $i \in \{\mathcal{I}_b, \mathcal{L}_1\}$
$P_{i,0\|0}^{D(19)} = \frac{1}{(1-0.99)^2}\sigma^2_{\eta_i}$	if $i \in \mathcal{L}_1$
$P_{i,0\|0}^{D(19)} = \sigma^2_{\epsilon_i}$	if $i \in \mathcal{L}_0$
$P_{i,0\|0}^{D(19)} = 0$	if $i \notin \{\mathcal{L}_0, \mathcal{L}_1\}$
$P_{i,0\|0}^{b(19)} = \frac{1}{(1-0.99)^2}\sigma^2_{\eta_i}$	if $i \in \mathcal{L}_1$
$\zeta_{i,0\|0}^{19} = \widehat{\xi}_{i1}^{(0),19}$	if $i \in \mathcal{I}_1$
$P_{i,0\|0}^{\zeta(19)} = \frac{1}{(1-0.99)^2}\widehat{\mathrm{Var}}\left(\Delta\widehat{\xi}_{it}^{(0),19}\right)$	if $i \in \mathcal{I}_1$

Table 1.C1 provides an overview of the initial values of the states for the Kalman filter.

Step 1: Estimate the model up to 2019:Q4 (pre-Covid step)

Given the initial values of the parameters and the states, we run the Kalman filter and smoother using a standardized version of the data in levels, up to 2019, that is:

$$\tilde{y}_{it}^{19} = \begin{cases} \frac{y_{it}^{19} - \breve{a}_i^{19}}{\widehat{\sigma}^2_{\Delta y_i^{19}}} & \text{if } i \in \{\mathcal{I}_b, \mathcal{L}_1\} \\ \frac{y_{it}^{19} - \bar{y}_i^{19}}{\widehat{\sigma}^2_{\Delta y_i^{19}}} & \text{otherwise} \end{cases}$$

Given $\tilde{\mathbf{y}}_t^{19} = (\tilde{y}_{1,t}, \ldots, \tilde{y}_{n,t})'$, we obtain a new estimate of the states, namely the factors $\mathbf{f}^{19}_{t|T}$, the time-varying secular components $\mathbf{D}^{19}_{t|T}$ and slopes $\mathbf{b}^{19}_{t|t}$, and the non-stationary idiosyncratic components $\boldsymbol{\zeta}^{19}_{t|T}$, along with the corresponding conditional covariances.

Given the smoothed states, we estimate all the parameters as follows:

- Factor loadings:

$$\widehat{\boldsymbol{\lambda}}_i^{19'} = \left(\sum_{t=1}^{T}\left(\tilde{y}_{it}^{19} - \mathrm{D}^{19}_{i,t|T} - \zeta^{19}_{i,t|T}\right)\mathbf{f}^{19'}_{t|T}\right)\left(\sum_{t=1}^{T}\mathbf{f}^{19}_{t|T}\mathbf{f}^{19'}_{t|T} + \mathbf{P}^{19}_{t|T}\right)^{-1}$$

- Parameters of the law of motion of the common factors:

$$\widehat{\mathbf{A}}^{19} = \left(\sum_{t=2}^{T}\mathbf{f}^{19}_{t|T}\mathbf{f}^{19'}_{t-1|T} + \mathbf{P}^{19}_{t,t-1|T}\right)\left(\sum_{t=2}^{T}\mathbf{f}^{19}_{t-1|T}\mathbf{f}^{19'}_{t-1|T} + \mathbf{P}^{19}_{t-1|T}\right)^{-1}$$

$$\widehat{\boldsymbol{\Sigma}}_u^{19} = \frac{1}{T}\left(\sum_{t=2}^{T}\left(\mathbf{f}^{19}_{t|T}\mathbf{f}^{19'}_{t|T} + \mathbf{P}^{19}_{t|T}\right) - \widehat{\mathbf{A}}^{19}\sum_{t=2}^{T}\left(\mathbf{f}^{19}_{t|T}\mathbf{f}^{19'}_{t-1|T} + \mathbf{P}^{19}_{t,t-1|T}\right)\right)$$

- Slopes of secular trend:

$$\widehat{b}_i^{19} = \left(\sum_{t=1}^{T}\left(\tilde{y}_{it}^{19} - \widehat{\boldsymbol{\lambda}}_i^{19'}\mathbf{f}^{19}_{t|T} - \zeta^{19}_{i,t|T}\right)t\right)\left(\sum_{t=1}^{T}t^2\right)^{-1}$$

- Variance of $I(1)$ idiosyncratic components:

$$\begin{aligned}\widehat{\sigma}_{e_i}^{2,19} &= \frac{1}{T}\sum_{t=2}^{T}\left(\zeta^{19}_{i,t|T}\zeta^{19'}_{i,t|T} + P^{\zeta(19)}_{i,t|T}\right) + \frac{1}{T}\sum_{t=2}^{T}\left(\zeta^{19}_{it-1|T}\zeta^{19'}_{it-1|T} + P^{\zeta(19)}_{i,t-1|T}\right) - \\ &\quad - \frac{2}{T}\sum_{t=2}^{T}\left(\zeta^{19}_{it|T}\zeta^{19'}_{it-1|T} + P^{\zeta(19)}_{i,t,t-1|T}\right)\end{aligned}$$

- Covariance prediction error:

$$\begin{aligned}\widehat{R}_i^{19} &= \frac{1}{T}\sum_{t=1}^{T}\left\{\left(\tilde{y}_{i,t}^{19} - \widehat{\boldsymbol{\lambda}}_i^{19'}\mathbf{f}^{19}_{t|T} - \mathbb{I}_{i\in\mathcal{I}_b}\mathrm{D}^{19}_{i,t|T} - \mathbb{I}_{i\in\mathcal{I}_1}\zeta^{19}_{i,t|T}\right)^2 + \widehat{\boldsymbol{\lambda}}_i^{19'}\mathbf{P}^{19}_{t,T|T}\widehat{\boldsymbol{\lambda}}_i^{19} + \right. \\ &\quad \left. + \mathbb{I}_{i\in\mathcal{I}_b}P^{\mathrm{D}(19)}_{i,t|T} + \mathbb{I}_{i\in\mathcal{I}_1}P^{\zeta(19)}_{i,t|T}\right\}\end{aligned}$$

Step 2: Estimate the Covid factor and volatility (Covid step)

Given the estimated parameters up to 2019:Q4, we run the Kalman filter and smoother using standardized data in levels for the entire sample, that is:

$$\tilde{y}_{it} = \begin{cases} \frac{y_{it} - \breve{a}_i}{\widehat{\sigma}^2_{\Delta y_i}} & \text{if } i \in \{\mathcal{I}_b, \mathcal{L}_1\} \\ \frac{y_{it} - \bar{y}_i}{\widehat{\sigma}^2_{\Delta y_i}} & \text{otherwise} \end{cases}$$

In computing $\bar{y}_i$, $\widehat{\sigma}^2_{\Delta y_i}$ and $\breve{a}_i$, we treat Covid outliers as missing values. Given $\tilde{\mathbf{y}}_t = (\tilde{y}_{1,t}, \ldots, \tilde{y}_{n,t})'$, we obtain the estimated states given the pre-Covid parameters. In doing so, we truncate the

Kalman smoother in correspondence of 2020:Q1, to avoid spurious backward effects from the presence of Covid outliers. The estimated states are denoted as $\mathbf{f}^{(0)}_{t|T}$, $\mathbf{D}^{(0)}_{t|T}$, $\mathbf{b}^{(0)}_{t|T}$ and $\boldsymbol{\zeta}^{(0)}_{t|T}$.

Given the smoothed states, let:

$$\widehat{\boldsymbol{\xi}}_t \;=\; \tilde{\mathbf{y}}_t - \widehat{\boldsymbol{\Lambda}}^{19}\mathbf{f}^{(0)}_{t|T} - \mathbf{D}^{(0)}_{t|T}$$

and denote as $\widehat{\boldsymbol{\Xi}} = (\boldsymbol{\xi}_1, \ldots, \boldsymbol{\xi}_t)'$ the $T \times n$ matrix of idiosyncratic components. Then we estimate the Covid factor by estimating the first principal component using the $n \times n$ variance-covariance matrix of the estimated idiosyncratic components from 2020:Q1 to 2021:Q4, denoted as $\widehat{\boldsymbol{\Sigma}}_{\boldsymbol{\Xi}^C}$. This is the procedure proposed by Stock and Watson (2025) that we modify to account for non-stationarity in the idiosyncratic component. This done by partitioning the matrix of idiosyncratic components during the Covid period as $\widehat{\boldsymbol{\Xi}}^C = (\widehat{\boldsymbol{\Xi}}^{C,1}|\widehat{\boldsymbol{\Xi}}^{C,0})$, where $\widehat{\boldsymbol{\Xi}}^{C,1}$ and $\widehat{\boldsymbol{\Xi}}^{C,1}$ are the matrices of estimated idiosyncratic components in the period 2020:Q1 to 2021:Q4 for $i \in \mathcal{I}_1$ and $i \in \mathcal{I}_0$, respectively. Then, we estimate $\widehat{\boldsymbol{\Sigma}}_{\boldsymbol{\Xi}^C}$ (Hamilton, 2020, Chapter 17; Bai, 2004):

$$\widehat{\boldsymbol{\Sigma}}_{\boldsymbol{\Xi}^C} \;=\; \begin{bmatrix} \frac{1}{(T^C)^2}\widehat{\boldsymbol{\Xi}}^{C,1\prime}\widehat{\boldsymbol{\Xi}}^{C,1} & \frac{1}{(T^C)^{3/2}}\widehat{\boldsymbol{\Xi}}^{C,1\prime}\widehat{\boldsymbol{\Xi}}^{C,0} \\ \frac{1}{(T^C)^{3/2}}\widehat{\boldsymbol{\Xi}}^{C,0\prime}\widehat{\boldsymbol{\Xi}}^{C,1} & \frac{1}{T^C}\widehat{\boldsymbol{\Xi}}^{C,0\prime}\widehat{\boldsymbol{\Xi}}^{C,0} \end{bmatrix}$$

where $T^c = 8$ denotes the time-periods between 2020:Q1 and 2021:Q4.

Given $\widehat{\boldsymbol{\Sigma}}_{\boldsymbol{\Xi}^C}$, we obtain the Covid factor and the corresponding loadings as:

$$\begin{aligned} \widehat{\gamma} \;&=\; \sqrt{n}\cdot\widehat{\mathbf{V}}_{\bar{\boldsymbol{\Xi}}^C} \\ \widehat{\mathbf{g}} \;&=\; \frac{1}{\sqrt{n}}\cdot(\widehat{\boldsymbol{\Xi}}^C\widehat{\mathbf{V}}_{\bar{\boldsymbol{\Xi}}^C}) \end{aligned}$$

where $\widehat{\mathbf{g}}$ is the $T^C \times 1$ vector with entries $\widehat{g}_t$ and $\widehat{\mathbf{V}}_{\boldsymbol{\Xi}^C}$ is the $n \times 1$ eigenvector corresponding to the largest eigenvalue of $\widehat{\boldsymbol{\Sigma}}_{\widehat{\boldsymbol{\Xi}}^C}$. Given $\widehat{\mathbf{g}}$, the associated loadings are $\widehat{\boldsymbol{\gamma}} = (\widehat{\gamma}_1, \ldots, \widehat{\gamma}_n)'$.

Next, give the estimate of states and the Covid factor, we account for the presence of changes in the volatility after the Covid shock by modifying the Lenza and Primiceri (2022) procedure to accommodate for quarterly data. Let $s^*_t = s_t\mathbb{I}_{t\geq t_{20\text{Q1}}} + (1 - \mathbb{I}_{t\geq t_{20\text{Q1}}})$, the likelihood writes as:

$$\begin{aligned} \mathcal{L}(\mathbf{f}^{(0)}\,|\,\mathbf{A}, \boldsymbol{\Sigma}_u, s^*_1, \ldots, s^*_T) \;&\propto\; \prod_{t=2}^{T}\left|(s^*_t)^2\boldsymbol{\Sigma}_u\right|^{-\frac{1}{2}}\cdot\exp\left\{-\frac{1}{2}\sum_{t=2}^{T}\left(\mathbf{f}^{(0)}_{t|T} - \mathbf{A}\mathbf{f}^{(0)}_{t-1|T}\right)'\left(s^2_t\boldsymbol{\Sigma}_u\right)^{-1}\left(\mathbf{f}^{(0)}_{t|T} - \mathbf{A}\mathbf{f}^{(0)}_{t-1|T}\right)\right\} \\ &\propto\; \left(\prod_{t=2}^{T}(s^*_t)^{-n}\right)|\boldsymbol{\Sigma}_u|^{-\frac{T-1}{2}}\cdot\exp\left\{-\frac{1}{2}\sum_{t=2}^{T}\left(\mathbf{f}^{*(0)}_{t|T} - \mathbf{A}\mathbf{f}^{*(0)}_{t-1|T}\right)'(\boldsymbol{\Sigma}_u)^{-1}\left(\mathbf{f}^{*(0)}_{t|T} - \mathbf{A}\mathbf{f}^{*(0)}_{t-1|T}\right)\right\} \end{aligned}$$

where $\mathbf{f}^{*(0)}_{t|T} = \mathbf{f}^{(0)}_{t|T}/s^*_t$, with corresponding variance-covariance matrix $\mathbf{P}^{*(0)}_{t|T}$.

The maximum-likelihood estimators of $\mathbf{A}$ and $\boldsymbol{\Sigma}_u$ given the factors are:

$$\begin{aligned} \check{\mathbf{A}} \;&=\; \left(\sum_{t=2}^{T}\mathbf{f}^{*(0)}_{t|T}\mathbf{f}^{*(0)\prime}_{t-1|T} + \mathbf{P}^{*(0)}_{t,t-1|T}\right)\left(\sum_{t=1}^{T}\mathbf{f}^{*(0)}_{t-1|T}\mathbf{f}^{*(0)\prime}_{t-1|T} + \mathbf{P}^{*(0)}_{t-1|T}\right)^{-1} \\ \check{\boldsymbol{\Sigma}}_u \;&=\; \frac{1}{T}\left(\sum_{t=2}^{T}\left(\mathbf{f}^{*(0)}_{t|T}\mathbf{f}^{*(0)\prime}_{t|T} + \mathbf{P}^{*(0)}_{t|T}\right) - \check{\mathbf{A}}\sum_{t=2}^{T}\left(\mathbf{f}^{*(0)}_{t|T}\mathbf{f}^{*(0)\prime}_{t-1|T} + \mathbf{P}^{*(0)}_{t,t-1|T}\right)\right) \end{aligned}$$

Substituting $\check{\mathbf{A}}$ and $\check{\boldsymbol{\Sigma}}_u$ in the likelihood, we obtain the concentrated likelihood:

$$\mathcal{L}(\mathbf{f}^{(0)}\,|\,\check{\mathbf{A}},\check{\mathbf{\Sigma}}_u,s_1^*,\ldots,s_T^*) \;=\; \prod_{t=2}^{T}(s_t^*)^{-n}\cdot\left|\check{\mathbf{\Sigma}}_u\right|^{-\frac{T}{2}}$$

By numerically maximizing the concentrated likelihood we obtain the volatility parameters $\widehat{s}_t$.

Step 3: Full sample estimation

Given the Covid factor estimated in Step 2, we obtain all the other parameters in the model:

- Factor loadings:

$$\widehat{\boldsymbol{\lambda}}_i' \;=\; \left(\sum_{t=1}^{T}\left(\tilde{y}_{it}-\mathrm{D}_{i,t|T}^{(0)}-\zeta_{i,t|T}^{(0)}\right)\mathbf{f}_{t|T}^{(0)\prime}-\widehat{\gamma}_i\widehat{g}_t\right)\left(\sum_{t=1}^{T}\mathbf{f}_{t|T}^{(0)}\mathbf{f}_{t|T}^{(0)\prime}+\mathbf{P}_{t|T}^{(0)}\right)^{-1}$$

- Slopes of secular trend:

$$\widehat{b}_i \;=\; \left(\sum_{t=1}^{T}\left(\tilde{y}_{it}-\widehat{\boldsymbol{\lambda}}_i'\mathbf{f}_{t|T}^{(0)}-\zeta_{i,t|T}^{(0)}-\widehat{\gamma}_i\widehat{g}_t\right)t\right)\left(\sum_{t=1}^{T}t^2\right)^{-1}$$

- Variance of $I(1)$ idiosyncratic components:

$$\begin{aligned}\widehat{\sigma}_{e_i}^2 \;&=\frac{1}{T}\sum_{t=2}^{T}\left(\zeta_{i,t|T}^{(0)}\zeta_{i,t|T}^{(0)\prime}+P_{i,t|T}^{\zeta(0)}\right)+\frac{1}{T}\sum_{t=2}^{T}\left(\zeta_{it-1|T}^{(0)}\zeta_{it-1|T}^{(0)\prime}+P_{i,t-1|T}^{\zeta(0)}\right)-\\&\quad-\frac{2}{T}\sum_{t=2}^{T}\left(\zeta_{it|T}^{(0)}\zeta_{it-1|T}^{(0)\prime}+P_{i,t,t-1|T}^{\zeta(0)}\right)\end{aligned}$$

- Covariance prediction error:

$$\begin{aligned}\widehat{R}_i \;&=\frac{1}{T}\left\{\sum_{t=1}^{T}\left(\tilde{y}_{i,t}^{(0)}-\widehat{\boldsymbol{\lambda}}_i^{(0)\prime}\mathbf{f}_{t|T}^{(0)}-\mathbb{I}_{i\in\mathcal{I}_b}\mathrm{D}_{i,t|T}^{(0)}-\mathbb{I}_{i\in\mathcal{I}_1}\zeta_{i,t|T}^{(0)}-\widehat{\gamma}_i\widehat{g}_t\right)^2+\widehat{\boldsymbol{\lambda}}_i'\mathbf{P}_{t,T|T}^{(0)}\widehat{\boldsymbol{\lambda}}_i+\right.\\&\quad\left.+\;\mathbb{I}_{i\in\mathcal{I}_b}P_{i,t|T}^{\mathrm{D}(0)}+\mathbb{I}_{i\in\mathcal{I}_1}P_{i,t|T}^{\zeta(0)}\right\}\end{aligned}$$

Given the estimated parameters, using data net of the Covid component, i.e. $\tilde{\mathbf{y}}_t-\widehat{\boldsymbol{\gamma}}\widehat{g}_t$, we obtain a final estimates of all the states, $\mathbf{f}_{t|T}$, $\mathbf{D}_{t|T}$, $\mathbf{b}_{t|T}$, $\boldsymbol{\zeta}_{t|T}$ and their conditional covariances with the Kalman filter and smoother. Note that, for this final run, the Kalman filter and smoother do not need to be truncated in 2019:Q4 because we have already controlled for the Covid pandemic.

Estimating the common trend

With the estimated factors, $\mathbf{f}_{t|T}$, we obtain an estimate of the trend and cyclical component by means of the EM algorithm. To run the algorithm, we need an initial estimate of the parameters $\boldsymbol{\psi}$, $\mathbf{\Sigma}_\omega$, and σ_ν^2.

(a) Let $\widehat{\tau}_t^{(0)}$ be the initial estimate of the common trend. We set $\widehat{\tau}_t^{(0)}=f_{j,t|T}$, where $f_{j,t|T}$ is the factor explaining the largest share of long-run dynamics. Specifically, let $\widehat{S}_j(\omega)$ denote the estimated spectral density of $\Delta f_{j,t|T}$ for frequency ω, and $\widehat{s}_j(\omega)$ be the corresponding standardized spectral density. Let $\bar{s}_j$ be the integral of $\widehat{s}_j(\omega)$ over frequencies ≥ 8 years. The common trend is initialized as the factor $f_{j,t|T}$ with the highest value of $\bar{s}_j$. This corresponds to an initial value of $\boldsymbol{\psi}$, denoted as $\widehat{\boldsymbol{\psi}}^{(0)}$, such that $\widehat{\psi}_j^{(0)} = 1$ and $\widehat{\psi}_{-j}^{(0)} = 0$.

(b) Given $\widehat{\boldsymbol{\psi}}^{(0)}$ and $\widehat{\tau}_t^{(0)}$, we obtain an initial estimate of the cyclical component $\widehat{\boldsymbol{\omega}}_t^{(0)} = \mathbf{f}_{t|T}^{(0)} - \widehat{\boldsymbol{\psi}}^{(0)}\widehat{\tau}_t^{(0)}$

(c) We initialize σ_ν^2 following Del Negro et al. (2017), so that $\widehat{\sigma}_\nu^{2,(0)} = (400\widehat{\sigma}^2_{\Delta\tau})^{-1}$, where $\widehat{\sigma}^2_{\Delta\tau}$ is the sample variance of $\Delta\widehat{\tau}_t^{(0)}$. We chose a very small value for the variance of $\widehat{\sigma}_\nu^{2,(0)}$ to incorporate our prior assumption of a slow-moving trend.

(d) Lastly, since by construction $\widehat{\boldsymbol{\omega}}_t^{(0)}$ has a sample covariance matrix of reduced rank $(q-1)$, in order to run the EM algorithm we initialize this covariance as $\widehat{\boldsymbol{\Sigma}}_\omega^{(0)} = T^{-1}\sum_{t=1}^T \widehat{\boldsymbol{\omega}}_t^{(0)}\widehat{\boldsymbol{\omega}}_t^{(0)\prime} + \kappa\mathbf{I}_q$, where we set $\kappa = 10^{-2}$, in agreement with the recommendations by Opschoor and van Dijk (2023).

Once the initial estimates for the algorithm have been computed, in the E-step we run the Kalman filter and smoother to obtain a new estimate of the trend, namely $\tau_{t|T}^{(1)}$, along with an estimate of its conditional variance and covariance, $P_{t|T}^{(1)}$ and $P_{t,t-1|T}^{(1)}$, respectively. The smoothed trend is then used to estimate the parameters in the M-step. This procedure is repeated iteratively until convergence.

For a generic iteration k of the algorithm, we estimate the parameters as follow:

- Trend loadings:

$$\widehat{\boldsymbol{\psi}}^{(k)} = \left(\sum_{t=1}^T \mathbf{f}_{t|T}\tau_{t|T}^{(k)}\right)\left(\sum_{t=1}^T \tau_{t|T}^{2(k)} + P_{t|T}^{\tau(k)}\right)^{-1}$$

- Variance of common trend:

$$\begin{aligned}\widehat{\sigma}_\nu^{2(k)} &= \frac{1}{T}\sum_{t=2}^T\left(\tau_{t|T}^{2(k)} + P_{t|T}^{\tau(k)}\right) + \frac{1}{T}\sum_{t=2}^T\left(\tau_{t-1|T}^{2(k)} + P_{t-1|T}^{\tau(k)}\right) - \\ &- \frac{2}{T}\sum_{t=2}^T\left(\tau_{t|T}^{(k)}\tau_{t-1|T}^{(k)} + P_{t,t-1|T}^{\tau(k)}\right)\end{aligned}$$

- Covariance of transitory component

$$\widehat{\boldsymbol{\Sigma}}_\omega^{(k)} = \frac{1}{T}\sum_{t=1}^T\left\{\left(\mathbf{f}_{t|T} - \widehat{\boldsymbol{\psi}}^{(k)}\tau_{t|T}^{(k)}\right)\left(\mathbf{f}_{t|T} - \widehat{\boldsymbol{\psi}}^{(k)}\tau_{t|T}^{(k)}\right)' + \widehat{\boldsymbol{\psi}}^{(k)}P_{t|T}^{\tau(k)}\widehat{\boldsymbol{\psi}}^{(k)\prime}\right\}$$

The algorithm is stopped using the likelihood-based criterion of Doz et al. (2012), with a threshold of 10^{-3}. At convergence, we obtain an estimate of the trend and transitory components, $\tau_{t|T}$ and $\boldsymbol{\omega}_{t|T}$, respectively, along with the estimated parameters $\widehat{\boldsymbol{\psi}}$, $\widehat{\sigma}_\nu^2$ and $\widehat{\boldsymbol{\Sigma}}_\omega$.

Ultimately, given the estimated trend and transitory components, the estimated output gap and potential output are defined as:

$$\begin{aligned}\widehat{\mathrm{PO}}_t &= \mathrm{D}_{\mathrm{GDP},t|T} + \widehat{\boldsymbol{\lambda}}'_{\mathrm{GDP}}\widehat{\boldsymbol{\psi}}\tau_{t|T}, \\ \widehat{\mathrm{OG}}_t &= \widehat{\boldsymbol{\lambda}}'_{\mathrm{GDP}}\boldsymbol{\omega}_{t|T}\end{aligned}$$

1.D Confidence bands

To obtain confidence bands for our quantities of interest, we follow the procedure outlined in Barigozzi and Luciani (2023). In particular, we simulate all the states in the model using the simulation smoother of Durbin and Koopman (2002), and we generate all the stationary residuals of the model using a stationary block bootstrap procedure (Politis and Romano, 1994). In practice, we have an estimate of all the states, namely $\mathbf{f}_{t|T}$, $\mathbf{D}_{t|T}$, $\mathbf{b}_{t|T}$ and $\boldsymbol{\zeta}_{t|T}$, an estimate of the Covid factor $\widehat{g}_t$ and the estimated volatility parameters $\widehat{s}_t$, $t \geq t_{\text{20Q1}}$. Then, the algorithm is structured as follows:

1. Simulate the states by the simulation smoother (Durbin and Koopman, 2002)

   (a) Common factors:

      i. simulate $\tilde{\mathbf{f}}_1^{(b)} \sim N\left(\mathbf{f}_{1|T}, \mathbf{P}_{1|T}\right)$;

      ii. simulate $\tilde{\mathbf{u}}_t^{(b)} \sim N\left(\mathbf{0}_q, \check{\boldsymbol{\Sigma}}_u\right)$;

      iii. for $t = 2, \ldots, T$ generate $\tilde{\mathbf{f}}_t^{(b)} = \sum_{k=1}^{p} \check{\mathbf{A}}_k \tilde{\mathbf{f}}_{t-k}^{(b)} + \{s_t \mathbb{I}_{t \geq t_{\text{20Q1}}} + (1 - \mathbb{I}_{t \geq t_{\text{20Q1}}})\} \tilde{\mathbf{u}}_t^{(b)}$.

   (b) $I(1)$ idiosyncratic components. For each $i \in \mathcal{I}_1$:

      i. simulate $\tilde{\xi}_{i1}^{(b)} \sim N\left(\xi_{i,1|T}, P_{i,1|T}^{\zeta}\right)$;

      ii. simulate $\tilde{e}_{it}^{(b)} \sim N\left(0, \widehat{\sigma}_{e_i}^2\right)$;

      iii. for $t = 2, \ldots, T$ generate $\tilde{\zeta}_{it}^{(b)} = \tilde{\xi}_{it}^{(b)}$; $\tilde{\xi}_{it}^{(b)} = \tilde{\xi}_{it-1}^{(b)} + \tilde{e}_{it}^{(b)}$.

   (c) Time-varying secular components:

      - $i \in \mathcal{L}_1$:

        i. simulate $\tilde{b}_{i,1}^{(b)} \sim N\left(b_{i,1|T}, P_{i,1|T}^{b}\right)$, and set $\tilde{\mathrm{D}}_{i,1}^{(b)} = \tilde{b}_{i,1}^{(b)}$;

        ii. simulate $\tilde{\eta}_t^{(b)} \sim N\left(0, \sigma_{\eta_i}^2\right)$;

        iii. for $t = 2, \ldots, T$ generate $\tilde{b}_{i,t}^{(b)} = \tilde{b}_{i,t-1}^{(b)} + \tilde{\eta}_t^{(b)}$;

        iv. for $t = 2, \ldots, T$ generate $\tilde{\mathrm{D}}_{i,t}^{(b)} = \tilde{\mathrm{D}}_{i,t-1}^{(b)} + \tilde{b}_{i,t}^{(b)}$.

      - $i \in \mathcal{L}_0$:

        i. simulate $\tilde{\mathrm{D}}_{i,1}^{(b)} \sim N\left(b_{i,1|T}, P_{i,1|T}^{\mathrm{D}}\right)$

        ii. simulate $\tilde{\epsilon}_t^{(b)} \sim N\left(0, \sigma_{\epsilon_i}^2\right)$;

        iii. for $t = 2, \ldots, T$ generate $\tilde{\mathrm{D}}_{i,t}^{(b)} = \tilde{\mathrm{D}}_{i,t-1} + \tilde{\epsilon}_t^{(b)}$.

2. Simulate the stationary residuals of the model, $\mathbf{z}_t = (z_{1,t}, \ldots, z_{n,t})'$, using a stationary block-bootstrap (Politis and Romano, 1994) with an average block length of four quarters. Denote the resulting simulated residuals as $\tilde{\mathbf{z}}_t^{(b)} = (\tilde{z}_{1,t}^{(b)}, \ldots, \tilde{z}_{n,t}^{(b)})'$.

3. Generate the data. For $t = 1, \ldots, T$, generate:

   (a) $\tilde{y}_{it}^{(b)} = \tilde{\mathrm{D}}_{it}^{(b)} + \widehat{\boldsymbol{\lambda}}_i' \tilde{\mathbf{f}}_t^{(b)} + \widehat{\gamma}_i \widehat{g}_t + \tilde{\zeta}_{it}^{(b)} + \tilde{z}_{it}^{(b)}$, for $i \in \{\mathcal{L}_0, \mathcal{L}_1\}$.

   (b) $\tilde{y}_{it}^{(b)} = \mathrm{D}_{i,t|T} + \widehat{\boldsymbol{\lambda}}_i' \tilde{\mathbf{f}}_t^{(b)} + \widehat{\gamma}_i \widehat{g}_t + \tilde{\zeta}_{it}^{(b)} + \tilde{z}_{it}^{(b)}$, for all other variables.

   where $\tilde{\zeta}_{it}^{(b)} = 0 \ \forall t = 1, \ldots, T$ if $i \notin \mathcal{I}_1$

4. Using $\tilde{\mathbf{y}}_t^{(b)} = (\tilde{y}_{1,t}^{(b)}, \dots, \tilde{y}_{n,t}^{(b)})'$, estimate the model as described in Appendix 1.C to get a new estimate of the loadings, $\widehat{\mathbf{\Lambda}}^{(b)} = (\widehat{\boldsymbol{\lambda}}_1^{(b)\prime}, \dots, \widehat{\boldsymbol{\lambda}}_N^{(b)\prime})'$, and all the other parameters in the model, as well as a new estimate of the states $\mathbf{f}_{t|T}^{(b)}, \mathbf{D}_{t|T}^{(b)}, \mathbf{b}_{t|T}^{(b)}$ and $\boldsymbol{\zeta}_{t|T}^{(b)}$.

5. Center the estimated states: $\bar{\mathbf{f}}_{t|T}^{(b)} = \mathbf{f}_{t|T} - \tilde{\mathbf{f}}_t^{(b)}$, $\bar{\mathbf{D}}_{t|T}^{(b)} = \mathbf{D}_{t|T} - \tilde{\mathbf{D}}_t^{(b)} + \mathbf{D}_{t|T}^{(b)}$, $\bar{\mathbf{b}}_{t|T}^{(b)} = \mathbf{b}_{t|T} - \tilde{\mathbf{b}}_t^{(b)} + \mathbf{b}_{t|T}^{(b)}$ and $\bar{\boldsymbol{\zeta}}_t^{(b)} = \boldsymbol{\zeta}_{t|T} - \tilde{\boldsymbol{\zeta}}_t^{(b)} + \boldsymbol{\zeta}_{t|T}^{(b)}$.

6. Run the trend cycle decomposition on the estimated factors $\bar{\mathbf{f}}_t^{(b)}$ to get a new estimate of the common trend $\tau_{t|T}^{(b)}$, the transitory component $\boldsymbol{\omega}_{t|T}^{(b)}$, and the parameter $\widehat{\boldsymbol{\psi}}^{(b)}$.

7. Estimate potential output as $\widehat{\mathrm{PO}}_t^{(b)} = \bar{\mathrm{D}}_{\mathrm{GDP},t|T}^{(b)} + \widehat{\boldsymbol{\lambda}}_{\mathrm{GDP}}^{(b)\prime} \widehat{\boldsymbol{\psi}}^{(b)} \tau_{t|T}^{(b)}$, and the output gap as $\widehat{\mathrm{OG}}_t^{(b)} = \widehat{\boldsymbol{\lambda}}_{\mathrm{GDP}}^{(b)\prime} \boldsymbol{\omega}_{t|T}^{(b)}$.

Repeating this procedure B times, we obtain a distribution of the output gap: $\{\widehat{\mathrm{OG}}_t^{(b)}, b = 1, \dots, B\}$. Then, we construct the $(1-\alpha)$ confidence interval as $[\widehat{\mathrm{OG}}_t + z_{\alpha/2}\widehat{\sigma}_t^{\mathrm{OG}}, \widehat{\mathrm{OG}}_t + z_{1-\alpha/2}\widehat{\sigma}_t^{\mathrm{OG}}]$, where $\widehat{\sigma}_t^{\mathrm{OG}}$ is the sample standard deviation of $\{\widehat{\mathrm{OG}}_t^{(b)} - \widehat{\mathrm{OG}}_t\}$ and $z_{\alpha/2} = -z_{1-\alpha/2}$ is the $\alpha/2$-th quantile of a standard normal distribution.

1.E Number of Common Factors

In this section, we present the results of various information criteria employed to select the number of common factors.

Assumptions (1)-(3), and (7) imply that the covariance and spectral density matrix of the differenced data $\Delta \mathbf{y}_t = (\Delta y_{1t} \cdots \Delta y_{nt})'$ has at most q eigenvalues diverging as $n \to \infty$, with all the others staying bounded. This allows us to consistently recover the numbers of common factors and common trends via the log-information criteria IC of Bai and Ng (2002), Hallin and Liška (2007), and Alessi et al. (2010), as well at the eigenvalue-ratio criterion by Ahn and Horenstein (2013), and the test proposed by Onatski (2009). In order to avoid spurious effects from the Covid period, we employ standardized and de-meaned first-differenced data up to 2019:Q4.

Table 1.E1: *Number of common factors*

Criteria	q
Alessi et al. (2010)	4
Ahn and Horenstein (2013)	1
Bai and Ng (2002)	4
Hallin and Liška (2007)	4
Onatski (2009)	1

As shown in Table 1.E1, the ABC, BN, and HL criteria suggest $q = 4$, while the AH criteria and the ON test suggest $q = 1$. We picked $q = 4$ because it is well documented that (i) the criteria of Ahn and Horenstein (2013) may underperform if there is a significant difference in the explanatory power of the different factors, which is the case in our dataset where the first factor has a much larger explanatory power than the others; and (ii) the Onatski (2009) may not perform well when T is small compared to n.

1.F Identification à la Morley et al. (2023)

Morley et al. (2024), henceforth MTW, propose an alternative trend smoothing approach to correct the estimated trend whenever it displays some serial correlation in first differences despite being assumed to be a random walk. We can apply the MTW approach in our setting by estimating an ARMA(1,1) model on the first difference of the estimated common trend $\Delta\widehat{\tau}_t^{(0)}$. The trend estimate corrected as in MTW is given by

$$\Delta\widetilde{\tau}_t \;=\; \left(\frac{1+\widehat{\theta}}{1-\widehat{\phi}}\right)\widehat{\varepsilon}_t, \tag{1.F1}$$

where $\widehat{\phi}$ and $\widehat{\theta}$ are the estimated ARMA parameters, and $\widehat{\varepsilon}_t$ are the ARMA residuals. By cumulating $\Delta\tilde{\tau}_t$, we obtain the corrected estimate of the common trend, $\tilde{\tau}_t$.

In practice, smoothing as in (1.F1) seems to be less efficient than our proposal of using the Kalman smoother due to the presence of some residual Covid volatility in the estimated factors that affects the ARMA estimation. In particular, $\widehat{\text{Var}}(\Delta\widehat{\tau}_t) = \widehat{\sigma}^2_\nu = 0.092$ (computed by excluding observation in 2020 and 2021 from the calculation) when estimating the model with our method, and $\widehat{\text{Var}}(\Delta\widetilde{\tau}_t) = (1+\widehat{\theta})(1-\widehat{\phi})^{-1}\widehat{\sigma}^2_\varepsilon = 0.17$, when estimating the model as in (1.F1), using MTW's method, where $\widehat{\sigma}^2_\varepsilon$ is the sample variance of $\widehat{\varepsilon}_t$. Although these values are quite similar, they become very different if we compute them using the whole sample; indeed, they increase to 0.095 and 0.52, respectively. This difference is essentially due to anomalous fluctuations in the ARMA residuals $\widehat{\varepsilon}_t$ during 2020-2021.

Figure 1.F1 compares our output gap estimate with the one obtained by applying the correction proposed by Morley et al. (2024). As expected, the two approaches yield very similar estimates, but in 2021 and 2022, when the MTW corrections reduce the estimate of the output gap from +4% to +3%.

FIGURE 1.F1: *Output gap estimate with identification à la Morley et al. (2024)*

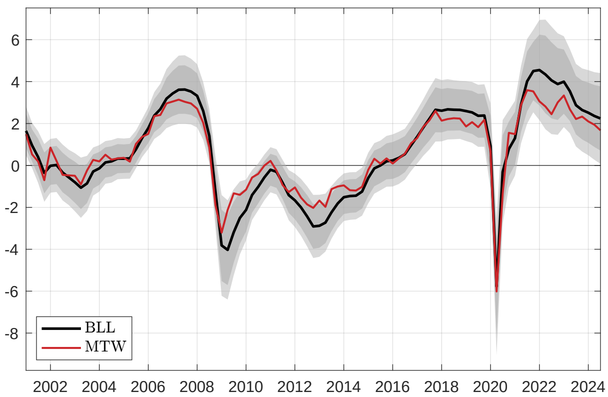

NOTES: The black bold line is our estimate of the output gap. The grey shaded areas are the 68% and 84% confidence bands. The light red line is the estimated output gap obtained applying the correction of the preliminary estimated trend proposed by Morley et al. (2024) (MTW).

1.G Accounting for Covid

1.G.1 Why adjusting for the Covid shock matters

Section 1.3.2 explained how we accounted for the Covid shock when estimating the model. The upper plots in Figure 1.G1 compare our benchmark estimates with the one we would have obtained if we had estimated the model over the full sample without applying any adjustment for the Covid shock ("no adj."). As can be seen, ignoring the Covid shock affects the estimates of potential output and the output gap throughout the sample, which is undesirable; moreover, ignoring the Covid shock distorts the estimate of common dynamics in 2020 and 2021.

FIGURE 1.G1: *Output gap when using pre-Covid parameters or without Covid adjustment*

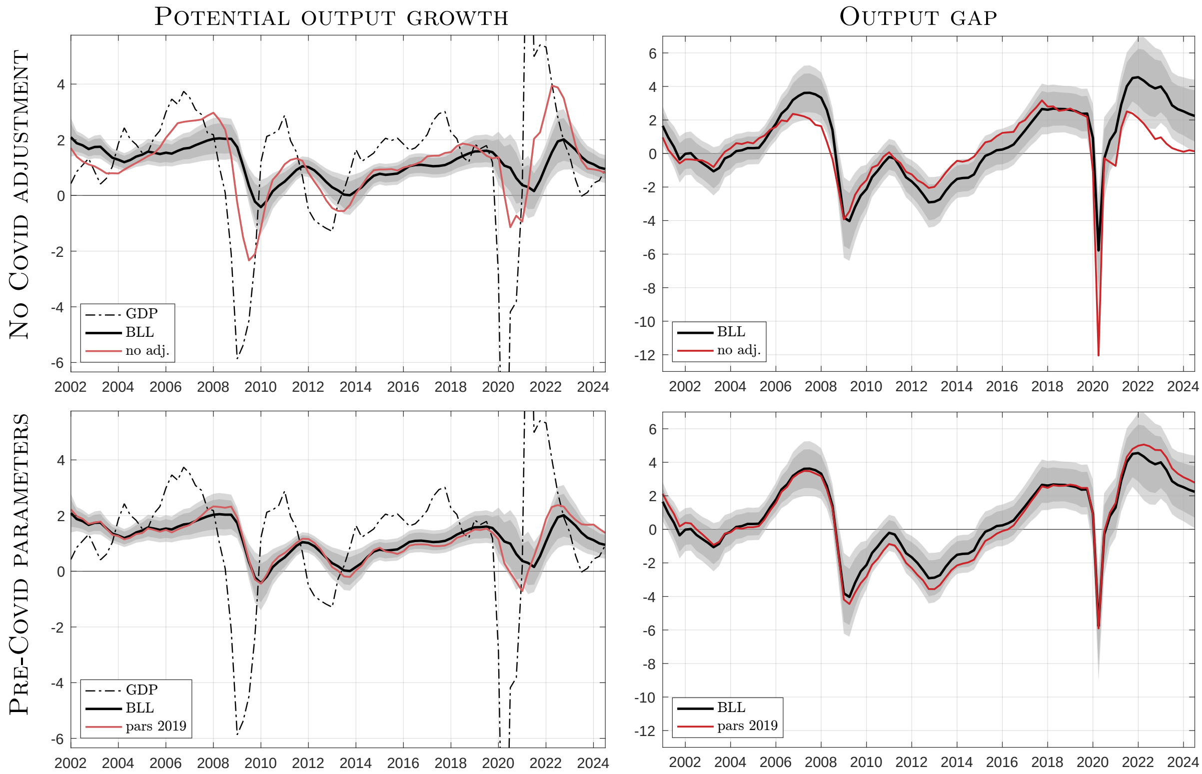

NOTES: The black solid line is our benchmark estimate and the grey shaded areas are the 68% and 84% confidence bands, the black dashed line is GDP YoY growth rate, the red lines are the estimates obtained with two alternative estimation strategies: 1. (left) fixing parameters estimated up to 2019:Q4 (pars 2019); 2. (right) estimating the model with no adjustment for Covid (no adj.).

Having shown that accounting for the Covid shock is necessary, the question is whether a strategy different from the one we adopted would have been desirable. For example, what if we had estimated all parameters up to 2019:Q4 and then extracted the states by simply truncating the Kalman smoother? Despite being effective, this strategy is sub-optimal because estimating the parameters up to 2019 becomes less and less justifiable as new data come in. Moreover, if the increase in volatility induced by the Covid shock turns out to be very persistent, confidence intervals would be underestimated because they only account for the pre-Covid volatility regime. By accounting for the Covid shock, we avoid both these issues.

The lower plots in Figure 1.G1 compare our benchmark estimate with the one obtained by estimating the parameters up to the last quarter of 2019 ("pars 2019"). The two estimates are very similar up to the pandemic, after which the estimate using the up-to-2019 parameters points towards much larger fluctuations in potential output growth and a much larger output gap, which, if taken at face value, signals a very tight economy.

1.G.2 Covid volatiliy

Section 1.3.2 explained how we accounted for the effect of the Covid shock on the volatility of the common factors. Specifically, we follow Lenza and Primiceri (2022) and introduce a factor s_t that scales the volatility of the common factors from the beginning of the pandemic onward. Lenza and Primiceri (2022) analyzed monthly US data and impose an exponential decay for s_t starting in June 2020. In contrast, we estimate one parameter for each period starting in 2020:Q1. This choice is motivated by both the different impact and policy response of the Covid pandemic in Europe and by the fact that, as Morley et al. (2023) pointed out, quarterly data do not allow for a sharp identification of the decay parameter.

The left plot in Figure 1.G2 shows the estimated scaling factor s_t obtained under both our parametrization (black line) and under the exponential decay parametrization proposed by Lenza and Primiceri (2022) (red line). Our estimate of the volatility closely tracks the evolution of the pandemic, as it spikes in the first two quarters of 2020 when mobility restrictions were most stringent in Europe, and pick-up again in 2021:Q1 when the spread of the Delta variant reached its peak. Moreover, we estimate that the volatility is very persistent—the decay we get is very close to 1 (≈ 0.98)—much more persistent than estimated by Lenza and Primiceri (2022), who estimated their model on monthly US data. This difference is likely due to the evolution of the pandemic in Europe, where mobility restriction measures were much more restrictive than in the US, lasted for longer, and were also implemented in 2021. Moreover, the Russia-Ukraine war had a much larger impact on Europe by pushing natural gas (and gasoline prices to a lesser extent) to the roof and creating a lot of macro-financial uncertainty. This result motivates the need to allow for time variation in the factor volatility until the end of the sample.

FIGURE 1.G2: *Output gap estimate with alternative Covid volatility*

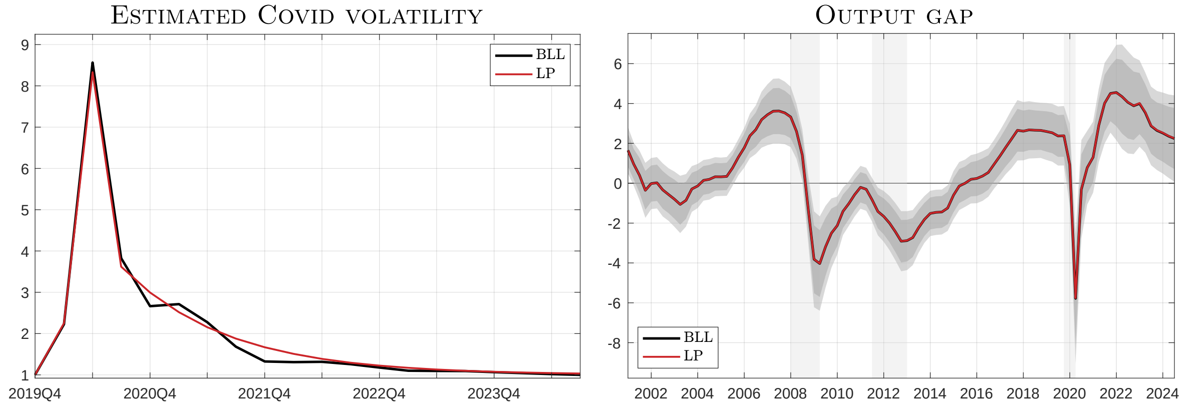

NOTES: In the left plot, the black line is our estimate of Covid volatility (s_t), the red line is the estimate obtained by assuming the exponential decay parametrization of the Covid volatility as in Lenza and Primiceri (2022). In the right plot, the black line is our benchmark estimate and the grey shaded areas are the 68% and 84% confidence bands, the red line is the estimate obtained with the exponential decay parametrization of the Covid volatility.

As shown in the right plot in Figure 1.G2, the two parametrizations lead to virtually identical results.

1.G.3 Alternative estimator for the Covid factor

The approach we described in Appendix 1.C to estimate the Covid factor has the benefit of retaining all the information in $\widehat{\boldsymbol{\xi}}_t$, but it has the problem of relying only on eight data points. That said, since we are only interested in the first eigenvector of $\widehat{\boldsymbol{\Sigma}}_{\widehat{\boldsymbol{\Xi}}^C}$, and given the extent to which the series co-moved during the Covid period, even a few data points should be informative. However, the estimates could be imprecise, thereby motivating an alternative estimation strategy.

As an alternative approach, we estimate the Covid factor by estimating the first principal component using the $T^C \times T^C$ variance-covariance matrix of the estimated idiosyncratic components from 2020:Q1 to 2021:Q4, denoted as $\tilde{\boldsymbol{\Sigma}}_{\boldsymbol{\Xi}^C}$. In order to estimate $\tilde{\boldsymbol{\Sigma}}_{\boldsymbol{\Xi}^C}$, we consider $\widehat{\xi}_{it}$ if $i \in \mathcal{I}_0$ and $\Delta\widehat{\xi}_{it}$ if $i \in \mathcal{I}_1$, i.e. we take first-differences of all non-stationary idiosyncratic components.(8) We obtain the Covid factor and the corresponding loadings as:

$$\tilde{\mathbf{g}} \;=\; \sqrt{T^C} \cdot \tilde{\mathbf{V}}_{\tilde{\boldsymbol{\Xi}}^C}$$
$$\tilde{\boldsymbol{\gamma}} \;=\; \frac{1}{\sqrt{T^C}} \cdot (\widehat{\boldsymbol{\Xi}}^C \tilde{\mathbf{V}}_{\tilde{\boldsymbol{\Xi}}^C})$$

where $\tilde{\mathbf{g}}$ is the $T^C \times 1$ vector with entries $\tilde{g}_t$ and $\tilde{\mathbf{V}}_{\boldsymbol{\Xi}^C}$ is the $T^C \times 1$ eigenvector corresponding to the largest eigenvalue of $\tilde{\boldsymbol{\Sigma}}_{\widehat{\boldsymbol{\Xi}}^C}$. Given $\tilde{\mathbf{g}}$, the associated loadings are $\tilde{\boldsymbol{\gamma}} = (\tilde{\gamma}_1, \ldots, \tilde{\gamma}_n)'$.

This second strategy allows us to estimate $\tilde{\boldsymbol{\Sigma}}_{\widehat{\boldsymbol{\Xi}}^C}$ with N data points, thereby yielding a more precise estimate. However, this comes at the cost of missing important information due to differencing of the non-stationary idiosyncratic component. Which one of the two approaches is better?

As a robustness exercise, in this Appendix we look at what would have been the output gap estimate, had we adopted the second strategy to estimate the Covid factor that we just laid out. As shown in Figure 1.G3, the results obtained with the alternative Covid factor are almost identical to those obtained in the benchmark specification. This is not surprising, since the co-movovements observed in most of the series during the Covid period are so large to be easily identified even with a limited range of observations.

Figure 1.G3: *Output gap estimate with the alternative Covid factor*

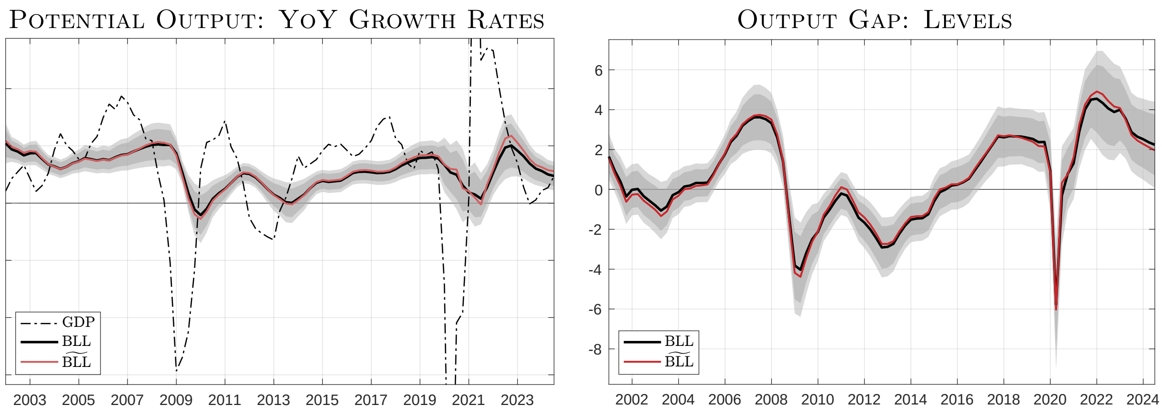

Notes: The black solid line is our benchmark estimate and the grey shaded areas are the 68% and 84% confidence bands. The red solid lines are the estimates obtained with the alternative Covid factor ($\widetilde{\text{BLL}}$). The level of the output gap is the percentage deviation from potential.

(8) In this case $\widehat{\boldsymbol{\xi}}_i$ will be a $T-1$ vector denoting at time t the level of the idiosyncratic component for $i \in \mathcal{I}_0$ and the growth rate of the idiosyncratic component for $i \in \mathcal{I}_1$.

1.H No time-varying parameters

Figure 1.H1 compares the benchmark estimates of the output gap (right plot) and YoY potential output growth (left plot) with those obtained without allowing for a local linear trend for GDP, household liabilities, and long-term loans and no time-varying mean for the unemployment rate and inflation indicators. Removing the time variation in the secular trends leads to a flatter estimate of potential output growth—hence, a lower output gap—in the post-pandemic periods. This result shows that allowing for a time-varying trend for GDP is crucial to properly capture the slowdown in potential output in the latter part of the sample.

FIGURE 1.H1: *Output gap estimate when imposing no time-varying parameters*

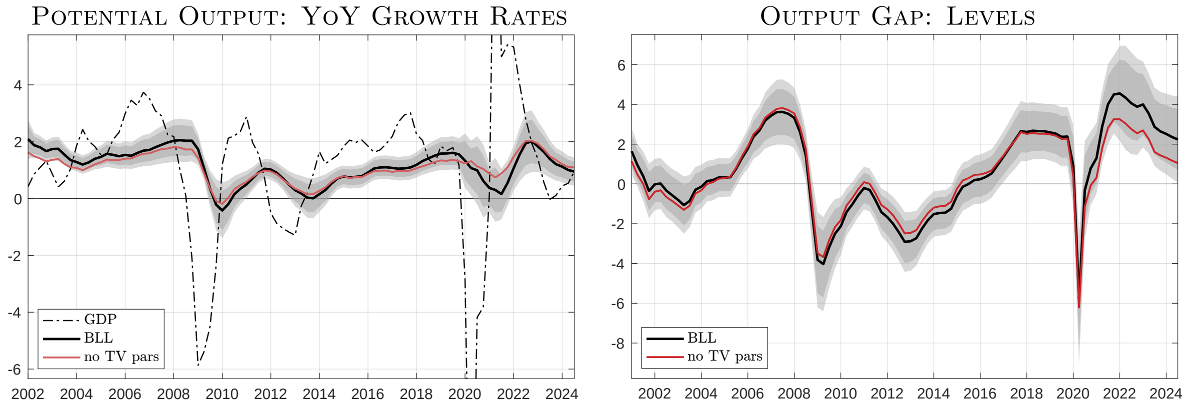

NOTES: The black solid line is our benchmark estimate, the grey shaded areas are the 68% and 84% confidence bands, the black dashed line is GDP YoY growth rate, the red line is the estimate obtained without time-varying parameters (no TV pars). The level of the output gap is the percentage deviation from potential.

1.I Comparison with alternative measures

In this section, we compare our estimates of potential output and the output gap with those obtained using four different univariate filters and one multivariate approach:

1) The Hodrick and Prescott (1997) filter (HP), with two different values for the smoothing parameter λ: (i) $\lambda = 1600$, commonly used for quarterly data, (ii) $\lambda = 51200$, as proposed by Borio (2014) to capture variability at lower frequencies.
2) The Hamilton (2018) filter (Ham), where the trend is the $8-$step ahead forecast of quarterly GDP growth, obtained using the 4 most recent values of quarterly GDP for each time t, and the cycle is the residual obtained from this regression.
3) The boosted HP filter (bHP) of Phillips and Shi (2021), which improves on the standard HP filter by applying the filter recursively on the residuals extracted from previous iterations. The number of iterations m is a tuning parameter that controls the intensity of the updating, and it is chosen to minimize the information criterion proposed by the authors.
4) The Christiano and Fitzgerald (2003) filter (CF), with cutoff frequencies for the transitory component between 8 and 32 quarters.
5) A Butterworth filter (BT) for the transitory component, as proposed by Canova (2025). This filter can be cast in state-space form, and its squared-gain function defines the frequencies attributed to the cycles. Here, we employ a first-order polynomial $n = 1$, with a cutoff point for the frequency set at $\omega = 0.04$ and scale $G_0 = 1$.

6) The multivariate Beveridge-Nelson (BN) decomposition based on a large Bayesian VAR, as proposed by Morley et al. (2023). The authors estimate the Euro Area output gap from 1999:Q1 to 2021:Q3. Here, due to the lack of availability of their data, we keep their original estimates, truncating the figure in correspondence with our starting point, i.e. 2001:Q1.

Figure 1.I1 presents the results of this exercise. Overall, the output gap obtained with our methodology aligns with those estimated with univariate models in terms of peaks and troughs. However, there are several differences in terms of shape and amplitude.

FIGURE 1.I1: *Output gap estimates with alternative methods*

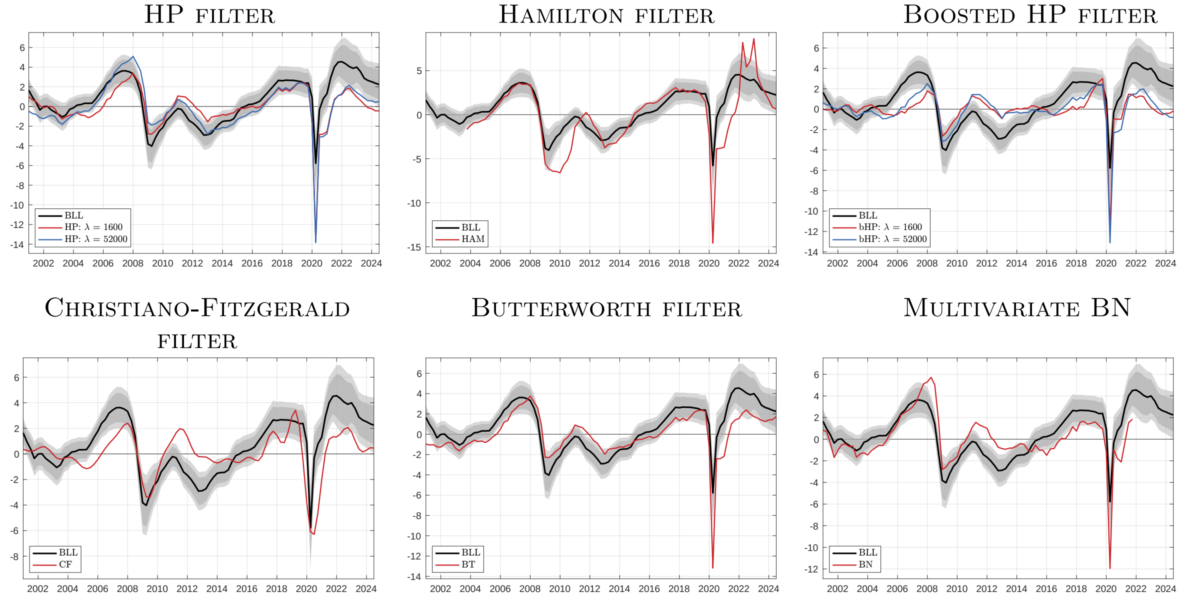

NOTES: The black line is our benchmark estimate and the grey shaded areas are the 68% and 84% confidence bands, the red and blue lines are alternative estimates.

1.J Real-time reliability

There is skepticism in the literature on the reliability of model-based output gap estimates in real time because of the size of end-of-sample revisions (Orphanides and van Norden, 2002). Model-based estimates of the output gap are subject to revisions in real time because new information leads to changes in both the estimates of the model parameters and the latent states. In this section, we assess the reliability of our output gap estimate through a *quasi*-real-time exercise on expanding windows, where the first window begins in 2000:Q1 ends in 2015:Q1 ($T = 57$).

Looking at the upper charts in Figure 1.J1, it is clear that the model is slow in recognizing how deep the 2012 Sovereign debt crisis is, only doing so once data for 2016 becomes available. Inasmuch as this result is disappointing, we cannot help but notice that 60 observations are probably too few to pin down the output gap accurately. As more information becomes available, the model's estimate of the output gap stabilizes, so much so that from 2017 onward, the *quasi*-real-time estimate is very close to the final estimate.

Moving to the Covid pandemic and its aftermath, it is evident that our strategy for adapting to the COVID shock was viable only starting from the second half of 2020 or even 2021. Moreover, it is reasonable to assume that anybody would have understood that doing nothing and allowing the Covid shock to affect the estimates was a huge mistake. Thus, we consider the

FIGURE 1.J1: *Output Gap: quasi-real time, expanding window*

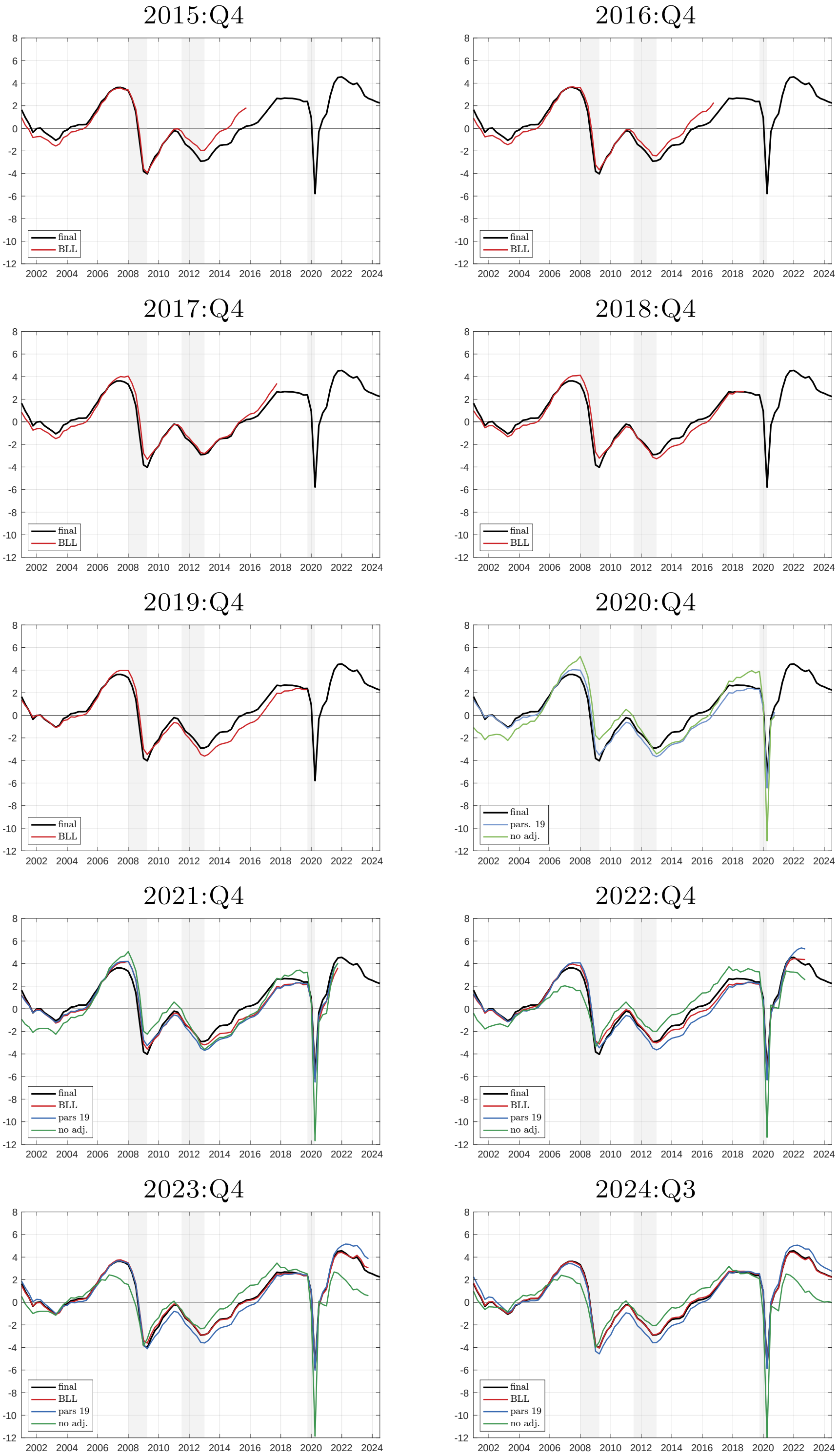

NOTES: The black line is the estimate of the output gap obtained using the final sample of data, up to 2024:Q3. The red line in Figure 1.J1 displays the evolution of our *quasi*-real-time estimate of the output gap obtained using the procedure outlined in Section 3.2. The blue line shows the estimate we would have obtained without any adjustment for the Covid shock. Lastly, the green line is the estimate we would have obtained if we had frozen the parameter estimate at the value in 2019:Q4.

quasi-real-time performance of the simple strategy of freezing the parameters to pre-Covid data. As shown by the green line, if we had followed this approach, we would have had very reliable output gap estimates, as opposed to extreme estimates, had we chosen to do nothing. Finally, by comparing the red and the green lines, we can appreciate the impact of the adjustment we implemented to account for the Covid shock.

Figure 1.J2: *Output gap: quasi-real time results*

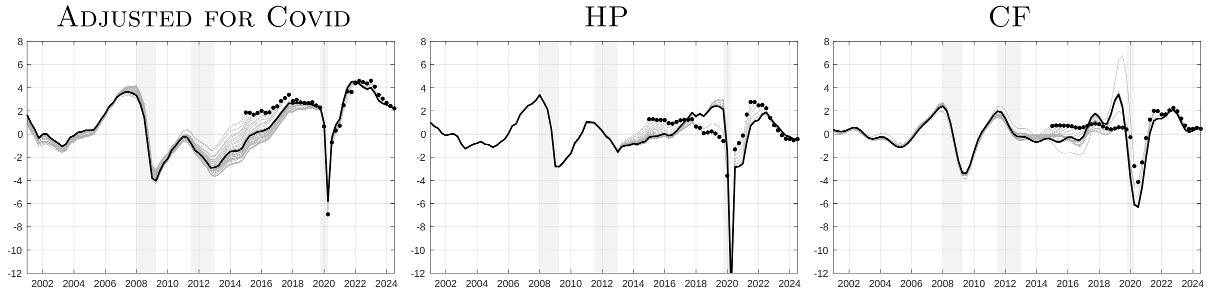

Notes: the black line is the estimate of the output gap obtained over the full sample, and the thin grey lines are the estimate obtained on all the other subsamples. Each black dots represent the estimate of the output gap for quarter Q and year Y obtained on the sample ending at quarter Q and year Y.

Figure 1.J2 compares the *quasi*-real-time estimate of the output gap from our model with those obtained from an HP filter and a Christiano-Fitzgerald band-pass filter. As mentioned earlier, our estimate's weakness is that the one obtained on the sample ending in 2015 is quite different from the final estimate. However, its strength is that from 2017 onward, the *quasi*-real-time estimates converge to the final and are very robust. In contrast, the HP filter and the Christiano-Fitzgerald filter yield *quasi*-real-time estimates that are never to far from the final estimate. However, they converge to the final estimate very late, making them unreliable for real-time analysis.

Appendix to Chapter 2

2.A Model and Estimation

2.A.1 State-space representation

In this Section, we present the complete state-space form of the two-level dynamic factor model employed for estimation, obtained by stacking the data of each group in a single n-dimensional vector, where $N = \sum_{c\in\mathcal{C}}\sum_{s\in\mathcal{S}} N_{c,s}$. Without loss of generality, let us order the groups by sector. Then, the model in compact form writes as:

$$\mathbf{x}_t \;=\; \mathbf{\Lambda}\mathbf{F}_t + \boldsymbol{\xi}_t; \quad \xi_{i,t} \sim \mathcal{N}(0, \sigma^2_{\xi_i}) \tag{2.A1a}$$

$$\mathbf{F}_t \;=\; \mathbf{A}\mathbf{F}_t + \mathbf{u}_t; \quad \mathbf{u}_t \sim \mathcal{N}(\mathbf{0}, \mathbf{Q}) \tag{2.A1b}$$

where:

$$\mathbf{x}_t \;=\; \left(\, \mathbf{x}_t^{(\mathrm{DE},F)\prime} \;\; \mathbf{x}_t^{(\mathrm{ES},F)\prime} \;\; \mathbf{x}_t^{(\mathrm{FR},F)\prime} \;\; \mathbf{x}_t^{(\mathrm{IT},F)\prime} \;\; \mathbf{x}_t^{(\mathrm{DE},M)\prime} \;\; \mathbf{x}_t^{(\mathrm{ES},M)\prime} \;\; \mathbf{x}_t^{(\mathrm{FR},M)\prime} \;\; \mathbf{x}_t^{(\mathrm{IT},M)\prime} \,\right)' \tag{2.A2a}$$

$$\mathbf{\Lambda} \;=\; \left(\begin{array}{cc|cccccccc}
\mathbf{\Gamma}^{(\mathrm{DE},F)} & \mathbf{0} & \mathbf{\Phi}^{(\mathrm{DE},F)} & \mathbf{0} & \mathbf{0} & \mathbf{0} & \mathbf{0} & \mathbf{0} & \mathbf{0} & \mathbf{0} \\
\mathbf{\Gamma}^{(\mathrm{ES},F)} & \mathbf{0} & \mathbf{0} & \mathbf{\Phi}^{(\mathrm{ES},F)} & \mathbf{0} & \mathbf{0} & \mathbf{0} & \mathbf{0} & \mathbf{0} & \mathbf{0} \\
\mathbf{\Gamma}^{(\mathrm{FR},F)} & \mathbf{0} & \mathbf{0} & \mathbf{0} & \mathbf{\Phi}^{(\mathrm{FR},F)} & \mathbf{0} & \mathbf{0} & \mathbf{0} & \mathbf{0} & \mathbf{0} \\
\mathbf{\Gamma}^{(\mathrm{IT},F)} & \mathbf{0} & \mathbf{0} & \mathbf{0} & \mathbf{0} & \mathbf{\Phi}^{(\mathrm{IT},F)} & \mathbf{0} & \mathbf{0} & \mathbf{0} & \mathbf{0} \\
\mathbf{0} & \mathbf{\Gamma}^{(\mathrm{DE},M)} & \mathbf{0} & \mathbf{0} & \mathbf{0} & \mathbf{0} & \mathbf{\Phi}^{(\mathrm{DE},M)} & \mathbf{0} & \mathbf{0} & \mathbf{0} \\
\mathbf{0} & \mathbf{\Gamma}^{(\mathrm{ES},M)} & \mathbf{0} & \mathbf{0} & \mathbf{0} & \mathbf{0} & \mathbf{0} & \mathbf{\Phi}^{(\mathrm{ES},M)} & \mathbf{0} & \mathbf{0} \\
\mathbf{0} & \mathbf{\Gamma}^{(\mathrm{FR},M)} & \mathbf{0} & \mathbf{0} & \mathbf{0} & \mathbf{0} & \mathbf{0} & \mathbf{0} & \mathbf{\Phi}^{(\mathrm{FR},M)} & \mathbf{0} \\
\mathbf{0} & \mathbf{\Gamma}^{(\mathrm{IT},M)} & \mathbf{0} & \mathbf{0} & \mathbf{0} & \mathbf{0} & \mathbf{0} & \mathbf{0} & \mathbf{0} & \mathbf{\Phi}^{(\mathrm{IT},M)}
\end{array}\right) \tag{2.A2b}$$

$$\mathbf{F}_t \;=\; \left(\, \mathbf{f}_t^{(F)\prime} \;\; \mathbf{f}_t^{(M)\prime} \;\; \mathbf{f}_t^{(\mathrm{DE},F)\prime} \;\; \mathbf{f}_t^{(\mathrm{ES},F)\prime} \;\; \mathbf{f}_t^{(\mathrm{FR},F)\prime} \;\; \mathbf{f}_t^{(\mathrm{IT},F)\prime} \;\; \mathbf{f}_t^{(\mathrm{DE},M)\prime} \;\; \mathbf{f}_t^{(\mathrm{ES},M)\prime} \;\; \mathbf{f}_t^{(\mathrm{FR},M)\prime} \;\; \mathbf{f}_t^{(\mathrm{IT},M)\prime} \,\right)' \tag{2.A2c}$$

$$\boldsymbol{\xi}_t \;=\; \left(\, \boldsymbol{\xi}_t^{(\mathrm{DE},F)\prime} \;\; \boldsymbol{\xi}_t^{(\mathrm{ES},F)\prime} \;\; \boldsymbol{\xi}_t^{(\mathrm{FR},F)\prime} \;\; \boldsymbol{\xi}_t^{(\mathrm{IT},F)\prime} \;\; \boldsymbol{\xi}_t^{(\mathrm{DE},M)\prime} \;\; \boldsymbol{\xi}_t^{(\mathrm{ES},M)\prime} \;\; \boldsymbol{\xi}_t^{(\mathrm{FR},M)\prime} \;\; \boldsymbol{\xi}_t^{(\mathrm{IT},M)\prime} \,\right)' \tag{2.A2d}$$

$$\mathbf{A} = \left(\begin{array}{cc|cccccccc} \mathbf{A}^{(F)'} & \mathbf{0} & \mathbf{0} & \mathbf{0} & \mathbf{0} & \mathbf{0} & \mathbf{0} & \mathbf{0} & \mathbf{0} & \mathbf{0} \\ \mathbf{0} & \mathbf{A}^{(M)'} & \mathbf{0} & \mathbf{0} & \mathbf{0} & \mathbf{0} & \mathbf{0} & \mathbf{0} & \mathbf{0} & \mathbf{0} \\ \hline \mathbf{0} & \mathbf{0} & \mathbf{A}^{(\text{DE},F)'} & \mathbf{0} & \mathbf{0} & \mathbf{0} & \mathbf{0} & \mathbf{0} & \mathbf{0} & \mathbf{0} \\ \mathbf{0} & \mathbf{0} & \mathbf{0} & \mathbf{A}^{(\text{ES},F)'} & \mathbf{0} & \mathbf{0} & \mathbf{0} & \mathbf{0} & \mathbf{0} & \mathbf{0} \\ \mathbf{0} & \mathbf{0} & \mathbf{0} & \mathbf{0} & \mathbf{A}^{(\text{FR},F)'} & \mathbf{0} & \mathbf{0} & \mathbf{0} & \mathbf{0} & \mathbf{0} \\ \mathbf{0} & \mathbf{0} & \mathbf{0} & \mathbf{0} & \mathbf{0} & \mathbf{A}^{(\text{IT},F)'} & \mathbf{0} & \mathbf{0} & \mathbf{0} & \mathbf{0} \\ \mathbf{0} & \mathbf{0} & \mathbf{0} & \mathbf{0} & \mathbf{0} & \mathbf{0} & \mathbf{A}^{(\text{DE},M)'} & \mathbf{0} & \mathbf{0} & \mathbf{0} \\ \mathbf{0} & \mathbf{0} & \mathbf{0} & \mathbf{0} & \mathbf{0} & \mathbf{0} & \mathbf{0} & \mathbf{A}^{(\text{ES},M)'} & \mathbf{0} & \mathbf{0} \\ \mathbf{0} & \mathbf{0} & \mathbf{0} & \mathbf{0} & \mathbf{0} & \mathbf{0} & \mathbf{0} & \mathbf{0} & \mathbf{A}^{(\text{FR},M)'} & \mathbf{0} \\ \mathbf{0} & \mathbf{0} & \mathbf{0} & \mathbf{0} & \mathbf{0} & \mathbf{0} & \mathbf{0} & \mathbf{0} & \mathbf{0} & \mathbf{A}^{(\text{IT},M)'} \end{array}\right) \tag{2.A2e}$$

$$\mathbf{u}_t = \left(\mathbf{u}_t^{(F)\prime} \; \mathbf{u}_t^{(M)\prime} \; \mathbf{u}_t^{(\text{DE},F)\prime} \; \mathbf{u}_t^{(\text{ES},F)\prime} \; \mathbf{u}_t^{(\text{FR},F)\prime} \; \mathbf{u}_t^{(\text{IT},F)\prime} \; \mathbf{u}_t^{(\text{DE},M)\prime} \; \mathbf{u}_t^{(\text{ES},M)\prime} \; \mathbf{u}_t^{(\text{FR},M)\prime} \; \mathbf{u}_t^{(\text{IT},M)\prime} \right)' \tag{2.A2f}$$

and:

$$\mathbf{A}^s = \begin{pmatrix} \mathbf{A}_1^{(s)} & \mathbf{A}_2^{(s)} & \dots & \mathbf{A}_{p_s}^{(s)} \\ \mathbf{I} & \mathbf{0} & \dots & \mathbf{0} \\ \mathbf{0} & \mathbf{I} & \dots & \mathbf{0} \\ \vdots & \vdots & \ddots & \vdots \\ \mathbf{0} & \mathbf{0} & \dots\ \mathbf{I} & \mathbf{0} \end{pmatrix} \qquad \mathbf{A}^{(c,s)} = \begin{pmatrix} \mathbf{A}_1^{(c,s)} & \mathbf{A}_2^{(c,s)} & \dots & \mathbf{A}_{p_s}^{(c,s)} \\ \mathbf{I} & \mathbf{0} & \dots & \mathbf{0} \\ \mathbf{0} & \mathbf{I} & \dots & \mathbf{0} \\ \vdots & \vdots & \ddots & \vdots \\ \mathbf{0} & \mathbf{0} & \dots\ \mathbf{I} & \mathbf{0} \end{pmatrix} \tag{2.A2g}$$

are the companion form representation of the transition matrices for $s \in \mathcal{S}$ and $c \in \mathcal{C}$.

Finally, let $\boldsymbol{\Gamma}^{(s)} = (\boldsymbol{\Gamma}^{(\text{DE},s)\prime}, \boldsymbol{\Gamma}^{(\text{ES},s)\prime}, \boldsymbol{\Gamma}^{(\text{FR},s)\prime}, \boldsymbol{\Gamma}^{(\text{IT},s)\prime})' = (\gamma_1^{(s)}, \dots, \gamma_{n_s}^{(s)})'$ denote the loadings of the pervasive factors for sector $s \in \mathcal{S}$.

2.A.2 EM algorithm

Initialization

To estimate the model in Equations (2.A1a)-(2.A1b), we need to initialize all the parameters and states in the model. To do so, we employ the two step (top-down) PC approach (Aastveit et al., 2016; Breitung and Eickmeier, 2016) to extract the estimated factors and the corresponding loadings, and we then use these estimated factors to obtain an estimate of the transition parameters in Equation (2.A1b).

Specifically, let $\mathbf{X}^{(s)} = (\mathbf{x}_1^{(s)}, \dots, \mathbf{x}_T^{(s)})'$ be the $T \times N_s$ vector of data for sector $s \in \mathcal{S}$, pooling all countries. Without loss of generality, let $\mathbf{X}^{(s)}$ be standardized so to have mean zero and unit variance. Given the data, we can estimate the global factor by means of principal components (PC) on the $N_s \times N_s$ sample variance-covariance matrix, say $\widehat{\boldsymbol{\Gamma}}^{X^s} = \frac{\mathbf{X}^{(s)\prime}\mathbf{X}^{(s)}}{T}$.

Following Barigozzi (2022), the least-squares estimation of the common factors within each sector, $\mathbf{f}^{(s)}$, and the corresponding loadings, $\boldsymbol{\Gamma}^{(s)}$, is given by:

$$\min_{\underline{\mathbf{F}}^{(s)}, \underline{\boldsymbol{\Gamma}}^{(s)}} \frac{1}{N_s T} \sum_{t=1}^{T} \left(\mathbf{X}^{(s)} - \underline{\mathbf{F}}^{(s)} \underline{\boldsymbol{\Gamma}}^{(s)\prime} \right)' \left(\mathbf{X}^{(s)} - \underline{\mathbf{F}}^{(s)} \underline{\boldsymbol{\Gamma}}^{(s)\prime} \right) \tag{2.A3}$$

where $\underline{\mathbf{F}}^{(s)} = (\underline{\mathbf{f}}_1^{(s)}, \dots, \underline{\mathbf{f}}_T^{(s)})'$. Under the identification conditions by Forni et al. (2009), i.e. $N_s^{-1} \underline{\boldsymbol{\Gamma}}^{(s)\prime} \underline{\boldsymbol{\Gamma}}^{(s)}$ diagonal, we solve Equation (2.A3) by $\underline{\boldsymbol{\Gamma}}^{(s)}$, to obtain the PC estimator:

$$\widehat{\boldsymbol{\Gamma}}^{(s),(0)} = \widehat{\mathbf{V}}^{\mathbf{X}^{(s)}} \left(\widehat{\mathbf{M}}^{\mathbf{X}^{(s)}} \right)^{\frac{1}{2}} \tag{2.A4}$$

where $\widehat{\mathbf{V}}^{\mathbf{X}^{(s)}}$ is the matrix of eigenvectors corresponding to the r_s- largest eigenvalues, $\widehat{\mathbf{M}}^{\mathbf{X}^{(s)}}$, of the sample variance-covariance matrix of the data. Given the estimated loadings, we obtain an estimate of the factor by projection onto matrix of data, that is:

$$\widehat{\mathbf{F}}^{(s),(0)} = \mathbf{X}^{(s)}\widehat{\mathbf{\Gamma}}^{(s)}\left(\widehat{\mathbf{\Gamma}}^{(s)\prime}\widehat{\mathbf{\Gamma}}^{(s)}\right)^{-1} = \mathbf{X}^{(s)}\widehat{\mathbf{V}}^{\mathbf{X}^{(s)}}\left(\widehat{\mathbf{M}}^{\mathbf{X}^{(s)}}\right)^{-\frac{1}{2}} \tag{2.A5}$$

Given the estimated factors in each sector, we still have to estimate the local factors within each country-sector block. Let $\overline{\mathbf{X}}^{(s)} = \mathbf{X}^{(s)} - \widehat{\mathbf{F}}^{(s),(0)}\widehat{\mathbf{\Gamma}}^{(s),(0)\prime}$ be the matrix of data for sector $s \in \mathcal{S}$ net of the comovements explained by the global factor (i.e., common to all countries) within the sector. We can repeat the procedure outlined above to obtain an estimate of the local factors within each country-sector subgroup. For each country-sector pair, the estimated loadings are given by:

$$\widehat{\mathbf{\Phi}}^{(s),(0)} = \widehat{\mathbf{V}}^{\overline{\mathbf{X}}^{(s)}}\left(\widehat{\mathbf{M}}^{\overline{\mathbf{X}}^{(s)}}\right)^{\frac{1}{2}} \tag{2.A6}$$

E-step

Let $k = 1, \ldots, k_{\max}$ denote the indicator for the current iteration of the EM algorithm, and let $\widehat{\boldsymbol{\theta}}^{(k-1)}$ denote the vector of parameters estimated at iteration $k-1$, while $\mathbf{F}_{0|0}^{(k-1)}$ and $\mathbf{P}_{0|0}^{(k-1)}$ denote the corresponding initial estimate of factor and their conditional variance. Then, conditional on these quantities, in the E-step we run the Kalman Filter and Smoother to obtain updated estimates the factors and their variance, i.e. $\mathbf{F}_{t|T}^{(k)}$ and $\mathbf{P}_{t|T}^{(k)}$, along with the conditional covariance across states, denoted as $\mathbf{P}_{t,t-1|T}^{(k)}$.

M-step

In the M-step, we maximize the expected log-likelihood with respect to the parameters.

1. **Factor Loadings**:

$$\begin{aligned}
\widehat{\gamma}_i^{(s),(k+1)} &= \left(\sum_{t=1}^{T} x_{i,t}^{(s)}\mathbf{f}_{t|T}^{(s),(k)}\right)\left(\sum_{t=1}^{T}\mathbf{f}_{t|T}^{(s),(k)}\mathbf{f}_{t|T}^{(s),(k)\prime} + \mathbf{P}_{t|T}^{\mathbf{f}^{(s)},(k)}\right)^{-1} \\
\widehat{\boldsymbol{\phi}}_i^{(c,s),(k)} &= \left(\sum_{t=1}^{T} x_{i,t}^{(c,s)}\mathbf{f}_{t|T}^{(c,s),(k)}\right)\left(\sum_{t=1}^{T}\mathbf{f}_{t|T}^{(c,s),(k)}\mathbf{f}_{t|T}^{(c,s),(k)\prime} + \mathbf{P}_{t|T}^{\mathbf{f}^{(c,s)},(k)}\right)^{-1}
\end{aligned}$$

   stacking the loadings, we denote the estimated loadings $\widehat{\mathbf{\Lambda}}^{(k+1)}$.

2. **Idiosyncratic variances**:

$$\widehat{\sigma}_{\xi_i}^{2,(k+1)} = \frac{1}{T}\sum_{t=1}^{T}\left[\left(x_{i,t} - \widehat{\boldsymbol{\lambda}}_i^{(k+1)\prime}\mathbf{F}_t^{(k)}\right)^2 + \widehat{\boldsymbol{\lambda}}_i^{(k+1)\prime}\mathbf{P}_{t|t-1}^{(k)}\widehat{\boldsymbol{\lambda}}_i^{(k+1)}\right]$$

   where $\boldsymbol{\lambda}_i$ is the i-th row of the matrix of stacked loadings $\mathbf{\Lambda} = (\boldsymbol{\lambda}_1, \ldots, \boldsymbol{\lambda}_n)'$.

3. **Parameters of the law of motion of the common factors**:

$$\begin{aligned}
\hat{\mathbf{A}}^{(s),(k+1)} &= \left(\sum_{t=2}^{T} \mathbf{f}_{t|T}^{(s),(k)} \mathbf{f}_{t-1|T}^{(s),(k)\prime} + \mathbf{P}_{t,t-1|T}^{\mathbf{f}^{(s)},(k)}\right)\left(\sum_{t=2}^{T} \mathbf{f}_{t-1|T}^{(s),(k)} \mathbf{f}_{t-1|T}^{(s),(k)\prime} + \mathbf{P}_{t-1|T}^{\mathbf{f}^{(s)},(k)}\right)^{-1} \\
\hat{\mathbf{A}}^{(c,s),(k+1)} &= \left(\sum_{t=2}^{T} \mathbf{f}_{t|T}^{(c,s),(k)} \mathbf{f}_{t-1|T}^{(c,s),(k)\prime} + \mathbf{P}_{t,t-1|T}^{\mathbf{f}^{(c,s)},(k)}\right)\left(\sum_{t=2}^{T} \mathbf{f}_{t-1|T}^{(c,s),(k)} \mathbf{f}_{t-1|T}^{(c,s),(k)\prime} + \mathbf{P}_{t-1|T}^{\mathbf{f}^{(c,s)},(k)}\right)^{-1} \\
\widehat{\mathbf{\Sigma}}_u^{(s),(k+1)} &= \frac{1}{T}\left[\sum_{t=2}^{T}\left(\mathbf{f}_{t|T}^{(s),(k)} \mathbf{f}_{t|T}^{(s),(k)\prime} + \mathbf{P}_{t|T}^{\mathbf{f}^{(s)},(k)}\right) - \hat{\mathbf{A}}\sum_{t=2}^{T}\left(\mathbf{f}_{t|T}^{(s),(k)} \mathbf{f}_{t-1|T}^{(s),(k)\prime} + \mathbf{P}_{t,t-1|T}^{\mathbf{f}^{(s)},(k)}\right)\right] \\
\widehat{\mathbf{\Sigma}}_u^{(c,s),(k+1)} &= \frac{1}{T}\left[\sum_{t=2}^{T}\left(\mathbf{f}_{t|T}^{(c,s),(k)} \mathbf{f}_{t|T}^{(c,s),(k)\prime} + \mathbf{P}_{t|T}^{\mathbf{f}^{(c,s)},(k)}\right) - \hat{\mathbf{A}}\sum_{t=2}^{T}\left(\mathbf{f}_{t|T}^{(c,s),(k)} \mathbf{f}_{t-1|T}^{(c,s),(k)\prime} + \mathbf{P}_{t,t-1|T}^{\mathbf{f}^{(c,s)},(k)}\right)\right]
\end{aligned}$$

Convergence

At each iteration k of the algorithm, an estimate of the log-likelihood conditional on the estimated parameters, $\ell(\mathbf{X}, \widehat{\boldsymbol{\theta}}^{(k)})$, is obtained from the Kalman Filter. To assess the convergence of the EM algorithm, we then employ the likelihood-based criterion introduced by Doz et al. (2012), based on the (scaled) difference between the log-likelihood across subsequent iterations of the algorithm:

$$\Delta\ell^{(k+1)} = \frac{\left|\ell\left(\mathbf{X}; \widehat{\boldsymbol{\theta}}^{(k+1)}\right) - \ell\left(\mathbf{X}; \widehat{\boldsymbol{\theta}}^{(k)}\right)\right|}{\frac{1}{2}\left|\ell\left(\boldsymbol{X}; \widehat{\boldsymbol{\theta}}^{(k+1)}\right) + \ell\left(\mathbf{X}; \widehat{\boldsymbol{\theta}}^{(k)}\right)\right|}$$

The algorithm is stopped when $\Delta\ell^{(k+1)} < \varepsilon$, for a predetermined threshold ε, which is set to 10^{-3}.

Confidence Intervals

In this chapter, we follow the procedure outlined in Barigozzi (2022) to compute confidence intervals for the factors estimated via the EM algorithm, properly modified so to account for the block structure within the model. Under the assumption of cross-sectionally uncorrelated idiosyncratic components the variance-covariance matrix of the common and country-specific factors can be estimated as:

$$\begin{aligned}
\tilde{\mathbf{\Gamma}}^{(s)} &= \left(\frac{1}{N^{(s)}} \sum_{i \in N^{(s)}} \widehat{\gamma}_i' (\widehat{\sigma}_{\xi_i}^2)^{-1} \widehat{\gamma}_i\right)^{-1} \\
\tilde{\mathbf{\Gamma}}^{(c,s)} &= \left(\frac{1}{N^{(c,s)}} \sum_{i \in N^{(c,s)}} \widehat{\boldsymbol{\phi}}_i' (\widehat{\sigma}_{\xi_i}^2)^{-1} \widehat{\boldsymbol{\phi}}_i\right)^{-1}
\end{aligned}$$

where $\widehat{\sigma}_{\xi_i}^2$ is the estimated variance of the idiosyncratic component of the i-th variable.

We also try implementing the adaptive thresholding procedure as outlined in Cai and Liu (2011), finding that only $\approx 3\%$ of outer-diagonal entries are actually shrinked to zero, yielding nearly identical results. Indeed, as shown also in Appendix 2.B, the block-structure is able to account for all relevant comovements in the panel, including local dynamics, which leave almost no relevant information in the idiosyncratic component

Although consistent, these estimates are likely to misrepresent the true uncertainty on the underlying factors. Indeed, as pointed out by Maldonado and Ruiz (2021), the estimated variance-covariance matrix of the factors depends on the loadings, which are themselves estimated. Hence, we need to account for the additional uncertainty which stems from the estimation of the loadings. This is particularly important in our setting, where we stress the factors at their 95% significance level. Failing to account for loadings uncertainty could make our results either upward or downward biased, resulting in an over- or under-estimation of the true level of stress for the factors.

In the chapter, we follow the subsampling procedure proposed by Maldonado and Ruiz (2021), properly modified to account for the block structure of our ML-DFM. Specifically, for each country-sector subgroup, we draw randomly, without replacement, a $T \times N^*_{c,s}$ sub-matrix of data, say $X_t^{(c,s)^*}$. The size of the sub-matrix is selected in a data-driven way, such that $N^*_{c,s} = p^{(c,s)} \cdot N^{(c,s)}$, where $p^{(c,s)} = 1 - \frac{235}{(N^{(c,s)}+25)^2} - 0.2\frac{\sqrt{N^{(c,s)}}}{T} - \frac{r^{c,s}}{N^{(c,s)}T}$. Given the sub-blocks for each country-sector pair, we then aggregate them to obtain the corresponding sub-blocks at the sectoral level, used to extract the sector-specific factors common to all countries. The reason for this "bottom-down" procedure is to avoid over- or under-representation of countries or sectors, which would be highly likely if we resampled the data being agnostic of the block-structure, especially since macroeconomic variables are sensibly more than financial ones.

Once the sub-matrix of data is selected, we extract the factors via PC, used to initialize the EM algorithm, which is run until convergence. This procedure is repeated B times and, at the end of each iteration, a new estimated of the factors, denoted as $\widehat{\mathbf{F}}_t^{(b)}$ for $b = 1, \ldots, B$, is stored. In this chapter we set $B = 199$ repetitions, as results are nearly identical using more replications, only being more computational demanding. Given the factors estimated at each iteration b, an estimate of the variance-covariance matrix of the factors which accounts for the uncertainty in the estimation of the loadings, can be finally computed. Specifically we define as $\widehat{\mathbf{\Gamma}}^{(s)}$ the estimated variance-covariance matrix for the sector-specific factors common to all countries, and with $\widehat{\mathbf{\Gamma}}^{(c,s)}$ the estimated variance-covariance matrix for the country-sector specific factors. Then:

$$
\begin{aligned}
\widehat{\mathbf{\Gamma}}^{(s)} &= \tilde{\mathbf{\Gamma}}^{(s)} + \frac{N^{(s)^*}}{N^{(s)}BT}\sum_{b=1}^{B}\sum_{t=1}^{T}\left(\widehat{\mathbf{f}}_t^{(s),(b)} - \widehat{\mathbf{f}}_t^{(s)}\right)\left(\widehat{\mathbf{f}}_t^{(s),(b)} - \widehat{\mathbf{f}}_t^{(s)}\right)' \\
\widehat{\mathbf{\Gamma}}^{(c,s)} &= \tilde{\mathbf{\Gamma}}^{(c,s)} + \frac{N^{(c,s)^*}}{N^{(c,s)}BT}\sum_{b=1}^{B}\sum_{t=1}^{T}\left(\widehat{\mathbf{f}}_t^{(c,s),(b)} - \widehat{\mathbf{f}}_t^{(s)}\right)\left(\widehat{\mathbf{f}}_t^{(c,s),(b)} - \widehat{\mathbf{f}}_t^{(c,s)}\right)'
\end{aligned}
$$

2.B Model Specification

The selection of the number of factors of the ML-DFM is carried out by analysing the structure of the sample covariance matrix of the idiosyncratic residuals obtained when estimating Model (2.3) via the EM algorithm with the most parsimonious specification, i.e. with just one global and one country-specific factor for each country, i.e. $\widehat{\mathbf{\Xi}} = (\widehat{\boldsymbol{\xi}}'_1, \ldots, \widehat{\boldsymbol{\xi}}'_N)'$. Figure 2.B1 is a heat-map of the corresponding pairwise cross-correlations. As we can see, although the most parsimonious model, with one country-specific factor, is able to capture the bulk of within-sector dynamics, there are still some small blocks of cross-correlated idiosyncratic components. This may be particularly relevant as the blocks are not randomly located, but they are concentrated around the same group of series for all countries (bottom-right corner). It turns out that these are mostly price series. Hence, it seems that one factor for macroeconomic variables is not able to account for some of the comovements across price series, either within or across countries (or both).

FIGURE 2.B1: *Idiosyncratic cross-correlation: $q = 1$ for each block*

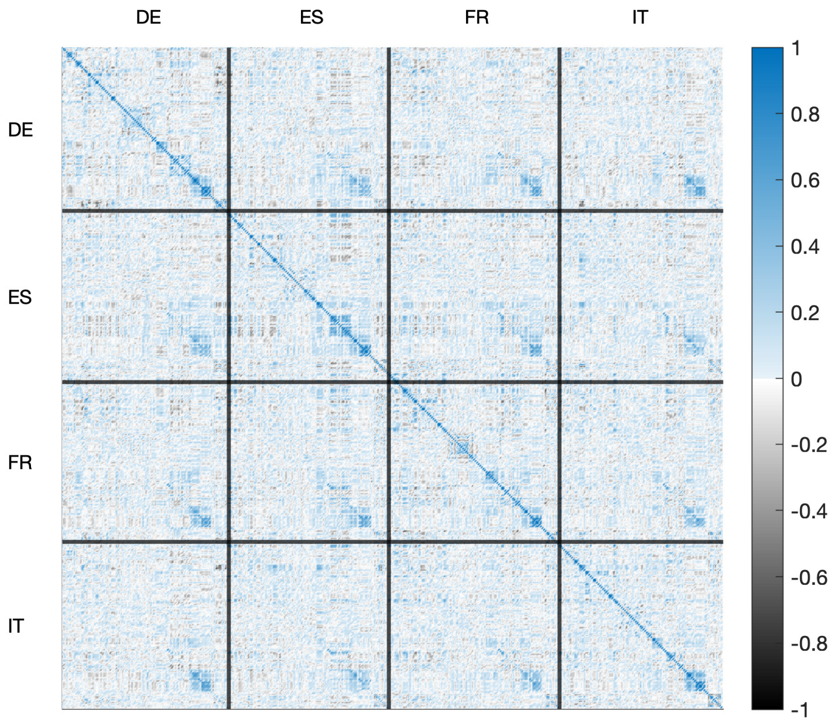

FIGURE 2.B2: *Idiosyncratic cross-correlation: alternative model specifications*

COMMON MACROECONOMIC FACTOR

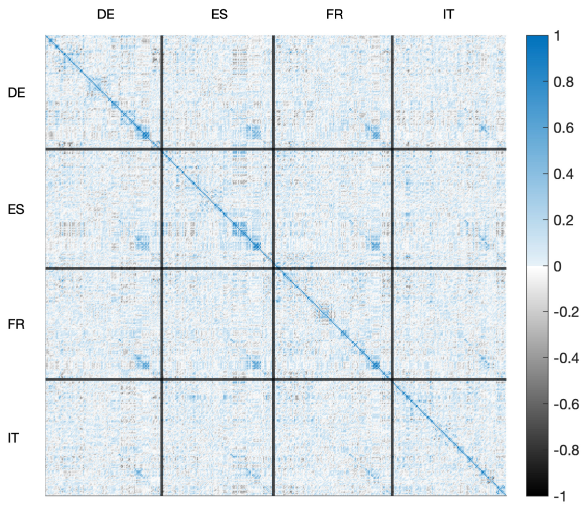

COUNTRY-SPECIFIC MACROECONOMIC FACTORS

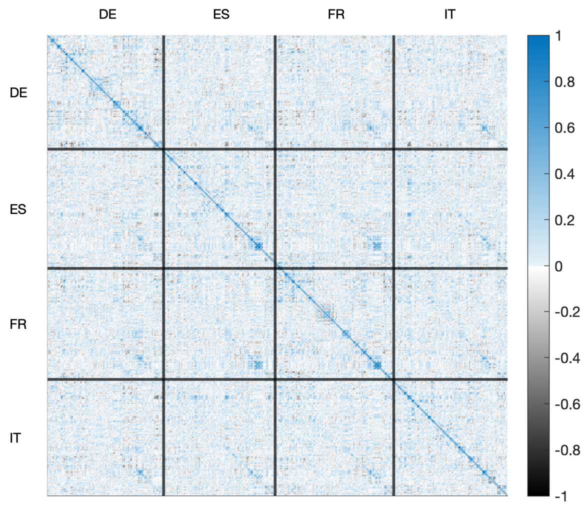

To account for the presence of cross-correlation across price series, we consider estimating an additional global macroeconomic factor and, alternatively, an country-specific additional macroeconomic factor for each country. If the price dynamics are mostly idiosyncratic within countries, then an additional macroeconomic factor for each country will incorporate this information.

Figure 2.B2 plots the matrix of cross-correlations across estimated idiosyncratic components in both the cases outlined above. From the graph, it emerges that one additional factor for each country seems to be the most appropriate solution to account for the presence of local dynamics within price series.

Appendix to Chapter 3

3.A Individual country responses

FIGURE 3.A1: *Difference between EA and country-level IRFs*

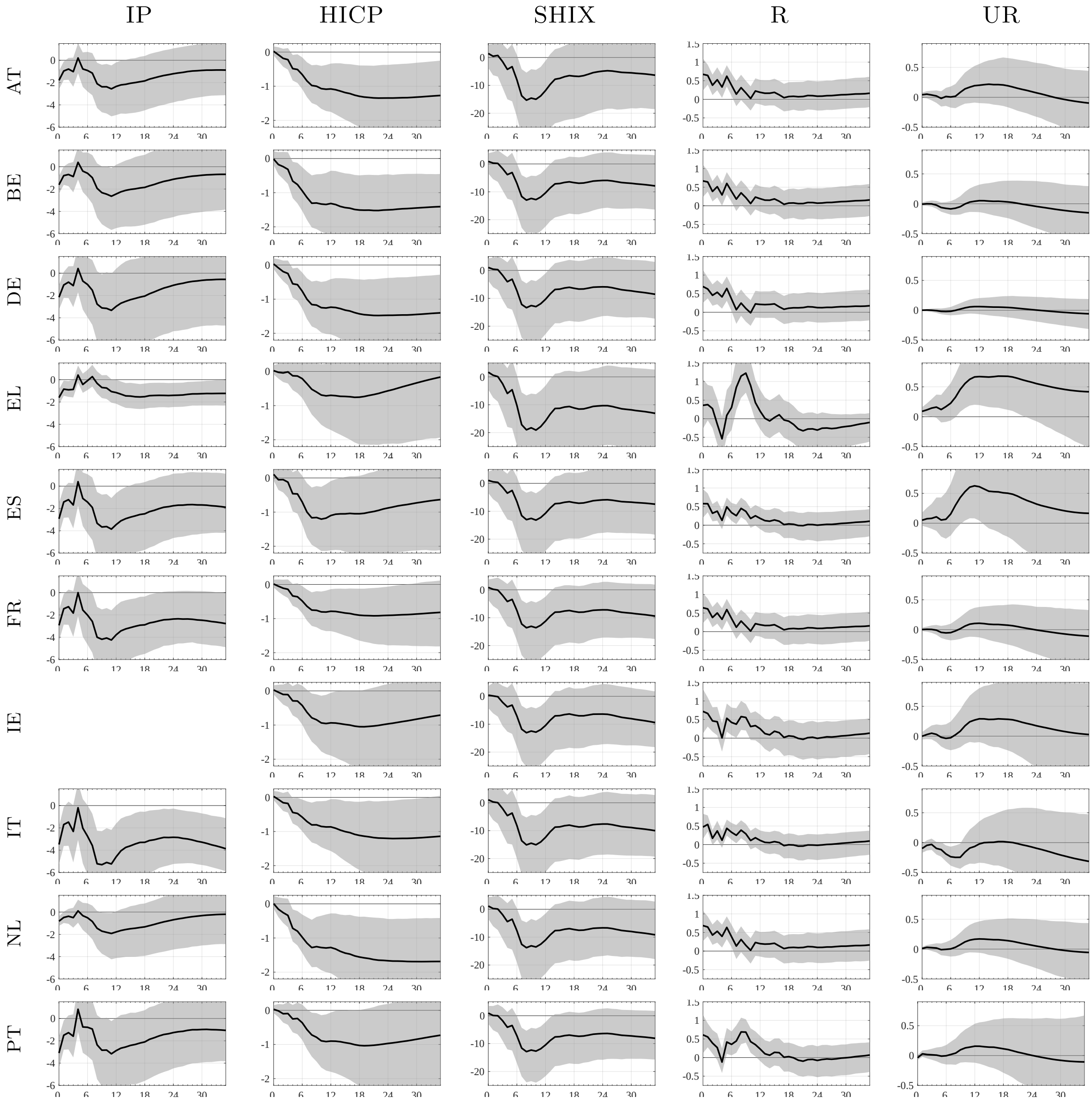

3.B Comparison with pre-Covid estimates

3.B.1 Euro Area IRFs

FIGURE 3.B2: *Euro Area IRFs: full sample vs 2019*

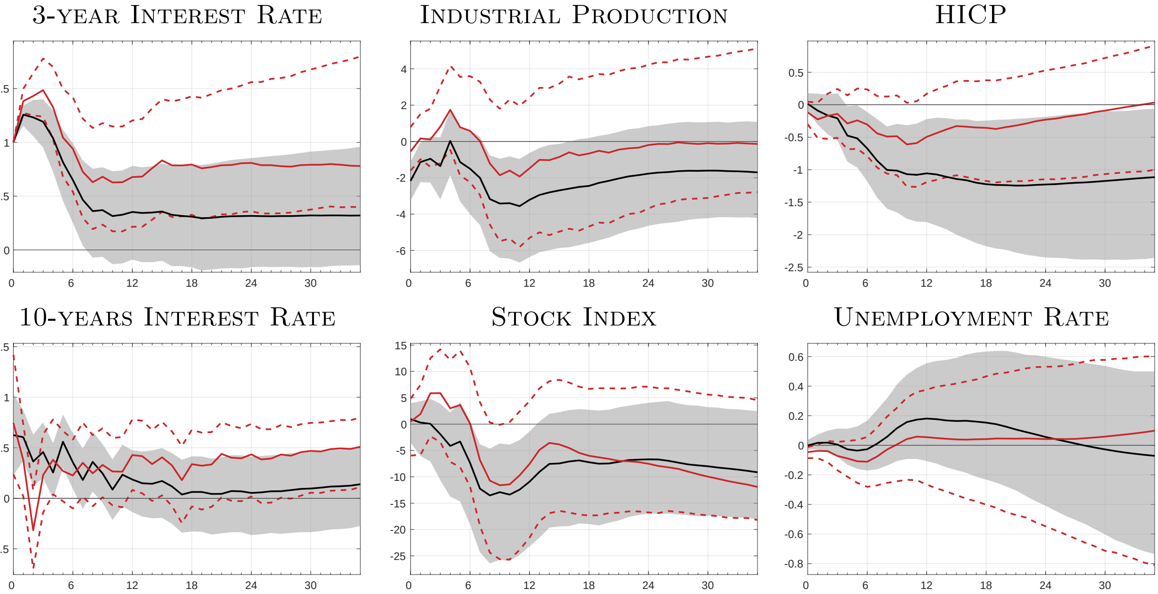

NOTES: Each sub-figure plots the impulse response of one EA variable to a 100bps contractionary monetary policy shock. The black solid line is the point estimate in our baseline setting, while the red solid line is the point estimate obtained with data truncated in 2019:M12. The gray shaded area and red dotted lines are the corresponding 68% confidence intervals.

3.B.2 Heterogeneous country responses

Figure 3.B3: *Difference between EA and country-level IRFs: full sample vs 2019*

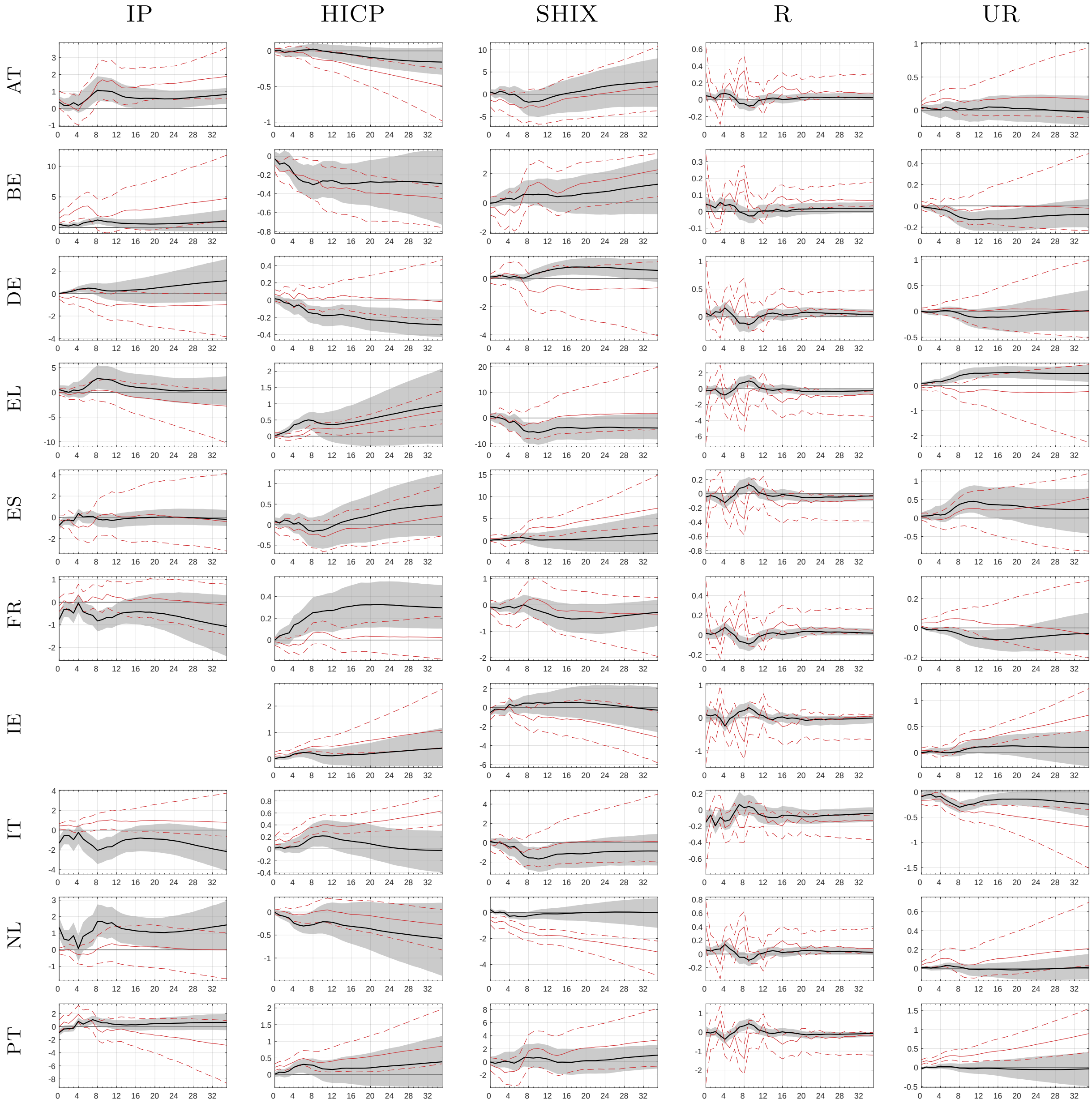

Notes: Each sub-figure plots the impulse response of one variable for each country to a 100bps contractionary monetary policy shock. Each column of the graph represents a variable, while each row represents a country. The black solid line is the point estimate in our baseline setting, while the red solid line is the point estimate obtained with data truncated in 2019:M12. The gray shaded area and red dotted lines are the corresponding 68% confidence intervals. The scale in the vertical axis differs across variables and countries.

3.C Comparison with alternative estimation strategies

3.C.1 VAR

Table 3.C1: *Components of* $\mathbf{Y}_t$ *in the VAR*

notation	ID	name
R_t	-	EA 2-Year Interest Rate
$\mathrm{IP}_t^{\mathrm{EA}}$	IPMN	EA Industrial Production
HICP_t^{EA}	HICPOV	EA HICP Overall
$\mathrm{R}_t^{\mathrm{long,EA}}$	LTIRT	EA Long-Term Interest Rate
$\mathrm{SHIX}_t^{\mathrm{EA}}$	SHIX	EA Share Prices
$\mathrm{UR}_t^{\mathrm{EA}}$	UNETOT	EA Unemployment Rate
$\mathrm{X}_t^{\mathrm{nat.}}$	-	National Variable

Figure 3.C4: *Euro Area IRFs: CC-VAR vs VAR*

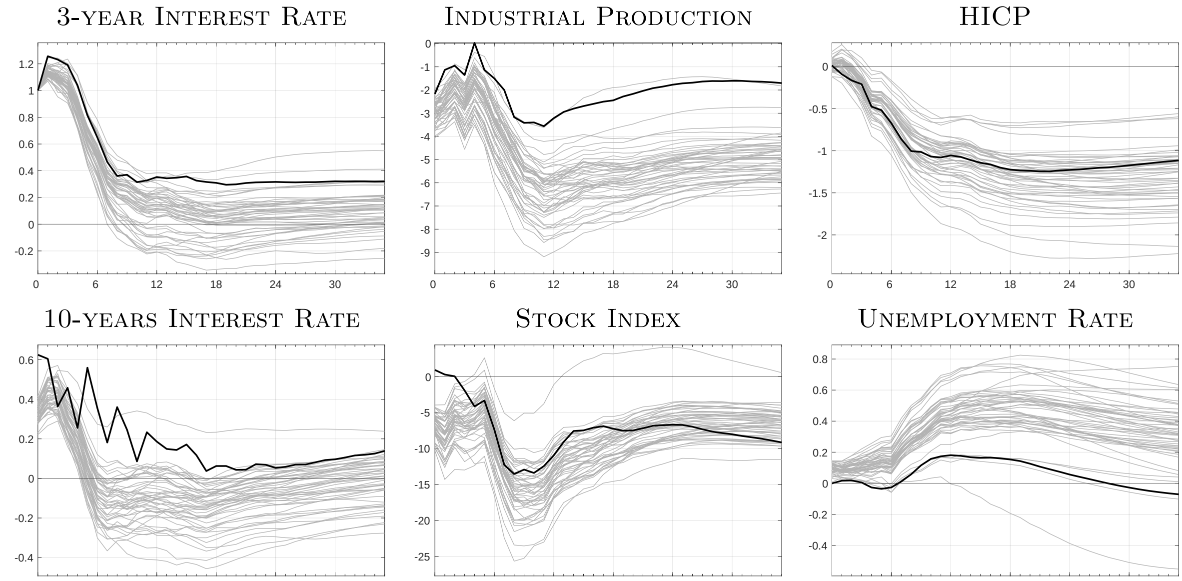

Notes: Each sub-figure plots the impulse response of one EA variable to a 100bps contractionary monetary policy shock. The black solid line is the point estimate obtained with the CC-VAR, which is the same regardless of the set of common components included in the model, as long as $n^* = r$. The thin gray lines are the point estimates obtained with the VAR model by rotating across different variables included in the model, i.e. the equivalent in our setting of rotating the common components.

3.C.2 FAVAR

TABLE 3.C2: *Components of* $\mathbf{Y}_t$ *in the FAVAR*

notation	ID	name
R_t	-	EA 2-Year Interest Rate
$\mathrm{IP}_t^{\mathrm{EA}}$	IPMN	EA Industrial Production
HICP_t^{EA}	HICPOV	EA HICP Overall
$\mathrm{R}_t^{\mathrm{long,EA}}$	LTIRT	EA Long-Term Interest Rate
$\mathrm{SHIX}_t^{\mathrm{EA}}$	SHIX	EA Share Prices
$\mathrm{UR}_t^{\mathrm{EA}}$	UNETOT	EA Unemployment Rate
$\widehat{f}_t$	-	First estimated factor
$\mathrm{X}_t^{\mathrm{nat.}}$	-	National Variable

FIGURE 3.C5: *Euro Area IRFs: CC-VAR vs FAVAR*

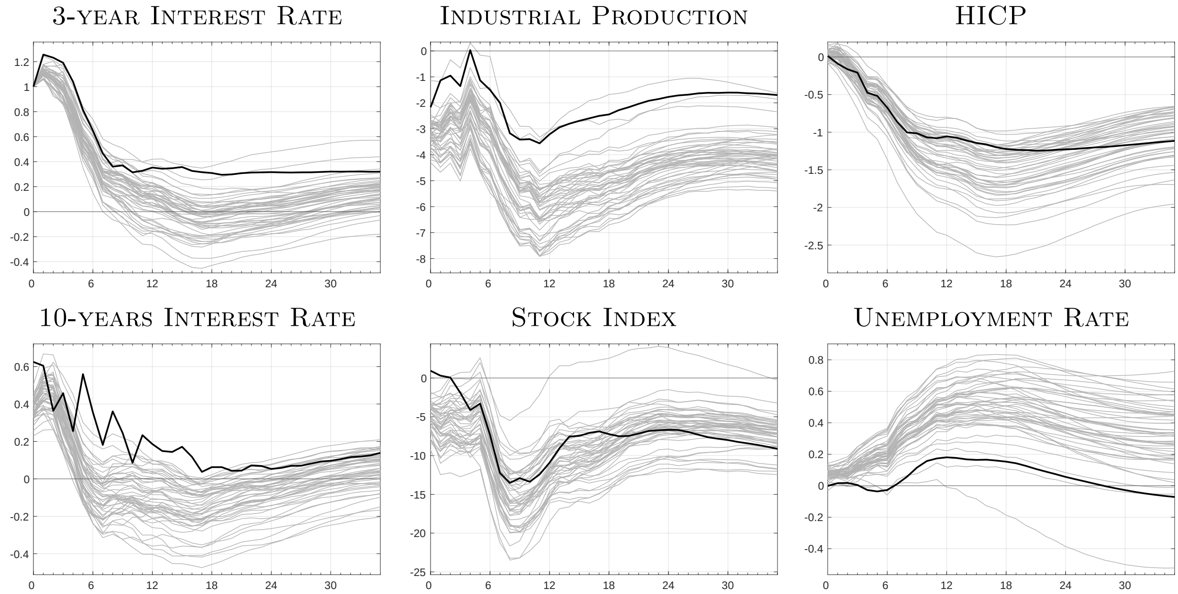

NOTES: Each sub-figure plots the impulse response of one EA variable to a 100bps contractionary monetary policy shock. The black solid line is the point estimate obtained with the CC-VAR, which is the same regardless of the set of common components included in the model, as long as $n^* = r$. The thin gray lines are the point estimates obtained with the FAVAR model by rotating across different variables included in the model, i.e. the equivalent in our setting of rotating the common components.

3.D Alternative set of transformations: statistical criteria

3.D.1 Euro Area IRFs

FIGURE 3.D6: *Euro Area IRFs: baseline vs alternative set of transformations (1)*

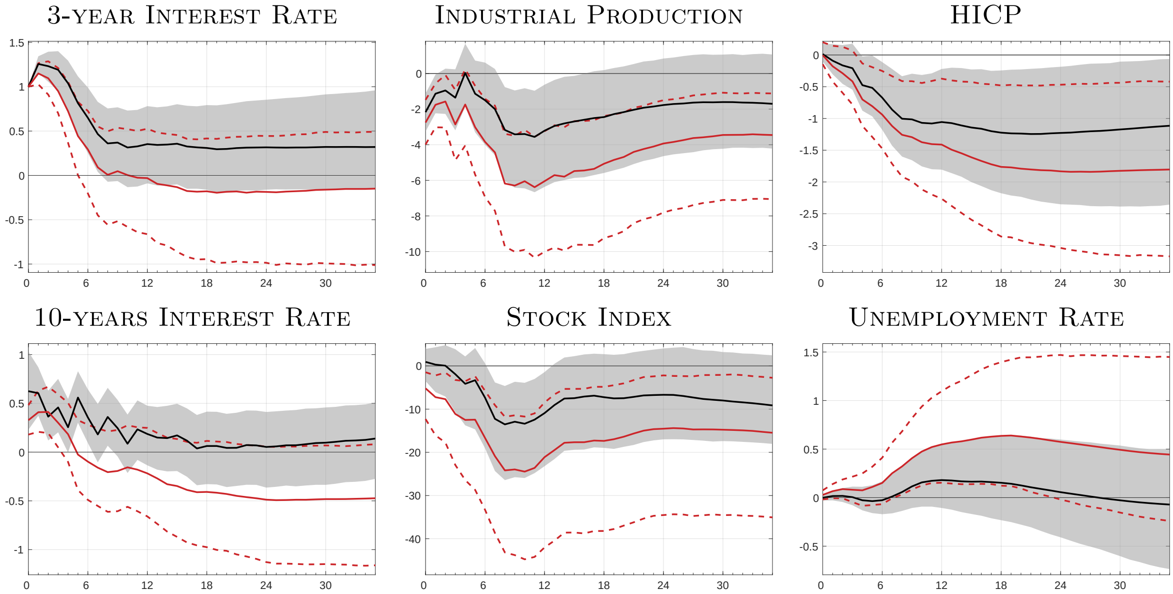

NOTES: Each sub-figure plots the impulse response of one EA variable to a 100bps contractionary monetary policy shock. The black solid line is the point estimate in our baseline setting, while the red solid line is the point estimate obtained with the alternative set of transformations based on statistical criteria. The gray shaded area and red dotted lines are the corresponding 68% confidence intervals.

3.D.2 Country-level IRFs

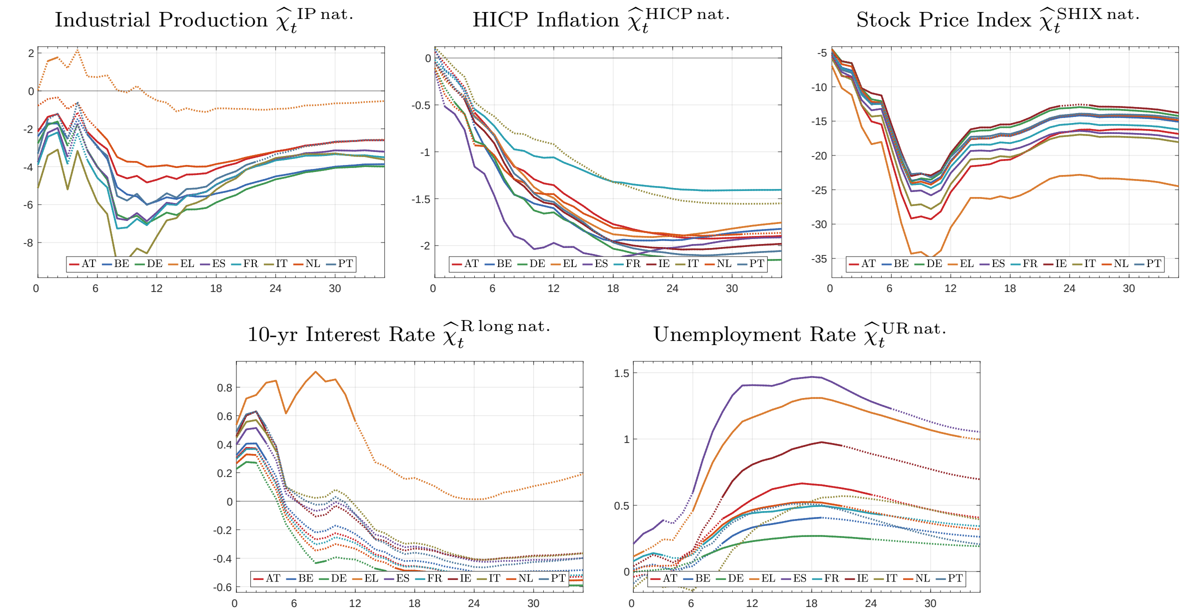

FIGURE 3.D7: *National IRFs - Monthly data. Cumulative percentage response.*

3.D.3 Heterogeneous country responses

FIGURE 3.D8: *Difference between EA and country-level IRFs: baseline vs. alternative transformations (1)*

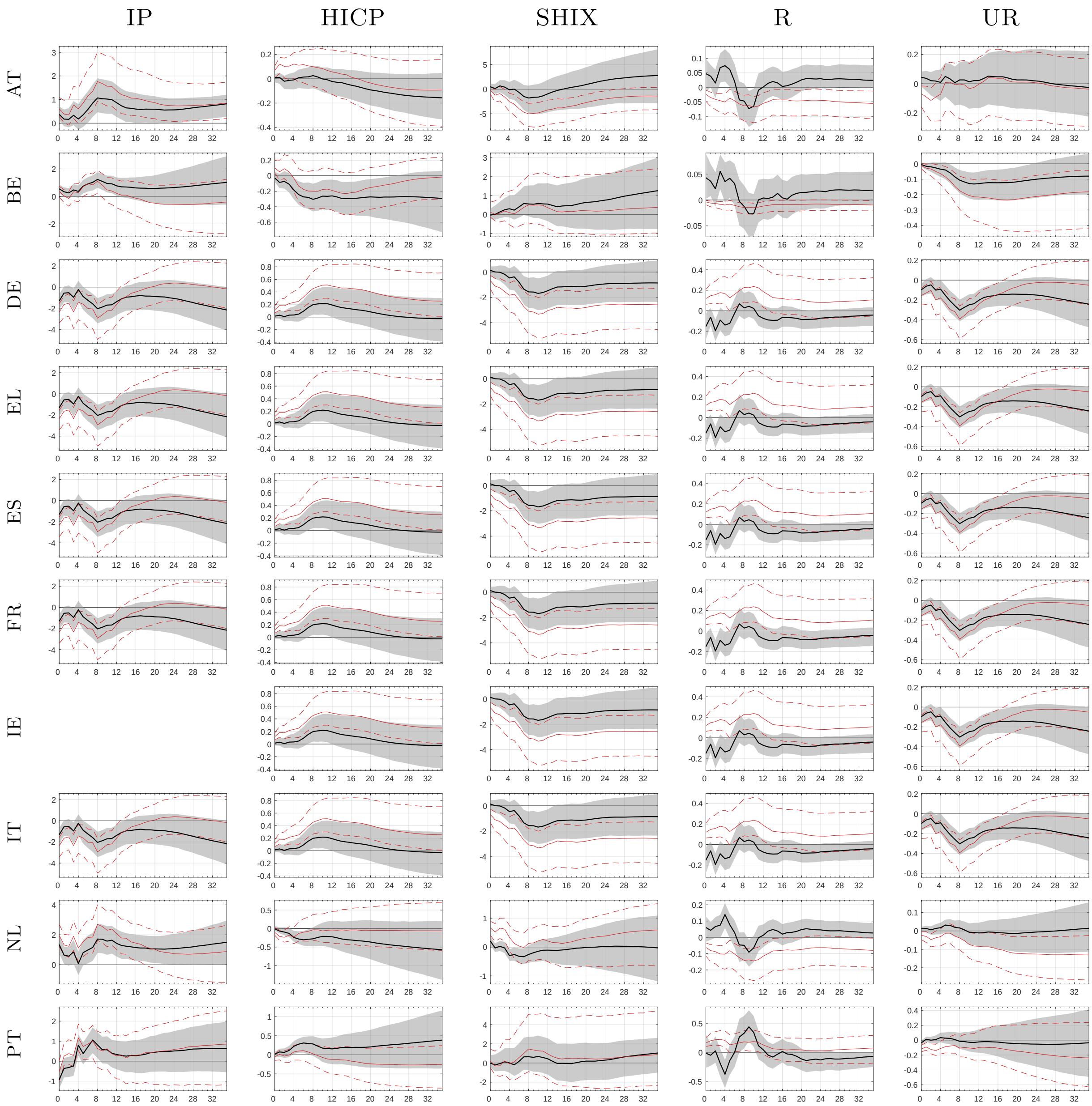

NOTES: Each sub-figure plots the impulse response of one variable for each country to a 100bps contractionary monetary policy shock. Each column of the graph represents a variable, while each row represents a country. The black solid line is the point estimate in our baseline setting, while the red solid line is the point estimate obtained with the alternative set of transformation based on statistical criteria. The gray shaded area and red dotted lines are the corresponding 68% confidence intervals. The scale in the vertical axis differs across variables and countries.

3.D.4 Correlation Analysis

Table 3.D3: *Cross-country characteristics and IRFs dynamics: correlation analysis*

ID	Variable	IP	HICP	R	SHIX	UR
1	Employment Protection	-0.05	0.17	-0.09	-0.05	-0.44
		(0.38)	(0.35)	(0.35)	(0.35)	(0.32)
2	Wage Adj. Frequency: more than once a year	0.16	0.28	-0.52	0.38	-0.51
		(0.44)	(0.39)	(0.35)	(0.38)	(0.35)
3	Wage Adj. Frequency: once a year	0.65	-0.15	-0.61	-0.22	0.11
		(0.34)	(0.40)	(0.32)	(0.40)	(0.41)
4	Wage Adj. Frequency: less than once a year	-0.65	0.38	0.42	-0.16	-0.22
		(0.34)	(0.38)	(0.37)	(0.40)	(0.40)
5	Price Flexibility	-0.09	-0.39	-0.39	0.64	-0.07
		(0.45)	(0.41)	(0.41)	(0.34)	(0.45)
6	NFC Leverage	0.00	-0.06	-0.36	0.68**	-0.15
		(0.38)	(0.35)	(0.33)	(0.26)	(0.35)
7	Homeownership	0.09	-0.02	0.67**	-0.09	0.57*
		(0.38)	(0.35)	(0.26)	(0.35)	(0.29)
8	Homeownership with mortgage	0.07	-0.21	-0.52	0.65**	-0.30
		(0.38)	(0.35)	(0.30)	(0.27)	(0.34)
9	Homeownership without mortgage	-0.01	0.17	0.81***	-0.59*	0.57*
		(0.38)	(0.35)	(0.21)	(0.28)	(0.29)
10	Fixed-Rate Mortgages	-0.28	0.33	-0.77***	0.43	-0.65**
		(0.36)	(0.33)	(0.23)	(0.32)	(0.27)
11	Loan to Value	-0.32	-0.26	-0.11	0.71**	-0.07
		(0.39)	(0.36)	(0.38)	(0.27)	(0.38)
12	Share of HtM	0.39	-0.53	0.49	0.17	0.35
		(0.35)	(0.30)	(0.31)	(0.35)	(0.33)
13	Share of WHtM	0.40	-0.48	0.70**	-0.02	0.51
		(0.35)	(0.31)	(0.25)	(0.35)	(0.30)
14	Saving Rate	-0.37	-0.12	-0.85***	0.60*	-0.37
		(0.35)	(0.35)	(0.19)	(0.28)	(0.33)
15	Explained Variance	-0.75**	0.13	-0.95***	0.37	0.37
		(0.25)	(0.35)	(0.11)	(0.33)	(0.33)

Notes: Each entry of the table corresponds to the correlation between each indicator (in the row) and the peak of the impulse response for a specific variable (in the columns). Standard errors in parentheses, asterisks denote statistical significance at 99% (***), 95% (**), and 90% (*). The first row reports the Employment Protection Index (OECD). Rows 2-4 show the frequency of wage adjustments by firms (Branten et al., 2018), while row 1 reports the frequency with which firms adjust output prices (Gautier et al., 2024). Row 6 shows the leverage of non-financial corporations relative to GDP (Eurostat). Row 7 reports the homeownership rate as a share of the population (Eurostat). Rows 8 and 9 indicate, respectively, the shares of residential properties with and without an outstanding mortgage (Eurostat). Row 10 reports the share of fixed-rate mortgages (De Stefani and Mano, 2025). Row 11 shows the average household loan-to-value ratio from the Eurosystem Household Finance and Consumption Survey (HFCS). Rows 12 and 13 display, respectively, the shares of "wealthy hand-to-mouth" and "poor hand-to-mouth" households, constructed as in Slacalek et al. (2020) based on HFCS data. Row 14 reports the household saving rate as a percentage of GDP (OECD). Finally, row 15 corresponds to the share of variance explained by the common factors for each variable in the columns, as reported in Table 3.3.

3.E Alternative set of transformations: all rates in levels

3.E.1 Euro Area IRFs

Figure 3.E9: *Euro Area IRFs: baseline vs alternative set of transformations (1)*

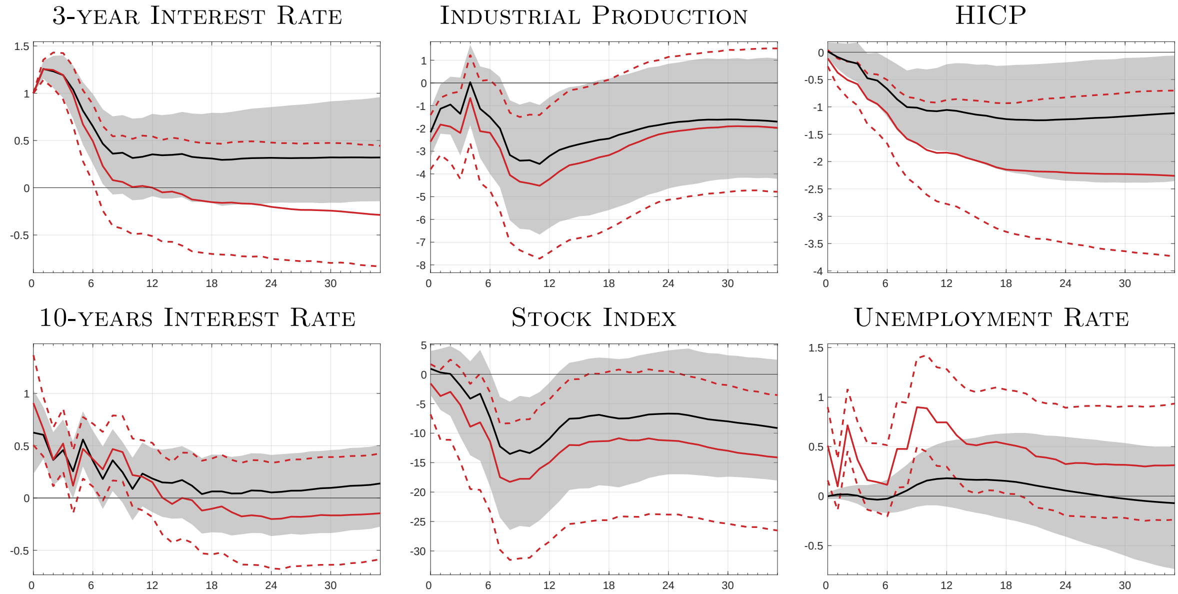

Notes: Each sub-figure plots the impulse response of one EA variable to a 100bps contractionary monetary policy shock. The black solid line is the point estimate in our baseline setting, while the red solid line is the point estimate obtained with the alternative set of transformations keeping all rates in levels. The gray shaded area and red dotted lines are the corresponding 68% confidence intervals.

3.E.2 Country-level IRFs

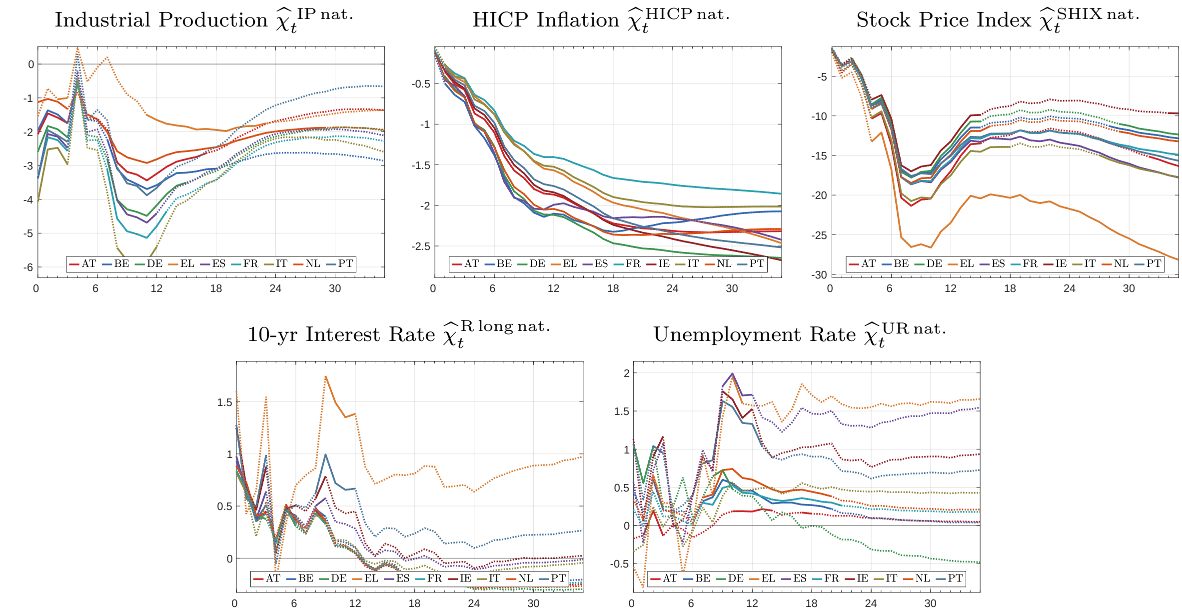

FIGURE 3.E10: *National IRFs - Monthly data. Cumulative percentage response.*

3.E.3 Heterogeneous country responses

Figure 3.E11: *Difference between EA and country-level IRFs: baseline vs. alternative transformations (2)*

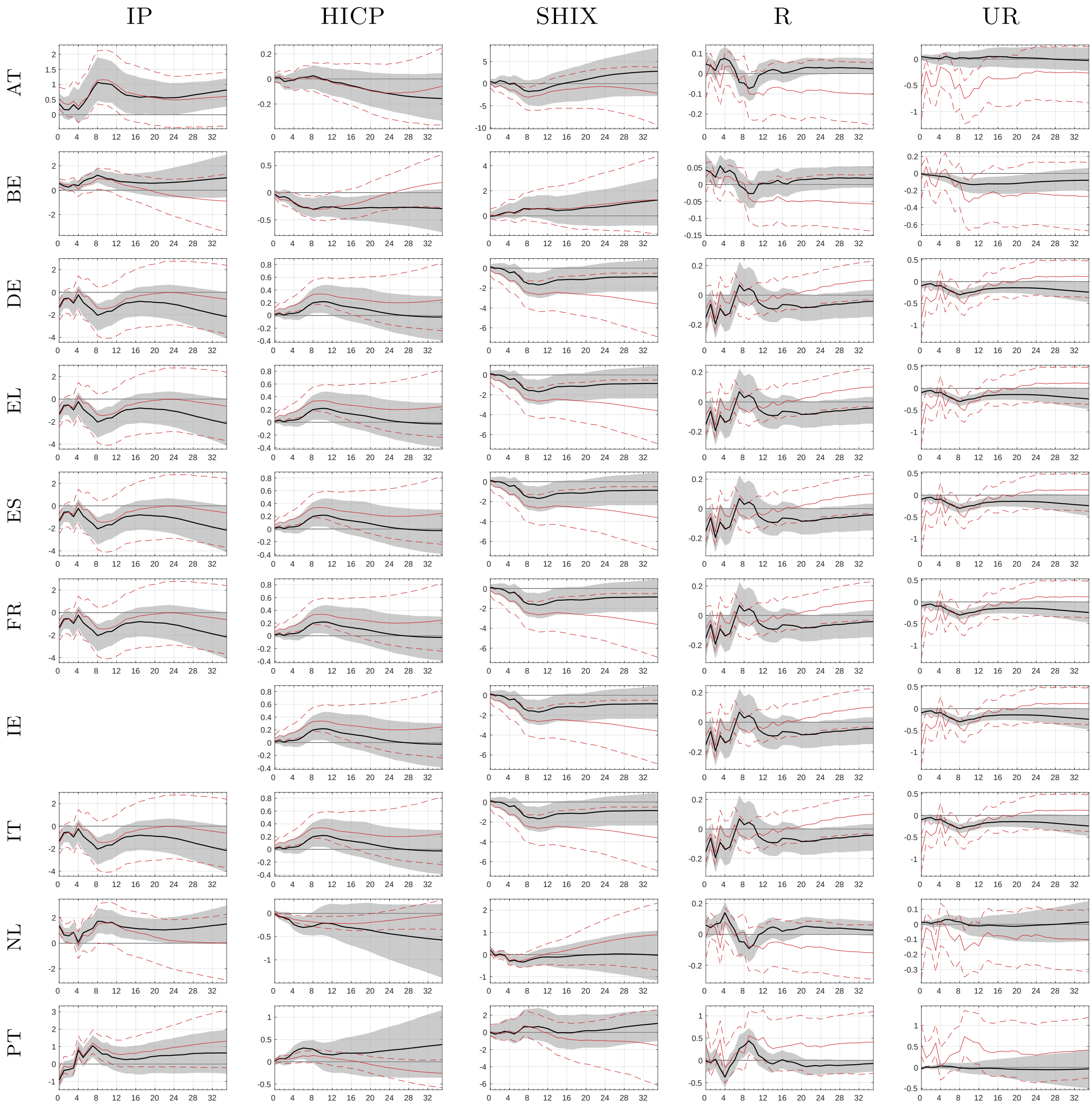

Notes: Each sub-figure plots the impulse response of one variable for each country to a 100bps contractionary monetary policy shock. Each column of the graph represents a variable, while each row represents a country. The black solid line is the point estimate in our baseline setting, while the red solid line is the point estimate obtained with the alternative set of transformation leaving all rates in levels. The gray shaded area and red dotted lines are the corresponding 68% confidence intervals. The scale in the vertical axis differs across variables and countries.

3.E.4 Correlation Analysis

TABLE 3.E4: *Cross-country characteristics and IRFs dynamics: correlation analysis*

ID	Variable	IP	HICP	R	SHIX	UR
1	Employment Protection	-0.05	0.17	-0.09	-0.05	-0.44
		(0.38)	(0.35)	(0.35)	(0.35)	(0.32)
2	Wage Adj. Frequency: more than once a year	0.16	0.28	-0.52	0.38	-0.51
		(0.44)	(0.39)	(0.35)	(0.38)	(0.35)
3	Wage Adj. Frequency: once a year	0.65	-0.15	-0.61	-0.22	0.11
		(0.34)	(0.40)	(0.32)	(0.40)	(0.41)
4	Wage Adj. Frequency: less than once a year	-0.65	0.38	0.42	-0.16	-0.22
		(0.34)	(0.38)	(0.37)	(0.40)	(0.40)
5	Price Flexibility	-0.09	-0.39	-0.39	0.64	-0.07
		(0.45)	(0.41)	(0.41)	(0.34)	(0.45)
6	NFC Leverage	0.00	-0.06	-0.36	0.68**	-0.15
		(0.38)	(0.35)	(0.33)	(0.26)	(0.35)
7	Homeownership	0.09	-0.02	0.67**	-0.09	0.57*
		(0.38)	(0.35)	(0.26)	(0.35)	(0.29)
8	Homeownership with mortgage	0.07	-0.21	-0.52	0.65**	-0.30
		(0.38)	(0.35)	(0.30)	(0.27)	(0.34)
9	Homeownership without mortgage	-0.01	0.17	0.81***	-0.59*	0.57*
		(0.38)	(0.35)	(0.21)	(0.28)	(0.29)
10	Fixed-Rate Mortgages	-0.28	0.33	-0.77***	0.43	-0.65**
		(0.36)	(0.33)	(0.23)	(0.32)	(0.27)
11	Loan to Value	-0.32	-0.26	-0.11	0.71**	-0.07
		(0.39)	(0.36)	(0.38)	(0.27)	(0.38)
12	Share of HtM	0.39	-0.53	0.49	0.17	0.35
		(0.35)	(0.30)	(0.31)	(0.35)	(0.33)
13	Share of WHtM	0.40	-0.48	0.70**	-0.02	0.51
		(0.35)	(0.31)	(0.25)	(0.35)	(0.30)
14	Saving Rate	-0.37	-0.12	-0.85***	0.60*	-0.37
		(0.35)	(0.35)	(0.19)	(0.28)	(0.33)
15	Explained Variance	-0.75**	0.13	-0.95***	0.37	0.37
		(0.25)	(0.35)	(0.11)	(0.33)	(0.33)

NOTES: Each entry of the table corresponds to the correlation between each indicator (in the row) and the peak of the impulse response for a specific variable (in the columns). Standard errors in parentheses, asterisks denote statistical significance at 99% (***), 95% (**), and 90% (*). The first row reports the Employment Protection Index (OECD). Rows 2-4 show the frequency of wage adjustments by firms (Branten et al., 2018), while row 1 reports the frequency with which firms adjust output prices (Gautier et al., 2024). Row 6 shows the leverage of non-financial corporations relative to GDP (Eurostat). Row 7 reports the homeownership rate as a share of the population (Eurostat). Rows 8 and 9 indicate, respectively, the shares of residential properties with and without an outstanding mortgage (Eurostat). Row 10 reports the share of fixed-rate mortgages (De Stefani and Mano, 2025). Row 11 shows the average household loan-to-value ratio from the Eurosystem Household Finance and Consumption Survey (HFCS). Rows 12 and 13 display, respectively, the shares of "wealthy hand-to-mouth" and "poor hand-to-mouth" households, constructed as in Slacalek et al. (2020) based on HFCS data. Row 14 reports the household saving rate as a percentage of GDP (OECD). Finally, row 15 corresponds to the share of variance explained by the common factors for each variable in the columns, as reported in Table 3.3.

3.F Identification via sign restrictions

Sign restrictions are imposed as summarized in Table 3.F5. Specifically, we impose a positive response of short- and long-term EA interest rates in the first two periods following the shock. For GDP, HICP, and share prices, we impose a negative response in the second and third periods. This choice accomodates possible nominal rigidities and delayed real adjustments, allowing for a gradual transmission of monetary policy effects.

TABLE 3.F5: *Sign Restrictions*

Horizon	R_t	$\widehat{\chi}_t^{\text{IP EA}}$	$\widehat{\chi}_t^{\text{HICP EA}}$	$\widehat{\chi}_t^{\text{R long EA}}$	$\widehat{\chi}_t^{\text{SHIX EA}}$
0	+			+	
1	+	−	−	+	−
2		−	−		−

Confidence intervals and point estimates are obtained using a bootstrap procedure with 10,000 replications. For each iteration, we proceed as follows. We draw an $n \times n$ matrix $\mathbf{W}$ whose rows are independently sampled from a $\mathcal{N}(\mathbf{0}, \mathbf{I}_n)$ distribution. We then compute the QR decomposition $\mathbf{W} = \mathbf{QR}$, where $\mathbf{Q}$ is orthogonal and $\mathbf{R}$ is upper triangular (Rubio-Ramirez et al., 2010). The candidate structural impact matrix is given by $\mathbf{S} = \mathbf{LQ'}$, where $\mathbf{L}$ denotes the lower triangular Cholesky factor of the reduced-form innovation covariance matrix $\mathbf{\Sigma}$.

If the resulting impulse responses satisfy the sign restrictions in Table 3.F5, the draw is accepted; otherwise, it is discarded. Within each bootstrap replication, we continue this process until $K = 30$ admissible draws are obtained. Following Fry and Pagan (2011), we retain only the IRF that is closest to the median across the K accepted draws. The same procedure is applied to the observed data. This yields 10,000+1 admissible IRFs, from which we construct the empirical distribution of responses. We take the median of this distribution as the point estimate, while the 16th and 84th percentiles serve as the lower and upper bounds of the confidence interval, respectively.

3.F.1 Euro Area IRFs

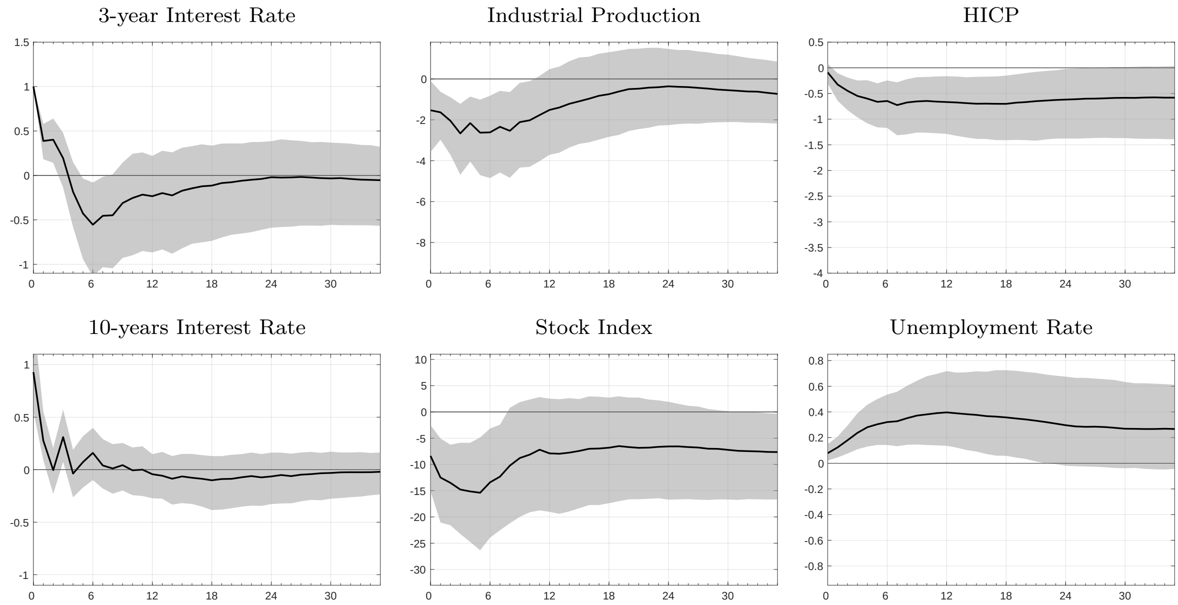

FIGURE 3.F12: *EA IRFs*

3.F.2 Country-level IRFs

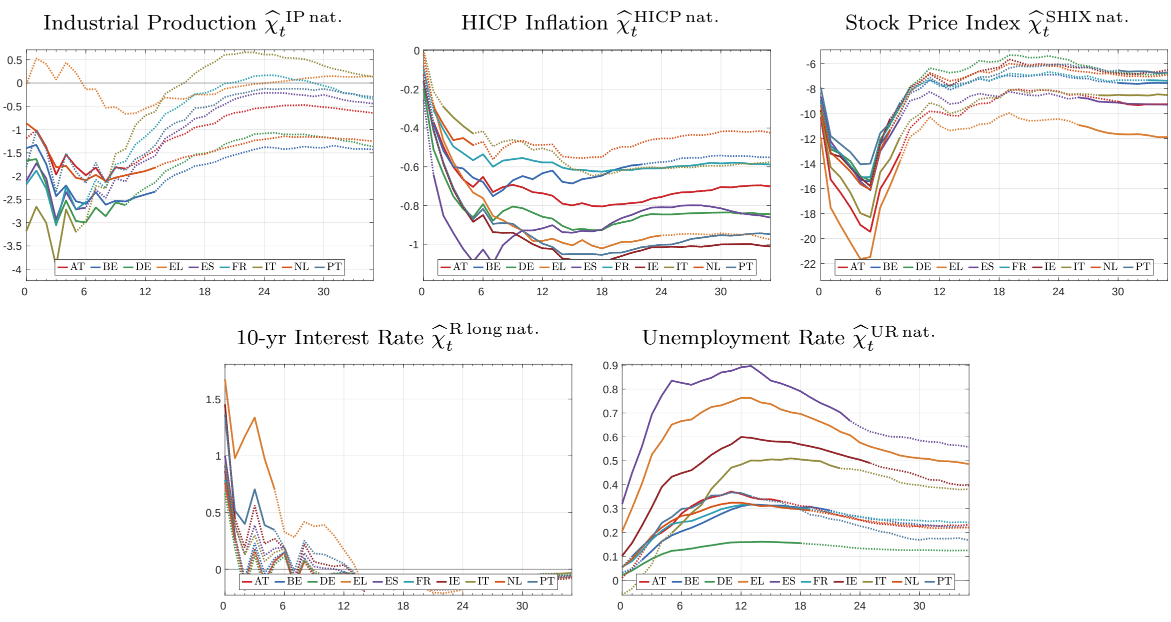

FIGURE 3.F13: *National IRFs - Monthly data. Cumulative percentage response.*

3.F.3 Heterogeneous country responses

Figure 3.F14: *Difference between Euro Area and country-specific IRFs: identification via sign restrictions*

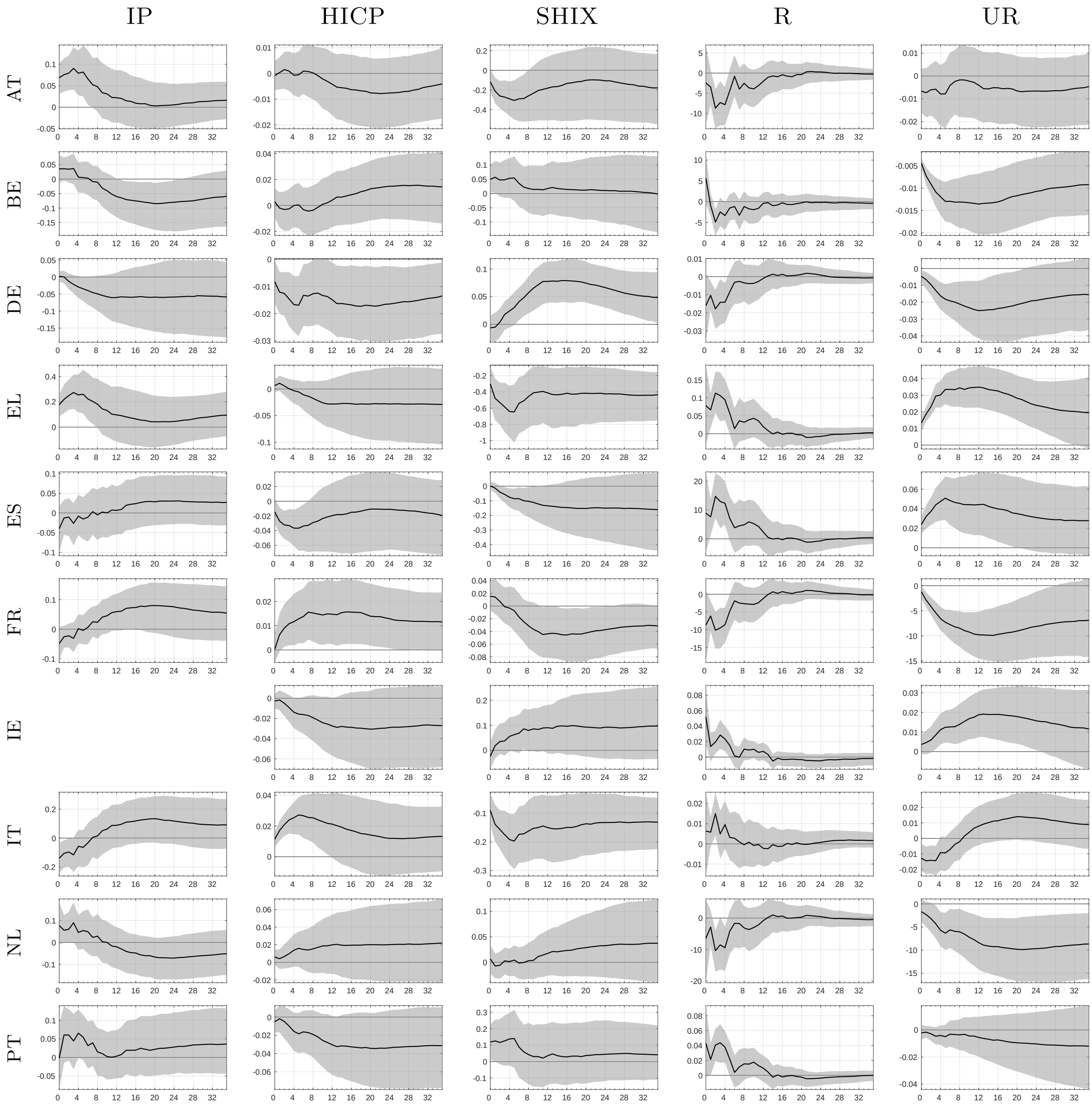

Notes: Each sub-figure plots the impulse response of one variable for each country to a 100bps contractionary monetary policy shock. Each column of the graph represents a variable, while each row represents a country. The black solid line is the point estimate obtained identifying the monetary policy shock via sign restrictions, while gray shaded area are the corresponding 68% confidence intervals. The scale in the vertical axis differs across variables and countries.

3.G Quarterly data

In this section, we present the results obtained using quarterly data, identifying the monetary policy shock through sign restrictions. We do not report results based on identification via instrumental variables, which are unreliable due to the extremely low explanatory power of the instrument at the quarterly frequency. As noted by Kilian (2024), time aggregation of high-frequency instruments can become problematic as the sampling frequency decreases.

Following the same procedure described in Appendix 3.F, we impose the sign restrictions summarized in Table 3.G6. Specifically, we require a positive response of short- and long-term EA interest rates during the first two periods after the shock. For GDP, HICP, and share prices, we impose a negative response in the second and third periods.

Table 3.G6: *Sign Restrictions - Quarterly data*

Horizon	R_t	$\widehat{\chi}_t^{\text{GDP EA}}$	$\widehat{\chi}_t^{\text{HICP EA}}$	$\widehat{\chi}_t^{\text{R long EA}}$	$\widehat{\chi}_t^{\text{SHIX EA}}$
0	+			+	
1	+	−	−	+	−
2		−	−		−

3.G.1 Euro Area IRFs

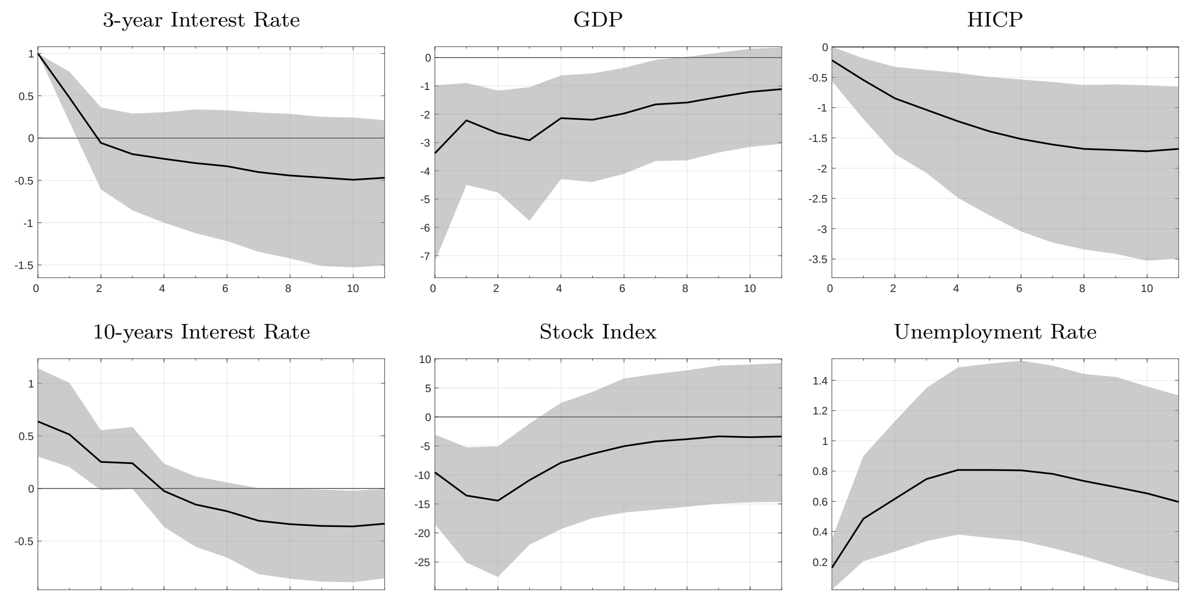

Figure 3.G15: *EA IRFs*

3.G.2 Country-level IRFs

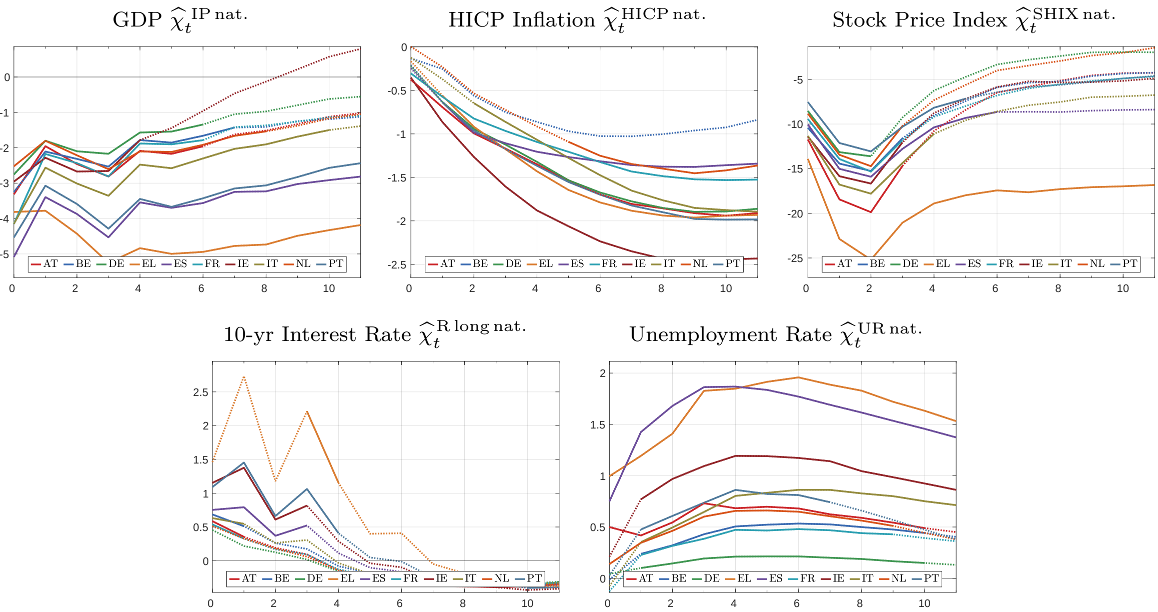

FIGURE 3.G16: *National IRFs - Monthly data. Cumulative percentage response.*

3.G.3 Heterogeneous country responses

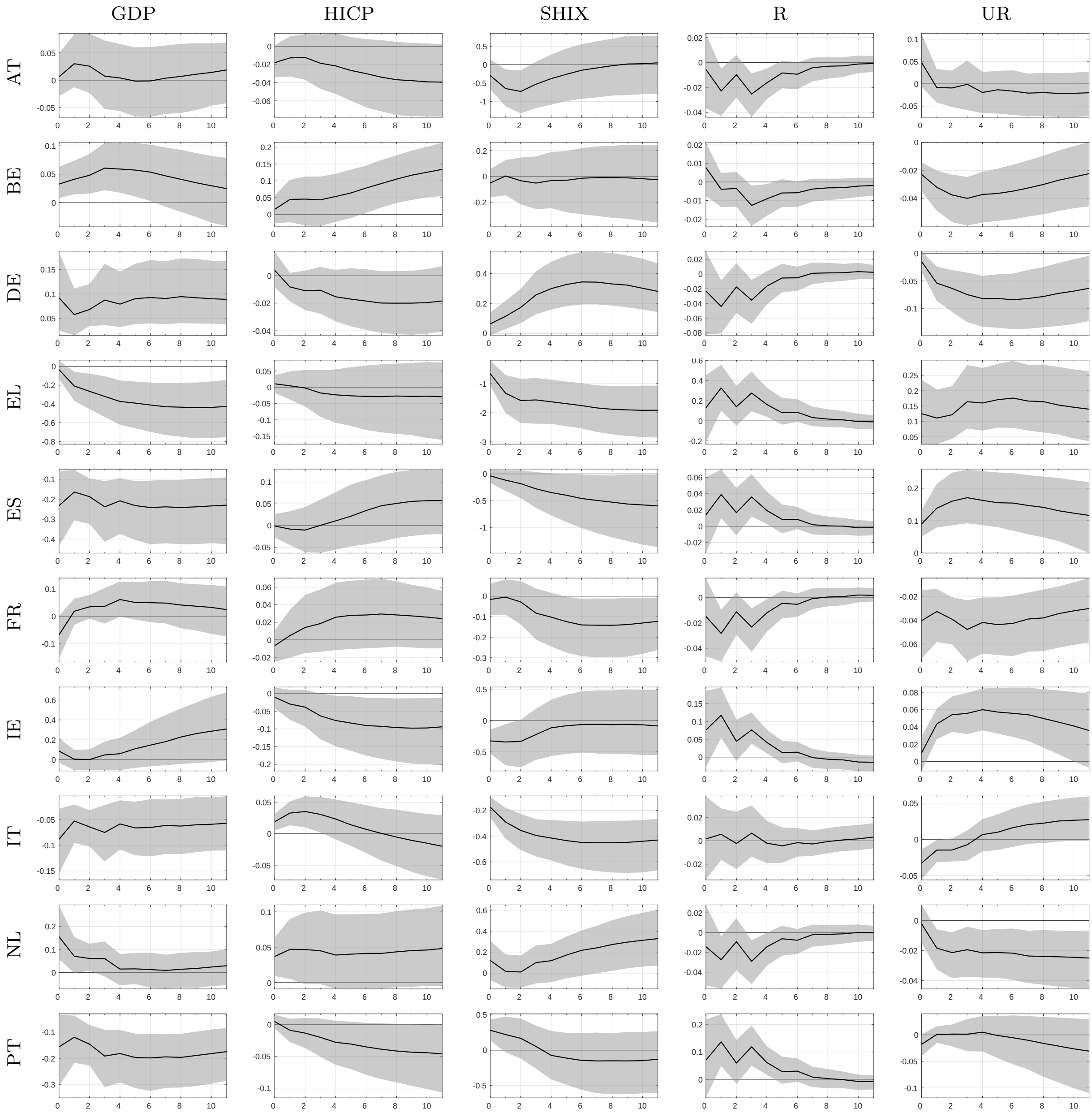

3.H Mixed Frequency estimation

3.H.1 Euro Area IRFs

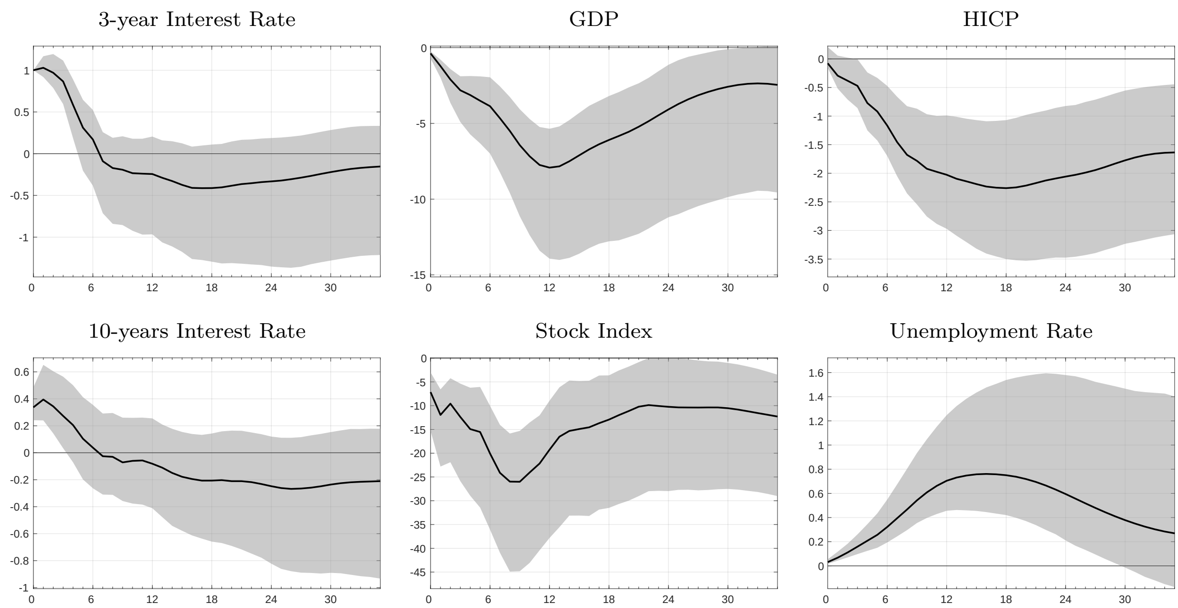

FIGURE 3.H17: *EA IRFs*

3.H.2 Country-level IRFs

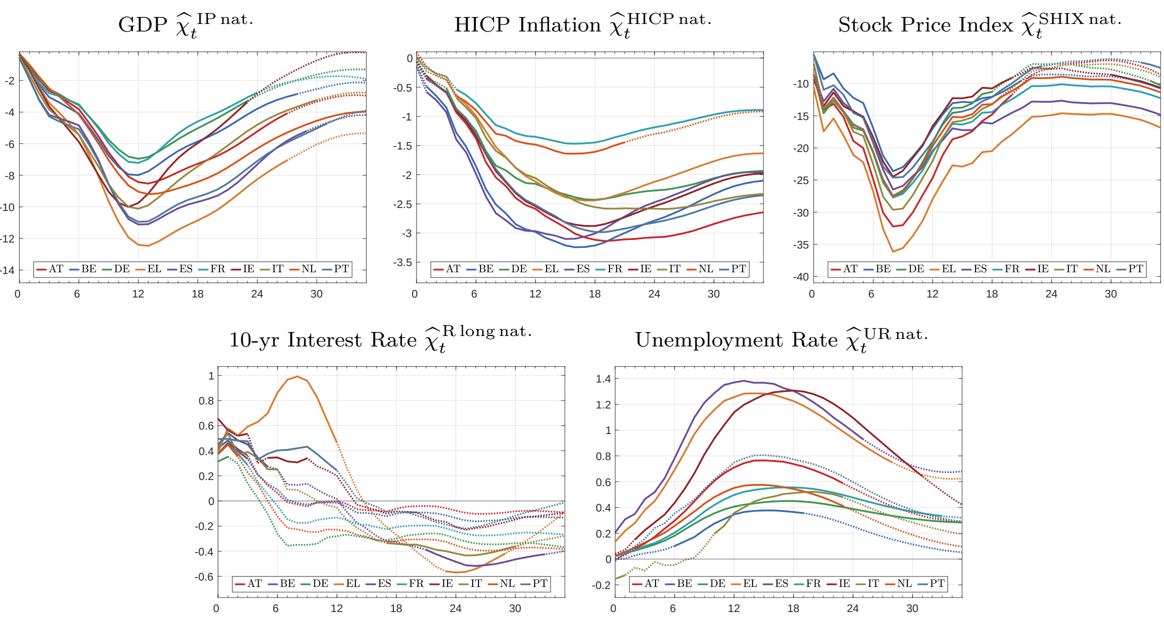

FIGURE 3.H18: *National IRFs - Monthly data. Cumulative percentage response.*

3.H.3 Heterogeneous country responses

Figure 3.H19: *Difference between EA and country-level IRFs: mixed-frequency estimation*

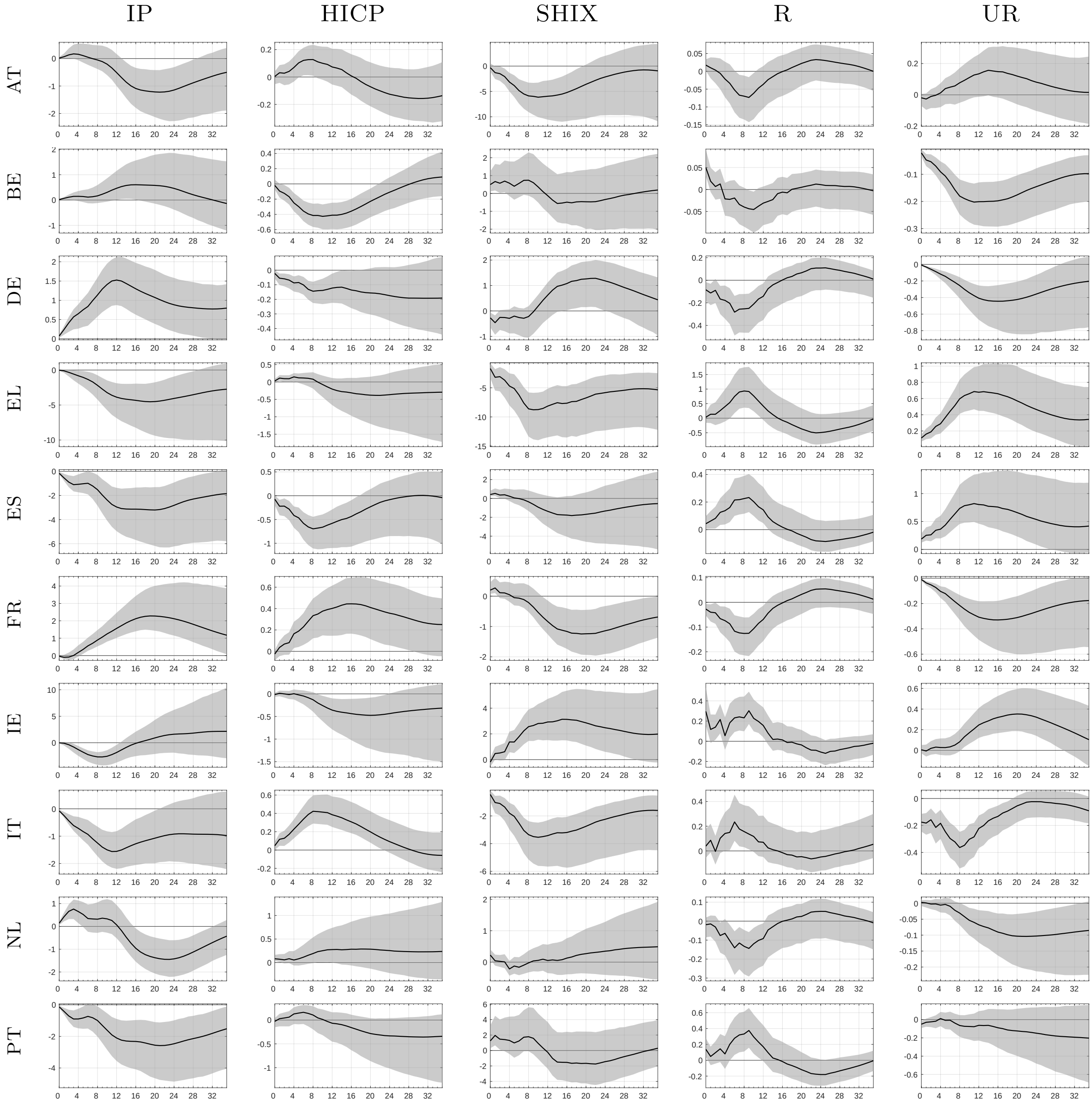

Notes: Each sub-figure plots the impulse response of one variable for each country to a 100bps contractionary monetary policy shock. Each column of the graph represents a variable, while each row represents a country. The black solid line is the point estimate obtained with a mixed-frequency model including GDP for all countries as quarterly variables. The gray shaded area is the corresponding 68% confidence interval.

Appendix to Chapter 4

4.A Data description

This appendix provides a detailed description of the dataset for the Euro Area and its ten largest member countries. All series are retrieved from institutional sources. For each series, we provide a brief description, the data source, the measurement unit, the seasonal adjustment procedure, and the transformation (if any) applied. Table 1.A1 presents a glossary to facilitate the interpretation of the data description reported in Table 4.A2.

The first eight columns of Table 4.A2 contain several identifiers for each series, namely: a numeric indicator (N), an alphabetical identifier (ID), a short description (Series), the unit of measure (Unit), the seasonal adjustment (SA), the frequency (F), the data provider (P), and the class (C) to which each variable belongs (real, nominal, or financial). The remaining columns list all countries included in the dataset, starting with the Euro Area aggregate, followed by individual countries in alphabetical order. Each entry in the country columns denotes the transformation applied to the corresponding series for that country. When a series is unavailable for a given country, the corresponding entry is marked with a "-".

We consider three sets of transformations in our application. For the baseline transformations, we determine the order of integration for each variable using standard statistical tests (Dickey and Fuller, 1979; Phillips and Perron, 1988) and difference once all I(1) variables and twice all I(2) variables, except for interest rates, which are kept in levels following Corsetti et al. (2022). In addition, we consider two sets of alternative transformations in the Appendix: (i) *statistical transformations*, which rely exclusively on statistical tests and therefore difference interest rates once; and (ii) *all rates in levels*, which also keep unemployment rates in levels. These alternative transformations are highlighted in Table 4.A2, with definitions provided in Table 4.A1.

The dataset for the Euro Area and individual countries is constructed with the objective of ensuring consistency across countries in terms of time coverage, number of indicators, and treatment of variables. Due to data limitations, full harmonization is not always possible. Specifically, the main differences across countries are as follows:

1. Labor market indicators are seasonally and calendar adjusted for all countries except France, Portugal, and Greece, where they are only seasonally adjusted.

2. Credit aggregates are available from 2000:Q1 for all countries except Ireland, for which they start in 2002:Q1.

3. Labor cost series are available from 2000:Q1 for all countries, except for the Euro Area, where they are available from 2001:Q1.

4. Turnover indicators are available from 2000:M1 for all countries except France, where data start in 2002:M1.

5. The Harmonized Index of Consumer Prices (HICP) is available for most countries from 2000:M1, with the exceptions of Spain (2000:M12), Ireland (2002:M1), and Belgium (2001:M1).

TABLE 4.A1: *Glossary*

Source	**Unit**
EUR = Eurostat	CLV = Chain-linked volumes
OECD = Organization for Economic Co-operation and Development	CP_MEUR = Current Prices (Million€)
ECB = European Central Bank	1000p = Thousands of persons
FRED = Federal Reserve Economic Data	1000-U = Thousands of Units

Seasonal Adjustment	**Frequency**	**Transformation**
NSA = No Seasonal Adjustment	Q = Quarterly	$1 = 100 \times \log(x_t)$
SA = Seasonal Adjustment	M = Monthly	$1.5 = 100 \times \Delta \log(x_t)$ (baseline); $100 \times \log(x_t)$ (statistical transformations)
SCA = Seasonal and Calendar Adjustment		$2 = 100 \times \Delta \log(x_t)$
MSA = Manual adjustment		$3 = 100 \times \Delta^2 \log(x_t)$
		$4 = x_t$ (No Transformation)
		$4.5 = \Delta x_t$ (baseline); x_t (all rates in levels)
		$5 = \Delta x_t$

Table 4.A2: *Data Description and Transformation by country*

Identifiers								Countries										
N	**ID**	**Series**	**Unit**	**SA**	**F**	**P**	**C**	**EA**	**AT**	**BE**	**DE**	**EL**	**ES**	**FR**	**IE**	**IT**	**NL**	**PT**
		(1) **National Accounts**																
1	GDP	Real Gross Domestic Product	CLV15	SCA	Q	EUR	R	2	2	2	2	2	2	2	2	2	2	2
2	EXPGS	Real Export Goods and services	CLV15	SCA	Q	EUR	R	2	2	2	2	2	2	2	2	2	2	2
3	IMPGS	Real Import Goods and services	CLV15	SCA	Q	EUR	R	2	2	2	2	2	2	2	2	2	2	2
4	GFCE	Real Government Final consumption expenditure	CLV15	SCA	Q	EUR	R	2	2	2	2	2	2	2	2	2	2	2
5	HFCE	Real Households consumption expenditure	CLV15	SCA	Q	EUR	R	2	2	2	2	2	2	2	2	2	2	2
6	CONSD	Real Households consumption expenditure: Durable Goods	CLV15	SCA	Q	EUR	R	2	2	2	2	2	2	2	2	2	2	2
7	CONSSD	Real Households consumption expenditure: Semi-Durable Goods	CLV15	SCA	Q	EUR	R	-	2	-	2	-	-	2	2	2	2	-
8	CONSSV	Real Households consumption expenditure: Services	CLV15	SCA	Q	EUR	R	-	2	-	2	-	-	2	2	2	2	-
9	CONSND	Real Households consumption expenditure: Non-Durable Goods	CLV15	SCA	Q	EUR	R	2	2	-	2	-	-	2	2	2	2	-
10	GCF	Real Gross capital formation	CLV15	SCA	Q	EUR	R	2	2	2	2	2	2	2	2	2	2	2
11	GCFC	Real Gross fixed capital formation	CLV15	SCA	Q	EUR	R	2	2	2	2	2	2	2	2	2	2	2
12	GFACON	Real Gross Fixed Capital Formation: Construction	CLV15	SCA	Q	EUR	R	2	2	-	2	2	3	2	2	2	2	2
13	GFAMG	Real Gross Fixed Capital Formation: Machinery and Equipment	CLV15	SCA	Q	EUR	R	2	2	-	2	2	2	2	2	2	2	2
14	AHRDI	Adjusted Households Real Disposable Income	%chg	SCA	Q	EUR	R	4	-	-	-	-	-	-	-	-	-	-
15	AHFCE	Actual Final Consumption Expenditure of Households	%chg	SCA	Q	EUR	R	4	-	-	-	-	-	-	-	-	-	-
16	GNFCPS	Gross Profit Share of Non-Financial Corporations	%	SCA	Q	EUR	R	5	5	5	5	5	5	5	5	5	5	5
17	GNFCIR	Gross Investment Share of Non-Financial Corporations	%	SCA	Q	EUR	R	5	5	5	5	5	5	5	5	5	5	5
18	GHIR	Gross Investment Rate of Households	%	SCA	Q	EUR	R	5	5	-	5	-	5	5	5	5	5	5
19	GHSR	Gross Households Savings Rate	%	SCA	Q	EUR	R	5	5	5	5	-	5	5	5	5	5	5
		(2) **Labor Market Indicators**																
20	TEMP	Total Employment (domestic concept)	1000p	SCA	Q	EUR	R	2	2	2	2	2	2	2	2	2	2	2
21	EMP	Employees (domestic concept)	1000p	SCA	Q	EUR	R	2	2	2	2	2	2	2	2	2	3	2
22	SEMP	Self Employment (domestic concept)	1000p	SCA	Q	EUR	R	2	2	3	3	2	2	3	2	2	2	2
23	THOURS	Hours Worked: Total	I15	SCA	Q	EUR	R	2	2	-	2	2	2	2	2	2	2	2
24	EMPAG	Quarterly Employment: Agriculture, Forestry, Fishing	1000p	SCA	Q	EUR	R	2	2	2	2	2	2	2	2	2	2	2
25	EMPIN	Quarterly Employment: Industry	1000p	SCA	Q	EUR	R	2	2	2	2	2	2	2	2	2	3	2
26	EMPMN	Quarterly Employment: Manufacturing	1000p	SCA	Q	EUR	R	2	2	2	2	2	2	2	2	2	3	2
27	EMPCON	Quarterly Employment: Construction	1000p	SCA	Q	EUR	R	2	2	3	2	2	2	3	2	2	2	2
28	EMPRT	Quarterly Employment: Wholesale/Retail trade, transport, food	1000p	SCA	Q	EUR	R	2	2	2	2	2	2	2	2	2	2	2
29	EMPIT	Quarterly Employment: Information and Communication	1000p	SCA	Q	EUR	R	2	2	2	2	2	2	2	2	2	2	2
30	EMPFC	Quarterly Employment: Financial and Insurance activities	1000p	SCA	Q	EUR	R	2	2	2	2	2	2	2	2	2	2	2
31	EMPRE	Quarterly Employment: Real Estate	1000p	SCA	Q	EUR	R	2	2	2	2	2	2	2	2	2	2	2
32	EMPPR	Quarterly Employment: Professional, Scientific, Technical activities	1000p	SCA	Q	EUR	R	2	2	2	2	2	2	2	2	2	2	2
33	EMPPA	Quarterly Employment: PA, education, health ad social services	1000p	SCA	Q	EUR	R	2	2	2	2	2	2	2	2	2	2	2
34	EMPENT	Quarterly Employment: Arts and recreational activities	1000p	SCA	Q	EUR	R	2	2	2	2	2	2	2	2	2	2	2
35	UNETOT	Unemployment: Total (% active population)	%	SA	M	EUR	R	4.5	4.5	4.5	4.5	4.5	4.5	4.5	4.5	4.5	4.5	4.5
36	UNEO25	Unemployment: Over 25 years (% active population)	%	SA	M	EUR	R	4.5	4.5	4.5	4.5	4.5	4.5	4.5	4.5	4.5	4.5	4.5
37	UNEU25	Unemployment: Under 25 years (% active population)	%	SA	M	EUR	R	4.5	4.5	4.5	4.5	4.5	4.5	4.5	4.5	4.5	4.5	4.5
38	RPRP	Real Labour Productivity (person)	I15	SCA	Q	EUR	R	2	2	2	2	2	2	2	2	2	2	2
39	WS	Wages and salaries	CP	SCA	Q	EUR	N	2	2	2	2	2	2	2	2	2	2	2
40	ESC	Employers' Social Contributions	CP	SCA	Q	EUR	N	2	2	2	2	2	2	2	2	2	2	2
		(3) **Credit Aggregates**																
41	TASS.SDB	Total Economy - Assets: Short-Term Debt Securities	MLN€	MSA	Q	EUR	F	2	2	2	2	2	2	2	2	2	2	2
42	TASS.LDB	Total Economy - Assets: Long-Term Debt Securities	MLN€	MSA	Q	EUR	F	2	2	2	2	2	2	2	2	2	2	2
43	TASS.SLN	Total Economy - Assets: Short-Term Loans	MLN€	MSA	Q	EUR	F	2	2	2	2	2	3	2	2	2	2	3
44	TASS.LLN	Total Economy - Assets: Long-Term Loans	MLN€	MSA	Q	EUR	F	2	2	2	2	2	3	2	2	3	2	2
45	TLB.SDB	Total Economy - Liabilities: Short-Term Debt Securities	MLN€	MSA	Q	EUR	F	2	2	2	2	-	2	2	2	2	2	2
46	TLB.LDB	Total Economy - Liabilities: Long-Term Debt Securities	MLN€	MSA	Q	EUR	F	2	2	2	2	2	2	2	2	2	2	2
47	TLB.SLN	Total Economy - Liabilities: Short-Term Loans	MLN€	MSA	Q	EUR	F	2	2	2	2	2	2	2	2	2	2	2
48	TLB.LLN	Total Economy - Liabilities: Long-Term Loans	MLN€	MSA	Q	EUR	F	2	2	2	2	2	3	2	2	3	2	3
49	NFCASS	Non-Financial Corporations: Total Financial Assets	MLN€	MSA	Q	EUR	F	2	2	2	2	2	2	2	2	2	2	2
50	NFCASS.SLN	Non-Financial Corporations - Assets: Short-Term Loans	MLN€	MSA	Q	EUR	F	2	2	2	2	-	2	2	2	2	2	2
51	NFCASS.LLN	Non-Financial Corporations - Assets: Long-Term Loans	MLN€	MSA	Q	EUR	F	2	2	2	2	-	2	2	2	2	2	2
52	NFCLB	Non-Financial Corporations: Total Financial Liabilities	MLN€	MSA	Q	EUR	F	2	2	2	2	2	2	2	2	2	2	2
53	NFCLB.SLN	Non-Financial Corporations - Liabilities - Short-Term Loans	MLN€	MSA	Q	EUR	F	2	2	2	2	2	2	2	-	2	2	2
54	NFCLB.LLN	Non-Financial Corporations - Liabilities - Long-Term Loans	MLN€	MSA	Q	EUR	F	2	2	2	2	3	2	2	-	3	2	3
55	GGASS	General Government: Total Financial Assets	MLN€	MSA	Q	EUR	F	2	2	2	2	2	2	2	2	2	2	2
56	GGASS.SLN	General Government - Assets: Short-Term Loans	MLN€	MSA	Q	EUR	F	2	2	-	-	-	-	-	-	-	2	-
57	GGASS.LLN	General Government - Assets: Short-Term Loans	MLN€	MSA	Q	EUR	F	2	2	-	2	-	-	2	-	-	2	2
58	GGLB	General Government: Total Financial Liabilities	MLN€	MSA	Q	EUR	F	2	2	2	2	2	2	2	2	2	2	2
59	GGLB.SLN	General Government - Liabilities: Short-Term Loans	MLN€	MSA	Q	EUR	F	2	2	2	2	-	2	2	2	2	2	2
60	GGLB.LLN	General Government - Liabilities: Long-Term Loans	MLN€	MSA	Q	EUR	F	2	2	2	2	-	2	2	2	2	2	3
61	HHASS	Households: Total Financial Assets	MLN€	MSA	Q	EUR	F	2	2	2	2	2	2	2	2	2	2	2
62	HHASS.SLN	Households - Assets: Short-Term Loans	MLN€	MSA	Q	EUR	F	2	-	-	-	-	-	2	-	-	-	-
63	HHASS.LLN	Households - Assets: Long-Term Loans	MLN€	MSA	Q	EUR	F	2	-	-	-	-	-	2	-	-	2	2
64	HHLB	Households: Total Financial Liabilities	MLN€	MSA	Q	EUR	F	3	2	2	3	3	3	3	2	3	2	3
65	HHLB.SLN	Households - Liabilities: Short-Term Loans	MLN€	MSA	Q	EUR	F	2	2	2	2	3	2	2	-	2	2	2
66	HHLB.LLN	Households - Liabilities: Long-Term Loans	MLN€	MSA	Q	EUR	F	3	2	2	3	3	3	3	-	3	3	3
		(4) **Labor Costs**																
67	ULCIN	Nominal Unit Labor Costs: Industry	I16	SCA	Q	EUR	N	2	2	2	2	2	2	2	2	2	2	2
68	ULCMQ	Nominal Unit Labor Costs: Mining and Quarrying	I16	SCA	Q	EUR	N	2	2	2	-	2	-	2	2	-	2	2
69	ULCMN	Nominal Unit Labor Costs: Manufacturing	I16	SCA	Q	EUR	N	2	2	2	2	2	2	2	2	2	2	2
70	ULCCON	Nominal Unit Labor Costs: Construction	I16	SCA	Q	EUR	N	2	2	2	2	2	2	2	-	2	2	2
71	ULCRT	Nominal Unit Labor Costs: Wholesale/Retail Trade, Transport, Food, IT	I16	SCA	Q	EUR	N	2	2	3	2	2	2	2	2	2	2	2
72	ULCFC	Nominal Unit Labor Costs: Financial Activities	I16	SCA	Q	EUR	N	2	2	2	2	2	2	2	2	2	2	2
73	ULCRE	Nominal Unit Labor Costs: Real Estate	I16	SCA	Q	EUR	N	2	2	2	2	2	2	2	-	2	2	2
74	ULCPR	Nominal Unit Labor Costs: Professional, Scientific, Technical activities	I16	SCA	Q	EUR	N	2	2	3	2	2	2	2	2	2	2	2
		(5) **Financial Markets**																
75	REER42	Real Exchange Rate (42 main industrial countries)	I10	NSA	M	EUR	F	2	2	2	2	2	2	2	2	2	2	2
76	ERUS	Exchange Rate (US dollar)	I10	NSA	M	EUR	F	2	-	-	-	-	-	-	-	-	-	-
77	SHIX	Share Prices	I10	SA	M	OECD	F	2	2	2	2	2	2	2	2	2	2	2
		(6) **Interest Rates**																
78	IRT3M	3-Months Interest Rates	%	NSA	M	EUR	F	1.5	-	-	-	-	-	-	-	-	-	-
79	IRT6M	6-Months Interest Rates	%	NSA	M	EUR	F	1.5	-	-	-	-	-	-	-	-	-	-
80	LTIRT	Long-Term Interest Rates (EMU Criterion)	%	NSA	M	EUR	F	1.5	1.5	1.5	1.5	1.5	1.5	1.5	1.5	1.5	1.5	1.5

TABLE 4.A2: *Data Description and Transformation by country*

Identifiers								Countries										
N	**ID**	**Series**	**Unit**	**SA**	**F**	**P**	**C**	**EA**	**AT**	**BE**	**DE**	**EL**	**ES**	**FR**	**IE**	**IT**	**NL**	**PT**
		(7) **Industrial Production and Turnover**																
81	IPMN	Industrial Production Index: Manufacturing	I21	SCA	M	EUR	R	2	2	2	2	2	2	2	-	2	2	2
82	IPCAG	Industrial Production Index: Capital Goods	I21	SCA	M	EUR	R	2	2	2	2	2	2	2	-	2	2	2
83	IPCOG	Industrial Production Index: Consumer Goods	I21	SCA	M	EUR	R	2	2	2	2	2	2	2	-	2	-	-
84	IPDCOG	Industrial Production Index: Durable Consumer Goods	I21	SCA	M	EUR	R	2	2	2	2	2	2	2	-	2	2	2
85	IPNDCOG	Industrial Production Index: Non Durable Consumer Goods	I21	SCA	M	EUR	R	2	2	2	2	2	2	2	-	2	2	2
86	IPING	Industrial Production Index: Intermediate Goods	I21	SCA	M	EUR	R	2	2	2	2	2	2	2	-	2	2	2
87	IPNRG	Industrial Production Index: Energy	I21	SCA	M	EUR	R	2	2	2	2	2	2	2	-	2	2	2
88	TRNMN	Turnover Index: Manufacturing	I21	SCA	M	EUR	R	2	2	2	2	2	2	2	-	-	2	2
89	TRNCAG	Turnover Index: Capital Goods	I21	SCA	M	EUR	R	2	2	2	2	2	2	2	-	2	2	2
90	TRNCOG	Turnover Index: Consumer Goods	I15	SCA	M	EUR	R	2	2	2	2	2	2	2	-	2	2	2
91	TRNDCOG	Turnover Index: Durable Consumer Goods	I21	SCA	M	EUR	R	2	2	2	2	2	2	2	-	2	2	2
92	TRNNDCOG	Turnover Index: Non Durable Consumer Goods	I21	SCA	M	EUR	R	2	2	2	2	2	2	2	-	2	2	2
93	TRNING	Turnover Index: Intermediate Goods	I21	SCA	M	EUR	R	2	2	2	2	2	2	2	-	2	2	2
94	TRNNRG	Turnover Index: Energy	I21	SCA	M	EUR	R	2	2	2	2	2	2	2	-	2	-	2
95	CAREG	Passenger's Cars Registrations	1000U	SCA	M	ECB	R	2	-	-	-	-	-	-	-	-	-	-
		(8) **Prices**																
96	PPICAG	Producer Price Index: Capital Goods	I21	MSA	M	EUR	N	2	2	2	2	2	2	2	-	2	2	-
97	PPICOG	Producer Price Index: Consumer Goods	I21	MSA	M	EUR	N	2	2	2	2	2	2	2	-	2	2	-
98	PPIDCOG	Producer Price Index: Durable Consumer Goods	I21	MSA	M	EUR	N	2	2	2	2	2	2	2	-	2	2	-
99	PPINDCOG	Producer Price Index: Non Durable Consumer Goods	I21	MSA	M	EUR	N	2	2	2	2	2	2	2	-	2	2	-
100	PPIING	Producer Price Index: Intermediate Goods	I21	MSA	M	EUR	N	2	2	2	2	2	2	2	-	2	2	-
101	PPINRG	Producer Price Index: Energy	I21	MSA	M	EUR	N	2	2	2	2	2	2	2	-	2	2	-
102	HICPOV	Harmonized Index of Consumer Prices: Overall Index	I10	SCA	M	ECB	N	2	2	2	2	2	2	2	2	2	2	2
103	HICPNEF	Harmonized Index of Consumer Prices: All Items, no Energy&Food	I10	SCA	M	ECB	N	2	2	2	2	2	2	2	2	2	2	2
104	HICPG	Harmonized Index of Consumer Prices: Goods	I10	SCA	M	ECB	N	2	2	2	2	2	2	2	2	2	2	2
105	HICPIN	Harmonized Index of Consumer Prices: Industrial Goods	I10	SCA	M	ECB	N	2	2	2	2	2	2	2	2	2	2	2
106	HICPSV	Harmonized Index of Consumer Prices: Services	I10	SCA	M	ECB	N	2	2	2	2	2	2	2	2	2	2	2
107	HICPNG	Harmonized Index of Consumer Prices: Energy	I10	MSA	M	EUR	N	2	2	2	2	2	2	2	2	2	2	2
108	DFGDP	Real Gross Domestic Product Deflator	I15	SCA	Q	EUR	N	2	2	2	2	2	2	2	2	2	2	2
109	HPRC	Residential Property Prices (BIS)	MLN€	SCA	Q	FRED	N	2	2	2	2	-	2	2	2	2	2	-
		(9) **Confidence Indicators**																
110	ICONFIX	Industrial Confidence Indicator	Index	SA	M	EUR	C	4	4	4	4	4	4	4	4	4	4	4
111	CCONFIX	Consumer Confidence Index	Index	SA	M	EUR	C	4	4	4	5	5	5	5	5	5	4	5
112	ESENTIX	Economic Sentiment Indicator	Index	SA	M	EUR	C	4	4	4	4	5	4	4	4	4	4	4
113	KCONFIX	Construction Sentiment Indicator	Index	SA	M	EUR	C	4	5	4	5	5	5	5	4	5	5	5
114	RTCONFIX	Retail Confidence Indicator	Index	SA	M	EUR	C	4	4	4	4	4	4	4	4	4	4	4
115	SCONFIX	Services Confidence Indicator	Index	SA	M	EUR	C	4	4	4	4	4	5	4	4	4	4	4
116	BCI	Business Confidence Index	2010=100	SA	M	OECD	C	4	4	4	4	5	4	4	4	4	4	4
117	CCI	Consumer Confidence Index	2010=100	SA	M	OECD	C	4	4	4	5	5	5	5	5	5	4	5
		(10) **Monetary Aggregates**																
118	CURR	Money Stock: Currency	MLN€	SCA	M	ECB	F	2	-	-	-	-	-	-	-	-	-	-
119	M1	Money Stock: M1	MLN€	SCA	M	ECB	F	2	-	-	-	-	-	-	-	-	-	-
120	M2	Money Stock: M2	MLN€	SCA	M	ECB	F	2	-	-	-	-	-	-	-	-	-	-

Bibliography

Aastveit, K. A. and T. Trovik (2014). Estimating the output gap in real time: A factor model approach. *The Quarterly Review of Economics and Finance 54*, 180–193.

Aastveit, K. A., H. C. Bjørnland, and L. A. Thorsrud (2016). The world is not enough! Small open economies and regional dependence. *The Scandinavian Journal of Economics 118*(1), 168–195.

Adrian, T., N. Boyarchenko, and D. Giannone (2019). Vulnerable growth. *American Economic Review 109*(4), 1263–1289.

Ahn, S. C. and A. R. Horenstein (2013). Eigenvalue ratio test for the number of factors. *Econometrica 81*, 1203–1227.

Ahn, H. J. and M. Luciani (2024). Common and idiosyncratic inflation. FEDS 2020-024r1, Board of Governors of the Federal Reserve System.

Ahn, H. J., S. Xie, and C. Yang (2024). Effects of monetary policy on household expectations: The role of homeownership. *Journal of Monetary Economics*, 147:103599.

Alessi, L., M. Barigozzi, and M. Capasso (2010). Improved penalization for determining the number of factors in approximate factor models. *Statistics & Probability Letters 80*(23-24), 1806–1813.

Alessi, L., M. Barigozzi, and M. Capasso (2011). Non-fundamentalness in structural econometric models: A review. *International Statistical Review*, 79(1):16–47.

Alessi, L., E. Ghysels, L. Onorante, R. Peach, and S. Potter (2014). Central bank macroeconomic forecasting during the global financial crisis: The European Central Bank and Federal Reserve Bank of New York experiences. *Journal of Business & Economic Statistics 32*(4), 483–500.

Altavilla, C., L. Brugnolini, R. S. Gürkaynak, R. Motto, and G. Ragusa (2019). Measuring euro area monetary policy. *Journal of Monetary Economics*, 108:162–179.

Alvarez, F., H. Le Bihan, and F. Lippi (2016). The real effects of monetary shocks in sticky price models: a sufficient statistic approach. *American Economic Review*, 106(10):2817–2851.

Ando, T. and R. S. Tsay (2011). Quantile regression models with factor-augmented predictors and information criterion. *The Econometrics Journal 14*(1), 1–24.

P. Andrade and F. Ferroni. Delphic and odyssean monetary policy shocks: Evidence from the euro area. *Journal of Monetary Economics*, 117:816–832, 2021.

Andreou, E., P. Gagliardini, E. Ghysels, and M. Rubin (2019). Inference in group factor models with an application to mixed-frequency data. *Econometrica 87*(4), 1267–1305.

Angelini, E., M. Lalik, M. Lenza, and J. Paredes (2019). Mind the gap: A multi-country BVAR benchmark for the eurosystem projections. *International Journal of Forecasting 35*(4), 1658–1668.

Antolin-Diaz, J., T. Drechsel, and I. Petrella (2017). Tracking the slowdown in long-run GDP growth. *The Review of Economics and Statistics 99*, 343–356.

Aruoba, S. B., F. X. Diebold, J. Nalewaik, F. Schorfheide, and D. Song (2016). Improving GDP measurement: A measurement-error perspective. *Journal of Econometrics 191*, 384–397.

Ascari, G., P. Bonomolo, M. Hoeberichts, and R. Trezzi (2023). The euro area great inflation surge. Policy Brief 548, SUERF.

Azqueta-Gavaldón, A., D. Hirschbühl, L. Onorante, and L. Saiz (2023). Sources of economic policy uncertainty in the euro area. *European Economic Review 152*, 104373.

Azzalini, A. (1985). A class of distributions which includes the normal ones. *Scandinavian Journal of Statistics 12*(2), 171–178.

Bai, J. (2003). Inferential theory for factor models of large dimensions. *Econometrica*, 71(1): 135–171.

Bai, J. (2004). Estimating cross-section common stochastic trends in nonstationary panel data. *Journal of Econometrics 122*, 137–183.

Bai, J. and S. Ng (2002). Determining the number of factors in approximate factor models. *Econometrica 70*, 191–221.

Bai, J. and S. Ng (2004). A PANIC attack on unit roots and cointegration. *Econometrica 72*, 1127–1177.

Bai, J. and S. Ng (2006). Confidence intervals for diffusion index forecasts and inference for factor-augmented regressions. *Econometrica*, 74(4):1133–1150.

Bai, J. and S. Ng (2008). Extremum estimation when the predictors are estimated from large panels. *Annals of Economics and Statistics 89–90*, 1–25.

Bai, J. and S. Ng (2013). Principal components estimation and identification of static factors. *Journal of Econometrics*, 176(1):18–29.

Bańbura, M. and E. Bobeica (2023). Does the Phillips curve help to forecast euro area inflation? *International Journal of Forecasting 39*, 364–390.

Bańbura, M., D. Giannone, and M. Lenza (2015). Conditional forecasts and scenario analysis with vector autoregressions for large cross-sections. *International Journal of Forecasting 31*(3), 739–756.

M. Bańbura and M. Modugno. Maximum likelihood estimation of factor models on datasets with arbitrary pattern of missing data. *Journal of Applied Econometrics*, 29(1):133–160, 2014.

M. Barigozzi. On estimation and inference of large approximate dynamic factor models via the principal component analysis. *arXiv preprint arXiv:2211.01921*, 2022.

Barigozzi, M., A. M. Conti, and M. Luciani (2014). Do euro area countries respond asymmetrically to the common monetary policy? *Oxford Bulletin of Economics and Statistics*, 76(5): 693–714.

Barigozzi, M., H. Cho, and P. Fryzlewicz (2018). Simultaneous multiple change-point and factor analysis for high-dimensional time series. *Journal of Econometrics*, 206(1):187–225.

Barigozzi, M., M. Lippi, and M. Luciani (2021). Large-dimensional dynamic factor models: Estimation of impulse-response functions with $I(1)$ cointegrated factors. *Journal of Econometrics 221*, 455–482.

Barigozzi, M. and M. Luciani (2023). Measuring the Output Gap using Large Datasets. *The Review of Economics and Statistics 105*, 1500–1514.

Barigozzi, M., C. Lissona, and L. Tonni (2024). Large datasets for the euro area and its member countries and the dynamic effects of the common monetary policy. *arXiv preprint arXiv:2410.05082*.

Barigozzi, M. and M. Luciani (2024). Quasi maximum likelihood estimation and inference of large approximate dynamic factor models via the EM algorithm. *arXiv preprint arXiv:1910.03821.v5 [math.ST].*

Benati, L. and T. A. Lubik (2021). Searching for hysteresis. Working Paper 21-03, Federal Reserve Bank of Richmond.

Berger, T., J. Richter, and B. Wong (2022). A unified approach for jointly estimating the business and financial cycle, and the role of financial factors. *Journal of Economic Dynamics and Control 136*, 104315.

Bergholt, D., F. Canova, F. Furlanetto, N. Maffei-Faccioli, and P. Ulvedal (2025). What drives the recent surge in inflation? the historical decomposition roller coaster. *American Economic Journal: Macroeconomics*, *forthcoming.*

Berson, C., V. Botelho, A. D. da Silva, C. Foroni, M. Mohr, C. Schroeder, and M. Weissler (2024). Explaining the resilience of the euro area labour market between 2022 and 2024. Economic Bulletin 8/2024, European Central Bank.

Bianchi, F., G. Nicoló, and D. Song (2023). Inflation and real activity over the business cycle. Finance and Economics Discussion Series 2023-038, Board of Governors of the Federal Reserve System.

Blanchard, O. J. and D. Quah (1989). The dynamic effects of aggregate demand and supply disturbance. *The American Economic Review 79*, 655–673.

Boivin, J. and S. Ng (2006). Are more data always better for factor analysis? *Journal of Econometrics 132*, 169–194.

Borio, C. (2014). The financial cycle and macroeconomics: What have we learnt? *Journal of Banking & Finance 45*, 182–198.

Borio, C., P. Disyatat, and M. Juselius (2017). Rethinking potential output: embedding information about the financial cycle. *Oxford Economic Papers 69*, 655–677.

Borio, C., P. Disyatat, and M. Juselius (2017). Rethinking potential output: embedding information about the financial cycle. *Oxford Economic Papers 69*, 655–677.

Botelho, V., C. Foroni, and A. Renzetti (2024). Labour at risk. *European Economic Review 170*, 104849.

Branten, E., A. Lamo, and T. Room (2018). Nominal wage rigidity in the eu countries before and after the great recession: evidence from the wdn surveys.

Breitung, J. and S. Eickmeier (2016). Analyzing international business and financial cycles using multi-level factor models: A comparison of alternative approaches. In *Dynamic Factor Models*, Volume 35, pp. 177–214. Emerald Group Publishing Limited.

Buncic, D., A. Pagan, and T. Robinson (2023). Recovering stars in macroeconomics. SSRN working paper 4562801.

Burlon, L. and P. D'Imperio (2020). Reliable real-time estimates of the euro-area output gap. *Journal of Macroeconomics 64*, 103191.

P. Burriel and A. Galesi. Uncovering the heterogeneous effects of ECB unconventional monetary policies across euro area countries. *European Economic Review*, 101:210–229, 2018.

Busetti, F., M. Caivano, D. Delle Monache, and C. Pacella (2021). The time-varying risk of Italian GDP. *Economic Modelling 101*, 105522.

Bussière, M., J. Cao, J. de Haan, R. Hills, S. Lloyd, B. Meunier, J. Pedrono, D. Reinhardt, S. Sinha, R. Sowerbutts, et al. (2021). The interaction between macroprudential policy and monetary policy: Overview. *Review of International Economics 29*(1), 1–19.

Cai, T. and W. Liu (2011). Adaptive thresholding for sparse covariance matrix estimation. *Journal of the American Statistical Association 106*(494), 672–684.

Canova, F. (2025). FAQ: How do I estimate the output gap? *The Economic Journal 135*, 59–80.

Carriero, A., T. E. Clark, M. Marcellino, and E. Mertens (2024). Addressing COVID-19 outliers in BVARs with stochastic volatility. *The Review of Economics and Statistics 106*, 1403–1417.

Casalis, A. and G. Krustev (2022). Cyclical drivers of euro area consumption: What can we learn from durable goods? *Journal of International Money and Finance 120*, 102241.

D. Cascaldi-Garcia, T. R. Ferreira, D. Giannone, and M. Modugno. Back to the present: Learning about the euro area through a now-casting model. *International Journal of Forecasting*, 40(2):661–686, 2024.

Cavallo, A. and A. Ribba (2015). Common macroeconomic shocks and business cycle fluctuations in euro area countries. *International Review of Economics & Finance 38*, 377–392.

Cecchetti, S. G. (2016). On the separation of monetary and prudential policy: How much of the precrisis consensus remains? *Journal of International Money and Finance 66*, 157–169.

Cette, G., J. Fernald, and B. Mojon (2016). The pre-Great Recession slowdown in productivity. *European Economic Review 88*, 3–20.

Choi, I., D. Kim, Y. J. Kim, and N.-S. Kwark (2018). A multilevel factor model: Identification, asymptotic theory and applications. *Journal of Applied Econometrics 33*(3), 355–377.

Choi, I., R. Lin, and Y. Shin (2023). Canonical correlation-based model selection for the multilevel factors. *Journal of Econometrics 233*(1), 22–44.

Christiano, L. J. and T. J. Fitzgerald (2003). The bandpass filter. *International Economic Review 44*, 435–465.

Christiano, L. J., M. Eichenbaum, and C. L. Evans (2005). Nominal rigidities and the dynamic effects of a shock to monetary policy. *Journal of Political Economy*, 113(1):1–45.

Ciccarelli, M. and C. Osbat (2017). Low inflation in the euro area: Causes and consequences. Occasional Paper Series 181, European Central Bank.

Claessens, S. (2015). An overview of macroprudential policy tools. *Annual Review of Financial Economics 7*(1), 397–422.

Claessens, S., M. A. Kose, and M. E. Terrones (2012). How do business and financial cycles interact? *Journal of International Economics 87*, 178–190.

Conti, A. M. (2021). Resurrecting the Phillips curve in low-inflation times. *Economic Modelling 96*, 172–195.

Corsello, F., S. Neri, and A. Tagliabracci (2021). Anchored or de-anchored? that is the question. *European Journal of Political Economy 69*, 102031.

G. Corsetti, J. B. Duarte, and S. Mann. One money, many markets. *Journal of the European Economic Association*, 20(1):513–548, 2022.

Crump, R. K., S. Eusepi, D. Giannone, E. Qian, and A. M. Sbordone (2021). A large bayesian var of the united states economy. *FRB of New York Staff Report* (976).

A. D'Agostino, D. Giannone, M. Lenza, and M. Modugno. Nowcasting business cycles: A Bayesian approach to dynamic heterogeneous factor models. In *Dynamic Factor Models*, pages 569–594. Emerald Group Publishing Limited, 2016.

R. Datsenko and J. Fleck. Country-specific effects of euro-area monetary policy: The role of sectoral differences. Technical report, FEDS Notes. Washington: Board of Governors of the Federal Reserve System, 2024.

De Masi, P. (1997). IMF estimates of potential output: Theory and practice. IMF Working Paper 97/177.

A. De Stefani and R. C. Mano. Long-term debt and short-term rates: Fixed-rate mortgages and monetary transmission. Technical report, International Monetary Fund, 2025.

L. Dedola and F. Lippi. The monetary transmission mechanism: Evidence from the industries of five OECD countries. *European Economic Review*, 49(6):1543–1569, 2005.

Del Negro, M., D. Giannone, M. P. Giannoni, and A. Tambalotti (2017). Safety, liquidity, and the natural rate of interest. *Brookings Papers on Economic Activity Spring 2017*, 235–316.

Del Negro, M., F. Schorfheide, F. Smets, and R. Wouters (2007). On the fit of new Keynesian models. *Journal of Business & Economic Statistics 25*, 123–143.

Delle Chiaie, S., L. Ferrara, and D. Giannone (2022). Common factors of commodity prices. *Journal of Applied Econometrics 37*(3), 461–476.

D. A. Dickey and W. A. Fuller. Distribution of the estimators for autoregressive time series with a unit root. *Journal of the American statistical association*, 74(366a):427–431, 1979.

Doz, C., D. Giannone, and L. Reichlin (2012). A quasi-maximum likelihood approach for large, approximate dynamic factor models. *The Review of Economics and Statistics 94*, 1014–1024.

Durbin, J. and S. J. Koopman (2002). A simple and efficient simulation smoother for state space time series analysis. *Biometrika 89*, 603–616.

Eickmeier, S. (2009). Comovements and heterogeneity in the euro area analyzed in a non-stationary dynamic factor model. *Journal of Applied Econometrics 24*(6), 933–959.

Elfsbacka Schmöller, M. and M. Spitzer (2021). Deep recessions, slowing productivity and missing (dis-) inflation in the euro area. *European Economic Review 134*, 103708.

Escribano, A. and D. Peña (1994). Cointegration and common factors. *Journal of Time Series Analysis 15*, 577–586.

European Commission (2018). Staff working document on the review of the flexibility under the Stability and Growth Pact. COM(2018) 335.

Ferrara, L., M. Mogliani, and J.-G. Sahuc (2022). High-frequency macroeconomic risk measures in the wake of the war in Ukraine. *VoxEU 7*.

Figueres, J. M. and M. Jarociński (2020). Vulnerable growth in the euro area: Measuring the financial conditions. *Economics Letters 191*, 109126.

Flood, M. D. and G. G. Korenko (2015). Systematic scenario selection: Stress testing and the nature of uncertainty. *Quantitative Finance 15*(1), 43–59.

D. F. Findley, B. C. Monsell, W. R. Bell, M. C. Otto, and B.-C. Chen. New capabilities and methods of the X-12-ARIMA seasonal-adjustment program. *Journal of Business & Economic Statistics*, 16(2):127–152, 1998.

Forni, M., D. Giannone, M. Lippi, and L. Reichlin (2009). Opening the black box: Structural factor models with large cross sections. *Econometric Theory 25*(5), 1319–1347.

Forni, M., L. Gambetti, A. Granese, L. Sala, and S. Soccorsi (2025). An American macroeconomic picture: Supply and demand shocks in the frequency domain. *American Economic Journal: Macroeconomics*. forthcoming.

M. Forni, L. Gambetti, M. Lippi, and L. Sala. Common components structural VARs. *Journal of Business & Economic Statistics*, (just-accepted):1–24, 2025.

O. Fortin-Gagnon, M. Leroux, D. Stevanovic, and S. Surprenant. A large Canadian database for macroeconomic analysis. *Canadian Journal of Economics*, 55(4):1799–1833, 2022.

Freyaldenhoven, S. (2022). Factor models with local factors—determining the number of relevant factors. *Journal of Econometrics 229*(1), 80–102.

R. Fry and A. Pagan. Sign restrictions in structural vector autoregressions: A critical review. *Journal of Economic Literature*, 49(4):938–960, 2011.

Furlanetto, F., P. Gelain, and M. T. Sanjani (2021). Output gap, monetary policy trade-offs, and financial frictions. *Review of Economic Dynamics 41*, 52–70.

Furlanetto, F., A. Lepetit, O. Robstad, J. Rubio-Ramírez, and P. Ulvedal (2025). Estimating hysteresis effects. *American Economic Journal: Macroeconomics 17*, 25–70.

Furno, F. and D. Giannone (2024). Nowcasting recession risk. In *Handbook of Research Methods and Applications in Macroeconomic Forecasting*, pp. 156–186. Edward Elgar Publishing.

Galesi, A. and O. Rachedi (2019). Services deepening and the transmission of monetary policy. *Journal of the European Economic Association*, 17(4):1261–1293.

Gambetti, L. and A. Musso (2017). Loan supply shocks and the business cycle. *Journal of Applied Econometrics 32*, 764–782.

Gautier, E., C. Conflitti, R. P. Faber, B. Fabo, L. Fadejeva, V. Jouvanceau, J.-O. Menz, T. Messner, P. Petroulas, P. Roldan-Blanco, et al. (2024). New facts on consumer price rigidity in the euro area. *American Economic Journal: Macroeconomics*, 16(4):386–431.

G. Georgiadis. Examining asymmetries in the transmission of monetary policy in the euro area: Evidence from a mixed cross-section global VAR model. *European Economic Review*, 75: 195–215, 2015.

M. Gertler and P. Karadi. Monetary policy surprises, credit costs, and economic activity. *American Economic Journal: Macroeconomics*, 7(1):44–76, 2015.

D. Giannone, J. Henry, M. Lalik, and M. Modugno. An area-wide real-time database for the euro area. *The Review of Economics and Statistics*, 94(4):1000–1013, 2012.

Giannone, D. and G. Primiceri (2024). The drivers of post-pandemic inflation. Working Paper 32859, National Bureau of Economic Research.

Giglio, S., B. Kelly, and S. Pruitt (2016). Systemic risk and the macroeconomy: An empirical evaluation. *Journal of Financial Economics 119*(3), 457–471.

Gilchrist, S. and B. Mojon (2018). Credit risk in the euro area. *The Economic Journal 128*(608), 118–158.

González-Astudillo, M. (2019). An output gap measure for the euro area: Exploiting country-level and cross-sectional data heterogeneity. *European Economic Review 120*, 103301.

Gonçalves, S. and L. Kilian (2004). Bootstrapping autoregressions with conditional heteroskedasticity of unknown form. *Journal of Econometrics*, 123(1):89–120.

Gonçalves, S., J. Koh, and B. Perron (2025). Bootstrap inference for group factor models. *Journal of Financial Econometrics 23*(2), nbae020.

González-Rivera, G., J. Maldonado, and E. Ruiz (2019). Growth in stress. *International Journal of Forecasting 35*(3), 948–966.

González-Rivera, G., C. Rodríguez-Caballero, and E. Ruiz (2024). Expecting the unexpected: Stressed scenarios for economic growth. *Journal of Applied Econometrics 39*(5), 926–942.

Gordon, R. J. (2018). Declining American economic growth despite ongoing innovation. *Explorations in Economic History 69*, 1–12.

Hallin, M. and R. Liška (2007). Determining the number of factors in the general dynamic factor model. *Journal of the American Statistical Association 102*, 603–617.

Hamilton, J. D. (2018). Why you should never use the Hodrick-Prescott filter. *The Review of Economics and Statistics 100*, 831–843.

Hamilton, J. D. (2020). *Time series analysis.* Princeton University Press.

Hartl, T., R. Tschernig, and E. Weber (2022). Solving the unobserved components puzzle: A fractional approach to measuring the business cycle. mimeo.

Hasenzagl, T., F. Pellegrino, L. Reichlin, and G. Ricco (2019). The inflation puzzle in the euro area. VoxEU 16 October 2019, CEPR.

Hasenzagl, T., F. Pellegrino, L. Reichlin, and G. Ricco (2022). A Model of the Fed's View on Inflation. *The Review of Economics and Statistics 104*, 686–704.

Havik, K., K. Mc Morrow, F. Orlandi, C. Planas, R. Raciborski, W. Röger, A. Rossi, A. Thum-Thysen, V. Vandermeulen, et al. (2014). The production function methodology for calculating potential growth rates & output gaps. Economic Papers 535, DG ECFIN, European Commission.

Hodrick, R. J. and E. C. Prescott (1997). Postwar US business cycles: an empirical investigation. *Journal of Money, Credit, and Banking 29*, 1–16.

Hoffmann, P., M. Kremer, and S. Zaharia (2020). Financial integration in Europe through the lens of composite indicators. *Economics Letters 194*, 109344.

Hollo, D., M. Kremer, and M. Lo Duca (2012). CISS – a composite indicator of systemic stress in the financial system.

Jarociński, M. and P. Karadi (2020). Deconstructing monetary policy surprises—the role of information shocks. *American Economic Journal: Macroeconomics*, 12(2):1–43.

Jarociński, M. and M. Lenza (2018). An inflation-predicting measure of the output gap in the euro area. *Journal of Money, Credit and Banking 50*, 1189–1224.

Justiniano, A., G. Primiceri, and A. Tambalotti (2013). Is there a trade-off between inflation and output stabilization? *American Economic Journal: Macroeconomics 5*, 1–31.

Kamber, G., J. Morley, and B. Wong (2018). Intuitive and reliable estimates of the output gap from a Beveridge-Nelson filter. *The Review of Economics and Statistics 100*, 550–566.

Kiley, M. T. (2013). Output gaps. *Journal of Macroeconomics 37*, 1–18.

Kim, C.-J. and J. Kim (2022). Trend-cycle decompositions of real GDP revisited: Classical and Bayesian perspectives on an unsolved puzzle. *Macroeconomic Dynamics 26*, 394–418.

Kilian, L. (1998). Small-sample confidence intervals for impulse response functions. *Review of Economics and Statistics*, 80(2):218–230.

Kilian, L. and S. Manganelli (2008). The central banker as a risk manager: Estimating the Federal Reserve's preferences under Greenspan. *Journal of Money, Credit and Banking 40*(6), 1103–1129.

Kilian, L. (2024). How to construct monthly var proxies based on daily surprises in futures markets. *Journal of Economic Dynamics and Control*, 168:104966.

Koenker, R. (2005). *Quantile regression.* Cambridge University Press.

Koenker, R. and G. Bassett, Jr (1978). Regression quantiles. *Econometrica 46*(1), 33–50.

Koenker, R. and J. Machado (1999). Goodness of fit and related inference processes for quantile regression. *Journal of the American Statistical Association 94*(448), 1296–1310.

Koenker, R. W. and V. d'Orey (1987). Algorithm as 229: Computing regression quantiles. *Applied Statistics*, 383–393.

Kose, M. A., C. Otrok, and C. H. Whiteman (2003). International business cycles: World, region, and country-specific factors. *American Economic Review 93*(4), 1216–1239.

Lane, P. R. (2024). The 2021-2022 inflation surges and the monetary policy response through the lens of macroeconomic models. Speech by Philip R. Lane, Executive Board of the ECB, SUERF Marjolin Lecture, Banca d'Italia, Rome, 18 November 2024.

Lenza, M. and G. E. Primiceri (2022). How to estimate a vector autoregression after March 2020. *Journal of Applied Econometrics 37*, 688–699.

Lhuissier, S. (2022). Financial conditions and macroeconomic downside risks in the euro area. *European Economic Review 143*, 104046.

Lippi, M. and L. Reichlin (1994). Diffusion of technical change and the decomposition of output into trend and cycle. *The Review of Economic Studies 61*, 19–30.

C. Lissona and E. Ruiz. Heterogeneous economic growth vulnerability across euro area countries under stressed scenarios. *arXiv preprint arXiv:2506.14321*, 2025.

Luciani, M. (2014). Forecasting with approximate dynamic factor models: The role of non-pervasive shocks. *International Journal of Forecasting 30*, 20–29.

Maldonado, J. and E. Ruiz (2021). Accurate confidence regions for principal components factors. *Oxford Bulletin of Economics and Statistics 83*(6), 1432–1453.

Mandler, M., M. Scharnagl, and U. Volz (2022). Heterogeneity in euro area monetary policy transmission: Results from a large multicountry BVAR model. *Journal of Money, Credit and Banking*, 54(2-3):627–649.

McCracken, M. W. and S. Ng (2016). FRED-MD: A monthly database for macroeconomic research. *Journal of Business & Economic Statistics 34*, 574–589.

McCracken, M. and S. Ng (2020). FRED-QD: A quarterly database for macroeconomic research. NBER working paper 26872.

Mertens, K. and M. O. Ravn (2013). The dynamic effects of personal and corporate income tax changes in the United States. *American Economic Review*, 103(4):1212–1247.

Mian, A. and A. Sufi (2018). Finance and business cycles: The credit-driven household demand channel. *Journal of Economic Perspectives 32*, 31–58.

Mian, A., A. Sufi, and E. Verner (2017). Household debt and business cycles worldwide. *The Quarterly Journal of Economics 132*(4), 1755–1817.

Morana, C. (2024). A new macro-financial condition index for the euro area. *Econometrics and Statistics 29*, 64–87.

Morley, J., C. R. Nelson, and E. Zivot (2003). Why are the Beveridge-Nelson and unobserved-components decompositions of GDP so different? *The Review of Economics and Statistics 85*, 235–243.

Morley, J. and B. Wong (2020). Estimating and accounting for the output gap with large Bayesian vector autoregressions. *Journal of Applied Econometrics 35*, 1–18.

Morley, J., D. Rodríguez-Palenzuela, Y. Sun, and B. Wong (2023). Estimating the euro area output gap using multivariate information and addressing the COVID-19 pandemic. *European Economic Review 153*, 104385.

Morley, J., T. D. Tran, and B. Wong (2024). A simple correction for misspecification in trend-cycle decompositions with an application to estimating r. *Journal of Business & Economic Statistics 42*, 665–680.

Ng, S. (2018). Comments on the cyclical sensitivity in estimates of potential output. *Brookings Papers on Economic Activity 49*, 412–423.

Ng, S. (2021). Modeling macroeconomic variations after COVID-19. NBER working paper 29060.

J. L. M. Olea and C. Pflueger. A robust test for weak instruments. *Journal of Business & Economic Statistics*, 31(3):358–369, 2013.

Oman, W. (2019). The synchronization of business cycles and financial cycles in the euro area. *International Journal of Central Banking 15*(1), 327–362.

on Banking Supervision, B. C. (2009). Principles for sound stress testing practices and supervision.

Onatski, A. (2009). Testing hypotheses about the number of factors in large factor models. *Econometrica 77*, 1447–1479.

Onatski, A. (2010). Determining the number of factors from empirical distribution of eigenvalues. *The Review of Economics and Statistics*, 92(4):1004–1016.

Onatski, A. and C. Wang (2021). Spurious factor analysis. *Econometrica 89*, 591–614.

Olea, J. L. M. and C. Pflueger (2013). A robust test for weak instruments. *Journal of Business & Economic Statistics*, 31(3):358–369.

Oman, W. (2019). The synchronization of business cycles and financial cycles in the euro area. *International Journal of Central Banking 15*(1), 327–362.

Opschoor, D. and D. J. van Dijk (2023). Slow Expectation-Maximization convergence in low-noise dynamic factor models. SSRN working paper 4408065.

A. Orphanides and S. van Norden. The unreliability of output-gap estimates in real time. *Review of Economics and Statistics*, 84(4):569–583, 2002.

Phillips, P. C. and P. Perron (1988). Testing for a unit root in time series regression. *Biometrika*, 75(2):335–346.

Phillips, P. C. and S. Jin (2021). Business cycles, trend elimination, and the HP filter. *International Economic Review 62*, 469–520.

Phillips, P. C. and Z. Shi (2021). Boosting: Why you can use the HP filter. *International Economic Review 62*, 521–570.

Plagborg-Møller, M., L. Reichlin, G. Ricco, and T. Hasenzagl (2020). When is growth at risk? *Brookings Papers on Economic Activity Spring 2020*, 167–229.

Politis, D. N. and J. P. Romano (1994). The stationary bootstrap. *Journal of the American Statistical Association 89*, 1303–1313.

Prasad, M. A., S. Elekdag, M. P. Jeasakul, R. Lafarguette, M. A. Alter, A. X. Feng, and C. Wang (2019). *Growth at risk: Concept and application in IMF country surveillance*. International Monetary Fund.

Proietti, T., M. Marczak, and G. Mazzi (2017). Euromind-: A density estimate of monthly gross domestic product for the euro area. *Journal of Applied Econometrics 32*(3), 683–703.

Rathke, A., S. Streicher, and J.-E. Sturm (2022). How similar are country- and sector-responses to common shocks within the euro area? *Journal of International Money and Finance 120*, 102313.

Reichlin, L., G. Ricco, and T. Hasenzagl (2020). Financial variables as predictors of real growth vulnerability. Deutsche Bundesbank Discussion Papers 05/2020.

Rodríguez-Caballero, C. and M. Caporin (2019). A multilevel factor approach for the analysis of CDS commonality and risk contribution. *Journal of International Financial Markets, Institutions and Money 63*, 101144.

Rubio-Ramirez, J. F., D. F. Waggoner, and T. Zha (2010). Structural vector autoregressions: Theory of identification and algorithms for inference. *The Review of Economic Studies*, 77 (2):665–696.

Rünstler, G. and M. Vlekke (2018). Business, housing, and credit cycles. *Journal of Applied Econometrics 33*(2), 212–226.

Slacalek, J., O. Tristani, and G. L. Violante (2020). Household balance sheet channels of monetary policy: A back-of-the- envelope calculation for the euro area. *Journal of Economic Dynamics and Control*, 115:103879.

Stock, J. H. and M. W. Watson (1996). Evidence on structural instability in macroeconomic time series relations. *Journal of Business & Economic Statistics*, 14(1):11.

Stock, J. H. and M. W. Watson (2002a). Forecasting using principal components from a large number of predictors. *Journal of the American Statistical Association*, 97(460):1167–1179.

Stock, J. H. and M. W. Watson (2002b). Macroeconomic forecasting using diffusion indexes. *Journal of Business & Economic Statistics*, 20(2):147–162.

J. H. Stock, J. H. Wright, and M. Yogo. A survey of weak instruments and weak identification in generalized method of moments. *Journal of Business & Economic Statistics*, 20(4):518–529, 2002.

Stock, J. H. and M. W. Watson (2012). Disentangling the channels of the 2007–09 recession. *Brookings Papers on Economic Activity*, (1):81–135.

Stock, J. H. and M. W. Watson (2016, January). Dynamic factor models, factor-augmented vector autoregressions, and structural vector autoregressions in macroeconomics. In J. B. Taylor and H. Uhlig (Eds.), *Handbook of Macroeconomics*, Volume 2, pp. 415–525. Elsevier.

Stock, J. H. and M. W. Watson (2025). Recovering from COVID. Brookings Paper on Economic Activity Conference Draft, March 27–28, 2025. link.

Suarez, J. (2022). Growth-at-risk and macroprudential policy design. *Journal of Financial Stability 60*, 101008.

Szendrei, T. and K. Varga (2023). Revisiting vulnerable growth in the euro area: Identifying the role of financial conditions in the distribution. *Economics Letters 223*, 110990.

Thum-Thysen, A., F. Blondeau, F. d'Auria, B. Döhring, A. Hristov, and K. Mc Morrow (2022). Potential output and output gaps against the backdrop of the COVID-19 pandemic. *Quarterly Report on the Euro Area 21*, 21–30.

Tóth, M. (2021). A multivariate unobserved components model to estimate potential output in the Euro Area: A production function based approach. ECB working paper 2523.

Wang, P. (2010). Large dimensional factor models with a multi-level factor structure: Identification, estimation and inference. *Unpublished manuscript, New York University.*

Winter, J. d., S. J. Koopman, and I. Hindrayanto (2022). Joint decomposition of business and financial cycles: Evidence from eight advanced economies. *Oxford Bulletin of Economics and Statistics 84*, 57–79.